5-2016

A Quantitative Genetic Analysis of Limb Segment Morphology in Humans and Other Primates: Genetic Variance, Morphological Integration, and Linkage Analysis

Brannon Irene Hulsey
University of Tennessee - Knoxville, bjones32@vols.utk.edu

To the Graduate Council:

I am submitting herewith a dissertation written by Brannon Irene Hulsey entitled "A Quantitative Genetic Analysis of Limb Segment Morphology in Humans and Other Primates: Genetic Variance, Morphological Integration, and Linkage Analysis." I have examined the final electronic copy of this dissertation for form and content and recommend that it be accepted in partial fulfillment of the requirements for the degree of Doctor of Philosophy, with a major in Anthropology.

Graciela S. Cabana, Major Professor

We have read this dissertation and recommend its acceptance:

Benjamin M. Auerbach, Lorena M. Havill, Andrew Kramer, Richard L. Jantz, Charles C. Roseman, Arnold M. Saxton

Accepted for the Council:
Dixie L. Thompson

Vice Provost and Dean of the Graduate School

(Original signatures are on file with official student records.)

A Quantitative Genetic Analysis of Limb Segment Morphology in Humans and Other Primates: Genetic Variance, Morphological Integration, and Linkage Analysis

A Dissertation Presented for the
Doctor of Philosophy
Degree
The University of Tennessee, Knoxville

Brannon Irene Hulsey
May 2016

ACKNOWLEDGEMENTS

There are many people that, without whom, this project would not have been completed. My sincere and heartfelt thanks goes out to each of them for their assistance and support.

To begin, thank you to Graciela Cabana for being an exceptionally supportive and patient advisor. I am grateful for the opportunities she has provided for me, from trusting me to help set up and maintain the Molecular Anthropology Laboratories at the University of Tennessee, to financially supporting me in ancient DNA training and dissertation data collection, to including me in various projects, presentations, and publications. I feel lucky to have had such an avid supporter in the academic arena that always provided an optimistic lens to view my work and allowed me to weave the demands of a dissertation into my very busy personal life.

Thank you also to my other UT committee members. Ben Auerbach provided statistical guidance and helped frame my work in the current literature. Richard Jantz, Andy Kramer, and Arnold Saxton each provided theoretical and statistical support through conversation and course work. And, thank you to the Department of Anthropology at UT for partially funding this work with the Kneberg-Lewis Award.

This project has afforded me the opportunity to work with several other committee members who are affiliated with different institutions. Thanks to Lorena Havill who granted access to the baboon skeletal collection at the Texas Biomedical Research Institute (TBRI) and who provided technical assistance, both from her own vast knowledge and by connecting me with the many brilliant people at TBRI (more on that below). And, many thanks to Charles Roseman at the University of Illinois Urbana-Champaign for providing endless statistical support

and helping me unravel the intricacies of R. Your patience with my many questions is much appreciated!

I would also like to thank the many other researchers and colleagues who are not on my committee that provided essential data, advice, and assistance. Thank you to Michael Crawford for providing access to the Mennonite data and to his former students Kristin Young and Anne Justice for their hospitality while I visited the University of Kansas. Many thanks to Dennis O'Rourke for allowing me to use the Sukhumi Baboon data. Thank you to Mark Algee-Hewitt for assistance in deciphering computer networking and helping me make computers "talk" to one another, a feat which was formerly so far outside my realm of knowledge I didn't even know where to begin. I am also indebted to a number of people at the TBRI: to Michael Mahaney for data access, to Debbie Newman for pedigree construction and SOLAR programming, to Charles Peterson and Linda Freeman-Shade for SOLAR assistance, to Jennifer Harris, Shayna Levine, and Ashan Choudary for general lab assistance, and to Courtney Roush and Tanya Lerma for assistance in bone cleaning. I also am extremely thankful for Jennifer Guida and Frankie West who each took time out of their summers to travel to San Antonio with me and spend a month cleaning baboon bones. You are both amazing women, and I appreciate you! In addition, there are several people in the San Antonio area who provided me with meals to eat and/or beds to sleep in: thank you Victoria Castellanos, Kate and Robert Crosby, Justin Schneider, Ellen Quillen, and Blake and Sarah Walsh.

I am immensely thankful for my extremely supportive friends and family, without whom I would have fallen flat on my face a long time ago. Thank you to my parents, Jeffrey and Susan Jones, and my brother, Matthew, for your unending love and understanding, especially when I

repeatedly told you not to ask me how the dissertation was going or when I would graduate. Thank you to my in-laws, Ron and Barbara Hulsey, for treating me like your own daughter and always agreeing to come into town and watch the kids when I needed to travel for conferences or data collection (or to go on a two-week journey to South Africa). Many thanks to my friends, both those within the academic world that understand the craziness that is grad school and dissertation writing and those outside of academia who love me and help me remember the bigger picture of life. The emotional support you have all provided is unparalleled. And a special thank you goes to my church family for always reminding me that my value in life does not come from what I do, but who I am. The community and support that I have found among the people of First Baptist Church Knoxville will always hold a special place in my heart.

Finally, there are really not words to express my love and gratitude for my amazing husband, Wade. Thank you for following me to Knoxville. Thank you for supporting me, emotionally, physically, financially, and spiritually, as I have grown and changed during my time in grad school. Thank you for being my best friend and biggest fan. You rock my face off! And, thank you for our beautiful children, Samuel, Ava, and this new little one growing in my belly.

ABSTRACT

Limb segment lengths (and, by extension, limb proportions) are widely studied postcranial features in biological anthropology due to the seemingly consistent phenotypic patterning among human and fossil hominin groups. This patterning, widely presumed to be the result of adaptation to thermoregulatory efficiency, has led to the assumption among biological anthropologists that limb proportions in humans are phenotypically stable unless long periods of extreme environmental conditions force adaptive change. Because these traits are considered stable, they have been used to inform multiple areas of anthropological inquiry, including investigations of phylogenetic relationships and fossil species identification, locomotor behavior and the evolution of bipedalism, and migration patterns.

The problem with this assumption is that phenotypic patterns may not accurately reflect evolutionary processes, and even if they do, there is no reason to expect phenotype to respond to natural selection solely. Investigations of phenotypic variation need to incorporate genetic variation and covariation to better understand the processes that produced observable patterns, including evolutionary processes. However, the incorporation of genetic parameters is often difficult given that knowledge of familial relationships are required. Therefore, the goal of this project is to use a quantitative genetics approach to estimate the genetic variance and covariance in limb segment lengths and then begin the task of identifying genes which may influence this normal variation. These tasks are accomplished using multiple large, pedigreed samples of primate species, including humans. Linkage analysis on a baboon sample, a well-accepted model

organism for humans, is used to identify regions of the genome which may influence limb segment variation.

The results presented here suggest that 1) while patterns of genetic and phenotypic variance and covariance across limb segments are broadly similar, there are differences in the details, and 2) while patterns of genetic and phenotypic variance and covariance within and among limb segments generally adhere to expectations set forth by developmental and evolutionary-based hypotheses, there are exceptions. Additionally, several genomic regions are identified which influence limb segment variation. Thus, biological anthropologists must use caution in their assumptions and interpretations regarding limb segment lengths and limb proportions in humans and other primates.

TABLE OF CONTENTS

LIST OF TABLES

LIST OF FIGURES

CHAPTER ONE
INTRODUCTION

Despite the fact that biological anthropologists understand that the relationship between genotype and phenotype is almost never one-to-one, phenotype (i.e., observable characteristics) is frequently used – often out of sheer necessity – as a proxy for genotype (i.e., a combination of alleles). This is often done because genetic parameters are difficult to estimate, requiring knowledge of familial relationships to tease them apart. Phenotypic data, alternatively, are relatively easier to measure and study. However, myriad factors influence the ways in which genes are transcribed, translated, and transformed into phenotypes. Factors such as canalization (Waddington, 1942), developmental constraint (Maynard Smith et al., 1985), genetic assimilation (West-Eberhard, 2003), and morphological integration (Olson and Miller, 1958) confound the way in which phenotypic variation is produced from genetic variation. Thus, investigations of phenotypic variation need to incorporate analyses of genotypic, or genetic, variation to better understand the processes that produced observable patterns, including evolutionary processes.

The phenotypic patterns found in modern human limb proportions would particularly benefit from a better understanding of the underlying genetic variation that shapes these traits. Limb segment lengths (and, by extension, limb proportions) are widely studied postcranial features. Anthropological interest in limb proportions began early in the 20th century due to the observation that human body shape, including limb morphology, seems to adhere to the thermoregulatory expectations set forth by Bergmann (1847) and Allen (1877). These

expectations postulate that individuals in warmer climates will have longer, leaner bodies and limbs to dissipate heat, while individuals in colder climates will have shorter, wider bodies and limbs to maintain heat. The phenotypic patterns found in modern humans (Roberts, 1978; Ruff, 1994, 2002) and fossil hominins (Jacobs, 1985; Ruff, 1991, 1993, 1994; Trinkaus, 1991; Ruff and Walker, 1993; Holliday, 1997, 1999) are typically thought to exhibit the predicted ecogeographic distribution of limb segment lengths and proportions.

The correlation between climate and limb patterning is much stronger in the Old World as compared to the New World (Auerbach, 2010; Jantz et al., 2010), suggesting that limb proportions take a long time to adapt to new climatic pressures (Holliday, 1997). Various forms of evidence support the idea of the stability of these traits over time. For instance, trait differences between geographically dispersed human populations appear early in fetal life (Schultz, 1923), migrant children who move to climatically different areas retain their ancestral limb proportions (Greulich, 1957; Froehlich, 1970; Martorell et al., 1988), and the relationship between intramembral proportions and geographic distributions of populations remains consistent over growth (Eleazer et al., 2010; Cowgill et al., 2012).

All these observations have led to the current operating assumption among biological anthropologists that limb proportions in humans are phenotypically stable unless long periods of extreme environmental conditions force adaptive change (Ruff 1994, 2002; Holliday, 1997). And, because limb proportions (and individual limb segments) are assumed to be stable across time, they have been used to inform multiple areas of anthropological inquiry: Investigations of phylogenetic relationships and fossil species identification (e.g., Jungers, 1982; Asfaw et al., 1999), locomotor behavior and the evolution of bipedalism (e.g., Haeusler and McHenry, 2004;

Harcourt-Smith and Aiello, 2004), and migration patterns (e.g., Holliday, 1997; Temple et al., 2008) are all predicated on the idea that limb proportions are phenotypically stable and thus useful in understanding various long-term evolutionary phenomena.

The problem with this assumption is that phenotypic patterns may not accurately reflect evolutionary processes, and even if they did, there is no reason to expect phenotype to respond to natural selection solely. Current research is finding, for example, that neutral evolutionary forces such as genetic drift may also play a role in human phenotypic variation (Betti et al., 2012; Roseman and Auerbach, 2015; Savell et al., in review). Therefore, the goal of this project is to use a quantitative genetics approach to estimate the genetic variance and covariance in limb segment lengths and then begin the task of identifying genes which may influence this normal variation. This goal will be accomplished using three approaches, two of which (numbers 2 and 3) are under-utilized in anthropology but are common in biomedical approaches.

1. *The use of multiple primate taxa* – Multiple primate species, both human and non-human, are used to infer how patterns may have changed over evolutionary time.

2. *The use of pedigreed samples* – Rather than relying on patterns of phenotypic variation, the use of pedigreed samples allows the direct estimation of genetic variation because familial relationships are known.

3. *The use of linkage analysis* – Linkage analysis relies on phenotypic, genotypic, and pedigree data to look for statistical associations between phenotypic and genetic

variation. The use of this approach will potentially allow precise areas of the genome that influence normal phenotypic variation to be identified.

This study is the first to use pedigree data to estimate genetic variation of limb segment length within and across multiple primate species and the first to use linkage analysis to identify genomic regions which may influence phenotypic variation in these traits. The use of the aforementioned approaches will be beneficial in describing the genetic variation and covariation of limb segment lengths, which may then be used to better investigate the evolutionary mechanisms leading to known patterns of human limb proportion variation.

Toward this end, *this project asks whether variation in limb segment morphology follow the expectations of a "developmental perspective," an "evolutionary perspective," or aspects of both*. Hypotheses will be developed pertaining to each perspective. These hypotheses are based on an abundance of literature, to be subsequently discussed (see *Limbs* and *Methodological Background*, below). The purpose of this study is not to not to pick one perspective over the other, but to show the ways in which limb morphology does or does not adhere to the assumptions frequently made in anthropological literature.

Structure of the Dissertation

The upcoming two chapters will provide essential background information for this study: Chapter Two, *Limbs: Development, Patterns, and Anthropological Inquiry*, discusses the wealth of literature pertaining to limbs. Limb development in humans is explored through the molecular and mechanical factors that influence limb development, followed by the effects of nutrition on

limb development and variation. From there, the patterns of limb variation in humans are described, first by defining the limb proportions of interest, then by describing the patterns of limb proportions seen across primates, and finally by elaborating on the ecogeographic patterning briefly described earlier. The chapter ends with a discussion on the applications of limb proportions in anthropology, namely phylogenetic relationships, the evolution of bipedalism, and migration patterns. Chapter Three, *Methodological Background*, is a technical chapter that dives into the quantitative genetic parameters used in this study. Specifically, the three main areas reviewed are genetic variance, morphological integration, and linkage analysis. Each section provides historical and theoretical background on method appropriateness.

The framework set up by Chapters Two and Three is then used in Chapter Four, *Research Design: Hypotheses, Materials, and Methods*, to lay out how the current study will be conducted. This chapter begins with laying out the specific hypotheses related to the developmental and evolutionary perspectives. It then discusses the samples, methods used for data preparation and screening, and the specific analyses conducted to explore genetic variance, morphological integration, and linkage analysis. Chapter Five, *Results*, presents a comprehensive report of the findings. Chapter Six, *Discussion and Conclusions*, explicitly assesses the results in light of the developmental and evolutionary perspective hypotheses. The chapter also discusses the implications of these results on anthropological research, as well as the limitations of the study and opportunities for future research.

CHAPTER TWO

LIMBS: DEVELOPMENT, PATTERNS, AND ANTHROPOLOGICAL INQUIRY

This chapter begins with a focus on the roles of molecular, mechanical, and nutritional factors in shaping limb morphology, and then moves into a review of the patterns of limb proportion variation in hominins. From there, several areas of anthropological inquiry that rely heavily upon limb proportions, namely phylogenetic relationships, locomotor behavior, and migration patterns, are reviewed.

The way in which anthropologists understand the development and evolution of limbs is currently shifting. Until very recently, limb development was believed to be the result of gradients of morphogens (Schoenwolf et al., 2015); current research is showing that limb patterning is formed by much more complicated developmental processes, which are explored further below (Mariani et al., 2008; Towers and Tickle, 2009). Additionally, previous interpretations of the way in which limb proportion variation across humans emerged relied on pattern recognition, thus postulating explanatory evolutionary mechanisms without firm knowledge of the underlying genetic variation (e.g., Trinkaus, 1981; Ruff, 1991; Holliday, 1997). Several authors are actively working on redressing this issue (e.g., Roseman and Auerbach, 2015; Savell et al., in review; this project).

Thus, many of the results reviewed here will likely be revised in the near future as evolutionary models are increasingly incorporated to understand limb morphology.

Limb Development in Humans

Molecular and Mechanical Factors in Development

Limb morphological development is a product of the interplay between genetically directed processes and environmental factors. Limb buds form during weeks four to eight after fertilization, with the upper limb forming slightly ahead of the lower limb. Normal limb development occurs in three axes simultaneously. The proximal-distal axis distinguishes the stylopod (i.e., humerus and femur), zeugopod (i.e., radius, ulna, tibia, and fibula), and autopod (i.e., carpals, metacarpals, tarsals, and metatarsals). The anterior-posterior axis specifies the pollex and hallux as the anterior side of each limb—these axes ultimately rotate to become the definitive medio-lateral axis for the autopod—and the dorsal-ventral axis identifies the palm of the hand and sole of the foot as the ventral side of each limb (Schoenwolf et al., 2015). This complex and critical spatial arrangement is made possible by multiple genes expressed at specific times during development in precise locations in the developing embryo; rather than classic models of limb development that advocate for patterning via morphogen gradients (e.g., as described in Schoenwolf et al., 2015), researchers now understand that, like other embryological structures, limb development is patterned by a four-dimensional interrelationship of genes, hormones, and factors (Bénazet and Zeller, 2009).

The exact specification of patterning in the developing limb bud is currently modeled as an interaction between direct specification, gradients, signal decay, and interactions between developmental factors (Towers et al., 2012). As this is a very active area of research, many developmental processes are subject to change; this section reflects our current understanding of molecular and mechanical factors that control limb development. Fibroblast growth factors

(FGFs) are secreted by the lateral plate mesoderm and cause a proliferation of cells that initiate limb formation. *Tbx* genes, which are transcriptional regulators that provide spatial and temporal expression (Showell et al., 2004), and retinoic acid (Stratford et al., 1996) work in conjunction with FGFs for limb initiation. The FGFs induce a thickening of the ectoderm at the distal tip of each limb bud known as the apical ectodermal ridge (AER). The AER is essential for limb outgrowth because it maintains proliferation of cells (i.e., is permissive) (Tanaka and Gann, 1995) as well as serving a specification of structure formation (i.e., is instructive) (Mariani et al., 2008; Towers and Tickle, 2009). These roles are temporally patterned, involving an interaction among FGFs and between the FGFs and retinoic acid (as well as Meis genes) (Towers and Tickle, 2009; Towers et al., 2012). A first wave of expression of *Hoxd* genes continues growth along the proximal-distal axis and triggers and maintains, along with FGFs (Yang and Niswander, 1995), the expression of a signaling molecule, or morphogen, known as Sonic hedgehog (*Shh*) (Tarchini and Duboule, 2006). A gradient of *Shh* forms the zone of polarizing activity (ZPA) on the posterior side of the limb bud, polarizing the limb into anterior and posterior sides (Riddle et al., 1993). The posterior location of *Shh* signaling causes anterior-posterior asymmetry in the expression of the second wave of expression of *Hoxd* genes in the distal limb (Tarchini and Duboule, 2006). Therefore, both *Shh* and *Hoxd* are responsible for the anterior-posterior patterning of the limbs, in addition to antagonistic signaling by other genes (i.e., *Wnt*) and protein mediators (i.e., *Gremlin*). *Wnt7a* is one of these antagonistic genes, and it also is a primary instructional gene for setting the dorsal-ventral axis (Yang and Niswander, 1995; Bui et al., 1997). As a result, FGFs, *Shh*, and *Wnt7a* are all intimately connected during

limb patterning and growth, making both anterio-posterior and dorsal-ventral patterning integrated processes (Towers and Tickle, 2009; Towers et al., 2012).

In addition to spatial patterning, genes play other roles in limb development. Genes encoding the *Tbx5* and *Tbx4* transcription factors are responsible for directing forelimb and hindlimb specificity, respectively (Ohuchi et al., 1998; Gilbert, 2013). Through work in specifying the proximal-distal axis, *Hox* genes stipulate whether a mesenchymal cell will become part of the stylopod, zeugopod, or autopod (Gilbert, 2013), though interactions between retinoic acid and *Fgf*s likely create a mutually suppressive gradient that, in turn, instructs the expression of *Hox* genes (Mariani et al., 2008; Mackem and Lewandoksi, 2011). Chondrogenesis, or cartilage development, is initiated by *Bmp* and *Fgf* induction of *Sox9* expression, which regulates collagen production. Additionally, Indian hedgehog (*Ihh*), parathyroid hormone-related protein (*PTHLH*), and *Fgf*18 control chondrogenesis by promoting or delaying hypertrophy, or maturation, of the chondrocytes, which in turn contributes to the formation of bone boundaries (Schoenwolf et al., 2015). *Wnt*s and the *Gdf5* gene are also pivotal to joint formation (Schoenwolf et al., 2015). Once the cartilaginous model of the bone is placed, *Ihh* induces the development of the bony collar around the diaphysis, beginning a process known as primary ossification (see below) (Schoenwolf et al., 2015).

While molecular signaling plays an imperative role in the early formation of the limbs, mechanical forces play a key role in the development of normal long bone shape. Ossification of most limb bones begins in weeks seven to twelve of gestation (Schoenwolf et al., 2015). The differentiation of osteoblasts, the cells that deposit bone matrix, is a prime example of the interplay between genetic signaling and mechanical stimuli. The *Runx2* and *Osterix* (i.e., *Sp7*)

genes are required for osteoblast differentiation from mesynchemal cells (Komori, 2010; Schoenwolf et al., 2015), but this does not occur until the cells are mechanically stimulated through involuntary fetal movement (Martin et al., 2015; Nowlan et al., 2007).

Mechanical forces produced by involuntary and voluntary muscle movements in the fetus, furthermore, direct the order of ossification in limb bones (Carter and Beaupré, 2001; Nowlan et al., 2007). External mechanical forces may also affect this progression (Nowlan et al., 2010). Once osteoblasts are differentiated, they may begin the task of ossifying the cartilage precursor known as the anlage. Primary ossification takes place as appositional deposition in the anlage, and subsequent ossification continues as endochondral ossification. Ossification even at this early stage requires the direction of involuntary and voluntary fetal movement and the mechanical forces it creates. Carter and colleagues (1996) discussed how mechanical stresses direct the ossification of long bones beginning in fetal life and continuing through primary growth. Because stresses are highest at the center of the anlage, this is where the primary ossification center begins to form. After this stage, greater stresses are found on both ends of the primary ossification center, causing endochondral bone formation to take over and begin extending the bone in both directions towards the epiphyseal ends. While the bone is extending in length, it also grows in breadth through endochondral ossification, primarily in the center of the bone where stresses remain high. The primary bone collar formed at the center of the bone continues to grow in breadth, and a medullary cavity is formed because stresses at the center of the bone are extremely low, allowing resorption to take place. As the bone continues to grow in length and produce a medullary cavity, secondary ossification centers begin to appear at the ends of the long bone, as these areas are now the ones experiencing the highest stresses. Forces tend to

decrease as the primary ossification center approaches the secondary ossification centers, allowing the ends of the bones to develop trabecular bone instead of cortical bone on their inner surfaces.

Another area where mechanical forces are necessary *in utero* to produce normal skeletal shape is in the diarthroidal joints of the limbs. Fetal movement is again involved in producing joints of correct shape. The characteristic convex/concave shape that most joints attain is due to movement of the fetus *in utero*, and without such movements, joints develop incorrectly (Carter and Wong, 1988; Schoenwolf et al., 2015). It is obvious that while genetic processes produce the basic form that the skeleton will take, mechanical forces are necessary to produce a normal version of the skeleton that will be fully functional (Carter and Beaupré, 2001; Nowlan et al., 2007).

The importance of mechanics in bone development continues after birth. Several key features of human long bones, particularly in the lower limb, are produced in early childhood. A notable feature to develop during childhood is the femoral bicondylar angle, a hominin feature associated with habitual bipedal locomotion (Tardieu and Trinkaus, 1994). The bicondylar angle begins at zero degrees at birth and begins to increase by the age of one to two. A final, adult angle of about six to eight degrees is achieved between the ages of four and eight. This progression follows the development of walking and the attainment of a mature, bipedal gait. Individuals who never walk do not show signs of a bicondylar angle, indicating that the development of a normal bicondylar angle is dependent upon the mechanical forces that act upon the skeleton during locomotion (Tardieu and Trinkaus, 1994).

Another similar example of the importance of locomotion and the mechanical forces it produces may be found by looking at the subtrochanteric shape of the femur. Wescott (2006) demonstrated that the characteristic platymeria (defined as a medio-laterally broad and anterio-posteriorly narrow shape) found in Native American groups develops in early childhood. Differences between Native Americans, and American Whites and Blacks are in place by the age of five, and, again, are hypothesized to be due to the adoption of bipedal locomotion in early childhood. Native Americans are purported to develop these medio-laterally broad femora because of their relatively short legs and relatively wide pelves, producing high medio-lateral stresses during locomotion (Wescott, 2006).

In addition to effects on external morphology, mechanical loading likewise affects the ontogenetic changes that occur in cortical bone morphology, especially in the diaphysis. Bone adapts to its mechanical environment during life (Ruff, 2008a), and diaphyses are known to be the area of long bones in which mechanical strain has great impact (Larsen, 1997). Long bone robusticity is defined as the amount of bone in a cross-section when scaled by the appropriate body measure, typically body mass and length of the long bone (Ruff, 2008a). While genetic variation produces variation in robusticity across individuals, increased robusticity also comes from increased mechanical strain placed on the bone, leading to bone deposition. A clear example of this comes from a series of papers by Trinkaus, Ruff, and Churchill (1993, 1994a, 1994b), which included analyses of bilateral asymmetry in young adult tennis players who had trained beginning as adolescents. While humeral length and articular breadths showed little asymmetry between sides, these individuals clearly show a bilateral difference in diaphyseal

robusticity, undoubtedly in response to a sport that encourages preferential loading on one side of the body.

The fact that diaphyseal dimensions seem to be highly responsive to mechanical loading means that behavior and lifeways can be inferred in archaeological skeletal remains. For instance, Ruff (2006, 2008a) explained that increased robusticity in the limbs is associated with rough terrain and/or an increase in the amount of walking (i.e., increased mobility). Both factors would cause greater strain responses from the bone cells, leading to increased bone deposition (for a thorough explanation of bone functional adaptation, see Turner, 1998; Pearson and Lieberman, 2004; Robling et al., 2006). Subsistence strategies may also be inferred. There is a decrease in robusticity with the transition to agriculture, most likely due to a decrease in mobility relative to hunter-gatherers. These same conclusions regarding robusticity and lifeways have been reached by numerous authors (Bridges, 1989, 1995; Holliday, 2002; Weiss 2003; Stock and Pfeiffer, 2004; Stock, 2006; Higgins, 2014); more recent research, furthermore, may indicate an interaction between local loading effects on bone and systemic metabolic effects (Eleazer and Jankauskas, 2016).

There are known differences in the response of adult and juvenile bone to mechanical loading (Pearson and Lieberman, 2004); the molecular and ontogenetic mechanical effects summarized in the preceding paragraphs are responsible for the morphological variation in limbs observed among adults, with only minor changes (barring traumatic or pathological processes) possible after primary growth ends. In juveniles, the periosteal surface is most responsive to mechanical loading, and this surface reacts to general growth hormones. In adolescents, the endosteal surface is most receptive, and acts in response to sex hormones (Ruff et al., 1994b).

The endosteal surface begins to resorb in later adulthood, and the periosteal surface again becomes more responsive (Pearson and Lieberman, 2004). This progression means that the effect that mechanical loading will have on cross-sectional shape and properties is dependent on the timing in which envelope is activated, presumably through genetic control (Ruff et al., 1994b). Martin and colleagues (2015) demonstrated through computer modeling that normal loading through primary growth and development followed by increases or decreases in loading during adulthood (i.e., after primary growth has ceased) will influence the cross-sectional properties differently than if the loading is increased or decreased during primary growth. These modeled patterns are also seen in living individuals. Bone strength gained as periosteal deposition during growth helps keep the skeleton strong despite bone loss on the endosteal surface during aging, making childhood known as the "window of opportunity" for optimizing bone health (Robling et al., 2014). And, finally, newer research using a mouse model has shown that greater differences are seen between mice with different genetic backgrounds than between mice with different degrees of functional loading on their limbs, regardless of genetic background, indicating that bone structure is strongly influenced by genetics which mitigate mechanical stimuli (Wallace et al., 2012). This evidence demonstrates that genetic constraints mediate mechanical loading, while mechanical loading likewise affects genetic expression.

There are two anatomical regions of long bones where mechanical loading does not appear to play a significant role in shaping morphological variation. The first is in the external size and shape of articulations. While diaphyses respond to mechanical loading during growth and development, articular external dimensions do not correlate with mechanical loadings during growth (Ruff et al., 1991; Ruff et al., 1994b; Ruff, 2007). The final adult sizes of the

articulations obtained at the end of growth and development, particularly in the lower limb, are appropriately sized for adult body mass, indicating genetic canalization[1] that will restrict the amount of possible morphological variance possible during development. Because long bone articulations are not sensitive to changes in mechanical loading, they are useful for estimating body mass in the archaeological record (Ruff, 1990; Auerbach and Ruff, 2004).

Another anatomical region in which biomechanical loading does not appear to play a significant role is in long bone length. Using the humerus and femur, Ruff (2003) looked at length proportions and strength proportions (i.e., cross-sectional properties) through development in humans. His results showed that upper to lower limb strength proportions change considerably once infants become primarily bipedal (i.e., the humerus shows a decrease in strength and the femur shows an increase in strength with the adoption of bipedality around one year of age), yet bone lengths show a log-linear increase with age independent of locomotor change, indicating that shifts in mechanical stimuli do not affect length. Similar results have been found in experimental animal studies (Lanyon, 1980; Biewener and Bertram, 1993). Trinkaus and colleagues (1994a) looked at bilateral asymmetry in the humerus and showed that the length of the humerus is less phenotypically variable than the diaphyseal breadth of the humerus, which is more phenotypically variable; however, the underlying mechanism creating that variability is unknown. Auerbach and Raxter (2008) showed that humeral and clavicular lengths are asymmetrical on opposite sides, while the breadths of the two bones are asymmetrical on the same side. This again supports the idea that mechanical forces influence the breadth of the cortices in long bone diaphyses since both bones on the same side are larger than the

[1] Genetic canalization is the buffering of a developmental process against mutations, meaning that the same phenotype will be produced despite underlying genetic variation (Waddington, 1942; Hallgrímsson et al., 2002).

corresponding bones on the opposite side. One major conclusion may be drawn from these studies: variation in long bone lengths and diaphyseal dimensions are partially independent, possibly as a result of different sensitivities and responses to environmental (e.g., mechanical) stimuli. Other studies have proffered the idea that long bone lengths are more highly genetically canalized than other bone dimensions, though this has not been empirically demonstrated (Auerbach and Ruff, 2006; Cowgill and Hager, 2007).

Nutrition

Nutrition and metabolism play a role in limb bone variation among human groups, in addition to genetics and mechanics. Anthropometric studies comparing generational groups within or between populations (collectively called secular change studies) have consistently shown that increased stature is associated with better nutrition and improved environmental conditions[2] (Steegman, 1985, 1986, 1991; Steckel, 1987, 1995; Floud et al., 1990; Komlos, 1990, 1994; Malina et al., 2004). Nutritional insufficiency is known to lead to a reduction in stature due to growth retardation (Hummert and Van Gerven, 1983; Jantz and Owsley, 1984; Eveleth and Tanner, 1990), so increased stature is presumably due to an increased capacity for bone production and maintenance during the growth period. Moreover, secular change studies in limb lengths specifically show that a change in nutritional status is correlated with changes in the length of the limbs more than the length of the torso, indicating that the fluctuations observed in

[2] Improved environmental conditions means, primarily, a decrease in disease load and work intensity (see Steckel, 1995). However, the focus here is on the role of nutrition rather than the complex interplay between nutrition and environmental load. For a detailed discussion, see Eleazer (2013).

stature due to nutrition are the result of lengthening or shortening of the legs (Tanner et al., 1982; Takamura et al., 1988; Malina et al., 2004, 2008; Cowgill et al., 2012).

Changes in long bone lengths from changes in nutrition do not occur evenly across sexes or across limbs. In the United States from 1800 to 1970, males showed greater secular change than females, the lower limb had more change than the upper limb, and distal segments were subject to more change than proximal segments (Meadows Jantz and Jantz, 1999). The differences between the upper and lower limb were echoed in a Japanese sample from 1961 to 1986 (Takamura et al., 1988). In the latter study, arm length increased over time, as did standing height (used here as a proxy for leg length as sitting height did not change considerably over this time), but the increase in arm length was delayed by ten years as compared to the leg. Given what is known about development (see above), this indicates dissimilar sensitivities and/or responses in the limbs to the environmental effects that occurred between generations in Japanese populations. Arguably, the differences between limbs and limb segments reflect known dissimilarities in early development. Perhaps faster growth trajectories in the lower limb are more readily impacted by nutritional stress, or the limbs and limb segments have distinct developmental envelopes of time in which they are more sensitive to perturbations. For instance, the lower limb grows faster than the upper limb (Bareggi et al., 1996; Cowgill et al. 2012) and distal segments grow faster than proximal segments (Cameron et al., 1982; Cowgill et al., 2012). This may extend across primate taxa, as the difference between proximal and distal segments has also been noted in nonhuman primates, with distal segments showing growth restrictions in nutritionally stressed individuals (Fleagle et al., 1975).

Differences in secular changes in long bones between males and females, as found in Meadows Jantz and Jantz (1999), bring up the interesting debate on the relative sensitivity of the sexes to environmental change. Some have argued that females are "buffered" against environmental insults (i.e., males are more sensitive to environmental stressors) (Stini, 1969; Wolański and Kasprzak, 1976; Stinson, 1985) and are therefore less likely to experience significant phenotypic responses to decreased nutrition. The hypothesized reason for this is that females have a greater physiological investment in reproduction and are therefore somehow protected against environmental fluctuations during growth (Stinson, 1985). Some empirical evidence supports the female buffering hypothesis (Stini, 1969; Wolański and Kasprzak, 1976; Dettwyler, 1992), but whether it acts throughout growth and development, only in the prenatal period, or at all, has yet to be determined (Stinson, 1985).

Limb Variation in Humans

While nutritional variation does have an effect on limb lengths and proportions, body proportions in general are considered fairly stable compared to other anthropometric measures (Ruff, 1994; Weaver and Steudel-Numbers, 2005; but see Roseman and Auerbach, 2015). A long research tradition in biological anthropology has explored variation in these proportions and developed a paradigm that links them to population differences ascribed to specific environmental factors, namely climate and population history. The following section reviews this history, though recent research (Betti et al., 2012; Roseman and Auerbach, 2015; Savell et al., in review) has provided significant revisions to this paradigm, as direct evolutionary models are

finally being applied to test long-held assumptions about the evolutionary forces that have shaped human limb variation.

Patterns of Limb Proportions

When comparing relative body size and shape across populations or species, "few absolute measurements are of interest by themselves" (Schultz, 1929:245). Rather, the size of one measurement in relation to another, known as a relative measure, index, or proportion, is used to explain patterns and variation. Before discussing the patterns and variation found in limb morphology throughout the human species, a review of the relevant limb proportions used in anthropological research is warranted. Specifically, limb *length* proportions are discussed here. There is also a wealth of literature using indices and proportions in regards to postcranial robusticity (for reviews, see Ruff et al., 1993; Pearson, 2000), but that is not a focus here.

Intralimb proportions are those which compare the two segments within a single limb to understand how the proximal and distal elements relate to one another. As stated by Davenport (1933:333-4), "[f]or convenience in locomotion a division of the appendages is necessary. The two segments constitute a pair of levers placed along one axis… According to the type of locomotion, whether springing, running, climbing, walking, burrowing, or swimming, the relative length of these levers to give greatest efficiency will vary." An appreciation and understanding of the wide variation in intralimb (and interlimb, discussed below) indices within primates is necessary as this variation is important for reconstructing locomotor behavior and phylogeny in fossil species (Jungers, 1985; Richmond et al., 2002). Intralimb indices are

calculated as the distal element relative to the proximal element; therefore, an index less than 100 indicates that the distal element is shorter than proximal element, and, conversely, an index greater than 100 indicates that the distal element is longer than the proximal element.

The brachial index is defined as the quotient of the length of the radius divided by the length of the humerus multiplied by 100 (Schultz, 1929)[3]. The majority of adult primates have radii that are longer or nearly equal in length to the humerus. Notable exceptions are humans, which show the lowest brachial index of all primates, averaging about 75, and gorillas, which average about 80 (Schultz, 1930; Aiello and Dean, 1990). The longest radii are found in species that primarily use suspensory locomotion, such as gibbons, orangutans, and spider monkeys (Schultz, 1930; Buschang, 1982). Primate species do not show significant differences in brachial indices between males and females, although evidence suggests that humans are an exception: human females consistently show a slightly lower brachial index than males (Martin, 1928; Schultz, 1930; Aiello and Dean, 1990).

The crural index is defined as the quotient of the length of the tibia divided by the bicondylar length of the femur multiplied by 100 (Davenport, 1933). Monkeys have tibiae that are closer to the length of the femur than apes and humans, with the former displaying crural indices above 90 and the latter having values averaging about 85 (Schultz, 1930; Davenport, 1933). Non-human primates do not show a significant difference in the crural index between males and females (Schultz, 1930). Humans show no differences between the sexes (Martin, 1928; Schultz, 1930) or show that females have consistently smaller crural indices (Davenport,

[3] It should be noted that while the majority of scholars use the radius in this equation, periodically the ulna is used (for example, Porter, 1999). While the radius and ulna are correlated in length, they are not isometrically scaled (i.e., while the size of both may change in the same direction, the proportion between the two bones is not constant). And, because the ulna is inherently a longer bone than the radius, using ulnar length will produce higher brachial indices.

1933). Based on his data, Schultz (1930) stated that the crural index is "more stable" than the brachial index because the range of values in each species are narrower for the crural index. Additionally, Trinkaus (1981) noted that there is less sexual dimorphism in humans in the crural index than the brachial index, although the exact reason for this is unknown (Holliday, 1995).

Interlimb indices are those that compare lengths between limbs, expressed as the upper limb element(s) relative to the lower limb element(s). Therefore, an interlimb index under 100 indicates that the upper limb segment(s) is shorter than the lower limb segment(s), and an interlimb index over 100 indicates that the upper limb segment(s) is longer than the lower limb segment(s). There are two main interlimb indices, the first being the intermembral index. The intermembral index is the length of the upper limb divided by the length of the lower limb multiplied by 100. Schultz (1929) defined the intermembral index using limb lengths which include both hand length and foot height but noted that these measurements are not particularly useful on skeletal material; therefore, a more practical definition of the sum of the length of the humerus and radius divided by the sum of the length of the femur and tibia multiplied by 100 is given (Schultz, 1929, 1930). Monkeys typically have intermembral indices less than 100, while apes have intermembral indices over 100. Humans have the lowest intermembral index of all simians, with an upper limb only about 65% of the length of the lower limb (Schultz, 1930). The other main interlimb index is the humerofemoral index, which, as the name suggests, compares the length of the humerus to that of the femur. This proportion is frequently studied because humans differ from other apes in that the humerus in apes is longer than the femur but shorter than the radius, a fact which is made evident by looking at both the humerofemoral index and the brachial index (Aiello and Dean, 1990). Additionally, the humerofemoral index has become

quite important in the study of primate evolution as humeri and femora are available for several fossil species, allowing hypotheses to be made regarding positional behavior, modern human ancestry, and evolution.

Several other indices involving the limbs are useful primarily when studying living populations using anthropometric measurements. These indices include relative sitting height, defined as sitting height divided by stature, and relative limb length, defined as the length of either the upper limb or the lower limb divided by stature (Roberts, 1978). These indices are less practical when studying skeletal material because they require many bones to be present in order to accurately estimate height. Therefore, these limb indices are not a focus here.

Overall body proportions change allometrically during growth (Bogin, 1997) and limb proportions specifically are known to change throughout ontogeny. For example, the intermembral index is higher in human fetuses and infants, who have long arms relative to legs, than in adults, who have long legs relative to arms (Schultz, 1930). During growth and development, the brachial index increases in humans and gorillas and decreases in orangutans and chimpanzees, while the crural index stays the same in chimpanzees and shows a slight increase in humans and other large apes (Aiello and Dean, 1990). The different changes in these indices are due to the lower limb growing faster than the upper limb (Takamura et al., 1988; Bareggi et al., 1996; Cowgill et al., 2012) and the distal limb segments growing faster than the proximal limb segments (Davenport, 1933; Cameron et al., 1982; Cowgill et al., 2012).

However, while limb proportions change during growth, there is also some relative consistency. Differences between species in intermembral proportions develop prior to birth in non-human primates (Lumer, 1939; Schultz, 1973) and humans (Schultz, 1973; Buschang,

1982). Within humans, differences between geographically dispersed human populations begin early in fetal life (Schultz, 1923). Ruff (2003) has shown that human infant femoral/humeral length proportions are within 10% of adult proportions, which is caused by the characteristically long femur of humans that begins to develop prior to birth. And, while these proportions do change during growth, the relationship between intramembral proportions and geographic distributions of populations remains consistent over growth (Eleazer et al., 2010; Cowgill et al., 2012). This consistency in limb proportions beginning in fetal life has supported the idea that "long bone length proportions are highly heritable" (Ruff 2003:338), have "strong genetic encoding" (Holliday, 1997:425), are "largely genetically controlled" (Holliday, 1999:563), and are "genetically determined" (Weaver and Steudel-Numbers, 2005:219). None of these authors tested a genetic model to determine whether these statements are supported. Nevertheless, the argument has consistently been made that limb proportion patterns are due to an underlying genetic process and are phenotypically constrained. Making genetic conclusions from phenotypic patterns is precarious; therefore, this project seeks to assess the genetic variance and covariance of limb segments to better understand human limb length and proportion variation.

Ecogeographic Patterning

There is a long-standing tendency within anthropology of discussing limb proportions as if the genetic and evolutionary processes that produced the known patterns of variation can be deduced from phenotypic variability alone. This section reviews traditional anthropological arguments with regard to the ecogeographic patterning of human limb proportions. Arguments

made here are likely to be revised in the near future as evolutionary models are increasingly developed.

Anthropological interest in limb proportions began early in the 20th century and stems from the observation that human limb morphology seems to adhere to the often-cited "Allen's Rule" (Allen, 1877). This "rule" and the corresponding "Bergmann's Rule" (Bergmann, 1847) state that differences in body proportions between populations are due to thermoregulation, or the efficient regulation of heat dissipation from the body. Specifically, Allen's rule observes that reduced limb lengths are often found in populations living in colder environments as compared to their counterparts in warmer environments, while Bergmann's rule explains that populations in colder environments will have larger bodies with higher body mass compared to groups in warmer environments. A longer, leaner body and limbs increases the surface area to volume, allowing heat to dissipate more easily in a warm environment; conversely, a shorter, wider body and limbs decreases the surface area to volume, preventing heat dissipation from the body, which would be advantageous in a colder environment. Critics of such thermoregulatory justifications, such as Scholander (1955) and Steegmann (2007), argued that 1) other physiological mechanisms (i.e., vasoconstriction, fat layers, fur) are more effective at preventing and promoting heat loss, and 2) multiple exceptions to these rules exist. Mayr (1956) explained, however, that these rules are merely "empirical generalizations" that have statistical validity. Whether climate is the causative agent in producing phenotypic data that parallels climatic variation is unknown, but their correlation allows implications regarding adaptation to climate to be made.

Ruff (1993) named the correlation between phenotypic variation and climatic variables the "thermoregulatory imperative." Ruff developed the cylindrical model (Ruff, 1991, 1994), which models the body as a cylinder, where the surface area (computed from length [i.e., stature] and width [i.e., body breadth]) to volume (i.e., body mass) is minimized in cold climates to reduce heat loss and maximized in warm climates to facilitate heat loss. This model accurately describes variation in fossil species and modern humans (Ruff, 1991, 1994; Ruff and Walker, 1993) (i.e., the patterns), but does not explain the evolutionary mechanisms underlying these patterns (i.e., the processes).

Numerous examples of non-human organisms adhering to Allen's and Bergmann's ecogeographic rules abound, such as birds (James, 1970; Graves, 1991) and mammals (for a review, see Ashton et al., 2000). Ashton and colleagues (2000) found that out of 78 out of 110 species show a positive intraspecific[4] correlation between size and latitude and 48 out of 64 species show a negative intraspecific correlation between size and temperature, providing empirical support for the existence of clines in body size, thereby adhering to Bergmann's rule. They did not, however, find evidence to support the idea that these clines exist to optimize surface area to volume ratios to enhance heat loss. Alternatively, in a test of Allen's rule, Nudds and Oswald (2007) found that not only do closely related endothermic (i.e., warm blooded) species follow expected patterns but limb length is correlated with temperature during the coldest part of the breeding season, suggesting that heat conservation is the mechanism producing these clines.

[4] Mayr (1956) warns that these rules should only be used to look at differences intraspecifically, but many studies look across species (e.g., Trinkaus, 1981; Holliday, 1999; Nudds and Oswald, 2007). How this impacts interpretations is unknown.

Ruff's "thermoregulatory imperative" has also been used to explain observed differences between fossil species. Trinkaus (1981) was an early advocate of climate as explanatory of differences among hominin groups. He looked at the limb proportions of Neandertals and early modern humans and found that while the intermembral and humerofemoral indices were similar between these two groups, the brachial and crural indices of the two species were different. Specifically, Neandertals exhibit low brachial and crural indices, indicating that their distal elements were relatively shorter (or distally abbreviated) compared to early modern humans. He attributed the difference to cold adaptations among Neandertals relative to early modern humans, and used this as support for the idea that early modern humans were more recent transplants into Europe, coming from Africa and bringing their warm-adapted limb proportions with them (i.e., evidence of gene flow). This idea has been supported by several other authors (Jacobs, 1985; Ruff, 1991, 2010; Holliday, 1997; Weaver, 2003). An alternative explanation for the difference in limb proportions between Neandertals and early modern humans is that Upper Paleolithic human populations were moving in and out of the area in response to climatic fluctuations, making them less likely to develop truly cold-adapted limb proportions, while Neandertals experienced a stable cold environment producing distally-abbreviated limbs (Jacobs, 1985). Either way, thermoregulation is touted as the reason for adaptive differences between these groups. The opposite body type, that of long limbs and a narrow body which would be advantageous in warmer environs, is found in *Homo erectus* (or *ergaster*) fossils from Africa (Ruff, 1991, 1993, 1994; Ruff and Walker, 1993; Potts, 1998). This warm-adapted body type is seen as further evidence of the Allen's rule being applicable in fossil species. Again, it is important to note that these studies all use phenotypic patterns to support an adaptationist view

of limb proportions without testing the genetic processes that would give rise to the phenotypic variation. This is not to say that these studies are wrong. Instead, they should be viewed as limited in their ability to estimate the genetic variation in the samples, and the adaptationist mechanism should be understood as a hypothesis rather than a conclusion with genetic support.

Holliday's research has similarly noted climatic adaptation as a source of variation, but it has also highlighted the importance of differential ancestry between groups. Holliday (1997) demonstrated that the limb proportions of early modern humans in Europe look more like that of modern Sub-Saharan Africans than later Mesolithic human groups, which look more like modern Europeans. Early modern humans also look different from the archaic humans that previously occupied the area, indicating that the early modern humans came from Africa and retained their long limbs through gene flow with their ancestral populations. Early modern humans then slowly adapted to the cold environment in their new home and developed shorter limbs by the Mesolithic, a condition that persists today in modern Europeans. This gene flow hypothesis coupled with thermoregulatory adaptation thus supports the idea that "long-term climatic selection is largely responsible for global variation in relative limb length" (Holliday and Falsetti, 1995). These studies are again based solely on phenotypic patterns without the addition of tested genetic models.

Besides climate and gene flow, another explanation that has been cited for differences between limb proportions in these fossil groups is mobility, or biomechanical advantage. Both Trinkaus (1981) and Porter (1999) claim that shorter distal elements in the lower limb would provide a biomechanical advantage for walking over rough terrain by lowering the moments of force about the knee; however, neither author provides any empirical support for this hypothesis.

In this argument, the shorter lower limbs of Neandertals would be advantageous if sheer mechanical power or walking over hilly terrain were necessary (Steudel-Numbers and Tilkens, 2004; Weaver and Steudel-Numbers, 2005; Higgins and Ruff, 2011). Longer lower limbs, on the other hand, have been touted as more efficient in normal bipedal walking and running (Steudel-Numbers and Tilkens, 2004; Steudel-Numbers, 2006; Stuedel-Numbers et al., 2007). Holliday and Falsetti (1995) attempted to test the idea that lower limb length is related to mobility, and found that the hypothesis that longer limbs provide greater mobility is not supported. Interestingly, though, they found that the hypothesis that lower limb length is associated with climate cannot be rejected.

Weaver and Steudel-Numbers (2005) suggested that variations in limb proportions are actually due to an interplay among all three factors. Population movement from Africa brought long-limbed Upper Paleolithic humans into the cold European environment of the Neandertals. Once there, selection would have acted against their long limbs for thermoregulatory efficiency, but this would have been mitigated by the "weaker but still consequential selection for energetic efficiency" in locomotion (Weaver and Steudel-Numbers, 2005:222). While a combination of factors likely did influence the observed pattern of limb proportion variation, the genetic mechanisms that produced phenotypic variation cannot be known from pattern recognition alone.

In modern humans, Old World populations exhibit the predicted ecogeographic distribution of limb lengths relative to torso length and of distal element relative to proximal element lengths (Roberts, 1978; Jacobs, 1985; Ruff, 1994; Holliday, 1997, 1999). Specifically, populations from lower latitudes (i.e., warmer environments) have relatively longer limbs, longer distal limb elements, narrower bodies, and lower body masses (Ruff, 1994, 2002a; Holliday,

1997). Clinal patterns are evident in humans who have colonized regions for millennia (as the Old World evidence shows), but these patterns can be confounded by effects of migration and colonization, as has been shown in the New World (Auerbach, 2010; Jantz et al., 2010).

Variation in the New World exhibits a mosaic, with limb proportions and pelvic widths showing different patterns. While pelvic breadths tend to be wide, suggestive of cold adaptation, limb proportions are more indicative of temperate environments (Jantz et al., 2010; Auerbach, 2012). This evidence supports the idea that limbs and pelves are potentially subject to different evolutionary forces (Betti et al., 2012; Auerbach, 2012). Additionally, the upper and lower limbs show different patterns: the relative length of the lower limb is relatively correlated with climate, but the relative length of the upper limb is not (Jantz et al., 2010), and intralimb indices show different patterns (for example, a high brachial index coupled with a low crural index) (Auerbach, 2012). Although dealing with Old World fossil specimens, Trinkaus (1981) shows that the brachial index has a higher correlation with latitude (used as a proxy for climate) than the crual index, which has been interpreted to mean that the upper limb, free from locomotor constraints, is "more likely to track climatic differences than the lower limb" (Holliday, 1995:165). This assumes that the upper limb is genetically independent of the lower limb, and it ascribes an evolutionary force (i.e., adaptation) and an evolutionary factor (i.e., climate) to the phenotypic patterns.

It has been argued that limb proportions take a long time to change. The fact that the New World phenotypic data does not correlate with climatic variables as well as Old World populations is interpreted to mean that limb proportions take a long time to adapt to climatic pressures (Holliday, 1997) (although not as long as the pelvis [Auerbach, 2012]). This is

evidenced not only by New World archaic skeletal and indigenous anthropometric data (as used by Auerbach [2012] and Jantz et al. [2010], respectively), but in modern juveniles. Martorell and colleagues (1988) showed that in migrant children who moved to climatically different areas, limb proportions remain consistent with those of their ancestral homeland populations, rather than adapting to those found in the new environment. This occurs despite an increase in stature. Other studies show similar findings (Greulich, 1957; Froehlich, 1970).

This suite of phenotypic clinal evidence has led to the current operating assumption among biological anthropologists that limb proportions in humans are phenotypically stable unless long periods of extreme environmental conditions force adaptive change (e.g., Ruff, 1994, 2002a; Holliday, 1997). In this view, Allen's rule applies to humans, as it accounts for the fundamental ecogeographic pattern of limb length proportions among hominins. Given the evidence that limb proportions are generally stable traits, humans have since tended to retain their ancestral proportions. Though extreme environmental conditions could still catalyze adaptive changes in limb proportions, it would likely take long periods of time to do so. This operating assumption is based purely on an adaptationist perspective without taking things such as genetic drift, gene flow, and conditional selection into account.

However, contrary to the assumption among biological anthropologists that limb proportions are stable traits is a suite of experimental data in nonhuman mammals. Experiments in rats (Lee et al., 1969; Risenfeld, 1973), pigs (Weaver and Ingram, 1969), rabbits (Ogle and Mills, 1933), and mice (Serrat et al., 2008) have shown that littermates raised in different environments produced differences in long bone lengths and, hence, proportions. For example, Serrat and colleagues (2008) raised mice in cold, moderate, and warm temperatures and found

that those raised in warm temperatures had significantly longer limbs than those in colder temperatures. Diet and activity level were higher in the cold-raised siblings, and as such cannot explain the differences. The research concluded that environmental temperature may regulate extremity growth by changing the temperature in and altering the growth rates of cartilage, the precursor to bone. While interesting, none of these studies on nonhuman species have tested to see if the observed changes are maintained over multiple generations (i.e., if evolution occurs).

Despite the limitations of previous studies, there has been a recent attempt at directly assessing the evolutionary forces influencing limb variation. While the previous studies were limited, the patterns they noted were important for setting up a foundation for this current research. Roseman and Auerbach (2015) found that distal limb segment lengths are shaped by both neutral evolutionary forces (genetic drift and potentially gene flow) and natural selection while the crural index is shaped primarily by population structure. In attempting to discern selection gradients in human limbs, Savell and colleagues (Savell et al., in review) have found that there are distinctions between the strength of selection and the actual responses to selection in the limbs. Moreover, selection on the tibia seems to be driving variation in all limb segments, likely because of the way in which the different limb segments covary (i.e., is a result of conditional evolution). Although focused on the autopods versus the other limb segments, a similar finding is echoed by Rolian (2009) who finds that the ability of a morphological trait to evolve is highly dependent on how strongly the traits covary. Therefore, an understanding of how these traits covary is important to accurately reconstruct evolutionary mechanisms for how limb proportion patterns emerged (Young and Hallgrímsson, 2005; Hallgrímsson et al., 2009; Young et al., 2010). This project contributes to this growing area of research by incorporating

genetic data to describe the genetic variance and covariance underlying limb segments in multiple primate groups. All these studies seek to better describe the evolutionary mechanisms that have shaped human limb proportion variation.

Applications of Limb Proportions in Anthropology

Why do anthropologists care about limb proportions? Up to this point, this chapter has focused on the observable phenotypic patterns and the assumptions that are made about how those patterns emerged. If the current operating assumption that limb proportions are highly phenotypically stable traits is true, then limb proportions may be informative in other areas of research, including phylogenetic relationships and fossil identification, locomotor behavior and the evolution of bipedalism, and migration patterns. In fact, while not overtly stated, research in these areas is predicated on the assumption that limb proportions are phenotypically stable and thus useful in understanding various evolutionary phenomena. However, this could be seen as contradictory given that evolution is inherently about change. It is convenient to suppose that limbs are phenotypically stable when observed patterns do not change yet indicative of evolution when patterns do change; phenotypic stability, though, is itself a product of evolution (e.g., via stabilizing selection). Without an understanding of how limb segments are capable of evolving, however, it is precarious to link their variation to specific causal factors. In light of this caveat, the following sections describe the current state of research that uses limb proportions to understand phylogenetic relationships and fossil identification, locomotor behavior and the evolution of bipedalism, and migration patterns.

Phylogenetic Relationships and Fossil Identification

Limb proportions of fossil species are often hard to determine as many long bones are broken or missing; however, partial and nearly complete bones are used to estimate long bone length (e.g., Johanson et al., 1987; Asfaw et al., 1999; Haeusler and McHenry, 2004). While there are inevitably problems with various estimation techniques, the details are beyond the scope of this paper (for a detailed discussion, see Reno et al., 2005). Limb segment lengths from fossil specimens are often compared to known limb proportions of extant species to make inferences about phylogeny and locomotion, and new fossil specimens are compared to previously studied fossils for species identification. Examples of these are below.

The limb proportions of *Australopithecus afarensis* (ca. 3.2 Ma) were first explored by Jungers (1982) by looking at allometric relationships between AL 288-1 ("Lucy"), modern humans, and catarrhine primates (Old World monkeys, lesser apes, and great apes). Modern humans and AL 288-1 show a similarity in relative humerus length (i.e., near isometry), but a large disparity in femur length (i.e., humans have extreme positive allometry). By comparing the relative length of the femur of AL 288-1 to the crural index of humans and apes, Jungers concluded that the short femur of *A. afarensis* is indicative of an overall short lower limb very unlike modern humans. However, given that humeral length is within the range of modern humans, the humerofemoral index of AL 288-1 (ca. 85) is intermediate compared to other species. Based on the AL 288-1 radii, as well as other specimens (Kimbel and Delezene, 2009) *A. afarensis* is thought to have a brachial index of ca. 91 (Asfaw et al., 1999; Reno et al., 2005; Kimbel and Delezene, 2009), making it similar to extant apes rather than modern humans. These proportions suggest that the climbing capabilities of AL 288-1 were reduced, that bipedality was

kinematically very different and less efficient than in modern humans, and that humeral reduction occurred prior to femoral elongation in hominin evolution (Jungers, 1982; Kimbel and Delezene, 2009).

Two other species, *Australopithecus africanus* and *Homo habilis*, have traditionally been interpreted to have more ape-like limb proportions than *A. afarensis*. Rather than being based on limb bone lengths, *A. africanus* (ca. 2.8 Ma) proportions are based on joint measures because of a lack of skeletal material. Assuming that the relationship between joint size and limb lengths does not differ between these taxa (Richmond et al., 2002), the pattern of limb joint sizes found in *A. africanus* (larger upper limb joint sizes compared to lower limb joint sizes) indicates that this species had more ape-like limb length proportions (McHenry and Berger, 1998; Berger, 2006). Similarly, few complete *H. habilis* limb bones are available for estimating limb proportions. Reconstructions of the *H. habilis* specimen OH-62 (ca. 1.8 Ma) indicate a humerofemoral index of about 95 (Johanson et al., 1987). Given that this is one of only a few *H. habilis* specimen where a humerofemoral index can be estimated, this specimen is often used as representative of the entire species. This estimation, however, is based on the assumption that the OH-62 femur was no longer than the AL 288-1 femur, which is uncertain, and on the assumption that reconstructions of the humerus are accurate, which is also questionable (Korey, 1990).

While some authors support the idea of more ape-like conditions of these taxa relative to *A. afarensis* (Hartwig-Scherer and Martin, 1991; McHenry and Berger, 1998; Green et al., 2007), other authors argue that there is no evidence of this if the specimens are reexamined while keeping the error rates of limb length reconstructions in mind (Asfaw et al., 1999; Reno et al., 2005; Haeusler and McHenry, 2007). For the camp accepting an ape-like condition for these

species, there are vast implications for phylogeny. If *A. afarensis* is thought to be the direct ancestor of *A. africanus* and *H. habilis*, then there had to have been an evolutionary reversal of limb proportions (McHenry and Berger, 1998). Alternatively, this could be considered evidence that *A. afarensis* is not ancestral to the other two taxa. For those who reject traditional indices produced using potentially faulty methods, the progression from *A. afarensis* to *A. africanus* to *A. habilis* is seen as a slow progression moving in the direction of modern human limb proportions (Reno et al., 2005).

A few other specimens which are complete enough to estimate limb proportions support the idea of this progression toward modern proportions. The BOU-VP 12/1 specimen (or, the Bouri skeleton) also has fairly complete limb bones, and it possibly represents the species *A. garhi* (ca. 2.5 Ma). It has a human-like humerofemoral index and an ape-like brachial index (i.e., an elongated forearm). If this specimen is actually representative of *A. garhi*, it would mark the earliest appearance of femoral elongation in the fossil record (Asfaw et al., 1999). These authors also say that these proportions are evidence of femoral elongation prior to forearm shortening in early hominids (Asfaw et al., 1999). Following this and the suggestion given by Jungers (1982) above, perhaps modern human limb proportions arose first through a reduction in the humerus, followed by an elongation of the femur, and then a shortening of the forearm. These modern human limb proportions are seen in *Homo erectus* (ca. 1.5 Ma), as evidenced by KNM-WT 15000 (the "Turkana Boy") (Walker and Leakey, 1993). This skeleton has the

relatively long femur and short radius, producing brachial and humerofemoral proportions that are indicative of modern humans[5].

As compared to humans, and as discussed above, Neandertals show low brachial and crural indices due to their short distal segments, but a humerofemoral index very similar to humans (Trinkaus, 1981). Given that Neandertals and early modern humans overlapped temporally and geographically and that their limb proportions differed, limb proportions are used to identify species affiliation when a new specimen is found (e.g., Arsuaga et al., 2007; Shang et al., 2007). Furthermore, limb proportions, along with other skeletal morphology, have been used to assess the relative Neandertal to modern human admixture proportions. For example, Duarte and colleagues cite the low crural index found in LV1 (the "Lagar Velho child") as evidence of admixture between early modern humans and Neandertals (Duarte et al., 1999). While this position has been critiqued (e.g., Tattersall and Schwartz, 1999), this example highlights how limb proportions have been used in paleoanthropological species identification. Similarly, the Dmanisi fossils have been identified as representing *H. habilis*, *H. rudolfensis*, *H. erectus*, a new species called *H. georgicus*, or a subspecies of *H. erectus* (Pontzer et al., 2010; Lordkipanidze et al., 2013; Schwartz et al., 2014). Analyses of the limbs show that the Dmanisi specimens have a humerofemoral index similar to modern humans and a crural index that is between Neandertals and early modern humans (Pontzer et al., 2010). Additionally, these fossils show a relatively long lower limb that is longer than both *A. afarensis* and *H. habilis* but shorter than Neandertals

[5]While previous work by Latimer and Ohman (2001) suggested that KNM-WT 15000 exhibited pathologies that would preclude it from being a useful reference for normal *H. erectus* skeletal morphology, recent work by Schiess and Haeusler (2013) determined that the specimen does not show signs of any congenital pathologies and belongs to a normal *H. erectus* youth.

and modern humans (Pontzer et al., 2010). This evidence firmly roots the Dmanisi fossils as early *Homo* specimens, but their exact taxonomic classification is still debated.

While grouping fossils with similar limb proportions into the same species categories is problematic, placing them into an evolutionary order is even more so. For example, without knowing the genetic covariance of the various limb segments and how they are capable of evolving, it is a stretch to say that humeral reduction occurred prior to femoral elongation in hominin evolution (Jungers, 1982; Kimbel and Delezene, 2009) or that femoral elongation occurred prior to forearm shortening in early hominids (Asfaw et al., 1999). These statements make assumptions about the genetic covariance structure of limb segments and about the independence of the limb segments from one another.

Locomotor Behavior and the Evolution of Bipedalism

Differences in limb proportions across primates are known to be related to locomotor differences. For instance, primates that leap (e.g., lemurs and lorises) have longer hindlimbs and thus lower intermembral indices than suspensory species (e.g., gibbons and siamangs) that have longer forelimbs and thus higher intermembral indices. Quadrupedal species (e.g., baboons and gorillas) generally have intermediate indices due to forelimbs and hindlimbs of similar lengths (Jungers, 1985; Fleagle, 1999). These known indices coupled with locomotor styles are used in interpreting the fossil record to determine how extinct species may have moved as well as how the distinct locomotive behavior of modern humans, namely bipedalism, developed.

While the reason or reasons that hominins first became bipedal is unknown (for varying hypotheses, see Prost, 1980; Rodman and McHenry, 1980; Wheeler, 1991; Jablonski and

Chaplain, 1993; Hunt, 1994; Leonard and Robertson, 1995; Sylvester, 2006), bipedality has been shown to be more energetically efficient than quadrupedal locomotion (Rodman and McHenry, 1980; Leonard and Robertson, 1995; Pontzer et al., 2009; but also see Jablonski and Chaplain, 1993). In addition, the long legs indicative of the genus *Homo* have been shown to also be more efficient than a shorter lower limb, both in walking (Steudel-Numbers and Tilkens, 2004; Steudel-Numbers, 2006; but see also Kramer and Eck, 2000) and running (Steudel-Numbers et al., 2007).

The characteristic bipedal gait of modern humans is first definitively seen in *Homo erectus*. This hominin has the elongated lower limb with similar intra- and intermembral indices to modern humans (Walker and Leakey, 1993). Additionally, the similarity in locomotive repertoire between *H. erectus* and modern humans has been shown through bone strength proportions (i.e., comparisons of cortical thickness between the humerus and femur). These strength proportions suggest that *H. erectus* walked the same way as modern humans (Ruff, 2008b). However, a similar analysis shows that *H. habilis* had different loading and locomotive patterns than humans (Ruff, 2009), despite showing an elongated lower limb (Haeusler and McHenry, 2004). The elongated lower limb of *H. habilis* is shown through both the femur (Haeusler and McHenry, 2004) and tibia (Susman and Stern, 1982). While lower limb morphology suggests that *H. habilis* was bipedal, upper limb morphology suggests that this species retained suspensory behaviors (Susman and Stern, 1982), which would explain the different strength proportion pattern (Ruff, 2009) and the ape-like intermembral index (Harcourt-Smith and Aiello, 2004).

The shorter hindlimb found in *A. afarensis*, combined with other morphological features of the pelvis, leg, and foot, has led to debate over the type of gait used by this species. Various suggestions include a bent hip, bent knee gait (Susman and Stern, 1982), a waddling gait (Berge, 1994), and bipedality specialized for a slower transition to running and a smaller daily range (Kramer and Eck, 2000). Others argue that there are no differences in the bipedality between *A. afarensis* and *Homo*, and that the longer legs of the latter are due to thermoregulation, allometry, efficiency, or reorganization of the pelvis (Wolfpoff, 1983; McHenry, 1986; Lovejoy, 2005).

While the way in which bipedality evolved is still unclear, what is clear is that there was a diversity of limb proportions in early hominin species. This diversity may well reflect diversity in locomotor adaptations (Harcourt-Smith and Aiello, 2004). The patterns that are shown in the literature are interesting relationships, but without an understanding of the underlying genetic variation of these limb segments, the processes that produced these patterns are not known. And, linking changes in limb proportions to efficiency in locomotion is again assigning an adaptationist perspective to these traits.

Migration patterns

Because they are considered stable traits that require an extremely long time to adapt to a climatically different environment, limb proportions are often used to infer modern human migration patterns (Holliday, 1997; Kurki et al., 2008; Temple et al., 2008; Auerbach, 2010). The migration of people is often used as an adequate explanation when individuals are found to have limb proportions that do not match with expected ecogeographic clines. For instance, Temple and colleagues (2008) looked at variation in limb proportions between the Jomon

(13,000-2,500 ybp) and Yayoi (2,500-1,700 ybp) of Japan. While both living in the temperate environment of the Japanese Islands, the two groups show differences in their limb proportions. Jomon people had elongated distal relative to proximal limb segment lengths as compared to the Yayoi people. In other words, the Jomon people had limb proportions that are expected for the environment in which they live, while the Yayoi people had proportions that resemble groups from colder environments. These authors suggest that the Yayoi people had limb proportions adapted for colder climates because they recently migrated to the Japanese Islands from Northeast Asia where their limb proportions would be much more typical. Additionally, evidence suggests that the Jomon people also migrated from a colder environment, but since they occupied Japan for a substantially longer period of time, their limb proportions adapted to the mild island climate.

Similar logic is applied when looking at limb proportion variation the New World. As previously mentioned, New World populations do not adhere to ecogeographic clines as well as Old World populations (Roberts, 1978; Auerbach, 2010; Jantz et al., 2010). Part of the justification for this is that New World populations have not been in their new environment long enough to have adapted to fit ecogeographic expectations. Analysis of Boas's anthropometric data shows that "climate is not the principal variable causing spatial patterning of body proportions" and that other factors, such as settlement history, may be producing the observed patterns (Jantz, 2006:788). That settlement history is the migration of peoples into and within the Americas.

Finally, as discussed above, migration has been used to explain the difference between archaic and early modern humans in Europe (Holliday, 1997). While early modern humans in the

Mesolithic look more like modern humans in Europe, early modern humans in the early Upper Paleolithic look more like individuals from sub-Saharan Africa. This has been interpreted as evidence that populations moved from Africa into Europe, and after occupying the new environment for a sufficient length of time, their limb proportions adapted to fit ecogeographic expectations.

The weakness with these interpretations is that they again make assumptions about the way in which limb segments can evolve without knowing the underlying genetic variance and covariance of these traits. They additionally assume that limb segments (and hence, proportions) change primarily due to adaptation to climate rather than to other factors such as genetic drift, gene flow, or population replacement. Many of these studies have archaeological context to support their interpretations, but the lack of genetic data weakens their conclusions.

Summary

There are many factors that influence limb segment lengths and limb proportions. Limb development is impacted by molecular signals, mechanical factors, and nutrition, and these features work in concert during growth and development to produce adult limb morphology. While there is undoubtedly an empirical pattern in humans that seems to show that variation in limb proportions is clinally distributed to match climatic variables (at least in the Old World), the evolutionary mechanisms by which these patterns developed is not well understood. The established body of literature has assumed an adaptationist explanation for limb variation; traditionally, climate has been the primary selective pressure purported to have made limb proportions adapt to fit ecogeographic expectations in fossil species and modern humans (e.g.,

Roberts, 1978; Trinkaus, 1981; Ruff, 1991). Recent research has shown, however, that human body variation is "evolutionarily dynamic and population historically contingent" (Roseman and Auerbach, 2015:87). In other words, neutral forces of evolution (i.e., random genetic drift and gene flow) likely play as big of a role as natural selection in producing the variation seen in modern human limb proportions. Other researchers have also begun to use genetic and evolutionary models to discern the processes that may have contributed to the known patterns of human limb morphology (e.g., Betti et al., 2012; Savell et al., in review).

Differences among groups are due in large part to genetic variance among groups (Brommer, 2011). Therefore, a better understanding of the genetic variation in limb proportions and the integration between limb segments is needed to better explain the process leading to the known patterns in limb proportion variation. The next chapter will look at limb variation in a genetic framework.

CHAPTER THREE
METHODOLOGICAL BACKGROUND

Phenotypic variation in limb morphology, both across human groups and among primate species, is due, at least in part, to genetic variation among these groups. Likewise, the differences seen among individuals of a population are partly due to genetic variation. These individual differences are the "materials for natural selection to act on and accumulate" (Darwin, [1859] 2003:60), and are thus important to understand the evolution of traits.

Unlike qualitative traits such as albinism or ABO blood groups, limb segment lengths are quantitative traits that show continuous variation. Such "continuous traits" are influenced by multiple genes at many loci, thereby complicating simple Mendelian assessment of ratios of inheritance. For this reason, the unit of study must go beyond individual offspring, as would be informative in a simple Mendelian cross with a qualitative trait, and consider the population as a whole. Because quantitative traits must be measured rather than counted or classified, calculating inheritance requires more complex mathematical methods. Therefore, a quantitative genetics framework that is built upon population genetics principles is necessary to analyze continuous, complex traits such as limb morphologies.

Quantitative genetics finds its basis in the work of Fisher (1918), Haldane (1932), and Wright (1921). Quantitative genetic theory deduces the effects of Mendelian inheritance when applied simultaneously to entire populations and the segregation of genes at many loci (Falconer and Mackay, 1996). These deductions are based on the premises that 1) quantitative differences are inherited through genes, and 2) these genes follow Mendelian laws of transmission. Quantitative genetic theory also takes the properties of dominance, epistasis, pleiotropy, linkage,

and mutation into account, making it a comprehensive field of study. Therefore, quantitative genetics provides a robust theoretical framework for understanding evolutionary change.

This chapter reviews the various methods that will be used to assess limb morphology variation in humans and other primates. Specifically, the areas to be reviewed are 1) estimates of variance (i.e., heritability and evolvability), 2) estimates of covariation (i.e., morphological integration), and 3) linkage analysis.

Estimates of Variance

Phenotypic variation can be partitioned into genetic and environmental components:

$$V_P = V_G + V_E \tag{3.1}$$

where V_P is the phenotypic variance, V_G is the genetic variance, and V_E is the environmental variance (Falconer and Mackay, 1996). This equation is a simplified version of reality because it assumes that there is neither genotype by environment covariance, nor an interaction between genotype and environment (Visscher et al., 2008). Genotype by environment covariance occurs when environmental conditions depend on genotype. An example is parents with high IQs providing an IQ-stimulating environment for their children. Here, environment is manifested as an IQ-stimulating setting and is dependent on the genotype of the parents, or IQ. When a covariation is present between genotype and environment, the term $2COV_{GE}$ (which is twice the covariance of genotypic values and environmental deviations) is added to Equation 3.1 (Falconer and Mackay, 1996). A genotype by environment interaction is when different genotypes respond to environmental variation in different ways. An example of this is the interaction between stressful life events (i.e., environment), the polymorphism of the serotonin transporter gene (i.e.,

genotype), and the effect of both on depression (Caspi et al., 2003; Visscher et al., 2008). When an interaction is present, the term V_{GE} is added to Equation 3.1 (Falconer and Mackay, 1996). While the inclusion of covariance and interaction between genotype and environment in phenotypic partitioning would lead to a more accurate representation of reality in some cases, these terms are usually not included because they are difficult to estimate.

Genetic variance itself can be divided into additive genetic variance (sometimes called "breeding values" [Visscher et al., 2008]), dominance genetic variance (due to interactions between alleles at the same locus), and interactive or epistatic genetic effects (due to interactions between alleles at different loci). Therefore:

$$V_G = V_A + V_D + V_I \tag{3.2}$$

and

$$V_P = V_A + V_D + V_I + V_E \tag{3.3}$$

where V_A is the additive genetic variance, V_D is the dominance genetic variance, and V_I is the interactive genetic variance. Of these three, only additive genetic variance is responsible for the resemblance between related individuals, and as such, is estimated by looking at the phenotypic covariation between related individuals. However, it should also be acknowledged that the interactive genetic variance (V_I) can impact the covariance between related individuals when epistasis is present in a trait; however, V_I is typically small (Falconer and Mackay, 1996).

Environmental variance (V_E), by definition, is any source of variation that is not due to genetics. Sources of environmental variance can include things such as variation in nutrition, climate, maternal effects, measurement error, and other "intangible" variation (Falconer and Mackay, 1996:135).

Heritability

While it is thought that Lush (1940) was the first to formally use the term "heritability" to describe the amount of variation in phenotypic traits that is due to heredity (Visscher et al., 2008), the concept of heritability goes back to two of the founders of the modern evolutionary synthesis, Ronald Fisher (1918) and Sewall Wright (1920). In his classical paper that founded quantitative genetic theory, Fisher (1918) described the resemblance between relatives with correlation and regression coefficients. He gives an example showing the percentage of total variance in adult human stature that is due to genotypes, which is then divided into "essential genotypes" and "dominance deviations" (pp. 424). The percentage attributed to genotypes corresponds to broad-sense heritability, and the percentage attributed to "essential genotypes" corresponds to narrow-sense heritability. Both broad-sense and narrow-sense heritability are discussed further below. Wright (1920) first used h^2 to represent the amount of variation in a phenotype that is due to genotype. His method, known as path analysis, estimates the relative importance of heredity, environment, and residual variation by using path coefficients. Each path coefficient measures the "importance of a given path of influence from cause to effect" (pp. 329). In this method, the path coefficient h (which stands for heredity) is the correlation between genotype and phenotype, and h^2 is the proportion of the overall phenotypic variation that is due to the path from genotype to phenotype (Visscher et al., 2008).

Partitioning phenotypic variance into components (Equations 3.1 and 3.3) allows the estimation of heritability. Heritability is a ratio of the amount of genetic variance relative to phenotypic variance for a given trait. Thus, heritability estimate values range between zero and one, and reflect the role of inherited variance in determining phenotypic variance (Falconer and

Mackay, 1996). Quantitative geneticists have two definitions of heritability. "Broad sense heritability" is defined as:

$$H^2 = V_G / V_P \quad (3.4)$$

and is a measure of how much of the total phenotypic variation in a population (V_P) is explained by genetic variation (V_G) (Falconer and Mackay, 1996). As shown in Equation 3.2, V_G includes several sources of genetic variation, making broad sense heritability different than the extent that phenotypes are determined by the genes passed on from parents (because parents pass on genes, not genotypes). This portion of variance is defined as "narrow-sense heritability:"

$$h^2 = V_A / V_P \quad (3.5)$$

(Falconer and Mackay, 1996) and will henceforth be called just "heritability" or h^2.

Heritability is a population-level estimate that requires pedigree information. Its values range from 0.0 to 1.0, with higher values indicating that much of the phenotypic variation in a trait is due to genetic variance (and the reverse for lower values). Though a high value means that a trait is relatively more influenced by the effects of genes rather than the environment in theory, the uniform environment typically encountered by pedigreed populations can artificially inflate the importance of genetic variance (Visscher et al., 2008). A further caveat is that heritability is population-specific and its estimation depends on the current genetic variation in a population under particular environmental conditions. Therefore, a change in either of these parameters—genetic variability or environmental factors—can lead to a different heritability estimate, meaning that estimates for one population should only be extrapolated to other populations with caution (Cheverud and Dittus, 1992; Falconer and Mackay, 1996; West-Eberhard, 2003).

However, given the fact that heritability is a dimensionless parameter that simply describes the importance of genetic factors in variation between individuals, it is nevertheless useful for comparing estimates made on the same trait across populations and different traits within a population. For example, body size exhibits similar heritability estimates not only across different populations, but also across multiple species, such that body size may be a trait that is universally robust to environmental insult (Visscher et al., 2008). Another more general example is the consistent pattern of low heritability estimates for fitness-related traits (e.g., fertility, number of offspring, life-history traits) compared to morphological traits (Cheverud and Buikstra, 1981; Mousseau and Roff, 1987; Falconer and Mackay, 1996; Visscher et al., 2008), a concept that is discussed further below.

Even though heritability is a widely used parameter, there are many misconceptions that plague its use. Visscher et al. (2008) lay out five common misconceptions that deserve further discussion here. First, heritability is not the proportion of a phenotype that is passed on to the next generation. This is untrue because it is genes that are passed on, not phenotypes, and the set of genes passed from parent to each offspring is unique. Second, high heritability does not imply genetic determinism; a high heritability simply means that much of the phenotypic variation in a population is attributable to genetic variation. While a high heritability estimate may mean that phenotype is a good predictor of genotype, it does not mean that genotype is a good predictor of phenotype because the environment can change and alter the phenotype. For example, secular change studies have shown that human stature has increased in many populations (Steegman, 1985, 1986, 1991; Steckel, 1987, 1995; Floud et al., 1990; Komlos, 1990, 1994; Malina et al., 2004) even with a commonly reported heritability value for stature of about 0.8 (Fisher, 1918;

Carmichael and McGue, 1996; Preece, 1996; Silventoinen et al., 2000, 2003; Macgregor et al., 2006; Perola et al., 2007). The increase in stature is likely due to better nutrition and improved environmental conditions. Therefore, the environment allowed for a change in phenotype even though the majority of the variation in that phenotype is due to variation in genotype.

Third, a low heritability value does not imply that there is no additive genetic variance. It simply means that compared to all the observed phenotypic variation, only a small portion of phenotypic variation is due to genotypic variation. Additive genetic variance can still be high, but if phenotypic variance is extremely high then heritability will be low. This distinction is particularly important when dealing with the response to natural or artificial selection and will be discussed further (see *Evolvability*, below). Fourth, heritability is not informative about the nature of between-group differences. Heritability is population and environment specific; a change in the environment or in gene frequencies can change heritability estimates. Therefore, heritability is not a useful predictor about changes within a population over time or about differences between different populations. Finally, a high heritability estimate does not imply genes of large effect. There is no relationship between the number or the effect size of genes affecting a trait and the heritability estimate. For example, stature, with its high heritability estimate of 0.8 (Fisher, 1918; Carmichael and McGue, 1996; Preece, 1996; Silventoinen et al., 2000, 2003; Macgregor et al., 2006; Perola et al., 2007), is influenced by numerous genetic loci that each individually only explain a small amount of genetic variance (Gudbjartsson et al., 2008; Lettre et al., 2008; Sanna et al., 2008; Weedon et al., 2008; Soranzo et al., 2009).

In regard to postcrania – the focus of this project – a significant amount of heritable variation has been found in the individual postcranial measurements of mice (Leamy, 1974),

horses (Dario et al., 2006), birds (Potti and Merino, 1994), and living (Cheverud and Dittus, 1992) and skeletal (Cheverud and Buikstra, 1981, 1982; Hulsey et al., 2010) non-human primates. Genetic variation also appears to play a large role in postcranial variation in humans (Susanne, 1977; Byard et al., 1984; Devor et al., 1986a,b; Arya et al., 2002; Livshits et al., 2002). For example, Devor and colleagues (1986a,b) used path analysis to estimate the transmissibility (i.e., heritability) of cranial and postcranial measures in a living human sample. Postcranial measurements of length showed higher heritability than breadth or circumference measures, a pattern suggested by Osborne and DeGeorge (1959), and cranial estimates of heritability were intermediate. Specifically, the heritability of limb and limb segment length measurements ranged from 0.640 to 0.741. These estimates are comparable to other similar studies, as is the general trend that measurements of length have higher h^2 estimates than other measurement types (Susanne, 1977; Kaur and Singh, 1981; Paganini-Hill et al., 1981; Byard et al., 1984). Despite the limitations (see *Anthropometrics vs. Osteometrics* in *Research Design*, below), all the human studies used anthropometric data, as skeletal data with associated pedigree data were not available. Within the limbs of skeletal primates, environmental variance increases while heritability decreases as one moves distally along the limb (Hallgrímsson et al., 2002). Given that development proceeds proximo-distally (see *Limbs*, above), variation is expected to accumulate in distal structures (Hallgrímsson et al., 2002; Young and Hallgrímsson, 2005).

Evolvability

Evolvability is defined as the ability of a population to respond to natural or artificial selection, which depends on the amount of additive genetic variation (V_A) present in the population (Houle, 1992). Narrow-sense heritability is often used as a measure of the evolutionary potential of a population, but as will be shown below, this is problematic. A different measure of evolvability, *e*, is discussed here.

As mentioned previously, one of the misconceptions regarding heritability is that a low value implies little to no additive genetic variance. In reality, low heritability means that only a small portion of the overall phenotypic variance is due to additive genetic variance. If the environmental variance (V_E in Equation 3.1) is very large as compared to the additive genetic variance, then heritability will be low. This distinction is particularly necessary to understand when discussing selection, as will be shown below.

The breeder's equation is:

$$R = h^2 * S \tag{3.6}$$

where R is the change in the mean phenotype between generations and S is the selection differential, or the difference in mean phenotype between parents selected for breeding and the overall mean in their generation (Lynch and Walsh, 1998). The response to selection (R) depends on the amount of genetic variation in the population, represented in Equation 3.6 by h^2. If there is no additive genetic variance (i.e., h^2 is zero), there will be no response to selection. Similarly, selection will reduce the amount of additive genetic variance, and, hence, heritability will decrease in the next generation (Konigsberg, 2000). The relationship between selection and heritability is described in Fisher's Fundamental Theorem of Natural Selection (Fisher, 1930) as:

$$R = V_A / W \quad (3.7)$$

where W is the mean fitness of the population. Fisher's theorem, then, shows that rates of trait change due to selection are related to the additive genetic variance in fitness (Fisher, 1930; Konigsberg, 2000). Combined with the decrease in additive genetic variance over generations, this leads to a decreased rate of evolution in response to selection over time. As stated above, estimates of heritability for fitness traits are typically low as compared to morphological traits (Cheverud and Buikstra, 1981; Mousseau and Roff, 1987; Falconer and Mackay, 1996; Visscher et al., 2008). Therefore, the response to selection should be low for fitness traits. However, as an example, the number of eggs produced by farmed chickens has a high response to artificial selection (Preisinger and Flock, 2000), indicating that a large amount of additive genetic variation exists. This is unexpected given that clutch size is a fitness trait with low heritability, meaning that it should have a limited response to selection.

The observation that many fitness traits have large additive genetic variance relative to the trait mean led Houle (1992) to propose a new dimensionless statistic that would more accurately estimate the ability of populations to respond to selection. Evolvability can be thought of as the expected evolutionary response to selection in a single trait or among multiple traits relative to the strength of selection (Hansen and Houle, 2008; Hansen et al., 2011). To effectively estimate evolutionary potential, the evolvability estimate should be comparable across traits and species. Therefore, the way that additive genetic variation is scaled is important.

Given that evolvability is effectively the response to selection scaled to the strength of selection (Hansen et al., 2011), it is closely related to the Lande equation. The multivariate Lande Equation gives the expected change in a trait mean per generation and is:

$$\Delta z = G * \beta \quad (3.8)$$

where Δz is the response to selection, G is the additive genetic variance/covariance matrix, and β is the directional selection gradient (Lande, 1979). The univariate version of the Lande Equation is:

$$R = V_A * \beta \quad (3.9)$$

where R is equivalent to the response to selection in Equation 3.6. Using this equation, evolvability is measured as:

$$e = R / \beta = V_A \quad (3.10)$$

following Hansen and colleagues (2011).

The additive genetic variance must be standardized in order to allow comparison across traits or species. Typically this is done by dividing the additive genetic variance by the phenotypic variance, which yields heritability and the breeder's equation seen in Equation 3.6. This variance-standardized measure of evolvability is inappropriate, as discussed above and in Houle (1992).

A more appropriate measure of evolvability is a mean-standardized one, such as:

$$e = V_A / m^2 \quad (3.11)$$

where m is the trait mean before selection, as suggested by Houle (1992) and Hansen and Houle (2008). Henceforth, this definition of *e* will be used when discussing evolvability. When using this mean-standardized statistic, fitness-related traits show higher levels of evolvability than morphological traits, opposite that seen in the pattern of heritability estimates. Therefore, fitness-related traits do indeed have high levels of additive genetic variance, but they also have even higher levels of total phenotypic variance due to high levels of environmental variance.

Furthermore, using data from over 200 quantitative genetic animal studies, Houle (1992) showed that the correlation between heritability and evolvability is near zero. As there is no predictive power between heritability and evolvability, the two measures should not be used interchangeably (Hansen et al., 2011). The one exception given by these authors is that a large heritability typically implies a non-zero evolvability. While both h^2 and e use additive genetic variance, the scale that is used to standardize that variance leads to very different conclusions.

Just like heritability, evolvability (e) is a population-level estimate that requires pedigree information. While estimates of e may seem quite small, they can have a large impact on quantitative traits. As described by Hansen and colleagues (Hansen et al., 2003b; Hansen et al., 2011), an evolvability of 0.001 predicts that for traits under unit selection there will be a tenth of a percent change per generation (Hansen et al., 2011). With a selection strength of 1, this level of evolvability, which was the median for linear morphological traits (i.e., single dimension traits rather than areas or volumes) in the large study comparing h^2 and e mentioned above (Houle, 1992), would produce a 10% change in just under 100 generations and a doubling of the trait in 700 generations (Hansen et al., 2011). Therefore, even seemingly small estimates of e are capable of producing significant changes.

Conditional evolvability is a closely related concept that takes the covariance of traits into account when estimating a trait's response to selection. Traits that share some of their additive genetic variance (V_A) through genetic covariance are not capable of evolving independently from one another. While most traits spend the majority of their time under stabilizing selection, as evidenced by the stability of organisms over time (Hansen, 1997; Hansen et al., 2003a), an environmental shift would cause some characters to experience directional

selection until they reached a new optimum; however, not all characters would be affected uniformly. In this situation, only the amount of V_A in a trait that is not shared with other traits through covariance is available for adaptation in the trait. Unconditional evolvability (*e*) can be thought of as the upper limit of evolvability for a trait because it does not take character correlations into account.

Conditional evolvability is computed from the G matrix, which includes additive genetic variance and covariance estimates for a set of traits. This is the same G as in the multivariate Lande Equation (Equation 3.8, above). The conditional evolvability of a trait is equivalent to the inverse of the corresponding diagonal element of the inverse G matrix. Therefore:

$$c(x_i) = 1 / [G^{-1}]_{ii} \quad (3.12)$$

where x is the *i*th trait and G^{-1} is the inverse G matrix (Hansen and Houle, 2008). Estimates of *c* are typically much smaller than *e* (Hansen et al., 2003a; Hansen and Houle, 2008). A low *c* relative to *e* indicates that a trait shares the majority of its variation with other traits. This type of trait would be constrained by evolution acting on other traits, and evolution acting on this trait would cause correlated responses in other traits (Hansen and Houle, 2008; Roseman et al., 2010).

There has been a surge in bioanthropological and related literature looking at the evolvability of human and non-human primate skeletal features, including the cranium (Marroig et al., 2009; Martínez-Abadías et al., 2009; Roseman et al., 2010), hands and feet (Rolian, 2009), pelvic girdle (Lewton, 2012), and limbs (Young et al., 2010; Villmoare et al., 2011). While most of these do not directly estimate *e* as defined above, they do evaluate the ability of a population to respond to selection via other statistical means. For instance, many of these studies analyze patterns of morphological integration (discussed further below) to determine the degree that traits

are able to independently evolve in a population. This is because genetic integration, which manifests as phenotypic covariance, impacts the amount of genetic variance available for the independent evolvability of traits (Young et al., 2010). Because estimating *e* and *c* requires pedigree information, the samples that can be used are limited. With the exception of Martínez-Abadías et al. (2009) and Roseman et al. (2010), none of the abovementioned papers use pedigreed samples and are thus unable to estimate the additive genetic variance of the samples.

The phenotypic variance/covariance matrix has been shown to be a good proxy for the genetic variance/covariance matrix (Cheverud, 1988), allowing non-pedigreed samples to be used to explore evolvability by other means. While the phenotypic and genetic variance/covariance matrices are broadly similar, some authors caution against such substitutions (Willis et al., 1991; Lewton, 2012). The direct estimation of *e* using additive genetic variance from pedigreed samples is largely not done. Therefore, while various features of the human and non-human primate skeleton have been found to be evolvable, there is a need to formally quantify the evolvability and conditional evolvability of independent traits in primate limbs using pedigreed samples. This project seeks to accomplish this goal.

Estimation of Covariation

The concept of evolvability is closely tied to the concept of morphological integration. While heritability and evolvability explore the genetic variation within a trait, morphological integration, like conditional evolvability, is an attempt to understand the covariation among traits. Phenotypic covariation occurs when traits are developmentally or functionally related

(Cheverud, 1982, 1996a) and can be the result of pleiotropic effects of genes acting on multiple traits (Cheverud, 1984, 2007; Hallgrímsson et al., 2002; Rolian, 2009; Young et al., 2010).

As originally conceptualized by Olson and Miller (1958), morphological integration is the process by which developmentally and/or functionally related parts interact to form an integrated organism with different parts that are capable of working together. In other words, morphological integration is "the summation of the totality of characters which, in their interdependency of form, produce an organism" (pp. v). These authors suggested the use of phenotypic correlation as a quantitative method of identifying sets of phenotypic traits that are more strongly integrated based on shared developmental pathways or functional purposes.

Modularity is a related concept that occurs when morphologically integrated sets of characters are relatively uncorrelated with other sets of characters (Wagner, 1996; Klingenberg, 2008; Mitteroecker and Bookstein, 2008; Hallgrímsson et al., 2009). The idea of modularity, which gained traction in the last two decades, has helped explain the various levels of heterogeneity found in an organism, whether that be structural or functional, and is considered an essential feature of biological organization (West-Eberhard, 2003). Various types of modules have been described in the literature, including variational modules (Wagner and Altenberg, 1996), functional modules (West-Eberhard, 2003) and developmental modules (Raff, 1996; Carroll et al., 2001). Each of these describes a part of an organism that is integrated due to natural variation or a functional or developmental process and that is also relatively uncorrelated with other parts of the organism (Wagner et al., 2007). Therefore, for example, a set of characters that work together to perform a function can be integrated in a functional module that is relatively independent from other modules. While different classes of modules have been

cited, the central issue facing studies of modularity is that their level of organization must be defined. What unifies all modules is that they are context-independent (Schlosser and Wagner, 2004). For an extensive overview of the evidence for and origins of modularity, see the review by Wagner and colleagues (2007).

The study of morphological integration in biological anthropology increased notably in the 1980s with Cheverud's work on macaque and tamarin crania (Cheverud 1982, 1995, 1996b). As explained by Rolian and Willmore (2009), Cheverud's work placed morphological integration in a quantitative genetics framework by relating the developmental and functional relationships among traits to the Lande Equation (Equations 3.8 and 3.9, above) and the evolution of genetic covariance structure. In addition, Cheverud established variance/covariance and correlation matrices as the method of identifying relationships among traits. These matrix-based methods, such as analysis of eigenvalues (e.g., Pavličev et al., 2009), principal component and factor analysis (e.g., Ackermann and Cheverud, 2000), and matrix correlations (e.g., Cheverud, 1996b; Ackermann and Cheverud, 2000), allow the identification of patterns and magnitudes of integration in large datasets and the testing of observed data against theoretical matrices for hypothesis testing.

Based on the abundance of empirical observations made using matrix-based methods in a quantitative genetics framework, integration theory began to shift focus in the mid-1990s. The new focus became the way that integration itself can evolve, and, again, Cheverud played a pivotal role. In his 1996 paper (Cheverud, 1996a), he defines four types of integration that are ordered hierarchically. The first two types of integration – functional and developmental – are seen within individuals; they are the same types of integration as described by Olson and Miller

(1958). Functional integration arises when phenotypic traits work together to perform a function and the efficiency of that performance is dependent upon the way that the traits interact. Developmental integration occurs when traits are directed by the same developmental process or interact during development. It should be noted that functional and developmental integration are not mutually exclusive because functional integration in adult individuals is partly achieved through developmental integration (Cheverud, 1996a). Moving from the individual level to the population level, there are two other types of integration: genetic and evolutionary. Genetic integration occurs when a set of morphological traits are inherited together as a module, through a process such as pleiotropy or linkage disequilibrium (defined below), independently from other sets of traits. Evolutionary integration occurs when morphological traits co-evolve because they are either inherited together (through genetic integration) or because they are selected together (even when inherited independently). In this framework, individual integration leads to genetic integration that in turn leads to the coordinated response to evolution known as evolutionary integration.

Cheverud's hierarchical framework points to the connection between morphological integration and evolvability. As traits become integrated at the population level and their response to selection becomes more coordinated through evolutionary integration, they are less capable of independently responding to selective pressures (i.e., their independent evolvability is reduced) (Rolian, 2009). Pleiotropic interactions between traits are either selected for or against depending on whether the covariation they produce at the phenotypic level increases or decreases fitness (Wagner, 1996; Wagner and Altenberg, 1996). If integration among traits is selected against, the process is known as parcellation (Wagner and Altenberg, 1996), and individual traits

become more independently evolvable. This may occur when traits that shared a common function or developmental basis are selected for specialization (Hallgrímsson et al., 2002). For an example of this, see Rolian (2009).

The hierarchical framework of morphological integration also highlights the importance of the underlying processes that produce integration among traits. This has led to a shift in focus from simply identifying *patterns* of integration to attempting to understand the *processes* (genetic, developmental, and functional) that create or contribute to the known patterns of covariation. In what is known as the Palimpsest Model[6], Hallgrímsson and colleagues (2009) explain that while integration and modularity are often investigated through phenotypic covariation or correlation, little thought is typically given as to whether the observed patterns accurately represent integration. The Palimpsest Model of covariation structure suggests that covariation structure arises through covariance-generating developmental processes (Hallgrímsson et al., 2007). Several of these processes may act to influence covariation, making it difficult to unravel the underpinnings of the covariation structure. Therefore, the underlying processes of integration and modularity can be hard to decipher from phenotypic covariance data. In fact, the authors state that, while integration and modularity are aspects of developmental architecture (defined as the connections between genetic and phenotypic variation during development [Hallgrímsson et al., 2009]) that influence evolvability by structuring how genetic variation is translated into phenotypic variation, they are not equivalent in any way to observed patterns of covariation (Hallgrímsson et al., 2009). This is because covariance and correlation depend on the existence of variance to be detected, yet integration and modularity exist even in

[6] A palimpsest is a velum scroll used in medieval times. The scroll would be reused, with the remnants of previous texts still visible. These various texts would accumulate over time, with newer text obliterating older text.

the absence of variance. The example given in this paper is a sample of clones raised under identical conditions and devoid of variation. These clones would exhibit no covariation structure, yet the developmental architecture would still be integrated in the same way as the parent population. Reintroduced variation would then be structured based on the integration and modularity of the developmental system. Therefore, these authors advocate a different definition of integration: the tendency of a developmental system to produce covariation.

Despite the limitations that the Palimpsest Model seems to posit on the study of integration, there are still viable methodological means to identify integration in samples. The scaled variance of eigenvalues shows how much variation is unequally distributed across principal components in a principle components analysis. As integration increases, more of the total variation is found in fewer principle components. Therefore, relative eigenvalue variance (following Pavličev et al., 2009) will be used here.

Studies looking at morphological integration in limbs support the idea that developmental factors play a role in limb variation. While evidence in avian datasets shows that integration is higher within limbs than between homologous elements (Van Valen, 1965; Wright, 1968; Magwene, 2001), the opposite appears true in primate datasets (Hallgrímsson et al., 2002; Young and Hallgrímsson, 2005). Specifically, when the limb girdle is removed from analysis, homologous elements of primates are more tightly integrated than elements within the individual limbs, signaling the similar developmental processes between homologous elements in the fore and hind limbs. However, evidence also suggests that functional factors impact the degree that limb elements are integrated. When a broader sample of mammals, including mice, gibbons, macaques, and bats, is analyzed, it becomes evident that the degree of integration between

homologous elements decreases with increased specialization and limb divergence (Young and Hallgrímsson, 2005). For example, the highly specialized forelimb of the bat shows much reduced integration with the homologous elements of the hind limb compared with the homologue integration found in the quadrupedal macaque. Selection for the increased functional specialization appears to reduce the common developmental factors between the limbs, leading to decreased covaration. This reduction in integration with increased specialization of the limbs can also be seen within primates. Young and colleagues demonstrate that apes and humans show lower levels of integration between limbs and higher levels of independent evolvability of the limbs than quadrupedal monkeys, arguably due to functionally divergent use of the limbs (Young et al., 2010). Similar results were also found in a large group of Strepsirrhine primates, with arboreal quadrupeds showing higher between limb integration than leapers (Villmoare et al., 2011).

There are few publications on the morphological integration of human limbs. Young and colleagues (2010) compared humans to other primate species (discussed above), and found human limbs to be less integrated than quadrupedal monkeys. DeLeon and Auerbach (2007) compared multiple human groups and found that patterns of integration differ between groups based on subsistence strategy, with agriculturalists showing higher between-limb integration than hunter-gatherers. And, finally, Auerbach and DeLeon (2013) looked at integration among multiple dimensions (articulations, diaphyses, and lengths) within the long bones of human limbs. These results suggest that similar dimensions among homologous elements are more integrated than elements in the same limb and that the highest levels of integration are found in long bone lengths.

Linkage Analysis

The previous sections reviewed quantitative genetics approaches to understanding variation and covariation in quantitative traits. Heritability and evolvability require an understanding of the phenotypic variance and familial relationships (i.e., pedigree data) to partition variance, and morphological integration requires knowledge of the covariance structure. The final analysis employed in this project, linkage analysis, necessitates not only phenotypic and pedigree data, but also genotypic data. These additional data are used to look for correlations between phenotypic and genotypic variation with the goal of identifying genomic regions that may contribute to quantitative trait variation. This section describes how linkage analysis works and reviews pertinent literature on quantitative trait loci (defined below) related to skeletal morphology, specifically with regards to the limbs.

Genetic mapping has been a staple of disease and complex trait research for a century because it "allows one to find where a gene is without knowing what it is" (Lander and Schork, 1994:2037). This is done by comparing the inheritance pattern of a trait to the inheritance pattern of chromosomal regions, and the goal is to create a graphical representation of the relative arrangement of genes on a chromosome. The first study to link a gene to a chromosomal location was Sturtevant's work that mathematically connected sex-linked traits in *Drosophila* to a linear arrangement on a chromosome (Sturtevant, 1913; Lander and Schork, 1994). The subsequent combination of new methods such as recombinant DNA (the artificial blending of DNA sequences) and positional cloning (the isolation of partially overlapping DNA segments that move toward a candidate gene) allowed the identification of genes based solely on chromosomal location rather than biochemical function (Bender et al., 1983; Lander and Schork, 1994). These

early methods to gene mapping worked well for model organisms such as *Drosophila* but were unfeasible in humans.

A genetic marker is a segment of DNA with an identifiable physical location on a chromosome with a recognizable inheritance pattern (Rubicz et al., 2007). There are several requirements for ideal genetic markers. Marker loci should be highly polymorphic so that individuals have different alleles, abundant so as to thoroughly cover the genome, neutral to both the trait and fitness, and co-dominant (Falconer and Mackay, 1996). The limitation prior to the molecular biology revolution and DNA technological advancements that began in the 1980s, however, was that there were only a few known genes to serve as genetic markers throughout a genome. For example, while blood antigen proteins meet the requirements of being neutral and co-dominant, they are neither highly polymorphic nor abundant enough to cover the genome (Falconer and Mackay, 1996).

A breakthrough in genetic mapping came with the work of Botstein and colleagues (Petes and Botstein, 1977; Botstein et al., 1980) who discovered that recombinant DNA probes could be used to identify marker loci that are polymorphic in DNA sequence. The differing lengths of these marker loci could then be detected using restriction endonucleases that cleave the DNA at sequence-specific locations, known as restriction fragment length polymorphisms (RFLPs). The recognition of these naturally-occurring RFLP DNA sequence variants meant that many genetic markers could be identified, and, if well-spaced throughout the genome, any trait caused completely or partially by a major locus segregating in a pedigree could be mapped (Botstein et al., 1980).

With the advent of polymerase chain reaction (PCR) (Saiki et al., 1985; Mullis et al., 1986; Mullis and Faloona, 1987), the number of markers available for mapping increased significantly. Short tandem repeats (STRs), which are segments of the genome with repetitive di-, tri-, or tetra-nucleotide sequences, were subsequently found to be ideal candidates for gene markers (Weber and May, 1989; Pulst, 1999). STR loci are multiallelic (i.e., there are multiple differing alleles), increasing the chance that an individual will be heterozygous and parental alleles can be differentiated (Pulst, 1999). STRs are also widely distributed throughout the genome, easily detected through PCR followed by electrophoresis (a method of visualizing PCR product [i.e., amplified DNA]), and can be multiplexed, allowing multiple STRs to be detected simultaneously (Pulst, 1999).

STRs are currently the genetic marker of choice for linkage analysis. Linkage analysis is a type of statistical analysis with the goal of mapping a gene to a region of a chromosome. These genes influence the expression of phenotypic traits, such as diseases or other complex traits (such as limb segment lengths). Oftentimes, however, what are actually being mapped are not individual genes but quantitative trait loci (QTL). A QTL is a segment of a chromosome that influences the trait of interest and is not necessarily a single gene (Falconer and Mackay, 1996). If a significant statistical result is found between the phenotypic trait of interest and a genetic marker, this indicates that a QTL lies somewhere in the region of the genetic marker (i.e., there is something in that area of the chromosome, whether it be a gene or a regulatory element, that affects variation in the phenotype). It does not mean that the marker itself is influencing the trait, only that something in the area of the genome around the marker is correlated with the phenotype.

The fact that QTLs can be located using genetic markers is based on the idea that genes on a chromosome can become "linked" during recombination. During meiosis, the process of cell replication and division that produces gametes (i.e., egg and sperm), genetic material is exchanged between homologous segments of chromosomes, a process known as crossing over or recombination (Bailey-Wilson and Wilson, 2011). Depending on how closely two genes are to one another on a chromosome will determine how often crossing over occurs between them. If syntenic loci (i.e., loci that are located on the same chromosome) are located far apart, they will have a high rate of recombination between them, typically about 50%. On the other hand, loci located very close to one another will have a much-reduced recombination rate, sometimes nearing zero if the loci are located next to each other. Recombination fractions that fall between zero and 1/2 indicate a level of linkage between the loci. This implies that the loci lie close enough to one another on a chromosome that they are sometimes transmitted together during crossing over and therefore do not recombine (Bailey-Wilson and Wilson, 2011)[7]. Genetic markers, therefore, can be especially useful in identifying QTLs if they are located near enough to each other to likely remain linked.

Linkage analysis requires pedigreed samples so that loci can be traced through generations to determine recombination rates. Classical linkage analysis involves offering a model that explains how phenotypes and genotypes in a pedigree are inherited. A hypothesized model that suggests a location for a trait locus near a genetic marker is compared to a null model

[7] Linkage disequilibrium (LD, also known as gametic phase disequilibrium) is a closely related concept. It is the non-random association of alleles at different loci that is different than would be expected if they were independent, randomly segregating alleles, making it appear that loci are associated. LD is a broad concept, with genetic linkage being only one of the ways that it occurs. Other causes of LD include the intermixture of populations, chance in small populations, and selection (Falconer and Mackay, 1996).

that suggests no linkage between the trait locus and the marker locus (Lander and Schork, 1994). These models are then compared to the observed data to see which offers a better fit. The hypothesized model is either accepted or rejected based on the likelihood ratio or corresponding logarithm of odds (LOD) score. Historically, a LOD of 3 (corresponding to a 1,000:1 chance) indicates that there is linkage between the trait loci and the genetic marker and that the null model should be rejected (Lander and Schorck, 1994; Bailey-Wilson and Wilson, 2011). However, Lander and Kruglyak (1995) proposed a modification to the LOD score to correct for multiple comparisons that are done with more dense genetic maps. Their new method of calculating significance thresholds helped to limit the genome-wide probability of observing a false positive linkage to 5% and has become a standard used in linkage analysis (Lander and Kruglyak, 1995; Bailey-Wilson and Wilson, 2011).

Another early limitation to linkage analysis specific to humans was that crosses cannot be experimentally controlled, family sizes are small, and generation times are long (Bailey-Wilson and Wilson, 2011). In addition, much of the information about relatedness between individuals could not be used in nuclear families as many statistical methods used only pairs of related individuals (e.g., sib-pairs) to garner information (e.g., Hasemon and Elston, 1972; Amos et al., 1989; Kruglyak and Lander, 1995; Risch and Zhang, 1995; Fulker and Cherny, 1996; Gu et al., 1996; Gu and Rao, 1997). However, pair-based methods have much lower power to identify genes than other methods that use larger configurations of relatives (Todorov et al., 1997; Williams and Blangero, 1999a,b; Blangero et al., 2000), and statistical methods have been developed to identify QTLs using all relationships in nuclear families and extended pedigrees

(Goldgar, 1990; Schork, 1993; Amos, 1994; Almasy and Blangero, 1998; Blangero et al., 2000; Prat et al., 2000).

A successful method for identifying QTLs in extended pedigrees is known as variance component linkage analysis, and it is based on the classical quantitative genetic method of partitioning phenotypic variance (see Equation 3.1 above). Here, the quantitative phenotype is expressed as a linear function of the *n* QTLs that influence it:

$$y = \mu + \sum_{i=1}^{n} \gamma_i + e \tag{3.13}$$

where y is the phenotype, μ is the grand mean, γ is the effect of the *i*th QTL, and e is the random environmental deviation (Almasy and Blangero, 1998). Using this equation, phenotypic trait covariance and correlation between pairs of relatives can be derived, the latter of which includes a heritability term representing the total phenotypic variance due to the additive genetic contribution of the *i*th QTL (for detailed equations and explanations, see Almasy and Blangero, 1998). Data from the pedigree are used to construct a covariance matrix for the pedigree, and a likelihood model is produced. The null hypothesis that additive genetic variance due to the *i*th QTL is equal to zero (i.e., there is no linkage) is tested against a model where the variance due to the *i*th QTL is estimated, and the difference between these is used to produce a LOD score (Almasy and Blangero, 1998). Variance component linkage analysis methods now exist for pedigrees of various sizes and complexities (Commuzie et al., 1997), and things such as pleiotropy (Almasy et al., 1997), genotype by environment interaction (Towne et al., 1997), and epistasis (Blangero et al., 2000) can be incorporated. For an in-depth review of variance component linkage analysis, see Blangero and colleagues (2007).

There are other methods available for identifying QTLs that are often cited in the literature, one of which is interval mapping. Interval mapping does not require pedigreed data, as linkage analysis does, and is commonly used in experimental animals where test crosses can be controlled (Soller et al., 1979; Jansen, 1993). This method works by using estimated genetic maps and statistically testing for the presence of a QTL in intervals defined by the ordered pairs of genetic markers (Doerge, 2002). While powerful in its use of non-pedigreed samples, interval mapping, as defined by Lander and Botstein (1989), statistically tests for the presence of a single QTL in each interval, not allowing for interactions between multiple QTLs to be considered. Methods for testing for multiple QTLs exist, but are beyond the scope of this chapter (for a review, see Doerge, 2002). Another commonly used method for identifying QTLs are genome wide association studies (GWAS), which also do not require pedigree data (Hirschhorn and Daly, 2005). The most abundant genetic marker in the human genome is single nucleotide polymorphisms (SNPs) (Wang et al., 1998a; Brookes, 1999), and GWAS studies rely upon SNPs to look for associations. While interval mapping and GWAS methods have their place, linkage analysis methods have made a recent comeback as the dominant method for identifying genes of interest in disease and complex trait studies because of the distinct ability to incorporate familial data and identify variants with large effect size (Bailey-Wilson and Wilson, 2011). For a review on the relationship between linkage analysis and next-generation sequencing, see Bailey-Wilson and Wilson (2011), and for the relationship between linkage analysis and whole-genome sequencing, see Ott and colleagues (2015).

Many studies that have identified QTLs in the human genome are centered on diseases, such as diabetes (e.g., Duggirala et al., 1999), cardiovascular disease (e.g., Wang and Paigen,

2002), and obesity (e.g., Rankinen et al., 2006). However, there are also studies that identify QTLs that influence skeletal attributes in humans. Height is a classic quantitative trait that has been extensively studied using GWAS methods, and a multitude of QTLs have been found that each have a small effect on variation in human height (Weedon et al., 2007; Gudbjartsson et al., 2008; Lettre et al., 2008; Sanna et al., 2008; Weedon et al., 2008; Soranzo et al., 2009). QTLs for skeletal attributes have been identified in humans for bone mineral density (Koller et al., 2000; Devoto et al., 2001; Ralston et al., 2005) and bone size (Koller et al., 2001; Deng et al., 2003). And, one study found a suggestive QTL associated with femur length in humans using linkage analysis on a cohort of twins (Chinappen-Horsley et al., 2008).

Animal models are frequently used to identify QTLs that influence skeletal attributes. This is because of the distinct lack of human skeletal samples that are associated with pedigree information and that have been adequately genotyped (discussed further in *Research Design*, below). Much work has been done to identify QTLs that influence skeletal attributes in mice, including such features as skeletal size (Christians et al., 2003), bone morphology (Drake et al., 2001; Masinde et al., 2003; Klinenberg et al., 2004), bone mineral density (Klein et al., 1998; Ishimori et al., 2006; Leamy et al., 2013), and bone mechanical properties (Robling et al., 2003; Kesevan et al., 2006). Some of these same skeletal features have been studied in other model animals, including bone mineral density in baboons (Havill et al., 2005) and chickens (Rubin et al., 2007), and bone morphology in fish (Kimmel at al., 2005). QTLs specific to long bone length have been found in mice (Leamy et al., 2002; Kenney-Hunt et al., 2006, 2008; Norgard et al., 2008, 2009; Pavličev et al., 2007), dogs (Chase et al., 2002; Carrier et al., 2005), and pigs (Mao et al., 2008); however, with the exception of Chinappen-Horsley and colleagues (2008), there is a

distinct lack of research that identifies QTLs that influence long bone length in humans and other primates. This project seeks to identify QTLs associated with long bone length in a model primate.

Considerable pleiotropy has been found between long bone lengths (Norgard et al., 2008, 2009; Mao et al., 2008), between long bone length and organ weight (Leamy et al., 2002; Kenney-Hunt et al., 2006), and between long bone length and body size (Chase et al., 2002; Kenney-Hunt 2006, 2008; Pavličev et al., 2007) in non-primate animals. Pleiotropy and phenotypic correlation are measures that are relatively strongly correlated (Kenney-Hunt, 2008), providing support for the idea that pleiotropy is one way that morphological features coevolve. Therefore, this project also seeks to identify pleiotropy in lone bone lengths in a primate model.

Summary

This chapter provides background on the various genetic approaches that are used in this study to understand variation and covariation in limb segment lengths. Limb segment lengths are complex traits that can be analyzed using the tenets of quantitative genetics to infer evolutionary change. By understanding the variance (i.e., heritability and evolvability) and covariance (i.e., morphological integration) of individual limb segments, the way that these traits are capable of evolving will be better understood. Additionally, identifying genomic regions (i.e., linkage analysis) that may impact the phenotypic variation of these traits provides another avenue of understanding the way that limb segments coevolve by potentially showing pleiotropic relationships between segments. Research that combines these various methodological

approaches is lacking in the literature, and this study could provide important insight into anthropological studies such as those reviewed in the previous chapter (see *Limbs*, above).

CHAPTER FOUR
RESEARCH DESIGN: HYPOTHESES, MATERIALS, AND METHODS

Hypotheses

The goal of this project is to use a quantitative genetics approach to estimate variance and covariance in limb segment lengths in humans and other primates using pedigreed samples and then begin the task of identifying genes which influence this normal genetic variation in primate limb bones. Pedigreed samples are by and large unused in previous research that has analyzed the variance and covariance of limb segments, and QTL analysis of primate limbs has not been done. The following hypotheses take into account findings from the literature discussed in the previous background chapters.

The way in which limb segments relate to one another will be explored here in two ways: 1) through hypotheses based on a developmental perspective, i.e., based on the way in which limbs develop, and 2) through hypotheses based on an evolutionary perspective, i.e., based on the way in which limbs change over time across species. The purpose is not to pick one perspective over the other, but to show the ways in which limb morphology does or does not adhere to the assumptions frequently made in anthropological literature.

Developmental Perspective Hypotheses

The Developmental Perspective is largely predicated by the notions that 1) limbs develop in a proximo-distal gradient (Tarchini and Duboule, 2006; Gilbert, 2013), 2) limb segment lengths are more genetically canalized than other limb features (Auerbach and Ruff, 2006;

Cowgill and Hager, 2007), and 3) homologous structures have similar developmental pathways (Hallgrímsson et al., 2002; Gilbert, 2013). These ideas give rise to the following hypotheses.

1. *While phenotypic variance increases from proximal to distal elements, heritability will decrease.* – Environmental variance has been shown to accumulate in distal elements in primates (Hallgrímsson et al., 2002) due to the way in which limbs form in a proximo-distal gradient (Tarchini and Duboule, 2006; Gilbert, 2013). Therefore, while phenotypic variance will increase due to increasing environmental variance, heritability will decrease because genetic variance plays a smaller role in overall phenotypic variance.

2. *Morphological integration will be higher among limb segment lengths and/or articulations and lower among diaphyseal measures.* – This is based on research which indicates that 1) diaphyseal measures are more influenced by mechanical loading than other limb features (Larsen, 1997; Ruff, 2008a), 2) limb articulations are less responsive to mechanical loading (Ruff et al., 1991), and 3) limb segment lengths are anecdotally considered to be more highly genetically canalized than other bone dimensions (Auerbach and Ruff, 2006; Cowgill and Hager, 2007).

3. *Proximal limb elements will shower higher morphological integration with one another than distal limb elements, and homologous elements will shower higher morphological integration than elements within the same limb.* - Homologous elements have similar developmental pathways, and molecular factors involved in limb development work in a

proximo-distal gradient (Tarchini and Duboule, 2006; Gilbert, 2013), allowing variation to accumulate in distal elements.

4. *Traits that show high morphological integration will have QTLs in the same genomic regions.* – Pleiotropy, defined as a single gene or region contributing to multiple phenotypic traits, is a genetic mechanism which leads to positive genetic correlation and integration because changes in that single gene or region causes phenotypic changes in multiple traits (Cheverud, 1984, 2007; Hallgrímsson et al., 2002; Rolian, 2009; Young et al., 2010). It can be identified as multiple traits showing significant correlations with similar genomic regions.

Evolutionary Perspective Hypotheses

The Evolutionary Perspective is driven largely by the ideas that 1) a major difference across primates is limb diversification from species that are quadrupeds to species that use suspension, leaping, or, as emphasized here, bipedalism, and 2) traits that evolve more independently share relatively less of their variation with other traits (Hansen and Houle, 2008). These factors lead to the following hypotheses.

1. *Evolvability will increase with limb diversification (i.e., as the upper and lower limbs evolve to perform different functions).* – Evolvability will increase as the limbs become more independent of one another, allowing the limbs to evolve to perform different functions. Additionally, the expectation is that evolvability estimates will be comparable

across limb segments in quadrupedal non-human primates and more variable across the limb segments in the bipedal human sample.

2. *The difference between conditional evolvability and evolvability will decrease with limb diversification.* – A trait that has low conditional evolvability relative to evolvability shares the majority of its variation with other traits, and evolution acting on this trait would cause correlated responses in other traits (Hansen and Houle, 2008; Roseman et al., 2010). Quadrupedal primates are expected to have low conditional evolvability relative to evolvability. A higher conditional evolvability relative to evolvability (i.e., a reduced difference between the two measures) means the trait is more able to evolve on its own. Therefore bipedal humans should show this latter pattern.

3. *Morphological integration will decrease with limb diversification.* – As the upper and lower limbs evolve to perform different functions, integration between the limbs (i.e., between homologous elements) will decrease (Young and Hallgrímsson, 2005). This means that humans, which are bipedal, will show lower integration than the other primate samples, which are quadrupeds.

Samples

A sample is defined here as a group of related individuals which meet the requirements listed below. This project includes four samples: a sample of skeletal tamarins, two samples of

baboons (one skeletal and one anthropometric), and a sample of anthropometric measurements from humans.

Sample Requirements

Sample selection for this project was based on the presence of a 1) large number of 2) pedigreed, adult individuals, with 3) data available or capable of being collected on the limbs or their skeletal elements. A total of four primate samples met these criteria, detailed further below. Permission was obtained to use all samples and data (see *Appendix I*).

A final criterion was the ability to collect QTL data. The genotyping of a large enough number of markers for linkage analysis was beyond the scope of this project. Therefore, rather than attempt to genotype all samples undergoing phenotypic analysis, one of the samples – a baboon colony housed at the Texas Biomedical Research Institute (TBRI) – was selected because it has already been genotyped. These baboons serve as a model organism for humans because the approximately 300 STR markers typed by the TBRI all have homologues in the human genome (Rogers et al., 2000; Cox et al., 2006). This means that any findings on the TBRI Baboon sample relate directly to the human genome (e.g., Havill et al., 2005; Sherwood et al., 2008). While the TBRI sample is an excellent resource and is the sole sample for which QTLs can be potentially located, not all limb bones are available for analysis, making a complete analysis of all limb segments unfeasible. For this reason, a second baboon sample with complete limb data from the Primate Colony at Sukhumi is included.

Model Organisms

Baboons are Old World monkeys belonging to the taxonomic family Cercopithecidae. These primates have been shown to be ideal model organisms for humans for a number of reasons. Baboons share a variety of socio-ecological features with humans, including large populations and breeding units, wide geographic distribution, and extensive, terrestrial home ranges (Jolly, 2001; Kramer, 2005). These behavioral features influence genetic variation by maximizing gene flow and creating genetic heterogeneity within groups and increasing homogeneity between groups, similar to humans (Kramer, 2005). In addition, these primates share several biological features with humans, such as large body size, a long life span, and comparable hormonal changes throughout life (Brommage, 2001; Martin et al., 2003). The skeletal biology of baboons is also extremely similar to humans in that these primates show bone loss with age (Aufdemorte et al., 1993), undergo skeletal remodeling, and have similar microstructural and compositional properties (Wang et al., 1998b). For a more comprehensive discussion of the usefulness of baboons as a model organism for humans, see Havill et al. (2003).

Tamarins are New World monkeys belonging to the family Callitrichidae. They have a small body size and display quadrupedal locomotion in arboreal territories. While more distantly related to humans than baboons, tamarins have been used as model organisms because of their small body size, ease of maintenance, and breeding capabilities in captivity, including consistently producing twins (Gengozian, 1969). In fact, they have been called an excellent "bridge between the laboratory rodent and the larger primates that are more closely related" to humans (Gengozian, 1969:336). For these reasons, tamarins were also used in this study to see how a more distantly related primate compares to baboons and humans.

Sample Descriptions

*Tamarins (*Saguinas oedipus*)*

The first sample consisted of 250 (136 males, 114 females) adult skeletal cotton-top tamarins, housed in the Department of Anthropology at the University of Tennessee. These tamarins were bred at the Marmoset Research Center, Oak Ridge Associated Universities' (ORAU) colony, which was founded in 1961 with animals from South America (Gengozian, 1969; Cheverud, 1995). Four hundred one animals were imported between 1961 and 1976, and an additional 50 animals were transferred from the Rush Presbyterian-St. Luke's Medical Center colony in 1981 (Clapp & Tardiff, 1985; Cheverud et al., 1994). The colony consisted of these wild-caught founders and their laboratory-born offspring, and while a small but significant morphological difference was found in the crania of wild versus captive-born individuals (Cheverud, 1996b:22), it is not known if a similar difference is found in the long bones. This cotton-top tamarin collection has been used extensively to study cranial variation (Hutchison & Cheverud, 1995; Cheverud, 1996b; Ackermann & Cheverud, 2000), body weight (Cheverud et al., 1994), the genetic epidemiology of colon cancer (Cheverud et al., 1993), infant-care behavior (Tardif et al., 1990), and long bone asymmetry (Reeves et al., 2016).

Adult status was defined here as individuals with fused long bones. Tamarin long bones fuse between 0.75 and 2.0 years (Kohn et al., 1997). While ages were not available for all individuals in the sample, the age range for those with age available was 1.5-17.3 years (with the exception of one individual that was 0.76 years). The majority of these individuals come from one large, extended pedigree sample that is six generations deep, with the remaining individuals coming from several smaller pedigrees that are two to three generations deep. The total number

of pedigreed individuals is 435. Because this was a skeletal sample, all four limb segments could be measured: the maximum length of the humerus, radius, and tibia were measured, as well as the bicondylar length of the femur (see *Skeletal Measurements*, below). The right and left side elements were measured; however, only the right side elements were used in this study since it has been shown that tamarins do not exhibit directional asymmetry (Reeves et al., 2016). All measures were taken in triplicate and averaged, and intraobserver measurement error was small (see *Intraobserver Error*, below).

*Sukhumi Baboons (*Papio hamadryas spp.*)*

The second sample consisted of anthropometric measurements on 214 (75 males, 139 females) sedated live adult baboons that were collected from the Primate Colony at Sukhumi in the former U.S.S.R. (O'Rourke, 1980). The colony began in 1927 with the arrival of four monkeys, including two hamadryas baboons, from Africa to the Black Sea coastal city of Sukhumi at what was a part of the Institute of Experimental Endocrinology in Moscow. The original mission of the Institute was to breed non-human primates for research, but as research opportunities increased at the Institute, breeding became secondary to research (O'Rourke, 1980; Lapin & Fridman, 1965). The center became known as the Institute of Experimental Pathology and Therapy in 1957, and extensive medical and behavioral research took place there until the fall of the Soviet Union in 1991. While the Institute is still in existence, the majority of the scientists and primates have moved to a newer facility in Russia.

The data from these baboons were collected in 1977, and all animals were sedated with ketamine hydrochloride prior to data collection. The original data set consisted of 1,125 animals;

however, only those individuals that were greater than or equal to 96 months (eight years) were used here, reducing the sample size to 214. This was done to ensure that only individuals that had reached skeletal maturity were used, as baboons reach morphometric maturity between six and seven years of age (O'Rourke, 1980). These baboons are part of several large, extended pedigrees that are five to seven generations deep and contain over 1,200 individuals. Measurements were available for all four limb segments (i.e., upper arm, forearm, thigh, and leg), which were used here as approximations of the maximum lengths of the humerus, radius, and tibia, and the bicondylar length of the femur.

The phenotype and pedigree data were obtained from Dr. Michael Crawford with permission from Dr. Dennis O'Rourke. All data were in paper form, datasheets were scanned, and data were transcribed into electronic format in Excel. The electronic data were then checked for transcription accuracy.

*Mennonites (*Homo sapiens*)*

The third sample consisted of anthropometric measurements from 410 adult Mennonite human individuals (208 males, 202 females) from Kansas and Nebraska. Although the sample is comprised of individuals from three different communities, all stem from one large founding community and are thus genetically related individuals. A large congregation of Alexanderwohl Mennonites immigrated to New York City in 1874 and continued on to Lincoln, Nebraska. The congregation then split into three major branches: 1) a group settled west of Lincoln in present-day Henderson, Nebraska, 2) a group moved south and settled in Goessel, Kansas, and 3) a group settled near Inman, Kansas and became known as the Meridian Mennonites (Crawford & Rogers,

1982; Devor et al., 1986a). The original data set consisted of 34 anthropometrics on 1,197 individuals from Henderson (n = 537), Goessel (n = 573), and Meridian (n = 87). These data were collected in the early 1980s (Crawford & Rogers, 1982) and have been used to study the transmissibility of anthropometric variation (Devor et al., 1986a,b), biological aging, and longevity (Crawford et al., 2000; Crawford, 2005).

The portion of the larger sample used in this study are those individuals that are a part of nuclear families, thus meeting the criteria for inclusion. The sample of 410 included 237 individuals from Henderson, 135 from Goessel, and 38 from Meridian. The pedigrees in this sample were not as complex as those in the other samples: there were 117 small nuclear family pedigrees, each two to three generations deep. Of the 34 anthropometric measurements taken on this population, measures of the limbs were included, which could be used to calculate all four limb segments (see *Limb Segment Calculations*, below). As with the Sukhumi Baboons, the limb segment lengths were used here as approximations of the maximum lengths of the humerus, radius, and tibia, and the bicondylar length of the femur.

The Mennonite phenotype data were obtained from Dr. Michael Crawford in paper form. All datasheets were scanned and data were transcribed into electronic format in Excel. The electronic data were then checked for transcription accuracy. The pedigree information was in electronic format in Excel. It was assembled by Dr. Ravi Duggirala and made available by Dr. Michael Crawford.

*TBRI Baboons (*Papio hamadryas ssp.*)*

The fourth and final sample was skeletal measurements from 479 (140 males, 339 females) adult baboons from the Havill Osteology Laboratory at the TBRI in San Antonio, Texas. The Southwest National Primate Research Center (SNPRC), which is housed at the TBRI, is home to the largest captive colony of baboons in the world (about 1,600 animals), and a large segment of those individuals are part of the largest pedigreed population of baboons in the world (about 1,200 animals) (SNPRC website). The majority of the animals are olive baboons (*Papio hamadyras anubis*), and there are also yellow baboons (*P. h. cynocephalus*) and hybrids between these two subspecies (Rogers et al., 2000).

This sample had the most complex pedigree, and two different pedigrees were used. The first, containing 4,686 individuals spanning six generations, was the larger of the two pedigrees and contained all 479 measured individuals. This larger pedigree was used in the heritability, evolvability, and morphological integration analyses (see *Analyses*, below) since only pedigree and phenotype data were needed. The second pedigree, containing 2,426 individuals spanning six generations, only contained 468 of the measured individuals; however, this smaller pedigree is associated with genotype data. Therefore, the smaller pedigree was used in the linkage analysis (see *Analyses*, below) since pedigree, phenotype, and genotype data were all needed. Of the 2,426 individuals in the smaller pedigree, 2,044 individuals have been genotyped at all (or nearly all) of the 284 autosomal STR markers and 25 X-linked STR markers and placed in the whole baboon genome map at 1000:1 odds. Additionally, these STRs have been mapped to homologous locations in the human genome (Rogers et al., 2000; Cox et al., 2006; SNPRC website). This attribute makes the TBRI Baboons an invaluable resource for studying the genetic and

environmental effects on baboon phenotypes and for localizing QTLs which impact human phenotypic variation. The TBRI Baboons have been used to study such complex diseases as osteoporosis (Havill et al., 2005; Havill, 2007), cardiovascular disease (Kammerer et al., 2002; Vinson et al., 2005), and diabetes (Quinn et al., 2012), as well as morphological attributes such as the craniofacial complex (Sherwood et al., 2008), dental morphology (Hlusko & Mahaney, 2009), brain size and structure (Rogers et al., 2007), and femoral cross-sections (Hansen et al., 2009).

The bones measured for this project came from individuals that died naturally or were culled from the pedigreed colony. Once deceased, the right humerus and left and right femora were collected at necropsy, wrapped in saline-soaked gauze, and stored in large, -80^{o} C freezers. Therefore, there was a large amount of preparatory work that came before osteological measurements could be obtained. The bones had to be thawed and unwrapped, and then the adhering soft tissue had to be removed with scalpels to allow the bone to be properly measured. After measuring, the bones had to be re-wrapped in new saline-soaked gauze and placed back in the freezer. Data collection occurred during two month-long trips to the TBRI, one in the summer of 2009 and one in the summer of 2011.

Adult status was defined here as any individual with fused long bones, with fusion typically occurring by eight years of age (Leigh, 2009). The age range for the baboons was 6.93 to 33.27 years, with only three individuals being younger than eight years. The right humerus was available for the majority of individuals; however, individuals differed on whether the right femur, the left femur, or both femora were available for study. All available bones were measured. For this study, whichever side was available was used, and one side was randomly

selected in cases where both the right and left femur were measured (see *Side Randomization*, below). In addition to the maximum length of the humerus and bicondylar length of the femur, measurements of the proximal and distal articulations, diaphyses, and muscle attachments were taken (see *Skeletal Measurements*, below). All measures were taken twice and averaged, and intraobserver error was small (see *Intraobserver Error*, below).

Measurements

Skeletal Measurements

For the Tamarin and TBRI Baboon skeletal samples, the measurements that were taken included the maximum length of the humerus, radius, and tibia, and the bicondylar length of the femur (following Hallgrímsson et al., 2002). These measurements follow Buikstra and Ubelaker (1994:80-83) and are described below.

1) Humerus Maximum Length – "direct distance from the most superior point on the head of the humerus to the most inferior point on the trochlea. Humerus shaft should be positioned parallel to the long axis of the osteometric board."
2) Radius Maximum Length – "distance from the most proximally positioned point on the head of the radius to the tip of the styloid process without regard for the long axis of the bone."
3) Femur Bicondylar Length – "distance from the most superior point on the head to a plane drawn along the inferior surfaces of the distal condyles."
4) Tibia Length – "distance from the superior articular surface of the lateral condyle to the tip of the medial malleolus."

Additional measurements of the articulations, diaphysis, and muscular attachments (Buikstra and Ubelaker, 1994; Ruff, 2002b) were also taken on the TBRI Baboons in order to further explore long bone morphology (for sample data collection sheets, see *Appendix II*). See Table 1[8] for a list of all TBRI Baboon skeletal measurements as well as citations for measurement definitions. All measurements were taken on both the right and left sides, when available.

Anthropometric Measurements

For the anthropometric data sets (Mennonites and Sukhumi Baboons), limb segments (either measured or calculated, see *Limb Segment Calculations in the Mennonites*, below) were used as approximations of the maximum lengths of the humerus, radius/ulna, and tibia and the bicondylar length of the femur. To distinguish the fact that these measurements were anthropometric rather than skeletal, they are hereafter referred to as arm, forearm, thigh, and leg lengths.

The Sukhumi Baboon data were collected following definitions found in Schultz (1929) and Gavan (1953). The measurement definitions are as follows:

1) Upper Arm Length (referred to simply as Arm Length hereafter) – the distance from the most superior point on the humerus to radiale when the arm is extended across the chest (Gavan, 1953:96; O'Rourke, 1980:37).

[8] All Tables and Figures are in *Appendix IV*.

2) Forearm Length – the distance "from the most distal point on the ulnar styloid process to the most proximal point on the olecranon process" when the arm is in the supine position across the chest (Gavan, 1953:96; O'Rourke, 1980:37)[9].
3) Thigh Length – the distance from "trochanterion summum to femorale parallel to the long axis of the femur" (Schultz, 1929:235; O'Rourke, 1980:36).
4) Leg Length – the distance between tibiale and sphyrion parallel to the long axis of the tibia (Schultz, 1929:236; O'Rourke, 1980:37).

The Mennonite data were collected following definitions found in Montagu (1960). The measurement definitions are as follows:

1) Total Upper Extremity Length (used to calculate Forearm Length, see *Limb Segment Calculations in the Mennonites*, below) – "From acromiale to dactylion, i.e. the tip of the middle finger" (Montagu, 1960:9).
2) Upper Arm Length (referred to simply as Arm Length hereafter) – "From acromiale to radiale when the arm is hanging down and the palm facing forward" (Montagu, 1960:9).
3) Maximum Hand Length (used to calculate Forearm Length, see *Limb Segment Calculations in the Mennonites*, below) – "The distance from the mid-point of a line connecting the styloid processes of radius and ulna to the most anterior projection of the skin of the middle finger" (Montagu, 1960:13).

[9] It should be noted that the Sukhumi forearm length approximates maximum ulnar length rather than maximal radial length. The extent to which this will influence results is unknown.

4) Trochanterion Height (used to calculate Thigh Length, see *Limb Segment Calculations in the Mennonites*, below) – "From the superior surface of the greater trochanter of the femur to the floor" (Montagu 1960:11).
5) Tibiale Height (referred to as Leg Length hereafter) – "From the superior surface of the medial condyle of the tibia to the floor" (Montagu, 1960:11)[10].

Anthropometrics vs. Osteometrics

The commensurability of skeletal and anthropometric data is potentially complicated by the presence of soft tissue in the latter. Most discussion on this topic has focused on comparisons of heritability estimates from skeletal and anthropometric measurements of cranial dimensions with the general conclusion being that one cannot be a proxy for the other (see Carson, 2006 for a review); however, studies have shown that "bony" craniofacial measurements (i.e., those where skeletal features are more palpable) have a higher heritability than those that include more soft tissue (Nakata et al., 1974; Susanne, 1975), indicating that "bony" measures may be preferable to use when anthropometric data are needed. In the postcranial skeleton, it has been shown that socioeconomic and nutritional status can influence heritability estimates (Arya et al., 2002), indicating that genetic and environmental influences have an impact on both soft tissue and bone (Carson, 2006); however, there is a general consensus (Clark, 1956; Vandenberg, 1962; Leamy, 1974; Devor et al., 1986a,b; with exceptions being Susanne, 1977; Arya et al., 2002) that length measures in the postcrania have higher heritabilities than measures of girth or breadth. Schultz

[10] While the measurement definition from Montagu (1960) states that Tibiale Height is measured to the floor, personal communication with Dr. Laurine Rogers, one of the original data collectors, indicates that this measurement was actually taken to the inferior point of the medial malleolus. Therefore, this measurement is roughly equivalent to the length of the tibia and is used here as its proxy.

(1929), in his descriptions on taking anthropometric measurements on human fetuses and primates, states that the measures for leg length and forearm length are "practically identical" to the lengths of the tibia and radius, respectively, while the measures of the thigh and arm surpass the length of the femur and humerus "by a small amount" because of soft tissue (Schultz, 1929:236-238). All this supports the idea that the length measurements of the postcrania used in this study are the most preferable when anthropometric data are analyzed. While this issue will likely introduce some imprecision, the lack of available pedigreed skeletal human populations that include postcrania of known provenience makes this issue unavoidable.

Data Preparation and Screening

Limb Segment Calculations in the Mennonites

The Mennonite data were collected following standard anthropometric definitions found in Montague's (1960) volume, *A Handbook of Anthropometry* (Dr. Laurine Rogers, personal communication. Dr. Rogers is one of the original data collectors). While there were 35 anthropometric measurements taken on the Mennonite individuals, a few of the limb segments were not directly measured and had to be calculated.

For the upper limb, the measurements of Upper Limb Length, Upper Arm Length, and Right and Left Hand Lengths were available in the original data set, but Forearm Length was not. Therefore, Forearm Length was calculated as:

Forearm Length = Upper Limb Length – Upper Arm Length – Right Hand Length

This calculation produced brachial index averages (after outlier removal, see *Outlier Detection*, below) of 80.29 (range of 69.10-92.88) and 78.29 (range of 66.35-91.43) for males and females,

respectively. These averages fall within the normal range of human variation (Schultz, 1930; Holliday, 1995; Auerbach, 2007), and therefore provided support for the calculated measure of Forearm Length.

For the lower limb, the measurements of Trochanteric Height and Leg Length were available in the original data set. While Leg Length is equivalent to the maximum length of the tibia, there was no Foot Height measurement available that could also be subtracted from Trochanteric Height to provide an accurate estimation of Thigh Length. Therefore, a more complicated estimation procedure was used.

Summary statistics and correlation coefficients from military personnel collected for the *1988 Anthropometric Survey of U.S. Army Personnel* (Gordon et al., 1988) were used to estimate Foot Height for the Mennonite individuals. Regression equations were produced for males and females separately using the standard deviations of Trochanteric Height and Lateral Malleolus Height (equivalent to foot height and used in place of Medial Malleolus Height, which was not available) and the covariance between these two variables. For males, the regression equation used was:

Lateral Malleolus Height = 0.03882 * Trochanteric Height + 31.03

For females, the regression equation used was:

Lateral Malleolus Height = 0.03343 * Trochanteric Height + 31.80

For further details on these calculations, see *Appendix III*.

After estimating Lateral Malleolus Height for the Mennonite males and females, Thigh Length was calculated as follows:

Thigh Length = Trochanteric Height – Leg Length – Lateral Malleolus Height

This calculation produced crural index averages (after outlier removal, see *Outlier Detection*, below) of 87.22 (range of 76.56-98.25) and 83.03 (range of 72.10-96.13) for males and females, respectively. These averages again fall within the normal range of human variation (Schultz, 1930; Davenport, 1933; Holliday, 1995; Auerbach, 2007), and therefore provided support for the calculated measures of Lateral Malleolus Height and Thigh Length.

Outlier Detection

Outlier detection and removal was performed prior to all statistical analyses. Multivariate outlier detection was used for the Tamarins, Sukhumi Baboons, and Mennonites as these samples had all four limb segments available. Males and females were treated separately, as were the upper and lower limbs. For each of the three samples, outliers for the four data subsets (male upper limb, male lower limb, female upper limb, and female lower limb) were detected using a robust Mahalanobis D^2, which was produced after running a principal components analysis in NCSS (Hintze, 2006). While this method identifies more data points as outliers than other methods, it was selected because robust statistics are useful with a wide array of data distributions.

In addition to this method, the lower limb measurements from an additional Mennonite individual were removed. These measurements produced a crural index over 100, which was deemed biologically inappropriate.

Sample sizes decreased once outliers were removed, and some individuals who previously had complete data now had incomplete data. The new sample sizes were 239

Tamarins (129 males, 110 females), 204 Sukhumi Baboons (72 males, 132 females), and 398 Mennonites (201 males, 197 females).

Because only two of the four limb segments, which did not belong to the same limb, were available for the TBRI Baboons, and because a multitude of other morphometric traits were included, a different approach was taken to outlier detection in this sample. A univariate approach known as the Outlier Labeling Rule (Tukey, 1977; Hoaglin et al., 1986; Hoaglin et al., 1987) was used on each individual trait. This rule uses the following equation to identify outliers:

$$(Q3 - Q1) * 2.2 = g \quad (4.1)$$

where Q1 and Q3 are the first and third quartiles, respectively. The product g was then added to Q3 and Q1 to produce upper and lower bounds. Any points falling outside of this range were considered outliers and removed from the data set. Males and females were analyzed separately. Using the Outlier Labeling Rule, only 16 data points were removed from the data set; however, the overall number of individuals did not decrease.

Side Randomization and Trait Reduction in TBRI Baboons

An abundance of data were collected on the TBRI Baboons since bone preparation was so time intensive; however, not all data that were collected were used for this study. The first step in data reduction was to select one femur to use for individuals (n = 104) in which both femora were available for study. Paired *t*-tests were run in SPSS (IBM Corp., 2012) to check for significant differences between measurements from the left and right femora. Six of the 15 femoral measurements (50% AP Diameter, 25% AP Diameter, 75% AP Diameter, Articular Breadth, Lateral Condyle Breadth, and Lateral Condyle Depth) were significantly different at the

$p = 0.05$ level (see Table 2). The mean differences between sides for these traits ranged from 0.09 mm to 0.28 mm. Therefore, these differences were deemed to be biologically insignificant, and it was determined that the right and left side femora could be used interchangeably. Half those individuals with both femora present were selected to use the left femur (26 males and 26 females), and the other half were selected to use the right femur (26 males and 26 females).

The second step in data reduction for the TBRI Baboons was to reduce the number of traits to analyze. Given the fact that many of the measurements were redundant and measured similar things (for example, the trochlear breadth and capitular breadth of the distal humerus were measured, as well as the distal articular breadth, which is the combination of these two measurements), the number of traits was reduced. Reduction was done in such a way to provide comparable measurements for the humerus and femur. The final suite of traits selected for analysis was comprised of five measurements from each bone, including: 1) a length measurement (Humerus Maximum Length and Femur Bicondylar Length), 2) a diaphyseal measurement (the average of anterio-posterior diameter and medio-lateral diameter at 50% of length for both the humerus and femur, which are called Humerus 50% Diameter Average and Femur 50% Diameter Average), 3) a proximal articulation (Humerus Head Length and Femur Head Diameter), 4) a distal articulation (Humerus Distal Articular Breadth and Femur Articular Breadth), and 5) a muscle attachment (Humerus Epicondylar Breadth and Femur Bicondylar Breadth).

Summary Statistics

Summary statistics, including mean, standard deviation, and range, were calculated independently for males and females separately and combined for all four samples and can be found in Tables 3 through 6.

Intraobserver Measurement Error

Intraobserver measurement error was calculated following White (2000) on the Tamarins and TBRI Baboons since these two samples were personally measured rather than transcribed from previously-collected data. The Tamarin skeletons were measured in triplicate over a short amount of time, and average intraobserver measurement error ranged between 0.009% and 0.015% (see Table 7).

The TBRI Baboons were measured twice, sometimes with a great length of time between successive measurements. For this reason, multiple intraobserver measurement errors are reported to show consistency in measuring across time. As shown in Table 8, average intraobserver error rates are given for those individuals measured twice in 2009, those measured once in 2009 and once in 2011, and those measured twice in 2011. Additionally, there is an overall average intraobserver error rate which was produced by looking at all individuals simultaneously. This error rate ranges between 0.071% and 0.915%.

Analyses

Genetic Variance

Both heritability and evolvability analyses, which look at the genetic variation in a sample, make use of pedigree and phenotype data. Pedigrees were formatted using Excel version 14 (2010) such that each individual had a separate row in the data file. Each line consisted of that individual's unique identification (ID) number, Father's unique ID number, and Mother's unique ID number. An unknown parent was coded as a 0, including the parents of founding individuals. For subsequent analyses to run properly, the pedigree had to be ordered so that no offspring were listed before their parents. The "OrderPed" command in the MasterBayes package (Hadfield, 2012) in R (R Core Team, 2014, version 3.1.2) was used to sort the pedigrees in this manner. Phenotype files were also formatted in Excel, again with each individual having a separate row. Each line included the individual ID number, sex (coded as either M/F or 1/2), and all phenotypes of interest. Individuals with unknown sex were not allowed, and missing phenotypic data were coded as NA.

Analyses were performed using the MCMCglmm package (Hadfield, 2010), also available in R, which uses a Markov Chain Monte Carlo (MCMC) Bayesian approach to work with generalized linear mixed models. This method requires the establishment of a prior distribution based on the data that the algorithm moves through in order to produce a posterior distribution. Pertinent results, such as heritability or evolvability, are then estimated from the posterior distribution. The MCMCglmm package uses an inverse-Wishart distribution for establishing priors, which incorporates *V*, variance, and *nu*, a belief parameter, both of which must be larger than 0 to establish proper priors (Hadfield, 2014). The belief parameter tells the

algorithm how much attention to give the prior distribution when creating the posterior distribution.

The MCMC portion of the analysis samples the posterior distribution, moving stochastically through the parameter space of the distribution (Hadfield, 2014). The Markov Chain determines what gets sampled from the distribution, while the Monte Carlo determines how the chain moves through parameter space. After initializing, the chain must decide where to go next in the parameter space. It will move to a new space and compare the new parameters located here (namely the mean and variance) to the old parameters at the previous location. If the new parameters have a higher posterior probability, then the chain moves to the new location. If the new parameters have a lower posterior probability, then the chain may or may not move to the new location. Each of these moves through parameter space is one iteration, and these iterations can be used together to generate an approximation of the posterior distribution (Hadfield, 2014). The goal of the chain is to reach the highest possible posterior probability.

The beginning iterations can have a strong dependence on the starting parameters, which then diminishes as the iterations continue. This is known as the Markov chain converging, and in order to only store iterations which are not dependent on the beginning parameters, a "burn-in" period is used. This is the number of iterations that are discarded before iterations are stored for later use. Autocorrelation in the chain reduces with an increase in the number of iterations, and autocorrelation between stored iterations is reduced by saving a portion of the total number of iterations, a process known as "thinning." For example, one in every 10 iterations may be stored for later use.

A multivariate model was run for each of the four samples with each limb segment as a dependent variable and sex as a fixed effect. The models also included *V*, *nu*, pedigree information, specifications for total number of iterations, burn-in period, and thinning interval, and the prior. Priors were established for both the random effect and the residual in each model with a belief parameter equivalent to the number of traits (*nu* = 4 for the Tamarins, Sukhumi Baboons, and Mennonites, and *nu* = 2 for the TBRI Baboons) and the assumption that a large portion of variation found in each trait was under genetic control (*V* = the trait phenotypic variance divided by 2). This set up is typical of analyses where large amounts of data are available relative to the complexity of the model (Wilson et al., 2009a,b). Each sample was initially run with 700,000 total iterations, a burn-in of 200,000 iterations, and a thinning interval of 50 iterations and checked for autocorrelation using the "autocorr" command. A reasonable goal is have autocorrelation less than 0.1 in 1,000 to 2,000 stored iterations (Hadfield, 2014). Each sample showed different levels of autocorrelation in the first run. For example, Mennonite autocorrelation was below the 0.1 threshold with the thinning interval of 50, while the other three samples had high autocorrelation at this thinning interval. Therefore, all four models were run a second time to: 1) reduce autocorrelation to an acceptable level, and 2) provide consistency in iteration sampling among the samples. The final model for each of the four samples had a run length of 900,000 iterations, a burn-in of 200,000 iterations, and a thinning interval of 350 iterations. This provided 2,000 stored iterations for each model with an autocorrelation below 0.1.

Posterior distributions were used to generate pertinent results. The posterior distribution of the genetic variance for each of the four samples can be thought of as a *k*-trait by *k*-trait by *i*-

sample array of output values from the MCMCglmm run. Each *k* x *k* slice of the *i*-length array is an estimated variance-covariance matrix for each stored iteration of the Markov chain, and *i* is equal to the number of stored iterations. For the Sukhumi Baboon, Mennonite, and Tamarin samples, this would be 2000 individual 4 x 4 matrices because there are four limb segments and 2000 stored iterations, and the TBRI Baboon sample would be 2000 2 x 2 matrices. So, for example, the posterior distribution of genetic variance for Humerus Length in the Tamarin sample is comprised of 2000 individual estimates, one from each MCMC iteration, each found in the same on-diagonal cell of all the 4 x 4 matrices. A similar *k* x *k* x *i* array is also available for the environmental variance, which is all variance that is not explained by the genetic variance. The element-wise sum of the genetic variance array and the environmental variance array produces the phenotypic variance array. A similar set up of posterior distributions for the means are also produced after the MCMCglmm run.

These arrays can be manipulated to produce relevant results within a sample, as described below. For each element in the array, whether an estimate of the mean or of the variance, a point estimate can be generated using the "posterior.mode" command. This is the estimate at the highest point on a plot of the posterior distribution. The command "HPDinterval" provides a 95% credibility interval for any estimate. The 95% credibility intervals for two estimates within a sample can be subtracted from one another to see if the estimates are statistically different. If the resulting interval crosses zero, then the posterior distributions for the two estimates are not different; however, if the resulting interval does not cross zero, then the posterior distributions for the two estimates are different.

The following matrices were then created for each sample: 1) a phenotypic VCV matrix, 2) a genetic VCV matrix, and 3) an environmental VCV matrix. The values on the diagonal of the genetic VCV matrix are the additive genetic variance of the trait. The environmental VCV matrix is all variance that cannot be explained by the genetic VCV. And, as mentioned earlier, the combination of the genetic and environmental variance produces the phenotypic variance. All three of these matrices included corresponding matrices of high and low credibility interval matrices and a matrix of standard error. Additionally, each of these three matrices was produced in the form of a correlation matrix with the same corresponding interval and standard error matrices. Genetic correlation is the proportion of variance that two traits share because of common genetic causes, while environmental correlation is the proportion of variance that two traits share due to common environmental effects.

Heritability

Narrow-sense heritability is calculated as:

$$h^2 = V_A / V_P \quad (4.2)$$

where V_A is the additive genetic variance and V_P is the phenotypic variance[11]. Therefore, heritability was calculated here as the posterior distribution of the genetic variance for the trait divided by the sum of the posterior distribution of the genetic variance for the trait and the posterior distribution of the environmental variance of the trait. A point estimate (posterior.mode) and credibility interval (HPDinterval) can then be produced from this calculation. The credibility

[11] This equation is the same as Equation 3.5, above.

intervals for two different traits can then be subtracted from one on another, as described above, to test whether they are different from one another.

Evolvability

Evolvability is calculated as:

$$e = V_A / m^2 \quad (4.3)$$

where V_A is the additive genetic variance and m^2 is the squared trait mean[12]. Therefore, evolvability was calculated here as the posterior distribution of the genetic variance for the trait divided by the squared posterior distribution of the mean of the trait. As before, a point estimate and credibility interval can be produced and tested for significance against other traits.

Conditional Evolvability

Conditional evolvability is calculated as:

$$c = 1 / [G^{-1}] \quad (4.4)$$

where G^{-1} is the inverse G matrix[13]. Therefore, conditional evolvability was calculated here as the 1 divided by the posterior distribution of the diagonal element of the inverse G matrix. As before, a point estimate and credibility interval can be produced and tested for significance against other traits.

[12] This equation is the same as Equation 3.11, above.
[13] This equation is the same as Equation 3.12, above.

Integration

Not to be confused with the measures of integration discussed below, this measure of integration looks at the relationship between evolvability and conditional evolvability to see how closely related the two measures are. It is calculated as:

$$i = 1 - (c / e) \quad (4.5)$$

Therefore, *i* was calculated as 1 minus the quotient of the posterior distribution of *c* divided by the posterior distribution of *e*. A point estimate and credibility interval can be produced and tested for significance against other traits.

Intra-Sample Comparisons

The phenotypic variance, genetic variance, heritability, evolvability, and conditional evolvability estimates for each limb segment within a sample were compared to test whether they were significantly different from one another. Additionally, phenotypic correlation and genetic correlation between pairs of limb segments were compared within each sample. If zero was included in the resulting interval produced from the difference between the credibility intervals of two traits, then the estimates for the two traits are not significantly different from one another.

Inter-Sample Comparisons

Similar comparisons were done to look for significance between the different samples. Because each of the individual Markov chains were well-mixed (i.e., the autocorrelation was brought down to acceptable levels), the four models may be compared. Phenotypic correlation, genetic correlation, heritability, evolvability, and conditional evolvability estimates were

compared the same way as in the intra-species comparisons. The genetic variance comparisons differed in that the inter-sample comparisons used the results of the genetic correlation matrices to make comparisons.

Morphological Integration

The morphological integration analyses, which look at the covariation in a sample, differ from the heritability and evolvability analyses in that they only require knowledge of phenotype data. Therefore, pedigree information was unnecessary for this segment of the analyses. Morphological integration was explored in two different ways. The first was to look at within-bone integration within the humerus and femur using the TBRI Baboons because multiple dimensions were available for only these two bones. The second method of exploring morphological integration was to look for integration across all four limb elements using the other three samples.

Within-Bone Morphological Integration

The within-bone integration analysis of the TBRI Baboon sample was divided into three separate analyses: 1) humerus only, 2) femur only, and 3) humerus and femur combined. The methodology outlined by Magwene (2001) was followed to test for within-bone integration in these three separate analyses. In this method, the relationship between two variables can be thought of as an edge. The Edge Exclusion Deviance determines whether an edge can be eliminated from a model because there is no significant relationship between those two variables. Edge Exclusion Deviance was calculated as:

$$-N * ln\left(1 - \left(\rho_{ij*\{K\}}\right)^2\right) \quad (4.6)$$

where N was the sample size and $\rho_{ij*\{K\}}$ was the partial correlation coefficient between the two variables with all other variables held constant. Partial correlation coefficients were calculated in SPSS (IBM Corp, 2012). Any edge with a deviance less than 3.84, which corresponds to a 5% point on the χ^2-distribution with 1 degree of freedom, was discarded. For those edges that were not eliminated from the model, an Edge Strength was calculated, which can be interpreted as an indicator of the copredictability among traits. Edge Strength was calculated as:

$$-0.5 * ln\left(1 - \left(\rho_{ij*\{K\}}\right)^2\right) \quad (4.7)$$

where $\rho_{ij*\{K\}}$ again represented the partial correlation between the two variables with all other variables held constant. A higher Edge Strength indicates a higher amount of morphological integration between the two traits.

To further test these within-bone integration patterns and provide verification for the Magwene (2001) methodology, Mantel (1967) tests were used to test for the significance of the correlation between correlation matrices and model matrices. For each of the three analyses (i.e., humerus only, femur only, and humerus and femur combined), correlation matrices for the five humerus and/or five femur measurements were produced using the PopTools add-in in Excel (Hood, 2011). Then, the humerus and femur were each divided into four different categories for analysis, including 1) length, 2) articulations, 3) diaphysis, and 4) muscle attachment. These four categories of measurements were then used to create multiple model matrices for the bones individually and combined. The models are listed below.

Model 1 – Lengths integrated

Model 2 – Articulations integrated

Model 3 – Diaphyses integrated

Model 4 – Muscle Attachments integrated

Model 5 – Lengths and Articulations integrated

Model 6 – Lengths and Diaphyses integrated

Model 7 – Lengths and Muscle Attachments integrated

Model 8 – Articulations and Diaphyses integrated

Model 9 – Articulations and Muscle Attachments integrated

Model 10 – Diaphyses and Muscle Attachments integrated

Models 1, 3, and 4 were only possible in the humerus and femur combined analysis, because there was only one measurement applicable to these categories in the humerus only and femur only analyses.

A sample model is shown in Table 9. A 1 indicates integration between the two measures, while a 0 indicates no integration. This example is a femoral model for integration between the proximal and distal articulations (or the Femur Head Diameter and Femur Distal Articular Breadth) and the muscle attachment (or the Femur Bicondylar Breadth), which corresponds to Model 9 listed above.

Mantel tests with 1000 iterations, performed in Pop-Tools (Hood, 2011), were used to compare the original correlation matrices with the various model matrices. A *p*-value was calculated for each model by determining the number of iterations with correlations higher than

the original correlation between the two matrices and dividing by 1000. The null hypothesis of no relationship between the two matrices was rejected when the *p*-value was less than 0.05.

Only individuals without missing data were used in the within-bone morphological integration analyses, so sample sizes were again reduced. Three separate data sets were used: 1) a humerus only sample size of 417 individuals (124 males, 293 females), 2) a femur only sample size of 344 individuals (111 males, 233 females), and 3) a combined humerus and femur sample size of 320 individuals (104 males, 216 females).

Morphological Integration Across Four Limb Segments

The second method of exploring morphological integration was to look for integration across all four limb elements using the Tamarin, Sukhumi Baboon, and Mennonite samples following the protocol set out by Pavličev et al. (2009). For each sample, correlation matrices were produced for the upper limb elements, the lower limb elements, the proximal limb elements, the distal limb elements, and all four elements. The relative eigenvalue variance of each matrix was calculated as:

$$V_{rel}(\lambda) = V(\lambda) \,/\, (n-1) \tag{4.8}$$

where V[14] is variance, λ is the eigenvalues, and n is the number of traits. Relative eigenvalue variance is used to explain the overall integration of each correlation matrix. It has a range of zero to one, and a higher number indicates more integration. Correlation matrices, eigenvalues, and relative eigenvalue variances were calculated in R using the posterior distributions from the models created for the genetic variance analyses. Point estimates and credibility intervals were

[14] Following Pavličev et al., (2009), variance is normalized by the number of traits (n) rather than n-1. In practice, this means using the population variance rather than the sample variance for calculations.

created using the posterior.mode and HPDinterval commands as described above. Because the eigenvalue variances were produced using the correlation matrix, rather than a variance/covariance matrix, and because each model was well-mixed, the results could be directly compared across samples. This was done by comparing the credibility intervals and seeing if zero is included in the resulting interval (with a zero meaning that the two estimates are not significantly different).

Linkage Analysis

Linkage analysis required the use of phenotype and pedigree data, as well as genotype data. This portion of the analyses was performed solely on the TBRI Baboons as it was the only sample with genotype data available. The phenotype file was formatted in Excel with each of the 468 measured individuals having a separate row. Each row consisted of the individual's unique identification number (ID), age, sex, and all ten of the humerus and femur traits. Age and sex were known for all individuals, and cells with missing data were left blank. The pedigree file, consisting of 2,426 individuals, was available through the TBRI server (details below) and included the individual's unique ID number, father's unique ID number, mother's unique ID number, and sex. Unknown parents, such as the parents of founders, were left blank.

Genotype data on 284 autosomal STRs and 25 X-linked STRs for 2,044 individuals in the pedigree were also previously formatted and available through the TBRI server (details below). Using the pedigree and allele frequencies, SOLAR (discussed below) creates Identity-By-Descent (IBD) matrices for each marker. These matrices contain a value for every pair of individuals in the pedigree, with each value being the probability that those two individuals share

an allele based on how closely related they are. A maximum likelihood estimation procedure is used to impute marker genotypes for individuals who have not been typed. The IBD files for each marker and a map of all markers on a single chromosome are then used to create Multipoint Identity-By-Descent (MIBD) files for each chromosome. The MIBD method used by SOLAR is useful in pedigrees of extensive size and complexity and is described in depth in Almasy & Blangero (1998). This method is an extension of the method by Fulker et al. (1995) which calculated multipoint identity-by-descent in sibships only. The allele frequencies, IBD files, map files, and MIBD files were previously generated and available on the TBRI server (details below).

All linkage analyses were run using the software SOLAR (Almasy & Blangero, 1998), version 7. SOLAR stands for Sequential Oligogenic Linkage Analysis Routines and is capable of working with large, complex pedigree data. SOLAR was accessed remotely through the TBRI server, with permission, using SSH Secure Shell Client version 3.2.9 (SSH Communications Security Corp., 2003).

Prior to linkage analyses, the data were checked for appropriate distribution and covariates were screened for significance. The variance components approach used in SOLAR is sensitive to non-normality, particularly high kurtosis, as this leads to biased parameter estimates and an increased false positive rate (Göring et al., 2001). Kurtosis of 0.8 or lower is desired, and if higher than that, data transformation is recommended. Therefore, an inverse normalization procedure was used to normalize all of the data. The "inormalize" procedure in SOLAR is a rank-based normalization method allows the variable to be normally distributed (with a mean of 0 and a standard deviation of 1). Even after inormalization, two traits (Femur Head Diameter

and Femur 50% Diameter Average) retained high kurtosis. For these two traits, the residuals from the inormalized data were inormalized to further reduce kurtosis and diminish the effects of skewed data (following Sherwood et al., 2008).

Covariates were screened for significance using two different methods, and covariates that were not significant were removed from subsequent analyses. The covariates that were screened were age, sex, age*sex (testing for an interaction between age and sex), age^2 (testing for a non-linear curve between age and the trait), and age^2*sex (testing for a non-linear curve between age and trait in each sex). The first method of screening was to use the polygenic screen function, which dropped one of the five covariates at a time, testing for a significant change in the model. If no change was found, then the covariate was considered non-significant and could be removed from further analyses. In this method, there were always at least four covariates in the model. The second method, the BayesAvg procedure, used a Bayesian approach and tested all possible combinations of covariates. Therefore, there was anywhere from one to five covariates in the model. The best combination of covariates was determined by the model with the lowest Bayesian Information Criterion (BIC). These two methods produced the same combination of covariates for six of the ten traits. For the other four traits, the covariates selected by the Bayesian method were used since more combinations of covariates were tested.

Once distribution issues were resolved and significant covariates were determined, linkage analyses were performed. The variance decomposition approach utilized in SOLAR specifies the expected genetic covariances between random relatives as a function of the identity by descent relationships at a given locus (Almasy & Blangero, 1998). The covariance matrix for the pedigree is then modeled as the sum of the additive genetic covariance due to the QTL, the

additive genetic covariance due to loci other than the QTL, and the variance due to environmental factors (Havill et al., 2005; Sherwood et al., 2008). Each of the ten traits was run in a univariate multipoint linkage to test for evidence of linkage between individual trait phenotypic variation and the 309 STR loci. All ten univariate linkage analyses were performed using the "multipoint" command in SOLAR. The hypothesis of linkage was tested at four-centimorgan (cM)[15] intervals by comparing the likelihood of a model in which the genetic variance due to the QTL was zero (i.e., a restricted model where there is no linkage) to the likelihood of a model in which the genetic variance due to the QTL was estimated (i.e., did not equal zero). A LOD score, calculated as the difference of the two *ln* likelihoods divided by *ln* 10 (Ott 1999), was produced every four cM, and areas with a LOD greater than 0.5 were rescanned every one cM.

The LOD score, or logarithm of odds, was developed by Morton (1955) and is used to compare the likelihood that a trait and marker are actually linked versus seeing the same data purely by chance. A LOD of three indicates 1000 to one odds that the observed linkage did not occur by chance. For the baboon pedigree, a LOD score associated with a genome-wide *p*-value of 0.05 was used. This LOD score, based on pedigree complexity and the finite marker locus density in the baboon linkage map, is a modification of Feingold et al. (1993) that was previously calculated and used in other studies utilizing the same baboon pedigree and marker maps (e.g., Sherwood et al., 2008). Based on these previous calculations, a LOD of 2.75 or greater was considered significant and corresponds to a false positive result once in 20 genome-wide linkage

[15] Named in 1919 by Haldane (1919), a centimorgan (cM) is a unit of chromosome length, with one cM corresponding to a 1% chance that a marker at a genetic locus will be separated from another locus due to crossing over during meiosis. In humans, 1 cM is equivalent to approximately one million base pairs (Lodish et al., 2004).

scans. Additionally, a LOD score of 1.5 was used as "suggestive" evidence of linkage, which is a result that would be expected to occur once in a genome-wide linkage scan (Lander & Kruglyak, 1995). While suggestive linkages may often be wrong, they are "worth reporting – if accompanied by an appropriate warning label about their tenuous nature" (Lander & Kruglyak, 1995:244).

String plots showing LOD scores for all chromosomes were produced for each of the ten univariate linkage analyses. SOLAR requires an X window system to produce graphics. The program Xming (Harrison, 2007), available as a free download, provided the appropriate X-based graphical user interface for producing plots. The TBRI server and Xming were connected using an alternative remote access program called PuTTY (Tatham, 2011), also available as a free download. Once the plots were created using PuTTY and Xming and saved as postscript (.ps) files to the TBRI server, they were transferred from the server to the PC using SSH. Adobe Acrobat XI (Adobe Systems Inc., 2012) was then used to open the postscript files and save them as either PDF or JPEG files.

Genomic areas in which significant LOD scores were found were then further analyzed to look for candidate genes influencing phenotypic variation. This was done using a few websites. First, the SNPRC Baboon to Human Comparative Maps website (SNPRC CompMaps website) was used to identify the STR markers which surround the region with the significant LOD score. While the chromosome numbers used by SNPRC are the orthologous human chromosome numbers, the locations of the LOD scores are based on the baboon maps. Each chromosome comparative map gives the location (in cM) of the STR loci on the baboon chromosome, as well

as the corresponding human location (Marshfield Position) and the base pairs (bps) where the STR physically lies on the human chromosome.

Once the range of bps of interest was determined, the next website used was the University of California, Santa Cruz (UCSC) Genome Browser (Kent et al., 2002; Karolchik et al., 2014). This website allowed the genes within the region of interest to be determined. An introductory tutorial useful for understanding basic search and display options in the UCSC Genome Browser is available from Open Helix (Open Helix website). Searching used the Genome Reference Consortium (GRC) h37/hg19 assembly from February 2009, the most recent reference assembly available. This assembly is highly accurate, with less than one error per 10,000 bases, and highly contiguous, with the only gaps being those where current technology cannot reliably sequence (UCSC Genome Browser website). Results were found in the UCSC Genes track based on data from multiple sources, including the National Center for Biotechnology Information (NCBI) RNA reference sequence collection (known as RefSeq), the National Institutes of Health genetic sequence database (known as GenBank), and others. The function of the genes was noted in the annotation section of each entry (Karlochik et al., 2014).

Protein Networks

After compiling a list of known genes from a region of interest, the coding genes (i.e., proteins) were further analyzed using a program called STRING version 10 (Szklarczyk et al., 2015), which stands for Search Tool for the Retrieval of Interacting Genes/Proteins. This program is a database of known and predicted protein interactions with evidence for gene interaction coming from genomic context, high-throughput experiments, coexpression of

proteins, and previously published literature (Jensen et al., 2009). Each list of genes was analyzed under the "multiple names" tab after setting the organism to *Homo sapiens*. The resulting pictures of protein interactions were visually analyzed for interesting connections. Additionally, proteins from each of the areas of interest were run a second time through STRING, this time including a list of proteins that are known to be involved in limb or bone formation (see *Results*, below), the majority of which are described previously (see *Limbs*, above). While this list is not exhaustive, those included are the major proteins involved in limb and bone formation. The resulting protein interactions were again visually analyzed for notable connections.

CHAPTER FIVE
RESULTS

Genetic Variance Analyses

The results of the genetic variance analyses (previously described, see *Research Design*, above), using the MCMCglmm package (Hadfield, 2010) in R (R Core Team, 2014) are described below. These results will be used to respond to Developmental Perspective Hypothesis 1 and Evolutionary Perspective Hypotheses 1 and 2[16]. For each sample, phenotypic, genetic, and environmental variance/covariance (VCV) matrices are provided, as well as phenotypic, genetic, and environmental correlation matrices. For all matrices (Tables 10 – 15, 17 – 22, 24 – 29, and 31 – 36), the variance/covariance/correlation estimates are in bold, the standard error of the estimate is in parentheses, and the 95% credibility interval for the estimate is below. Additionally, a table is available for each sample (Tables 16, 23, 30, and 37) showing the results of the heritability, evolvability, and conditional evolvability estimates.

To compare limb segment values within and across samples, many independent tests were performed, as described in the previous chapter. The results of these comparisons are found in seven tables (Tables 38 through 44). Table 38 shows the results of the intra-sample comparisons for phenotypic variance, which looks at the phenotypic variance across limb segments (i.e., compares the phenotypic variance of the humerus and the radius within one sample, as well as all other comparisons of the limb segments). (Inter-sample comparisons of phenotypic variance were not possible as the phenotypic correlation values would be used to

[16] All formal responses to hypotheses are included in the *Discussion and Conclusions* chapter, below.

compare across samples, and all on-diagonal phenotypic correlation values are 1). Table 39 shows the intra- and inter-sample comparisons for phenotypic correlation. For the intra-sample comparisons, the correlation between two limb segments is compared to the correlations from all other pairs of limb segments (for example, the correlation between the humerus and femur was compared to the correlation between the humerus and radius, as well as all other limb combinations). The inter-sample comparisons compare the correlation between the same two limb segments across samples (for example, the correlation between the humerus and femur in the Tamarins was compared to the same phenotypic correlation in the other three samples). Table 40 shows the results of the intra- and inter-sample comparisons for genetic variance. Intra-sample comparisons look at the genetic variance across limb segments (similar to the phenotypic variance comparisons), while inter-sample comparisons look at differences in genetic variance for a single limb segment in two different samples using values from the genetic correlation tables. Table 41 shows intra- and inter-sample comparisons for genetic correlation, which is similar to the Table 39 showing the intra- and inter-sample comparisons for phenotypic correlation. Tables 42, 43, and 44 show the intra- and inter-sample comparisons for heritability, evolvability, and conditional evolvability, respectively. For all three of these tables, intra-species comparisons look at the estimates across limb segments, while inter-sample comparisons looked at differences in estimates for a single limb segment in two different samples. The results in these tables should be used to aid in interpreting the tables for each individual sample.

For ease of interpretation in Tables 38 through 44, all four samples use the abbreviations of H (humerus), R (radius), F (femur), and T (tibia) despite the fact that these limb segments are called the arm, forearm, thigh, and leg for the Sukhumi Baboons and Mennonites throughout the

text. There are also many gray cells in these tables, which indicate comparisons that are either 1) redundant, 2) self-comparisons in intra-sample comparisons (e.g., humerus and humerus in the Tamarins), 3) not done (e.g., comparing the humerus of one sample to the tibia of another sample), or 4) not possible (because the TBRI Baboon sample is limited to two limb segments).

Intra-Sample Comparisons

Tamarins

Tables 10, 11, and 12 are the phenotypic, genetic, and environmental VCV matrices for the Tamarins, respectively, and Tables 13, 14, and 15 are the corresponding correlation matrices. Heritability (h^2), evolvability (*e*), conditional evolvability (*c*), and integration (*i*) estimates, along with 95% credibility intervals for each, are found in Table 16. The posterior distributions for h^2, *e*, and *c* for each of the four limb segments are found in Figures 1, 2, and 3, respectively. All of these figures show good, even distributions of the posterior estimates produced by the MCMCglmm model.

Phenotypic variances for the Tamarin limb segments, found on the diagonal of Table 10, range from 2.772 to 5.167. Table 38, which shows the results of the intra- and inter-sample comparisons for phenotypic variance, indicates that all but one of the phenotypic variance comparisons within the Tamarins are significant (i.e., the interval resulting from the difference between the two credibility intervals did not include zero), the exception being the comparison between the humerus phenotypic variance and the radius phenotypic variance. The elements of the upper limb have a reduced phenotypic variance compared to elements of the lower limb. Within the lower limb, the tibia has more phenotypic variance than the femur. The phenotypic

correlation comparisons, shown in Tables 13 and 39, indicate that the phenotypic correlation between the humerus and radius ($corr_p$ = 0.861) is significantly different from that of the humerus and femur ($corr_p$ = 0.788), the humerus and tibia ($corr_p$ = 0.812), and the radius and femur ($corr_p$ = 0.794). Additionally, the phenotypic correlation of the femur and tibia ($corr_p$ = 0.874) is significantly different from the same three limb combinations. This means that the elements of the upper limb have a higher correlation with each other than the humerus does with either of the lower limb elements, and the elements of the lower limb have a higher correlation with each other than the femur does with either element of the upper limb.

Additive genetic variances for the Tamarin limb segments, found on the diagonal of Table 11, range from 1.276 to 2.431. Table 40, which shows the results of the intra- and inter-sample comparisons for additive genetic variance, indicates that several of the genetic variance comparisons within the Tamarins are significant. The comparisons between the humerus (σ_g^2 = 1.276) and femur (σ_g^2 = 2.284), between the radius (σ_g^2 = 1.282) and femur, between the humerus and tibia (σ_g^2 = 2.431), and between the radius and tibia are all significantly different from one another. This means that homologous elements and non-homologous elements in different limbs show different levels of additive genetic variance, but additive genetic variance for limb segments found within the same limb are not significantly different from one another. However, when the genetic correlations of these limb segments are compared to one another, there is no significant difference found between any of them (Table 14). Additionally, there are no significant differences between any of the pairs of genetic correlations (i.e., off-diagonal values, Table 41) for the Tamarins, results which are much different than the phenotypic correlation comparisons described above.

Despite the significant differences found in the phenotypic variances and correlations and additive genetic variances of the Tamarin limb segments, Tables 42, 43, and 44 show that none of the heritability (ranging from 0.445 to 0.527, as seen in Table 16), evolvability (ranging from 0.000519 to 0.000616), conditional evolvability (ranging from 0.000101 to 0.000129), or *i* estimates[17] (ranging from 0.773 to 0.832) are significantly different from one another within the Tamarin sample.

Sukhumi Baboons

Tables 17, 18, and 19 are the phenotypic, genetic, and environmental VCV matrices for the Sukhumi Baboons, respectively. Tables 20, 21, and 22 are the corresponding correlation matrices. Heritability (h^2), evolvability (*e*), conditional evolvability (*c*), and integration (*i*) estimates, along with 95% credibility intervals for each, are found in Table 23. The posterior distributions for h^2, *e*, and *c* for each of the four limb segments are found in Figures 4, 5, and 6, respectively. All of these figures again show good, even distributions of the posterior estimates produced by the MCMCglmm model.

Phenotypic variances for the Sukhumi Baboon limb segments, found on the diagonal of Table 17, range from 66.366 to 158.179. Table 38 shows that all but one of the phenotypic variance comparisons within the Sukhumi Baboons are significant, the exception being the comparison between the phenotypic variances of the arm and the forearm. The thigh has the highest level of phenotypic variance and the tibia has the lowest level of phenotypic variance, while the elements of the upper limb are in the middle. The phenotypic correlation comparisons

[17] The results of the intra- and inter-sample comparisons for *i* are not shown as there are very few significant differences. These differences are noted in the text.

(Tables 20 and 39) show no significant differences between any pairs of limb segments, indicating that all pairs of limb segments are equally phenotypically correlated.

Additive genetic variances for the Sukhumi Baboon limb segments, found on the diagonal of Table 18, range from 39.868 to 102.449. Table 40 indicates that the only significant difference in additive genetic variance between the four limb segments is found between the thigh (σ_g^2 = 102.449) and leg (σ_g^2 = 39.868), mirroring the vast difference seen in these limb segments in the phenotypic variance. All other limb segment comparisons for additive genetic variance are not different from each other. This significant difference, however, is no longer significant when looking at the genetic correlations. Looking at Table 21, none of the limb segments (on-diagonal) are significantly different in their level of genetic correlation, nor are any of the pairs of genetic correlations (off-diagonal).

Looking at Tables 23 and 42 and 43, none of the heritability (ranging from 0.479 to 0.602), evolvability (ranging from 0.00100 to 0.001628), or *i* (ranging from 0.515 to 0.646) comparisons are significantly different for the Sukhumi Baboons; however, when looking at Table 44, there are several conditional evolvability estimates that are significantly different in this sample. The conditional evolvability estimates for the arm (*c* = 0.000715) and forearm (*c* = 0.000374), the arm and leg (*c* = 0.000390), and the thigh (*c* = 0.000639) and leg are significantly different. This means that limb segments within the same limb have significantly different conditional evolvability estimates, as do the non-homologous elements of the arm and leg. Homologous elements show non-significant conditional evolvability estimates, as do the non-homologous elements of the forearm and thigh.

Mennonites

Tables 24, 25, and 26 are the phenotypic, genetic, and environmental VCV matrices for the Mennonites, respectively, and Tables 27, 28, and 29 are the corresponding correlation matrices. Heritability (h^2), evolvability (e), conditional evolvability (c), and integration (i) estimates, along with 95% credibility intervals for each, are found in Table 30. The posterior distributions for h^2, e, and c for each of the four limb segments are found in Figures 7, 8, and 9, respectively. All of these figures again show good, even distributions of the posterior estimates produced by the MCMCglmm model.

Phenotypic variances for the Mennonite limb segments, found on the diagonal of Table 24, range from 211.721 to 821.957. Table 38, shows that all but one of the phenotypic variance comparisons within the Mennonites are significant, the exception being the comparison between the arm phenotypic variance and the forearm phenotypic variance. The elements of the upper limb have a reduced phenotypic variance compared to elements of the lower limb, and within the lower limb, the thigh has much more phenotypic variance than the leg. The phenotypic correlation comparisons, shown in Tables 27 and 39 indicate that there are numerous limb combinations that have significantly different correlations from one another. The phenotypic correlation between the elements of the upper limb ($corr_p = 0.249$) is significantly lower than all of the inter-limb comparisons (with the exception of the correlation between the forearm and thigh). The phenotypic correlation of the elements of the lower limb ($corr_p = 0.344$) is also lower than the same inter-limb comparisons but is higher than the correlation of the upper limb elements. The highest phenotypic correlations for this sample are the inter-limb combinations with the exception of the correlation between the forearm and thigh.

Additive genetic variances for the Mennonite limb segments, found on the diagonal of Table 28, range from 106.778 to 541.050. Table 40 shows that several of the genetic variance comparisons within the Mennonites are significant. The comparisons between the arm (σ_g^2 = 162.104) and forearm (σ_g^2 = 106.778), between the arm and thigh (σ_g^2 = 541.050), between the forearm and thigh, and between the leg (σ_g^2 = 154.188) and thigh are all significantly different from one another. This means that all elements have a significantly different genetic variance from the thigh, and the elements of the upper limb are also significantly different from one another. When genetic correlations are considered, the only significant difference is between the forearm ($corr_g$ = 0.475) and thigh ($corr_g$ = 0.716) (Table 28). Additionally, Table 41 shows that the genetic correlation between the arm and forearm ($corr_g$ = 0.376) is significantly lower than the correlation between the arm and thigh ($corr_g$ = 0.694) and the correlation between the arm and leg ($corr_g$ = 0.592).

Looking at Tables 30 and 42, the heritability of the forearm (h^2 = 0.475) and the thigh (h^2 = 0.716) are significantly different from one another. All other heritability comparisons are the same. Tables 30 and 43 show that the evolvability of the thigh (e = 0.002263) is significantly different from all other limb segments (arm e = 0.001463, forearm e = 0.001529, and leg e = 0.000859). Finally, when looking at Tables 30 and 44, there are two conditional evolvability comparisons that are significantly different in the Mennonite sample. The forearm (c = 0.000903) and thigh (c = 0.001234) are both significantly different from the leg (c = 0.000443). None of the i estimates are significantly different from one another.

TBRI Baboons

Tables 31, 32, and 33 are the phenotypic, genetic, and environmental VCV matrices for the TBRI Baboons, respectively. Tables 34, 35, and 36 are the corresponding correlation matrices. Heritability (h^2), evolvability (e), conditional evolvability (c), and integration (i) estimates, along with 95% credibility intervals for each, are found in Table 37. The posterior distributions for h^2, e, and c for the two limb segments are found in Figures 10, 11, and 12, respectively. All of these figures again show good, even distributions of the posterior estimates produced by the MCMCglmm model.

Phenotypic variances for the TBRI limb segments, found on the diagonal of Table 31, are 66.546 for the humerus and 99.099 for the femur. Table 38 shows that these two values are significantly different from one another.

Additive genetic variances for the TBRI Baboon limb segments, found on the diagonal of Table 32, are 39.818 for the humerus and 58.524 for the femur. Table 40 shows that comparison of these genetic variances is significant; however, the genetic correlation values for these limb segments (humerus $corr_g = 0.595$, femur $corr_g = 0.649$) are not significantly different (Table 35).

Despite the difference in additive genetic variance, Tables 37, 42, 43, and 44 show that the heritability (humerus $h^2 = 0.595$, femur $h^2 = 0.649$), evolvability (humerus $e = 0.001064$, femur $e = 0.001260$), and conditional evolvability (humerus $c = 0.000359$, femur $c = 0.000410$) comparisons for the TBRI Baboons are not significant, nor are the i estimates.

Inter-Sample Comparisons

Tamarins vs. Sukhumi Baboons

While there are no differences in genetic variances (Table 40) or genetic correlations (Table 41) between the Tamarin and Sukhumi Baboon samples, all combinations of phenotypic correlations are significantly different (Table 39). The Tamarins show consistently higher levels of phenotypic correlation than the Sukhumi Baboons. There is a stark difference between the patterns seen in the phenotypic and genetic correlation data.

There are also no differences heritability estimates (Table 42) or *i* estimates between these samples. However, the evolvability (Table 43) of the humerus (Tamarin humerus e = 0.000519, Table 16; Sukhumi Baboon arm e = 0.001330, Table 23) is significantly different between the two samples, as is the evolvability of the femur (Tamarin femur e = 0.000527, Sukhumi Baboon thigh e = 0.001628). The homologous proximal elements show different evolvability estimates while the homologous distal elements are not significantly different in their evolvability estimates. The conditional evolvability estimates (Table 44) for all four limb segments are significantly different from one another: 1) Tamarin humerus c = 0.000101, Table 16; Sukhumi Baboon arm c = 0.000715, Table 23; 2) Tamarin radius c = 0.000129, Sukhumi Baboon forearm c = 0.000374; 3) Tamarin femur c = 0.000108, Sukhumi Baboon thigh c = 0.000639; and 4) Tamarin tibia c = 0.000120, Sukhumi Baboon leg c = 0.000390. The Sukhumi Baboons have higher evolvability and conditional evolvability estimates than the Tamarins.

Tamarins vs. Mennonites

There are no differences between genetic variances (Table 40) between the Tamarin and the Mennonite samples. There are, however, significant differences between all of the phenotypic correlations (Table 39) and all but one of the genetic correlations (Table 41) (the exception being the correlation between the humerus and femur [i.e., the arm and thigh in the Mennonites]). The Tamarins have both higher levels of genetic correlation and phenotypic correlation than the Mennonites.

While there are no differences in heritability estimates (Table 42), the evolvability estimates (Table 43) of the humerus (Tamarin humerus e = 0.000519, Table 16; Mennonite arm e = 0.001463, Table 30), radius (Tamarin radius e = 0.000605, Mennonite forearm e = 0.001529), and femur (Tamarin femur e = 0.000527, Mennonite thigh e = 0.00263) are significantly different between the two groups. The conditional evolvability estimates (Table 44) for all four limb segments are also significantly different: 1) Tamarin humerus c = 0.000101, Table 16; Mennonite arm c = 0.000711, Table 30; 2) Tamarin radius c = 0.000129, Mennonite forearm c = 0.000903; 3) Tamarin femur c = 0.000108, Mennonite thigh c = 0.001234; and 4) Tamarin tibia c = 0.000120, Mennonite leg c = 0.000443. The Mennonite sample shows both higher evolvability estimates and higher conditional evolvability estimates than the Tamarins. Additionally, the only significant differences in integration found among the samples are between these samples. The estimates for i for the humerus, radius, and tibia are significantly higher in the Tamarins than in the Mennonites (Tables 16 and 30).

Tamarins vs. TBRI Baboons

There are no differences between genetic variances (Table 40), genetic correlations (Table 41), or phenotypic correlations (Table 39) between the Tamarin and TBRI Baboon samples.

There is also no difference between heritability estimates (Table 42) and *i* estimates for these samples. Only two limb segments are comparable here, and both are significantly different in evolvability estimates (Table 43) between the two samples (Tamarin humerus $e = 0.000519$, Table 16; TBRI Baboon humerus $e = 0.001064$, Table 37; Tamarin femur $e = 0.000527$, TBRI Baboon femur $e = 0.001260$). Both limb segments are also significantly different in their conditional evolvability estimates (Table 44): Tamarin humerus $c = 0.000101$, Table 16; TBRI Baboon humerus $c = 0.000359$, Table 37; Tamarin femur $c = 0.000108$, TBRI Baboon femur $c = 0.000410$. The TBRI Baboons have higher evolvability and conditional evolvability estimates than the Tamarins.

Sukhumi Baboons vs. Mennonites

There are no differences in genetic variances (Table 40) between the Sukhumi Baboon and Mennonite samples. The only genetic correlation (Table 41) that is significantly different between the two samples is the correlation between the humerus and radius (i.e., the arm and forearm for both of these samples), with the Sukhumi Baboons having a higher correlation. The majority of the phenotypic correlations (Table 39) between these two samples are significantly different form one another, with the Sukhumi Baboons having higher correlations than the Mennonites.

There are no differences in heritability estimates (Table 42), evolvability estimates (Table 43), or *i* estimates between the Sukhumi Baboon and Mennonite samples. The conditional evolvability estimate (Table 44) of the radius differs for the two samples (Sukhumi Baboon forearm $c = 0.000374$, Table 23; Mennonite forearm $c = 0.000903$, Table 30).

Sukhumi Baboons vs. TBRI Baboons

There are no differences in the genetic variances (Table 40) for the Sukhumi Baboons and TBRI Baboons. The genetic correlation (Table 41) between the humerus and femur differs between the two groups (Sukhumi Baboon arm and thigh $corr_g = 0.634$, Table 21; TBRI Baboon humerus and femur $corr_g = 0.827$, Table 35). Additionally, the phenotypic correlation between the two samples differs (Sukhumi Baboon arm and thigh $corr_p = 0.580$, Table 20; TBRI Baboon humerus and femur $corr_p = 0.793$, Table 34). The TBRI Baboon estimate is higher in both cases.

There are no differences in heritability estimates (Table 42), evolvability estimates (Table 43), or *i* estimates between the Sukhumi Baboon and TBRI Baboon samples. However, the conditional evolvability estimates (Table 44) for both limb segments available for comparison here are significantly different between the samples (Sukhumi Baboon arm $c = 0.000715$, Table 23; TBRI Baboon humerus $c = 0.000359$, Table 37; Sukhumi Baboon thigh $c = 0.000639$, TBRI Baboon femur $c = 0.000410$), with the Sukhumi Baboons showing higher estimates.

Mennonites vs. TBRI Baboons

There are no differences between the genetic variances (Table 40) or genetic correlations (Table 41) between the Mennonite and TBRI Baboon samples. However, the phenotypic correlation between the humerus and femur of each samples does differ (Mennonite arm and thigh $corr_p = 0.482$, Table 27; TBRI Baboon humerus and femur $corr_p = 0.793$, Table 34).

There are also no differences in heritability estimates (Table 42) or *i* estimates between the Mennonites and TBRI Baboons. There is a significant difference in the evolvability estimate (Table 43) of the femur between the two samples (Mennonite thigh $e = 0.00263$, Table 30; TBRI Baboon femur $e = 0.001260$, Table 37). Additionally, the conditional evolvability estimates (Table 44) of both the humerus (Mennonite arm $c = 0.000711$, Table 30; TBRI Baboon humerus $c = 0.000359$, Table 37) and femur (Mennonite thigh $c = 0.001234$, TBRI Baboon femur $c = 0.000410$) are significantly different between the two samples. The Mennonites show consistently higher estimates for evolvability and conditional evolvability than the TBRI Baboons.

Summary of Genetic Variance Results

Estimates of variance are not comparable across species. This is because phenotypic variance is tied to differences in size, meaning that larger limb elements will typically have larger variances. Therefore, larger species will have larger variances, a pattern that holds true here (Tables 10, 17, 24, and 31). Additionally, elements of the lower limb are more likely to have larger variances than elements of the upper limb simply because of their larger size. This pattern also holds true for all four of the samples here, with the exception of the leg in the Sukhumi

Baboons (Table 17). Another pattern seen in three of the four samples (and not possible in the TBRI Baboon sample) is that the phenotypic variances of the humerus and radius are not significantly different from one another (Table 38). This may be explained by the fact that the humerus and radius are similarly-sized elements in all these samples. This phenomenon of larger elements having larger phenotypic variances explains why the phenotypic correlation values were used when comparing across species (and, similarly, why genetic correlation values were used to compare across species [Table 41]).

When phenotypic correlation values are used, there are still many significant results (Table 39) indicating differences between the species. Eighteen of the 21 inter-sample comparisons are significant for phenotypic correlation. The general trend is that phenotypic correlation values between pairs of limb elements decrease from Tamarins to the baboon samples (Sukhumi Baboons and TBRI Baboons) and from the baboons to the Mennonites. The same trend of decreasing correlation values from Tamarins to baboons to Mennonites is seen for the genetic correlation values (Table 41). However, only seven of the 21 comparisons are significant for genetic correlation, the majority of those being between the Tamarin and Mennonite samples. These results show that while phenotypic data may be similar to genetic data, it does not exactly mirror it.

While not strictly comparable across species (see discussion in *Methodological Background*, above), heritability is a dimensionless ratio. Heritability estimates are quite uniform both within and across samples (Table 42). In fact, of all of the intra- and inter-sample comparisons, only one comparison shows a significant result: the comparison between the Mennonite forearm and thigh. This result highlights two things: 1) heritability is a relatively

uninformative ratio here, given that only one out of 21 comparisons is significant, and 2) the genetic variance of the Mennonite thigh is very high compared to the forearm given how large the phenotypic variance of the thigh is for this sample (See Tables 24, 25, and 30).

Evolvability estimates show less uniformity across samples (Table 43). Opposite the correlation results above, there is a general trend of evolvability estimates increasing from the Tamarins to the baboon samples to the Mennonites, although there is some overlap (Tables 16, 23, 30, and 37). The majority of the intra-sample comparisons are insignificant. The exception here is the Mennonite thigh that is significantly different from all three of the other limb segments. All but one of the eight inter-sample significant results is found between the Tamarins and the other samples. The Tamarin humerus and femur has a significantly lower evolvability than all of the other samples, and the radius of the Tamarin is significantly lower evolvability than the Mennonite forearm. The only significant inter-sample comparison not associated with the Tamarins is the difference between the evolvability of the Mennonite thigh which is higher than the TBRI Baboon femur.

The most variable results are found in the conditional evolvability estimates (Table 44). Again, there is a general trend of conditional evolvability estimates increasing from the Tamarins to the baboon samples to the Mennonites (Tables 16, 23, 30, and 37). There are intra-sample differences within the Sukhumi baboons and the Mennonites. The Sukhumi baboons show that the conditional evolvability of the humerus and tibia are each significantly different from their non-homologous elements, while the Mennonites show that the conditional evolvability of the leg is different from the homologous element of the forearm and the intra-limb element of the femur. Fifteen of the 21 inter-sample conditional evolvability comparisons are significant. The

Tamarins differ from all other samples for all four limb elements – conditional evolvability estimates for this sample are lower than for the others. The TBRI Baboons also differ from all other samples for two limb elements available (i.e., humerus and femur), with estimates that are higher than the Tamarins and lower than the Sukhumi Baboons and Mennonites. The conditional evolvability of the radius differs for all three samples that it is available, with the Tamarins showing the lowest estimate and the Mennonites showing the highest. The Sukhumi Baboons and Mennonites are the most similar, with three of the four limb elements not being significantly different from one another.

The estimates of *i*, which look at the relationship between *e* and *c*, are almost entirely uniform across all four samples. The one exception is that the estimations of *i* for the Tamarin humerus, radius, and tibia are significantly higher than for the corresponding limb segments in the Mennonites.

These results demonstrate that phenotypic data alone do not fully describe how limb elements are related to one another or how they can change over time. Phenotypic correlation cannot predict how limb elements will respond to selection pressures, as seen in the differences between patterns of phenotypic correlation and patterns of genetic variance, heritability, evolvability, and conditional evolvability, both within and across samples. While phenotypic data help us understand patterns and hypothesize about evolutionary mechanisms, the addition of genetic data help us better understand those processes.

Morphological Integration

Within-Bone Morphological Integration

The results of the within-bone morphological integration analyses using the TBRI Baboons are below. These results will be used to respond to Developmental Perspective Hypothesis 2.

Following the Magwene (2001) methodology, partial correlation coefficients (i.e., the correlation between two variables with all other variables held constant) for the humerus only, femur only, and humerus and femur combined were calculated and are given in Tables 45 through 47. Using these partial correlations and the Edge Exclusion Deviance formula (see *Research Design*, above), the Edge Exclusion Deviances were calculated for the humerus only, femur only, and humerus and femur combined. Results are reported in Tables 48 through 50. In these tables, any edges that are below 3.84, corresponding to a 5% point on the χ^2-distribution with one degree of freedom, have already been omitted. The results of humerus only and femur only Edge Exclusion Deviances (Tables 48 and 49, respectively) show that all sets of variables, with the exception of one in each matrix, have a statistically significant relationship. The humerus and femur combined model (Table 50) has many more blank cells, which represent combinations of variables that do not have a significant relationship and can therefore be removed from the model.

A strength was calculated for the edges which remained following the Edge Exclusion Deviance calculations using the Edge Strength formula (see *Research Design*, above). The Edge Strength provides a measure of the strength of the relationship between two variables, otherwise thought of the as the copredictability between the two traits. The results of the Edge Strength

calculations for the humerus only, femur only, and humerus and femur combined are given in Tables 51 through 53. To more easily visualize the differences in Edge Strengths that are represented in these matrices, the cells are given different colors based on the order of magnitude of the strength. An Edge Strength ranging from 0.001-0.009 is yellow, from 0.01-0.09 is orange, and from 0.1-0.9 is red. Blank white cells again represent combinations of variables which do not have a significant relationship.

The Edge Strength results show the following trends. The humerus itself is moderately integrated, with the majority of edges being orange (Table 51). The two yellow edges, representing the lowest level of strength, are between the Humerus Maximum Length and both the 50% Diaphysis Average and the Distal Articular Breadth. The femur itself is also moderately integrated, with the majority of the edges again being orange (Table 52). The two yellow edges are between the Femur Head Diameter and the 50% Diaphysis Average and between the Femur Bicondylar Length and the Bicondylar Breadth. The significant result within the femur is that the Articular Breadth and the Bicondylar Breadth are relatively highly integrated, showing an edge strength of 0.268. The model including both the humerus and femur (Table 53) again shows the relative high integration between the Articular Breadth and Bicondylar Breadth within the femur. Additionally, the combined model shows high integration between the Humerus Maximum Length and the Femur Bicondylar Length. Otherwise, integration between the other humerus and femur traits are low to moderate.

The second within-bone analysis was to perform Mantel tests comparing correlation matrices based on the data and model matrices based on various tests of integration. Correlation matrices for the humerus only, femur only, and humerus and femur combined are given in Tables

54 through 56. While the correlations between two traits within one bone (e.g., Humerus Maximum Length and Humerus 50% Diameter Average) should be the same in the matrix for the humerus only and the matrix for the humerus and femur combined, the numbers here differ slightly. This is due to the different samples sizes, which are the result of the inability to include individuals with missing data (see *Research Design*, above).

The correlation matrices in Tables 54 through 56 were compared to the seven model matrices for the humerus only and femur only analyses and the 10 model matrices for the humerus and femur combined analyses (see *Research Design*, above). The 10 different models are listed in Table 57. A *p*-value was calculated for each model by determining the number of iterations with correlations higher than the original correlation between the two matrices and dividing by 1000, and the null hypothesis of no relationship between the two matrices was rejected when the *p*-value was less than 0.05.

The Mantel tests resulted in only two significant models at the 0.05 level. The first is a model in the femur only data indicating integration between the articulations of the femur and the femoral muscle attachment, Femur Bicondylar Breadth. This is also reflected in the Magwene methodology as red cells in both the femur only and the humerus and femur combined Edge Strength results (Tables 52 and 53). The second significant model indicates integration between the Humerus Maximum Length and the Femur Bicondylar Length. This result also corresponds to the high Edge Strength found between these traits using the Magwene methodology (see Table 53). Table 58 summarizes the results of the Mantel tests and includes the original correlations between the correlation matrices and the various model matrices and the *p*-value associated with each model. Significant results are in bold.

Morphological Integration Across Four Limb Segments

The relative eigenvalue variance results, produced in R (R Core Team, 2014, version 3.1.2) and following Pavličev et al. (2009), are presented here. These results will be used to respond to Developmental Perspective Hypothesis 3 and Evolutionary Perspective Hypothesis 3. Defined as the variance of the eigenvalues divided by one less than the number of traits, the relative eigenvalue variance is used here to explain the overall level of integration of a correlation matrix. The relative eigenvalue variance is given for five different matrices for three samples (Tamarins, Sukhumi Baboons, and Mennonites) to compare integration in the upper limb, the lower limb, the proximal elements, the distal elements, and all four elements. These results, along with 95% credibility intervals, can be seen in Table 59. Additionally, Table 60 shows the results of the intra- and inter-sample comparisons for significance.

The levels of integration are higher for both of the non-human primates than they are for the humans. When comparing overall integration by looking at all four limb segments, the Tamarins ($V_{rel}\lambda = 0.679$) are significantly more integrated than the Sukhumi Baboons ($V_{rel}\lambda = 0.381$), and both are significantly more integrated than the Mennonites ($V_{rel}\lambda = 0.154$). This pattern continues for the other four measures of integration (i.e., upper limb, lower limb, proximal elements, and distal elements), with the Tamarins consistently showing higher levels of integration than the Sukhumi Baboons and both samples showing significantly higher integration than the Mennonites. The one exception to this is that the Sukhumi Baboon proximal elements ($V_{rel}\lambda = 0.337$) are not significantly different than the Mennonite proximal elements ($V_{rel}\lambda = 0.196$).

Within the Tamarins, the integration of the proximal elements ($V_{rel}\lambda = 0.621$) is significantly lower than the integration of the distal elements, upper limb, and lower limb. These latter three measures of integration are not significantly different from one another, but they are all significantly higher than the overall level of integration (i.e., when all four limb segments are used) for the Tamarins. The Sukhumi Baboons show a much different pattern than the Tamarins: there are no significant differences across the five measures of integration for this sample. Within the Mennonite sample, homologous elements (i.e., proximal elements and distal elements) have significantly higher levels of integration than elements within the same limbs (i.e., upper limb and lower limb), while the two measures within each of these categories are not significantly different from one another.

Summary of Morphological Integration Results

When looking within a single bone using the Magwene methodology, relatively low to moderate levels of integration are found within both the humerus and femur, as evidenced by the TBRI Baboons (Tables 51 and 52). A higher level of integration is found between the Bicondylar Breadth and Articular Breadth of the femur (Table 52). When looking across these two limb segments, the Humerus Maximum Length and the Femur Bicondylar Length show the highest level of integration (Table 53). These results are mirrored in the Mantel tests, as seen in Table 58.

The Relative Eigenvalue Variance results, used to compare integration across all four limb segments in the Tamarins, Sukhumi Baboons, and Mennonites, show that the Tamarins and Sukhumi Baboons have higher levels of integration than the Mennonites, with the Tamarins

having the highest level overall. The pattern of integration within each species for the four additional measures of integration (i.e., upper limb, lower limb, proximal elements, and distal elements) is different for each species. These results can be seen in Tables 59 and 60.

Linkage Analysis

The results of the 10 univariate multipoint linkage analyses run in SOLAR (Almasy & Blangero, 1998) are reported below. These results will be used to respond to Developmental Perspective Hypothesis 4. Each of these analyses was run to test for evidence of linkage between individual trait phenotypic variation and the 309 STR loci previously genotyped by TBRI personnel (see *Research Design*, above).

The final residual kurtosis and covariates used in the 10 models as well as the heritability associated with each model can be seen in Table 61. All traits (except two) are inormalized traits. The two exceptions, Femur 50% Diameter Average and Femur Head Diameter, are the inormalized residuals from the inormalized data (following Sherwood et al., 2008). These transformations ensure that residual kurtosis is kept below 0.8, as recommended by the SOLAR documentation (2013) (section 6.8.2). Sex is included as a significant covariate in all 10 traits, while age is included in six of the traits. The only other significant covariates used are age*sex in two traits and age^2 in three traits.

All 10 phenotypic traits have at least one area of suggestive linkage (i.e., a LOD score of 1.5 or higher), and one trait, Humerus Head Length, has an area of significant linkage (i.e., a LOD score of 2.75 or higher). All areas of suggestive and significant linkages are listed in Table 5.53. Due to the fact that areas with LOD scores above 0.5 were rescanned and LOD scores were

calculated every 1 cM (see *Research Design*, above), there is typically a range of locations above the suggestive or significant threshold. The entire range of suggestive/significant LOD scores is given in the "location" column, while the "peak" column gives the position of the highest LOD score in the entire region. These highest LOD scores are reported in the final column. Additionally, the locations of the LOD scores are based on the Baboon chromosome maps, but the chromosome numbers used by SNPRC reflect the orthologous human chromosome numbers. Therefore, both the human and corresponding baboon chromosome numbers are given here.

The string plots for each of the 10 univariate linkage analyses can be seen in Figures 13 - 22. Each of these plots shows the LOD scores for the complete length of all 21 baboon chromosomes. The small tick marks on each of the straight lines representing the chromosomes show the locations of the STRs. Larger curves indicate higher LOD scores, and the chromosome with the highest LOD score for that trait has a LOD scale below.

The results of three of the traits are discussed in further detail here. Humerus Head Length (Figure 15) had the only significant LOD score, so it is included here. And, because limb segment lengths are the focus of the overall project, the areas with suggestive LOD scores for Humerus Maximum Length (Figure 13) and Femur Bicondylar Length (Figure 18) are also examined. It should be remembered throughout that the LOD scores associated with both Humerus Maximum Length and Femur Bicondylar Length are merely suggestive, not significant; therefore they may be wrong. However, as stated by Lander and Kruglyak (1995), they are "worth reporting." Figure 23 shows the significant peak for Humerus Head Length found on human chromosome 11. Figure 24 shows the suggestive peak for Humerus Maximum Length on

human chromosome 12. There are two peaks with suggestive LOD score for Femur Bicondylar Length found on chromosome human 7[18] (Figure 25) and human chromosome 14 (Figure 26).

Significant LOD Score Associated with Humerus Head Length

The region around the significant peak LOD score for Humerus Head Length was further analyzed to look for candidate genes which may influence phenotypic variation. The peak location associated with a LOD score of 3.7985 is location 46 on baboon chromosome 14 (see Table 62). As shown in the plot in Figure 23, this peak is between STR markers D11S4203 and D11S907. The SNPRC Baboon to Human Comparative Maps website (SNPRC CompMaps website) is used to determine the location of these STR loci in the human genome. These two STRs have corresponding locations on human chromosome 11 (using Marshfield Position) of 45.94 cM and 42.55 cM, respectively. Figure 23 also shows a second peak, located at 62 cM and associated with a LOD score of 3.5410. This peak is between STR markers D11S904 and D11S1349, which have locations in the human genome at 33.57 cM and 18.26 cM. A map of the relative positions of the STRs on the baboon and human chromosomes can also be seen on the SNPRC website (SNPRC CompMaps website). A reduced version of these maps, focusing on only the locations of the STRs of interest on human chromosome 11/baboon chromosome 14, can be seen in Figure 27. While D11S907 is not shown on the SNPRC map, D11S4200, which is right next to it on Figure 23, is. Of significance in this map is that STRs D11S4200 and

[18] Figure 25 is the plot associated with both human chromosome 7 and human chromosome 21. This is because human chromosomes 7 and 21 are combined into one chromosome (chromosome 3) in the baboon genome. However, the location of the suggestive peak is in the area that is orthologous to human chromosome 7. Similarly, human chromosomes 14 and 15 are combined to make baboon chromosome 7, but the location of the suggestive peak is in the area that is orthologous to human chromosome 14 and is shown in Figure 26.

D11S4203 are located next to one another in both species, as are D11S904 and D11S1349. Furthermore, there are nine STR loci occurring in the same order, although inverted on the human chromosome, which can be seen on the SNPRC maps. This further highlights the orthologous nature of the human genome as compared to the baboon genome and the utility of the baboon genome to look for candidate genes in the human genome.

The SNPRC website (SNPRC CompMaps website) also provides the physical location of the STRs on the human chromosome in base pairs (bps). D11S4203 is located between bps 35,769,948 and 35,770,298 and D11S907 is located between bps 34,624,001 and 34,624,268. Therefore, the region of interest to look for candidate genes associated with the highest peak is between bps 34,624,001 and 35,770,298 on human chromosome 11. Similarly, D11S904 is located between bps 26,637,090 and 26,637,375 and D11S1349 is located between bps 11,709,077 and 11,709,431. Therefore, the region of interest to look for candidate genes in the secondary peak is between bps 11,709,077 and 26,637,375 on human chromosome 11.

Genes within these regions of interest on human chromosome 11 were determined using the UCSC Genome Browser (UCSC Genome Browser website). Within these regions, there are nine genes that are listed in the UCSC Genes track associated with the highest peak and 98 genes associated with the secondary peak. When the Genome Browser returns results there is typically more than one entry for each gene, which can be due to different splice variants of the gene. Each entry is also color-coded: black entries are those which are well known and are in the Protein Data Bank, dark blue entries are transcripts which have been reviewed or validated by another source (such as RefSeq), and light blue entries are transcripts that are not found in RefSeq. Only one entry for each gene is used, with the darkest colored entry being selected.

Table 63 lists the nine genes found on human chromosome 11 between bps 34,624,001 and 35,770,298, in alphabetical order. Each row lists the gene abbreviation, the unique search term given for the selected gene entry, the color of the selected gene entry, whether the gene is coding or noncoding, and the function of the gene. All but one of these genes are coding (i.e., produce proteins), and the one noncoding gene is for a microRNA. The functions are known for most of these nine genes, and they range from epithelial differentiation to muscle regeneration and from transcription repression to cell-cell interactions.

Determining the gene or genes that may be causing a significant LOD score on human chromosome 11 is not possible in this project, but there are two genes in the highest peak that would be candidates for further study. The first is CD44, which is located at bps 35,160,417 to 35,253,949 on the p arm of chromosome 11. The protein produced by this gene is a cell-surface glycoprotein and it is involved in cell-cell interactions. Specifically, it is a receptor for hyaluronic acid, which is found in joint cavities (Schoenwolf et al., 2015). Alternatively, this protein can be a receptor for osteopontin, which, among other things, is involved with bone formation (Denhardt & Guo, 1993). In addition, one of the biological processes listed for CD44 is a *Wnt* signaling pathway. *Wnt* genes are responsible for limb bud formation and dorsal-ventral patterning in the developing limb (Gilbert, 2013). These features make CD44 a candidate gene influencing variation in Humerus Head Length.

The second candidate gene associated with the highest peak on chromosome 11 is FJX1 (full name is four jointed box 1). It is located at bps 35,639,735 to 35,642,421 on the p arm of chromosome 11. While the exact function of this gene is unknown in humans, the ortholog of this gene is known in mouse and *Drosophila*. In *Drosophila*, the protein is important in the

differentiation of legs and wings. Because this gene is closely related to genes that are known to be involved with limb development in other species, FJX1 is a candidate gene here.

Table 64 lists the 98 genes found on human chromosome 11 between bps 11,709,077 and 26,637,375, the area of the second highest peak. While 79 of the genes are coding, 21 of the genes are noncoding. Noncoding genes may result in products such as endogenous retroviruses, noncoding RNAs (including ribosomal RNA or microRNAs), and pseudogenes. A majority of the genes have a function listed; however, 33 genes did not have a clear function described in the UCSC files. Most (19) of the 33 without functions are noncoding genes.

The functions of the genes listed in Table 64 are wide-ranging, from DNA activities, such as DNA repair and transcription activation, to cellular activities, such as metabolism, protein transport, apoptosis, and organelle biogenesis, to tissue production, such as myogenesis, and chondrogenesis. There are several genes involved with pain modulation, two that are specific to cochlear hair cell production, and a few that impact tumor susceptibility and suppression. Of specific interest to this project, there are several genes which are important for bone formation (CALCA, NELL1) or that have been implicated as influencing body height (TEAD1, PTH, SERGEF).

There are a few genes associated with the second highest peak on chromosome 11 which have functions that would make them candidates for further study. The first is DKK3 (dickkopf WNT signaling pathway inhibitor 3). This gene is located at bps 11,984,543 to 12,030,917 on the p arm of chromosome 11. A member of the dikkopf family, the protein encoded by this gene is involved with embryonic development due to its interactions in the *Wnt* signaling pathway. *Wnt* signaling is responsible for limb bud formation as well as dorsal-ventral patterning in the

developing limb (Gilbert, 2013). The DKK genes are local inhibitors of *Wnt* signaling, making them important for vertebrate development. Among other things DKK3 is implicated in limb development, making it a candidate gene here.

The second candidate gene is NELL1 (NEL-like protein 1). This gene is located at bps 20,691,117 to 21,597,229 on the p arm of chromosome 11. The protein is involved in cell growth regulation and differentiation, and, specifically, it is involved with osteoblast cell differentiation and bone mineralization. Osteoblasts are the bone-forming cells which deposit matrix that is then mineralized. Because this gene is implicated in bone formation, it is a candidate gene for the Humerus Head Length phenotype.

There are several other genes that seem to be peripherally related to limb bone formation and could thus also be considered candidate genes. One of the functions of TEAD1 is organ size control, and it has also been implicated as contributing to body height, as have PTH and SERGEF. Finally, CALCA regulates bone ossification and bone resorption and has been associated with bone mineral density, as has INSC.

Suggestive LOD Scores Associated with Limb Segment Lengths

The suggestive LOD score peak associated with the Humerus Maximum Length (Figure 13 and Figure 24) was analyzed following the same protocol as above. As shown in Table 62, the highest suggestive LOD score on chromosome 12 was 1.7153 at location 42. Looking at Figure 24, this falls between STR markers PHA11S2 and PHA11S3. These STRs are baboon specific and do not have an orthologous location in the humans genome. Therefore, the area of interest was widened to STR markers D12S364, which is located between bps 13,724,569 and

13,724,907 on human chromosome 12, and D12S85, which is located between bps 45,622,953 and 45,623,129 on the same chromosome. Therefore, the region of interest for Human Maximum Length is between bps 13,724,569 and 45,622,953 on human chromosome 12.

The UCSC Genome Browser returned 153 genes in this region of chromosome 12, which are listed in Table 65. Of these, 121 are coding genes which produce proteins, while the remaining 32 are antisense, near coding, or noncoding genes. There are a variety of functions among the coding genes, and four in particular are considered candidate genes here. The first is MGP (matrix gla protein), located at bps 15,034,115 to 15,038,853 on the p arm of chromosome 12. The protein produced by this gene associates with the organic matrix of bone and cartilage and is an inhibitor to bone formation. The second gene is PTHLH (parathyroid hormone-related protein), located at bps 28,111,017 to 28,124,916 on the p arm of chromosome 12. This protein regulates endochondral bone development and is required for skeletal homeostasis. Third, PTPRO (protein tyrosine phosphatase, receptor type, O) is located at bps 15,475,191 to 15,751,265 on the p arm of chromosome 12. Its function is to regulate osteoclast production, cells which resorb bone tissue during bone growth and remodeling. And, finally, SOX5 (sex determining region Y-box 5) is located at bps 23,685,231 to 24,102,637 on the p arm of chromosome 12. This gene helps regulate embryonic development and plays a role in chondrogenesis.

The two suggestive LOD score peaks associated with Femur Bicondylar Length (Figure 18) are located on chromosomes 7 and 14. On chromosome 7 (Figure 25), the peak is located between STRs D7S496 (located between bps 106,941,921 and 106,942,086) and D7S480 (located between bps 120,752,256 and 120,752,501), making the area of interest located between

bps 106,941,921 and 120,752,501 on human chromosome 7. On chromosome 14 (Figure 26), the peak is located between STRs D14S66 (located between bps 56,120,368 and 56,120,628) and D14S277 (located between bps 72,097,057 and 72,097,415), making the area of interest located between bps 56,120,368 and 72,097,415 on human chromosome 14.

For chromosome 7, 69 genes were identified, 45 of which are coding genes (Table 66). Two of these, TFEC and WNT2, are considered candidate genes here. TFEC (transcription factor EC) is located at bps 115,575,202 to 115,670,867 on the q arm of chromosome 7, and it co-regulates genes in osteoclasts. WNT2 (wingless-type MMTV integration site family member 2) is located at bps 116,916,686 to 116,963,343 on the q arm of chromosome 7. *Wnts* are known to control cell fate and patterning in embryogenesis. For chromosome 14, 143 genes were identified in the region of interest using the UCSC Genome Browser (Table 67). Of these, 101 are coding and two are identified as candidate genes. KIAA0586 is located at bps 58,894,103 to 59,015,549 on the q arm of chromosome 14. It is important in SHH signaling, which is imperative for limb patterning during embryogenesis. And finally, SMOC1 (SPARC related modular calcium binding 1) is located at bps 70,346,114 to 70,499,083 on the q arm of chromosome 14. The protein created by this gene plays a critical role in limb development. Candidate genes for all three traits are listed in Table 68.

It should also be noted that the string plot for Humerus Maximum Length (Figure 13) shows a peak on chromosome 7 that looks strikingly similar to the peak in the same location of chromosome 7 for Femur Bicondylar Length (Figure 18). The maximum LOD score for this peak is 1.4737 at location 137 of chromosome 7, which is nearing the “suggestive” cutoff LOD

score of 1.5. This suggests that the length of both proximal bones may be influenced by the same area of the genome.

There are several other homologous traits that show similar patterns in their string plots. For instance, both Humerus Head Length and Femur Head Diameter show a small peak in the same location of baboon chromosome 20_22, and Femur Head Diameter shows a peak in the same area as the suggestive QTL for Humerus Head Length on chromosome 2q (Figures 15 and 20). The suggestive QTLs for both Humerus 50% Diameter Average and Femur 50% Diameter Average are in the same area of chromosome 6 (Figures 14 and 19). Also of note is the fact that the only two traits with high morphological integration, aside from the limb segment lengths, were Femur Articular Breadth and Femur Bicondylar Breadth. These traits show similar peaks on chromosomes 2q, 7_21, and 14_15 (Figures 21 and 22). The majority of these do not even reach the level of a suggestive QTL, but an increased sample size may bring them up to the level of significance.

Protein Networks

To look for connections among proteins within each region of interest, the lists of genes were reduced to only those that produce proteins (i.e., coding genes). This reduced the number of genes to 85 for Humerus Head Length, 120 for Humerus Maximum Length, and 146 (45 on chromosome 7 and 101 on chromosome 14) for Femur Bicondylar Length. These three lists of proteins were each run independently through STRING using the "multiple names" function. A few of the proteins in these lists were not found in the STRING database, reducing the number of proteins to 77 for Humerus Head Length, 115 for Humerus Maximum Length, and 137 for

Femur Bicondylar Length. These proteins are identified with an asterisk next to the gene abbreviation in Tables 63 through 67. Additionally, a few proteins were identified by different names in STRING, and those names are found in parentheses next to the gene abbreviation in the same tables. A second round of STRING analyses were performed by running each list of proteins separately through the database again, this time including the 35 known proteins involved in bone and limb development (Table 69).

The figures produced by STRING are circles (i.e., nodes) connected by lines. Each circle represents a different protein, while lines represent connections between them. The various colors of the protein circles do not mean anything and are simply used as a visual aid when comparing the figure to the list of included proteins on the website. The various sizes of the nodes reflect whether any structural information is known about the protein; if a structure is known for the protein, then a small image appears inside the node indicating that information. The different colors of the lines represent the type of evidence that is used to support an interaction between the proteins, and a legend is found in Table 70.

The protein network for Humerus Head Length is found in Figure 28. Candidate genes CD44 (light blue, left side) and DKK3 (yellow, bottom left) are not connected to any other proteins. NELL1 (light green, right side) is connected by text mining evidence to ANO5, while FJX1 (dark blue, right side) is connected by text mining evidence to TRIM44.

The second run for Humerus Head Length, which includes the list of known bone and limb development proteins, is found in Figure 29 (which has been cropped from a larger image). There is a messy web of interconnectivity where the known bone and limb proteins cluster, which is expected. The majority of the connections are due to text mining, databases, and

experiments. There are several proteins which were not connected in Figure 28 but are now connected to bone or limb proteins, including SOX6 and MYOD1. DKK3 and CD44, the two previously unconnected candidate genes, are now connected to other bone and limb genes, providing support for the idea that these genes may be involved in bone or limb development.

Figure 30 shows the protein network for Humerus Maximum Length. Candidate genes PTPRO (light green, right side) and MGP (light blue, left side) are not connected to any other proteins. SOX5 (dark blue, lower left side) is connected by text mining evidence to LRMP, ETNK1, and ATF71P. PTPLH (light blue, left side) is connected by text mining evidence to KIF21A and by text mining and database evidence to IAPP.

Figure 31 shows the second run for Humerus Maximum Length (which has also been cropped from a larger image). Several proteins which were not connected in Figure 30 are now connected via these bone and limb proteins, including KRAS, MGP, YAF2, DBX2, PRICKLE1, and TMTC1, indicating that these genes may be peripherally involved in bone or limb development.

The protein network for Femur Bicondylar Length is found in Figure 32. TFEC (yellow, center) is connected by text mining evidence to MAX and by text mining and experimental evidence to ING3. WNT2 (yellow, top left) is connected by text mining evidence to ST7 and CAPZA2 and by text mining and experimental evidence to MET. KIAA0586 (yellow, lower right side) is connected by text mining evidence to DACT1 and ARID4A. And, finally, SMOC1 (light blue, top) is not connected to any other proteins.

Figure 33 shows the second run for Femur Bicondylar Length (again, cropped from a larger image). Several new connections are made in this figure. OTX2, SIX6, and MET each

have multiple connections to the known bone and limb development proteins and may be involved in bone or limb development.

Summary of Linkage Analysis and Protein Network Results

The results of the 10 univariate multipoint linkage analyses show that there are several suggestive LOD scores and one significant LOD score of interest to this project, including suggestive LOD scores for both Humerus Maximum Length and Femur Bicondylar Length. Additionally, there is a peak on the string plot for Humerus Maximum Length (Figure 13) on chromosome 7 that nearly reaches the level of a suggestive LOD score and that is located in the same area of a suggestive LOD score for Femur Bicondylar Length (Figure 18). These results suggest that the same area of chromosome 7 may be impacting the length of both the humerus and the femur.

In addition, there are genes within all of the examined regions (the significant region of chromosome 11 for Humerus Head Length, the suggestive region chromosome 12 for Humerus Maximum Length, and the suggestive regions on chromosomes 7 and 14 for Femur Bicondylar Length) that are good candidates for further study because they play some role in bone formation, limb development, or some other related function (Table 68). This indicates that variation found in the genome is indeed influencing variation found in phenotype.

Finally, the protein networks show that the candidate genes identified here are indeed associated with many proteins that are known to influence bone and limb development (Figures 29, 31, and 33), thereby adding weight to the argument that these genes are good candidates which are likely influencing phenotypic variation in limb segment lengths.

CHAPTER SIX
DISCUSSION AND CONCLUSIONS

This study set out to use a quantitative genetics approach to better estimate the variance and covariance in limb segment lengths in humans and other primates using pedigreed samples and then begin the task of identifying genes which influence this normal genetic variation in primate limb bones. The study's results have important implications for how limb segment lengths and proportions are used in anthropological research.

This chapter will begin with responding to the hypotheses detailed in *Research Design*, above, using details from *Results*, also above. Following this there will be a discussion on the implications that these results have on current anthropological and related literature which was described in *Limbs* and *Methodological Background*, above. There will then be a discussion of the limitations to this study as well as a section on future research.

Responding to the Hypotheses

Developmental Perspective Hypotheses

1. *While phenotypic variance increases from proximal to distal elements, heritability will decrease.*

Previous research has shown that environmental variance accumulates in distal elements in primates species (Hallgrímsson et al., 2002) arguably because of the way in which limbs form in a proximo-distal gradient (Tarchini and Duboule, 2006; Gilbert, 2013). Therefore, while phenotypic variance will increase due to increasing environmental variance, heritability will

decrease because genetic variance plays a smaller role in overall phenotypic variance. This is not supported by the results presented here.

Phenotypic variance does indeed increase from proximal (humerus/arm and femur/thigh) to distal (radius/forearm and tibia/leg) elements when looking at the Tamarin sample (Table 10); however, the same does not hold true for the other samples. Phenotypic variance decreases from proximal to distal elements in the Sukhumi Baboons (Table 17) and Mennonites (Table 24). The TBRI Baboons are not included here because that sample only has the proximal elements available. When looking at the heritability estimates presented in Tables 16, 23, and 30 for the Tamarin, Sukhumi Baboon, and Mennonite samples, respectively, it can be seen that heritability does not consistently decrease as expected from the proximal segments to distal segments. The Tamarins show a slight decrease in h^2 from the humerus to radius but a slight increase from femur to tibia (Table 16). The Sukhumi Baboons actually show an increase in h^2 from proximal to distal segments (Table 23). Finally, the Mennonites do show a decrease from proximal to distal segments (Table 30), as expected.

However, all results must be viewed while simultaneously looking at Tables 38 and 42 which show the intra- and inter-sample comparisons for phenotypic variance and heritability, respectively. Given that these estimates have quite large credibility intervals generated from the posterior distributions of the MCMCglmm models, patterns seen in the estimates themselves are not all that informative. When the posterior distributions for phenotypic variance are compared within species, all three samples show that there is no significant difference between the humerus and radius. However, the difference between the femur and tibia is significantly different for all three samples. That still means that only the Tamarins show the expected increase in phenotypic

variance from proximal to distal segments, albeit only in the lower limb. When the posterior distributions for h^2 are compared within and across species, there is only one significant difference – the Mennonite forearm has a significantly lower h^2 than the Mennonite thigh. All other comparisons of limb segment heritability estimates are not significantly different. Given that the significant difference found in the Mennonites is between elements from different limbs, even this result does not support the hypothesis that h^2 should decrease from proximal to distal segments.

There are a few explanations as to why this hypothesis is not supported by the analyses presented here. First, the paper that purported that phenotypic variance increases and heritability decreases from proximal to distal segments (i.e., Hallgrímsson et al., 2002) included the autopod, in addition to the stylopod and zeugopod, in the analysis. As a reminder, the stylopod makes up the proximal elements of the limbs (i.e., humerus and femur), the zeugopod makes up what have been referred to here as the distal elements of the limbs (i.e., radius, ulna, tibia, and fibula), and the autopod makes up the hands and feet (i.e., carpals, metacarpals, tarsals, and metatarsals). Hallgrímsson et al. (2002: Figure 7[19]) do indeed show that environmental and phenotypic variance increase from stylopod to zeugopod to autopod; however, the majority of the increase seems to be in the autopod, which is not included in the current analysis. Second, the analysis in Hallgrímsson et al. (2002) uses skeletal data from a sample of Rhesus macaques (*Macaca mulatta*), similar to the skeletal data used here from the Tamarins. The Sukhumi Baboon and Mennonite data, on the other hand, are both anthropometric data. Therefore, it is perhaps not surprising that the Tamarin sample used here is the one that most closely adheres to their

[19] Not shown here.

findings. The potential limitations of anthropometric versus osteometric data will be discussed further below, in *Limitations*.

2. *Morphological integration will be higher among limb segment lengths and/or articulations and lower among diaphyseal measures*.

This hypothesis brings together several sources of information to make the claim that limb segment lengths and/or articulations should show higher levels of integration to one another than to diaphyseal measures. First, diaphyseal measures have been shown to be more influenced by mechanical loading than other limb features (Larsen, 1997; Ruff, 2008a). Second, limb articulations are less responsive to mechanical loading (Ruff et al., 1991) and show a degree of genetic canalization and/or are influenced by more general systemic factors such as nutrition (Ruff et al., 1994). Finally, variation in limb segment lengths appears independent from variation in diaphyseal dimensions (Ruff, 2003; Trinkaus et al., 2004; Auerbach and Raxter, 2008) and is anecdotally considered to be more highly genetically canalized than other bone dimensions (Auerbach and Ruff, 2006; Cowgill and Hager, 2007).

The within-bone morphological integration analyses show that this hypothesis is well supported. Table 53, which shows Edge Strengths for the TBRI Baboon humerus and femur indicates that the highest levels of morphological integration within the features of these two bones are found in two comparisons: 1) the Humerus Maximum Length and the Femur Bicondylar Length, and 2) the Femur Articular Breadth and the Femur Bicondylar Breadth. Mantel test results show the same two significant results.

These within-bone morphological integration analyses support the hypothesis that long bone lengths are more highly integrated than other limb bone features since the two long bone lengths included are relatively highly integrated. Additionally, while only one articulation (Femur Articular Breadth) was included in a significant result, diaphyseal measures were not included in any. This supports the idea that diaphyseal measures, which are highly influenced by mechanical loading, are not tightly integrated with other limb features.

Of interest is the fact that Femur Bicondylar Breadth, a muscle attachment, was included in the significant result with Femur Articular Breadth. While muscle attachments would be considered less genetically canalized because their size may be dependent on activity and muscle size (Robb, 1998), the fact that it is highly integrated with Femur Articular Breadth is not surprising. Both these measures are taken at the distal end of the femur, not far from one another, and the breadth of the muscle attachment is partially dependent upon the breadth of the articular surface.

3. *Proximal limb elements will show higher morphological integration with one another than distal limb elements, and homologous elements will show higher morphological integration than elements within the same limb.*

Homologous elements (i.e., the humerus/femur and the radius/tibia) have similar developmental pathways (Hallgrímsson et al., 2002; Gilbert, 2013), indicating that these structures should have higher levels of integration than elements within the same limb (Young et al., 2010). Additionally, molecular factors involved in limb development work in a proximo-distal gradient (Tarchini and Duboule, 2006; Gilbert, 2013), which allows variation to

accumulate in distal elements. Therefore, proximal elements are expected to show higher levels of integration with one another than distal elements. The results of this study are split on whether they support his hypothesis. See Tables 59 and 60.

With regard to the proximal versus distal elements, all three samples show a similar, unexpected pattern: the proximal elements show a lower level of integration with one another than the distal elements show with one another. For the Tamarins and Sukhumi Baboons, the estimation of integration for the proximal elements is the lowest level of integration of any of the measures of integration (i.e., proximal elements, distal elements, upper limb, lower limb, all four limbs). The difference between these two non-human primate samples is that the difference between the proximal element integration is significantly lower than all other measures for the Tamarins, while the difference is not significant for the Sukhumi Baboons (in fact, none of the comparisons among the different measures of integration are significantly different for this sample). The Mennonite sample follows the same pattern of proximal elements showing lower levels of integration than the distal elements, although the difference between them is not significant. Therefore, for two of the samples (Sukhumi Baboons and Mennonites) the level of integration for the proximal elements is not significantly different than then level of integration for the distal elements. For the remaining sample, the Tamarins, the proximal elements show a significantly lower level of integration than the distal elements, which goes against the expectations of this hypothesis.

With regard to the homologous elements versus within-limb elements, the non-human primates show a different pattern than the human sample. The Tamarins and Sukhumi Baboons show that there is no significant difference between the integration levels of the upper limb,

lower limb, and distal elements, and the Sukhumi Baboons also show no difference between these three and the proximal elements. The Tamarins do show a significant difference between the proximal elements and the other three measures of integration, but as discussed before, the proximal elements have a lower level of integration than the other measures. Therefore, the non-human primate samples do not adhere to the expectations of the hypothesis. The Mennonites, on the other hand, do support the expectations of the hypothesis. There are no significant differences in the level of integration between either the upper limb and the lower limb or the proximal elements and the distal elements; however, there are significant differences between homologous elements and within-limb elements with homologous elements showing significantly higher levels of integration than within-limb elements. Thus, while the non-human primate samples do not support the hypothesis, the human sample does.

4. *Traits that show high morphological integration will have QTLs in the same genomic regions*.

Pleiotropy, defined as a single gene or region contributing to multiple phenotypic traits, is a genetic mechanism which leads to positive genetic correlation and integration because changes in that single gene or region causes phenotypic changes in multiple traits (Cheverud, 1984, 2007; Hallgrímsson et al., 2002; Rolian, 2009; Young et al., 2010). Pleiotropy can be identified as multiple traits showing significant correlations with similar genomic regions.

The results of the linkage analysis show that this hypothesis is well supported. In this study, there are two sets of individual traits which show high levels of integration in the within-bone morphological integration analysis, as detailed in the Developmental Perspective

Hypothesis 2, above. The first set of traits, Humerus Maximum Length and Femur Bicondylar Length, do indeed have QTLs in the same genomic region. One of the two suggestive LOD scores for Femur Bicondylar Length is found on chromosome 7 between locations 134 and 159 (Table 62). The Humerus Maximum Length shows a very similar peak in the same region of chromosome 7, with a maximum LOD score of 1.4737 at location 37. While this peak does not reach significance, or even the suggestive cutoff value, the string plots for the two traits (Figures 13 and 18) are strikingly similar. The issue of non-significance in LOD scores will be discussed below.

The other set of traits which show a high level of within-bone morphological integration are Femur Articular Breadth and Femur Bicondylar Breadth. These traits show very similar peaks on three chromosomes: 2q, 7_21, and 14_15 (Figures 21 and 22). The only one of these QTLs to reach the level of suggestive significance is the peak on chromosome 2q for Femur Bicondylar Length, with a LOD score of 1.5137, but the similarities shown in the string plots suggests that similar genomic regions are influencing variation in these traits.

Many of the results reported for the linkage analyses do not reach the level of a suggestive LOD score, much less a significant LOD score. As described in *Research Design*, above, a LOD score is used to compare the likelihood that a trait and marker are actually linked versus seeing the same data purely by chance. Using a modification of Feingold et al. (1993), which takes pedigree complexity and finite marker locus density of the linkage map into account, a suggestive LOD score for this sample is 1.5 and a significant LOD score is 2.75 (following Sherwood et al., 2008). The significant LOD score is associated with a genome-wide *p*-value of 0.5, while the suggestive LOD score provides a result that would be expected to occur once in a

genome-wide linkage scan. Therefore, not all of the suggestive LOD scores that are reported here are going to be results that eventually lead to the identification of candidate genes which influence phenotypic variation. Some of these will be associations that are produced purely by chance. However, these suggestive LOD scores are worthy of reporting as they are currently the most noteworthy sections of the genome that are associated with the known phenotypic variation. And, given that many of the candidate genes that were identified here connected directly to proteins that are known to be involved in limb development (Figures 29, 31, 33), this suggests that the LOD scores where these genes were found, while not significant, are picking up on areas of the genome that are associated with phenotypic variation in these traits.

Even more precarious than reporting suggestive LOD scores is the reporting of LOD scores which are nearing the level of being suggestive (for instance, the small peak on chromosome 7 for Humerus Maximum Length that is located in the same region as the suggestive peak for Femur Bicondylar Length, described above). The reporting of these peaks here is not meant to say that these peaks are definitively showing the areas of gene(s) which influence phenotypic variation. Rather, they are noted here as interesting areas which overlap areas that do reach the level of a suggestive LOD score in traits which are either highly integrated or homologous to the trait being discussed.

A LOD score may reach the level of significance by increasing the number of individuals included in the pedigree. If linkage does exist between the trait and the area of the genome where the (near) suggestive LOD score peak is located, then increasing the sample size will increase the strength of the relationship between the two.

Evolutionary Perspective Hypotheses

1. *Evolvability will increase with limb diversification (i.e., as the upper and lower limbs evolve to perform different functions).*

Evolvability, or the expected evolutionary response to selection in a trait, is expected to increase across species to allow the limbs to evolve to perform different functions. Additionally, the expectation is that evolvability estimates will be comparable across limb segments in quadrupedal non-human primates and more variable across the limb segments in the bipedal human sample. This is because limbs that do not need to adapt to different functions (i.e., the limbs of quadrupeds) should show consistent levels of evolvability, while limbs that need to adapt to differing functions (i.e., limbs of bipeds) may need different levels of evolvability to allow limb segments to change. The results of this study are again split on whether they support this hypothesis.

With regard to whether evolvability increases with limb diversification, there are some interesting patterns which support the hypothesis (Tables 16, 23, 30, 37, and 43). Given that all the non-human primate samples are quadrupeds, the results are expected to show that the Tamarins, Sukhumi Baboons, and TBRI Baboons are very similar and all are significantly different from the Mennonites. This is only partially the case. The patterns of evolvability estimates do indeed show that they increase from the quadrupedal non-human primates to the bipedal humans; however, the differences are not significant across the board. The evolvability estimates for the Tamarins are significantly lower than the Mennonites for the humerus, radius, and femur, and the TBRI Baboons are significantly lower for the femur only. However, none of the comparisons between the Sukhumi Baboon and Mennonite evolvability estimates are significantly different. In fact, the Sukhumi Baboons differ only from the Tamarin proximal

elements, which are significantly lower. Thus, the significant difference between the Tamarins and the Mennonites supports the hypothesis expectation of increasing evolvability with limb diversification, but the lack of significance between the Sukhumi Baboons and the Mennonites does not support the hypothesis.

With regard to the expectation that evolvability estimates should be more uniform in quadrupedal samples versus bipedal samples, the results do support the hypothesis. Intra-sample comparisons for the Tamarins, Sukhumi Baboons, and TBRI Baboons show that none of the evolvability estimates are significantly different within each sample. Alternatively, the Mennonites do show some significant differences in the intra-sample comparisons. The thigh has a higher level of evolvability than all of the other limb segments.

2. *The difference between conditional evolvability and evolvability will decrease with limb diversification.*

A trait that has a low conditional evolvability relative to evolvability shares the majority of its variation with other traits, and evolution acting on this trait would cause correlated responses in other traits (Hansen and Houle, 2008; Roseman et al., 2010). Quadrupedal primates are expected to have low conditional evolvability relative to evolvability because all limbs are expected to be highly correlated. A higher conditional evolvability relative to evolvability (i.e., a reduced difference between the two measures) means the trait is more able to evolve on its own. Therefore, bipedal humans should show this latter pattern.

In these analyses, the difference between *e* and *c* is measured using a measure known as *i* (for integration, although this should not be confused with the other measures of integration

discussed here). As shown in Equation 4.5, *i* is calculated as the difference between 1 and the quotient of *c* and *e*. Therefore, as the difference between *c* and *e* decreases, *i* will decrease. If there is a large difference between *c* and *e*, then *i* will be closer to 1. Traits with *i* values closer to 1 are less capable of evolving independently, while lower values of *i* indicate that the trait can evolve more independently because it is less correlated with other traits. For this hypothesis, then, the quadrupedal non-human primate samples are expected to have higher *i* values than the human sample. The results of the estimates of *i* in this study are again split on whether they support this hypothesis.

The *i* estimates for each sample are listed in Tables 16, 23, 30, and 37, and while there is no table showing the results of the intra- and inter-sample comparisons, the only significant results are noted in the *Tamarins vs. Mennonites* section in *Results*, above. The patterns of *i* estimates in the abovementioned tables do indeed show that the difference between evolvability and conditional evolvability decreases for limb segments from the non-human primate samples to the human sample. However, like so many other patterns seen in this study, not all of the results are significant. There are no significant differences found within any of the individual samples, indicating that all limb segments within each sample have the same level of independence to evolve. As for inter-sample comparisons, the only significant differences are found between the humerus, radius, and tibia of the Tamarins and the Mennonites. The Tamarins show significantly higher *i* estimates for these three limb segments compared to the Mennonites, which indicates that these traits are less capable of evolving independently in the Tamarins than the Mennonites. These significant results support the expectations of the hypothesis; however the

fact that neither of the quadrupedal baboon samples shows significant differences from the bipedal humans does not align with the hypothesis.

The fact that so few *i* estimates are significant is somewhat unexpected given that so many of the conditional evolvability estimates within and across samples are significantly different from one another (Table 44). As a reminder, *c* is a measure of evolvability that takes the covariance of traits into account when estimating a trait's response to selection. As shown in the *c* results previously (see *Results*, above), the Tamarins show the lowest levels of *c* and the highest levels of phenotypic and genetic correlation across limb segments. Conversely, the Mennonites show the highest levels of *c* and the lowest levels of phenotypic and genetic correlation across limbs. The Sukhumi Baboons and TBRI Baboons fall in the middle. However, when the correlation between traits is not included and the upper limit of evolvability (unconditional evolvability, or *e*) is calculated, there is less of a difference between the samples (i.e., fewer significant differences), as seen in Table 43. Because *i* is a ratio *c* and *e* subtracted from 1, the large differences seen within and among samples in the estimates of *c* are tempered by the smaller differences seen within and among samples in the estimates of *e*.

3. *Morphological integration will decrease with limb diversification.*

As the limbs evolve to perform different functions, integration between the limbs (i.e., between homologous elements) will decrease (Young and Hallgrímsson, 2005). This means that humans, which are bipedal, will show lower integration than the other primate samples, which are quadrupeds. The results from this study support this hypothesis.

As shown in Tables 59 and 60, the Tamarins have the highest level of relative eigenvalue variance (i.e., morphological integration), the Mennonites have the lowest level of relative eigenvalue variance, and the Sukhumi Baboons have relative eigenvalue variance estimates in the middle. All of the comparisons across species are significantly different except for the comparison between the Sukhumi Baboon and Mennonite proximal elements which are not significantly different. These results show that the human sample has quite low levels of morphological integration for all measures of integration (i.e., upper limb, lower limb, proximal elements, distal elements, and all four elements), and specifically for the measures looking at homologous elements (i.e., proximal elements and distal elements). The one exception of non-significance between the Sukhumi Baboon and Mennonite proximal elements does not fit with the expectations of hypothesis.

The patterns presented by the results of the relative eigenvalue variance analyses for morphological integration analysis accord well with the results shown in the previous hypothesis (*Evolutionary Perspective Hypothesis 2*) which looked at integration through the comparison of *c* and *e* using the measure *i*. Both sets of results indicate that the Tamarin limb segments are significantly more highly integrated and less capable of evolving independently of one another than the Mennonite limb segments. The Sukhumi Baboon limb segments show the same pattern in each set of analyses by having intermediate values of *i* and relative eigenvalue variance; however, while the difference between the Sukhumi Baboons and the other two samples is significant in the majority of the cases in the relative eigenvalue variance analyses, none of the comparisons of *i* are significant for this sample.

One interesting observation regarding these data is the fact that the patterns presented here do not conform identically to previous research that looked at morphological integration in primate limbs (Young et al., 2010). While Young and colleagues did not use baboons and tamarins in their samples, they did include multiple species of both Old World and New World monkeys, which were also used here (i.e., baboons are Old World monkeys and tamarins are New World monkeys). In their analyses, the Old World monkeys have higher levels of morphological integration than the New World monkeys, which is opposite the pattern seen in this study (the Sukhumi Baboons, as Old World monkeys, have lower morphological integration than the Tamarins, the New World monkey sample). However, there is some overlap between the Old World and New World monkeys, and the larger point of their analyses is that humans and apes show much reduced levels of integration as compared to the quadrupedal monkeys. The specific results between the Young et al. (2010) paper and this study cannot be directly compared as the former used eigenvalue variance as the measure of integration rather than the relative eigenvalue variance used here.

Implications for Anthropological Research

Heritability is not the Same as Evolvability

The results of this study support the statement made by Hansen, Houle, and colleagues (Houle, 1992; Hansen et al., 2011) that heritability is not evolvability. These papers show that when looking at traits from over 200 quantitative genetic animal studies, the correlation between heritability and evolvability is near zero. The correlation between the heritability estimates and evolvability estimates presented in this study is 0.64. While this may seem like a fairly strong

correlation between heritability and evolvability, it is likely a result of the small number of data points included (only 14 estimates of each) and would decrease as more data were added.

Perhaps what is more important than the low correlation between heritability and evolvability is the lack of correspondence between the heritability and evolvability results. As shown in Tables 42 and 43, the pattern of significance within and between samples is very different. The only significant difference within the heritability estimates is that the Mennonite thigh has a significantly higher heritability than the Mennonite forearm. This is explained by the dramatically higher phenotypic and genetic variance found in the Mennonite thigh (both of which are four times higher than the same values for the forearm). The remaining comparisons of heritability are not significantly different from one another because, for these samples, as genetic variance increases, so does phenotypic variance. This is partly due to the fact that, as explained by Hansen and colleagues (2011), "scaling additive variance with phenotypic variance becomes akin to a rubber scale that gets stretched when measuring something large" (pp. 268). However, when genetic variance is scaled by the squared trait mean, as is done when estimating *e*, there are many more significant differences within and among the groups. The "rubber scale" of phenotypic variance is replaced with the squared trait mean as a way to scale the genetic variance seen in each trait.

This is not to say that heritability does not have a purpose. Given that heritability is population and environment specific it can be useful when used in specific situations. For example, heritability is useful as a predictor of response in artificial selection (following the breeder's equation [Equation 3.6, above]). However, heritability is not a useful predictor of evolutionary potential in natural selection and is not meaningful when compared across

populations. Using heritability in these ways leads to dubious conclusions, such as the idea that life-history traits have low genetic variance when in fact they simply have very high phenotypic variance (as discussed in *Methodological Background*, above).

The evolvability results reported here align nicely with expectations following Hansen and colleagues (2011). That paper reports that the median *e* for linear traits in their database is 0.001, which corresponds to a tenth of a percent change per generation for traits under unit selection or a 10% change in about 100 generations. Evolvability estimates in this study range from 0.000519 (Tamarin humerus) to 0.002263 (Mennonite thigh), which are slightly higher than the median reported above. However, given that lengths have been shown to be more highly heritable than other measures, such as measurements of breadth (Clark, 1956; Osborne and DeGeorge, 1959; Vandenberg, 1962; Leamy, 1974; Devor et al., 1986a,b; with exceptions being Susanne, 1977; Arya et al., 2002), it is not all that surprising that the *e* estimates here are slightly higher than reported by Hansen et al. (2011) which likely included measures other than just length.

The evolvability estimates presented here do indeed indicate that limb segment lengths in humans and other primates are capable of changing rather significantly if under directional selection to do so. They will not have changed as much as these evolvability estimates may suggest though, given than *e* is the upper limit of evolvability and must be tempered by the correlation between traits. Therefore, conditional evolvability estimates will show a more accurate representation of the ability of these limb segments to change through time.

Genetic Data Change the Phenotypic Story

The results of this study also support another important idea: phenotypic variance alone cannot predict how limb elements will respond to selection pressures. Many times, simply as a result of the type of specimens available in anthropological collections, studies rely solely upon patterns of phenotypic variance and correlation to make statements about the way in which populations or species are related, how they evolved, and where they migrated from (see *Limbs*, above). These studies use phenotype alone to postulate explanatory evolutionary mechanisms without firm knowledge of the underlying genetic variation (e.g., Trinkaus, 1981; Ruff, 1991; Holliday, 1997). As this study shows, such a jump from phenotypic patterns to genetic mechanisms is not always a good idea.

Cheverud demonstrated that the phenotypic variance/covariance matrix can be a good proxy for the genetic variance/covariance matrix (Cheverud, 1988). However, he noted that his method of multiplying the phenotypic covariance matrix by a factor equal to the average heritability of the traits "will certainly lead to errors in evolutionary inference in specific instances" (pp. 965). Some authors, in particular Willis and colleagues (1991), argue that the substitution of phenotypic correlations for genetic correlations is unreliable and should be approached with caution.

The results of this study support the idea that patterns of phenotypic variance and correlation do not exactly mirror genetic variance and correlation. As shown in Tables 38 and 40, the patterns of significant differences across limb segments within individual samples are not the same for phenotypic variance and genetic variance. There are many more significantly different phenotypic variance values than there are genetic variance values. Similarly, looking at Tables

39 and 41, there are many fewer significant intra- and inter-sample comparisons for genetic correlations than phenotypic correlations. If phenotypic values alone are used to explain the variation within and across species, the conclusion would be that many of the individual limb segments have differing levels of additive genetic variance and would thus potentially respond to directional selection at different rates that are tempered by many significant correlations between segments. However, if the more appropriate genetic values are used to explain variation within and across species, different conclusions about the response to directional selection would be drawn.

This is not to say that studies which are unable to estimate genetic parameters and substitute the phenotypic covariance matrix are useless. Estimating genetic parameters is a known difficulty in anthropological studies because of the need for pedigree information. There are many solid studies whose results are likely similar to what would be found if genetic data were available. Like many other issues in anthropology (i.e., small sample sizes, missing data, fragmented specimens, etc.), there are limits to what can be done, and many creative solutions have been implemented to work around those limits. But, the limitations must be acknowledged, and in cases where genetic data is lacking, results must be interpreted with an understanding that phenotype is not the whole story.

The Fossil Record

Perhaps the area of anthropological research where the most speculation about the way in which limbs evolve is found is in reconstructing the fossil record. This is for a good reason – paleoanthropological samples are notoriously difficult to work with: the limitations of small

sample sizes, fragmented specimens, and lack of genetic data are very real. There are a few areas of paleoanthropological research which will be discussed here to see how results from this study may impact our understanding of the fossil record.

The first of these areas to be reviewed is the pattern of limb segments changes discussed in *Phylogenetic Relationships and Fossil Identification* in *Limbs*, above. According to various authors, humeral reduction occurred prior to femoral elongation in hominin evolution (Jungers, 1982; Kimbel and Delezene, 2009), and femoral elongation occurred prior to forearm shortening in early hominids (Asfaw et al., 1999). Whether or not these claims are possible depends on the genetic correlation structure of these traits and, by extension, the conditional evolvability and *i* estimates of each limb segment.

Looking at the genetic correlations for the Tamarins (Table 14), Sukhumi Baboons (Table 21), and Mennonites (Table 30), there are some patterns that can be seen. The correlation between the femur and radius is the lowest of all genetic correlations for the Tamarins, indicating that perhaps these two limb segments would be the most likely to evolve independently. Likewise, the correlation between the humerus and radius is one of the highest, indicating that these two limb segments would be less likely to evolve independently. However, none of the genetic correlations for the Tamarins are significantly different from one another (Table 41). The same is true for the Sukhumi Baboons. For the Mennonites, the correlation between the humerus and radius is the lowest of all genetic correlations, and the correlation between humerus and femur is the highest. These two correlations are significantly different from one another, indicating that perhaps the humerus and radius are more likely to evolve independently than the humerus and femur because they share less genetic variance.

Yet, when looking at the evolvability, conditional evolvability, and *i* results for the Tamarins (Table 16), Sukhumi Baboons (Table 23), and Mennonites (Table 30) as well as the comparisons between these (Tables 43 and 44), there is very little significance. While the radius shows the lowest *i* value within the Tamarin and Mennonites samples, indicating that it may have more of an ability to evolve independently than other limb segments, it is not significantly different within either sample. The Mennonite femur does have a significantly higher evolvability than the other three limb segments, suggesting that it has more of an ability to evolve, but the conditional evolvability of this limb segment is not significantly different from either the humerus or the radius, and the *i* estimate is not significant either. The Sukhumi Baboons do show a significantly different conditional evolvability for the humerus and radius, with the humerus having a greater ability to evolve, but the *i* estimates for these limb segments are not different from one another.

These results suggest that, when looking within individual samples, none of the limb segments are any more or less likely to evolve independently than any of the others. Any response to directional selection pressure for one limb segment to elongate or shorten would be met with correlated responses among the other limb segments. This is not to say that femoral elongation or humeral or forearm shortening could not happen, just that these events likely did not occur in isolation from other changes occurring at the same time in other limb segments.

However, as argued in Young and colleagues (2010), the combination of reduced integration and increased independent evolvability of the limbs across species shows the evolution of adaptations for functionally divergent limbs. The significant pattern of reduced morphological integration (as measured with relative eigenvalue variance) (Tables 59 and 60)

and increased evolvability and conditional evolvability (Tables 43 and 44) seen here across taxa supports this idea.

The evolution of bipedalism is another area of the fossil record in which may gain insight from these results. The modern bipedal gait is often definitively attributed first to *H. erectus* (for a review, see *Locomotor Behavior and the Evolution of Bipedalism* in *Limbs*, above), some specimens of which possessed the long legs that are indicative of modern members of the genus *Homo*. The significantly high evolvability of the thigh in the Mennonite sample (Tables 30 and 43) supports the idea that the lower limb was able to change as needed for limb diversification due to new functional demands (i.e., bipedalism). However, these results must be viewed in conjunction with the conditional evolvability and *i* results which show that a good portion of the genetic variance of the thigh is shared with other limb segments, and, therefore, the femur does not evolve independently. The morphological integration results show that, while limb elements are still integrated, the level of integration (as measured with relative eigenvalue variance) is much reduced as compared to the quadrupedal non-human primate samples. This suggests that while the limb segments of the Mennonites do share genetic variance across elements, they are more capable of evolving independently than quadrupeds. So, just as when discussing limb segment elongation and shortening as above, these results do not suggest that lower limb elongation in general, and femoral elongation specifically, did not occur – it very clearly did. What these results do suggest is that femoral elongation was tempered by the genetic variance that the femur shares with the other limb segments. The results of this study cannot assess whether locomotor efficiency was the adaptive cause of the shift to bipedalism in the genus

Homo, as suggested by several authors (Rodman and McHenry, 1980; Leonard and Robertson, 1995; Pontzer, 2009).

Likewise, this study cannot determine if adaptations due to thermoregulation or mechanical loading were responsible for the distal limb shortening found in Neandertals (for a review, see *Ecogeographic Patterning* in *Limbs*, above). What this study can do is comment on the ability of distal limb elements to change independently of proximal limb elements. This independent change of the distal limb elements would require a higher conditional evolvability relative to evolvability (i.e., a lower *i*) in the distal elements than the proximal elements and decreased morphological integration within limbs. Unlike the non-human samples, the Mennonite sample does show a pattern of reduced estimates of *i* in the distal segment of each limb as compared to the proximal segment of the same limb (Table 30); however, these differences are not significant. As for the morphological integration expectations, the relative eigenvalue variance within limbs is significantly smaller than the relative eigenvalue variance of homologous elements in the Mennonites (Table 59). This suggests that the homologous distal elements would have been more likely than the elements within a limb to change together. Like all other scenarios discussed here, a change in the distal limb elements of Neandertals (or for that matter, early modern humans that may have adapted to a cold European climate, following Holliday [1997]) likely did not occur in isolation but in correlated response with the other limb segments.

All this discussion highlights the fact that researchers should use caution when interpreting differences across specimens in the fossil record and not automatically assign adaptation via natural selection as an explanation. While adaptation likely plays a large role in

many of the differences seen across species, some of the changes will be due to correlated responses from selection acting on another bone. It would probably make anthropological analyses much easier if each bone or trait acted independently and selection on that bone affected that bone alone, but such is not the case. Body plans in general, and primate limb morphologies specifically, are correlated structures that, because of developmental constraints and morphological integration, cannot change without altering multiple traits along the way.

Clinical Applications of QTLs

One goal of this study was to begin to identify genes which are involved in the normal variation of limb segment morphology, most importantly limb segment length. This is important because genetic variation must be present in order for evolution to occur; thus, there must be genes which are involved in producing normal variation in limb segment length and other features. A better understanding of the genes involved in producing normal variation provides an avenue to deciphering how limb morphology evolves.

The first step in identifying genes which may be involved in producing variation in a phenotype such as limb segment length is to identify regions of the genome which may harbor these genes through the process of identifying quantitative trait loci. The QTLs that are identified may be of interest outside of the evolutionary anthropology/biology sphere if they are applicable in a clinical sense. The potential clinical significance of the QTLs identified in this study is discussed here.

There are several peaks for Humerus Maximum Length and Femur Bicondylar Length that correspond closely with areas of the genome which are known to contribute to limb

malformation when mutations are present. The best example is hypophosphatasia, a form of osteochondrodysplasia which involves abnormal bone or cartilage growth and leads to skeletal malformation, often manifesting as a form of short-limbed dwarfism. Hypophosphatasia presents with a wide range of lethal abnormalities, including poorly formed limb bones, and is known to be caused by various mutations in the tissue-nonspecific alkaline phosphatase (TNSALP) gene located on the p arm of chromosome 1 (specifically 1p36.1-1p34) (Greenberg et al., 1990; Jones, 2006). As seen in Figure 13, there are several non-significant peaks located on chromosome 1 for Humerus Maximum Length. One of these peaks, with a LOD score of 1.0592, is found at location 19, which resides between STR markers D1S548 and D1S2130. The location of these STRs in the human genome is between bps 7,365,332 and 41,590,405 on the p arm of chromosome 1. This corresponds specifically to 1p36.23-1p.34.2, almost exactly the same region known to influence hypophosphatasia.

There are several other patterns of malformation which have known mutations near a QTL that was identified here. First, Robinow syndrome presents with a variety of symptoms, including relatively short limbs. It is known to be caused by mutations in the ROR2 gene located on chromosome 9q22 (Afzal et al., 2000; Jones, 2006). As seen in Figure 18 there is a non-significant peak on chromosome 9 for Femur Bicondylar Length. This peak has a LOD score of 1.0873, is found at location 134, and is located between STR markers D9S934 and D9S1798. The corresponding bps are 120,135,476 to 128,212,507, which corresponds to location q33.1-q33.3. Second, Shwachman-Diamond syndrome, another form of osteochondrodysplasia, is known to be caused by mutations in the gene SBDS located at chromosome 7q11 (Boocock et al., 2003; Jones, 2006). Both the femur and the humerus show a peak on chromosome 7 (the

QTL for Femur Bicondylar Length is suggestive while the QTL for Humerus Maximum Length is non-significant). This peak is previously described in *Suggestive LOD Scores Associated with Limb Segment Lengths* in *Results*, above, and resides at chromosome 7q22.3-1q31.31. While neither of the QTLs on chromosomes 9 or 7 exactly aligns with the known mutations associated with these syndromes, there are suggestive and non-significant peaks which are nearby.

While identifying correspondence between known mutations that cause limb malformation and the results found in this study is interesting, it does not necessarily provide new insight into areas of the genome which may contribute to different syndromes. There are multiple patterns of malformation which do not have known genes that influence the abnormal development that is seen in some individuals. For instance, femoral hypoplasia-unusual facies syndrome presents with abnormalities of the face, pelvis, spine, and limbs, and the cause of this syndrome is unknown (Franz and O'Rahilly, 1961; Jones, 2006). The same is true of numerous other skeletal malformations which involve the limbs, including, but not limited to, fibrochondrogenesis, Roberts syndrome, metatropic dysplasia, Schinzel-Giedion syndrome, short rib-polydactyly syndrome types 1 and II, and Peters'-Plus syndrome (all described in Jones, 2006). The inheritance pattern of many of these syndromes is known (for example, autosomal recessive), but the specific gene(s) which, when mutated, may lead to these syndromes are unknown. The identification of new areas of the genome which are statistically associated (although not always significantly) with normal phenotypic variation in limb segment lengths may lead to new connections being made between these syndromes and possible responsible genes.

Limitations of the Study

Osteometrics vs. Anthropometrics

One area of likely imprecision in the present study is the use and comparison of both osteometric and anthropometric data. The presence of soft tissue in anthropometric measures obviously increases those measurements, however slightly, over what they would be if the bone itself were being measured. Additionally, the way in which bones are held and measured cannot be precisely mimicked when the bones are being measured within the body. Therefore, the comparison of results from both data types likely introduces some error into the study that cannot be quantified.

Given that the anthropometric data used here (i.e., the Sukhumi Baboons and the Mennonites) were collected by other observers (as described in *Samples* in *Research Design*, above), it cannot be said with certainty how carefully the measurements were taken. However, it is assumed that the individuals that collected the data were well-trained in anthropometric procedures, were capable of correctly measuring the individuals following the measurement definitions, and exercised every precaution to minimize intraobserver measurement error. If these assumptions are true, then the data used here should be acceptable for these analyses even if caution is warranted when interpreting the results between the two datatypes.

Several precautions were used in this study to minimize the amount of imprecision that the problem of anthropometric and osteometric data would introduce. First, bicondylar length of the femur, rather than maximum length of the femur, was measured for both of the skeletal samples (i.e., the Tamarins and the TBRI Baboons) to more closely approximate the length that is measured in the anthropometric measurement of thigh length. Secondly, the use of two baboon

samples was done to not only make up for the missing limb segments in the TBRI Baboons, but also to serve as a comparison for the two types of data. As described in the *Sukhumi Baboons vs. TBRI Baboons* section in *Results*, above, the samples were not significantly different from one another in many regards. Estimates of genetic variance, heritability, evolvability, and *i* were the same between the samples. However, the TBRI Baboons had significantly higher estimates of genetic correlation and phenotypic correlation while the Sukhumi Baboons had significantly higher estimates of conditional evolvability. Whether these differences are due to inconsistencies in datatype or the fact that they are different populations of baboons with unique mixtures of subspecies is unknown. Despite these differences, the two samples did consistently seem to fall as intermediates between the Tamarins and the Mennonites.

One issue which could not be circumvented is that the forearm length of the Sukhumi Baboons was measured so that the length of the ulna, rather than the radius, was approximated. As noted in *Limbs*, above, while the lengths of the radius and ulna are correlated, they are not isometrically scaled (i.e., while the size of both may change in the same direction, the proportion between the two bones is not constant). Therefore, the forearm measure from the Sukhumi Baboon sample is known to be inaccurate compared to the other samples, but it is a problem that is unavoidable.

Mennonite Limb Segments Calculations

Another area in which error was potentially introduced into the study was the way in which two limb segments were calculated from other anthropometric measurements in the Mennonite sample. As a reminder, Forearm Length was approximated by subtracting Upper Arm

Length and Right Hand Length from Upper Limb Length. While the results produced forearm measurements that, in conjunction with Upper Arm Length, produced brachial indices that fall within normal human ranges (see *Limb Segment Calculations in the Mennonites* in *Research Design*, above), the way in which Forearm Length was calculated may induce a negative estimation bias between Forearm Length and the other quantities, namely Upper Limb Length. However, without this approximation of the Forearm Length, the Mennonite sample would not have been useful for this study.

A more complicated route was taken to estimate Thigh Length for the Mennonite sample. The available anthropometrics included Trochanteric Height and Leg Length, but no measure of Foot Height to calculate Thigh Length in a similar fashion as Forearm Length. This is where the anthropometric data on U.S. Army Personnel (Gordon et al., 1988) were used to create regression equations (see *Appendix III*, below) to estimate Foot Height (i.e., Lateral Malleolus Height). Thigh Length was then approximated by subtracting Leg Length and Foot Height from Trochanteric Height. This method once again produced estimates which, in conjunction with Leg Length, produced crural indices that fall in normal human ranges (see *Limb Segment Calculations in the Mennonites* in *Research Design*, above). However, there are several potential issues with this methodology. First, there is again the possibility of negative estimation bias for Thigh Length as compared to Leg Length. Second, the regression equations were produced using trait averages, standard deviations, and correlations from a different sample (U.S. Army Personnel). It is unknown how closely the U.S. Army Personnel data aligns with the true values of the Mennonite individuals. Yet, despite these issues, the Mennonite data would not have been available for inclusion in this study without an estimation of Thigh Length.

The Mennonite Thigh Length shows the highest estimate of phenotypic variance, genetic variance, heritability, evolvability, and conditional evolvability of all limb segments across all samples. It is also rather consistently reaches significance when in comparison with other limb segments, both within and across samples. Whether these results are due to the way in which Thigh Length was estimated or simply due to the fact that the human femur is highly variable and evolvable compared to other limb segments is unknown. Interpretations of the results pertaining to the Mennonites, therefore, warrant caution.

Future Research

The primary goals of this study were to describe the genetic variance and morphological integration of individual limb segment lengths and to begin the task of identifying genomic regions which may play a role in producing that normal genetic variation. The results of this study provide some interesting insights but are far from conclusive. Future research could help to bring more of these results from interesting patterns to significant results.

One way in which to aid in this task would be to add the outliers that were removed from the analyses. Only a small percentage (about 4%) of all individuals were removed from analysis (for details, see *Outlier Removal* in *Research Design*, above), but these individuals may harbor helpful information. While outliers are typically removed so as to not skew results, they could be useful in this situation. Individuals with greater phenotypic variation may also have greater genetic variation, and this greater variation could lead to significance between samples for quantitative genetic measures. Additionally, the presence of greater genetic variation from outlier data in linkage analysis may increase likelihood of finding suggestive or significant QTLs.

Another way to improve this study would be to increase sample sizes. While 1,353 individuals across four samples may seem like an adequate sample size to accurately describe genetic variance, increased sample sizes will increase the accuracy with which genetic parameters are estimated. An increased sample size for the TBRI Baboons would also increase the accuracy and significance of QTLs. A large number of individuals is needed to detect QTLs given that many of the QTLs for quantitative traits, such as limb segment length, likely have very small effects on phenotypic variance. For example, some of the genome wide association studies looking for genomic variants for height used anywhere from 4,000 to over 30,000 individuals (Gudbjartsson et al., 2008; Lettre et al., 2008; Sanna et al., 2008; Weedon et al., 2008; Soranzo et al., 2009). However, increasing the sample size of the Sukhumi Baboons and Mennonites is not possible as those data were collected decades ago. Also, all the Tamarins that were available to measure were included here. All TBRI Baboons that met age requirements were included at the time of measurement, but additional specimens may have been added to the collection since then. Therefore, it may be possible to increase the sample size of the TBRI Baboons for future research.

Conclusions

In conclusion, this study set out to describe the genetic variance and covariance in limb segment lengths in humans and other primates and then and begin the initial investigation into identifying genomic regions which are statistically associated with normal phenotypic variation in these traits. This study is noteworthy for several reasons: 1) Pedigreed samples were used to assess additive genetic variance, allowing direct estimation of evolvability and conditional

evolvability in these traits, 2) multiple primate samples, consisting of humans and non-humans, were used to identify differences between species which may help to explain evolutionary changes over time, and 3) linkage analysis was used to identify QTLs associated with limb segment lengths and other limb features. This approach, while limited in some of the technical details (discussed in *Limitations of the Study*, above), allowed the following overarching questions, to be answered.

1. *Does variation in limb segment morphology follow the expectations of a Developmental Perspective, an Evolutionary Perspective, or aspects of both?*

The results of this study suggest that the limb morphology of humans and other primates largely adheres to expectations set forth from both a Developmental Perspective and an Evolutionary Perspective, but there are some details which do not fit as anticipated. The overall expectation and reality of each set of hypotheses is laid out below.

The Developmental Perspective was largely driven by the notions that 1) limbs develop in a proximo-distal gradient (Tarchini and Duboule, 2006; Gilbert, 2013), 2) limb segment lengths are more genetically canalized than other limb features (Auerbach and Ruff, 2006; Cowgill and Hager, 2007), and 3) homologous structures have similar developmental pathways (Hallgrímsson et al., 2002; Gilbert, 2013). These ideas led to hypotheses which supposed that 1) phenotypic variance should increase and heritability should decrease in a proximo-distal gradient, 2) limb segments lengths should be more highly integrated than other limb features, and 3) proximal elements should show higher levels of morphological integration than distal elements while homologous structures should be more highly integrated than elements within the

same limb. Additionally, the proximal elements, with presumed high heritability and high morphological integration, should have QTLs in similar areas of the genome which are statistically associated with phenotypic variation.

There are aspects of each of these hypotheses that are supported by the results, as detailed above. Developmental Perspective Hypotheses 2 and 4 are supported by these results: limb segment lengths show higher levels of integration than do other limb features (most notably diaphyseal measures), and limb traits with high morphological integration have QTLs in similar genomic regions (most notably Humerus Maximum Length and Femur Bicondylar Length). Developmental Perspective Hypotheses 1 and 3 are more mixed in their adherence to expectations. While phenotypic variance does not increase from proximal to distal elements in the upper limb for the three samples analyzed, it does increase from the femur to the tibia in the Tamarin sample; however, the Sukhumi Baboons and Mennonites show a reduction in phenotypic variance from the femur to the tibia. And, none of the samples show the expected decrease in h^2 from proximal to distal elements. Additionally, the expected higher integration in proximal elements as opposed to distal elements is not seen, and there is no difference between integration for homologous structures and within-limb structures for the non-human primates. The human sample does, however, show the expected pattern of higher integration between homologous structures than within-limb structures. The results of the Developmental Perspective Hypotheses suggest that, overall, limb morphology adheres to the expectations set forth using what is known about the way in which limbs develop.

The Evolutionary Perspective was driven largely by the ideas that 1) a major difference across primates is limb diversification from species that are quadrupeds to species that use

suspension, leaping, or, as emphasized here, bipedalism, and 2) traits that evolve more independently share relatively less of their variation with other traits (Hansen and Houle, 2008). These ideas led to hypotheses which postulated that with limb diversification comes 1) an increase in evolvability, 2) a reduction in the difference between conditional evolvability and evolvability, and 3) a decrease in morphological integration.

The expectations of these hypotheses are largely supported by the results, as detailed above. All three Evolutionary Perspective Hypotheses find support in these analyses. First, evolvability does indeed increase from the Tamarins, where it is uniform across limb segments, to the Mennonites, where the femur has higher evolvability than the other limb segments. The Sukhumi Baboons fit expectations with the pattern of evolvability (i.e., they are intermediate between the Tamarins and the Mennonites), but not in significance (i.e., they are not significantly different from the Mennonites). Second, there is a reduction in the difference between conditional evolvability and evolvability from the Tamarins to the Mennonites, indicating that quadrupedal non-human primate limb segments are less capable of evolving independently as compared to bipedal humans. Again, the baboon samples are not significantly different from the humans. Finally, morphological integration, as measured by relative eigenvalue variance, does indeed decrease from the Tamarins to the Sukhumi Baboons to the Mennonites. The results of the Evolutionary Perspective Hypotheses suggest that limb morphology in humans and other primates adheres well to the expectations set forth using what is known about the way in which limbs evolve.

2. *How accurate is the current operating assumption used by biological anthropologists regarding limb segment lengths and proportions?*

As discussed in *Limbs*, above, the current operating assumption among biological anthropologists regarding limb segment lengths (and by extension, limb proportions) is that limb proportions in humans are phenotypically stable unless long periods of extreme environmental conditions force adaptive change (e.g., Ruff, 1994; Holliday, 1997; Ruff, 2002). This assumption can be broken down into two different parts, each discussed in turn.

The first part of the current operating assumption among biological anthropologists regarding limb proportions is that they are phenotypically stable traits. A wealth of evidence in the literature supports this notion, including the geographic patterning of limb proportions across fossil species and modern humans (e.g., Roberts, 1978; Ruff, 1994; Ruff, 2002a), the disparity between Old World and New World data in adhering to thermoregulatory expectations (e.g., Auerbach, 2010; Jantz et al., 2010), and the consistency of ancestral limb proportions of migrant children in new climatic settings (e.g., Froehlich, 1970; Martorell et al., 1988). But do the results of this study support the idea that limb segment lengths (and limb proportions) are phenotypically stable traits? Overall, yes, they do. While evidence from the conditional evolvability, *i*, and relative eigenvalue variance estimates indicate that humans are much more capable of independently altering their limb segment lengths in response to directional selection (because of the combination of increased evolvability and decreased morphological integration), these changes must occur in conjunction with the underlying correlation structure between traits.

Additionally, while there is a significantly higher level of evolvability in the human sample as compared to the non-human primate samples, the rate of evolution that would occur

given these estimates is still slow. Recall that an *e* estimate of 0.001 leads to a 10% change in the trait in about 100 generations (Hansen et al., 2011); however, unconditional evolvability estimates (i.e., *e*) are the upper limit of evolutionary potential, and a more accurate reflection of the rate of evolution comes from using conditional evolvability estimates. These estimates are, again, tempered by the correlation structure between individual traits, and as the results show here, none of the limb segments are capable of altering completely independently. And, any change that could occur as a result of higher conditional evolvability estimates would be the result of direct selection on that trait to change.

This brings us to the second part of the assumption that biological anthropologists make regarding limb proportions: that differences in limb proportions are the direct result of adaptive responses. While this may very well be true in many cases, and phenotypic patterns in the literature strongly advocate for climate (e.g., Trinkaus, 1991; Ruff, 1994; Holliday, 1997) or increased mechanical efficiency (e.g., Trinkaus, 1991; Porter, 1999; Steudel-Numbers and Tilkens, 2004) as selective pressures, this part of the assumption should not be made without caution. The models purported in the literature accurately reflect the phenotypic patterns that are seen, but that does not mean that they inherently explain the processes (i.e., evolutionary mechanisms) which produced those patterns. As discussed above, the addition of genetic data adds a new dimension to the understanding of limb proportion variation and should be included in model building and analyses whenever possible. Newer research is beginning to explicitly investigate the evolutionary mechanisms that have produced the patterns of variation seen in modern human limb proportions (Betti et al., 2012; Roseman and Auerbach, 2015; Savell et al., in review). These results are suggesting that the evolutionary forces beyond selection (i.e.,

random genetic drift and gene flow) have played a large role in producing the patterns of phenotypic variation that are seen in limb proportions in modern humans. The results of this study should aid in future work designed to continue unravelling these questions.

REFERENCES

Ackermann RR, Cheverud JM. 2000. Phenotypic covariance structure in tamarins (genus *Saguinus*): A comparison of variation patterns using matrix correlation and common principal component analysis. *American Journal of Physical Anthropology* 111:489-501.

Adobe Systems Inc. 2012. Adobe Acrobat XI. Version 11.0.07. www.adobe.com.

Afzal AR, Rajab A, Fenske1 CD, Oldridge M, Elanko N, Ternes-Pereira E, Tüysüz B, Murday VA, PattonMA, Wilkie AOM, Jeffery S. 2000. Recessive Robinow syndrome, allelic to brachydactyly type B, is caused by mutations of ROR2. *Nauture Genetics* 25:419.

Aiello L, Dean C. 1990. *An Introduction to Human Evolutionary Anatomy*. New York: Academic Press.

Allen, JA. 1877. The influence of physical conditions on the genesis of species. *Radical Review* 1:108-140.

Almasy L, Blangero J. 1998. Multipoint quantitative-trait linkage analysis in general pedigrees. *American Journal of Human Genetics* 62:1198-1211.

Almasy L, Dyer TD, Blangero J. 1997. Bivariate quantitative trait linkage analysis: pleiotropy versus coincident linkages. *Genetic Epidemiology* 14:953–958.

Amos CI. 1994. Robust variance-components approach for assessing genetic linkage in pedigrees. *American Journal of Human Genetics* 54:535–543.

Amos CI, Elston RC, Wilson AF, Bailey-Wilson JE. 1989. A more powerful robust sib-pair test of linkage for quantitative traits. *Genetic Epidemiology* 6:435-449.

Arsuaga JL, Villaverde V, Quama R, Martíneza I, Carreteroa JM, Lorenzoa C, Gracia A. 2007. New Neandertal remains from Cova Negra (Valencia, Spain). *Journal of Human Evolution* 52(1):31–58.

Arya R, Duggirala R, Comuzzie AG, Puppala S, Modem S, Busi BR, Crawford MH. 2002. Heritability of anthropometric phenotypes in caste populations of Visakhapatnam, India. *Human Biology* 74:325-344.

Asfaw B, White T, Lovejoy C, Latimer B, Simpson S, Suwa G. 1999. *Australopithecus garhi*: A new species of early hominid from Ethiopia. *Science* 284:629-635.

Ashton KG, Tracy MC, de Queiroz A. 2000. Is Bergmann's rule valid for mammals? *The American Naturalist* 156(4):390-415.

Auerbach, BM. 2007. *Human skeletal variation in the New World during the Holocene: Effects of climate and subsistence across geography and time*. Ph.D. dissertation. Baltimore, MD: Johns Hopkins University.

Auerbach BM. 2010. Giants among us? Morphological variation and migration on the Great Plains. In: Auerbach BM, editor. *Human Variation in the Americas: The Integration of Archaeology and Biological Anthropology*. Carbondale, IL: Southern Illinois University Carbondale. pp. 172-214.

Auerbach BM. 2012. Skeletal variation among early Holocene North American humans: Implications for origins and diversity in the Americas. *American Journal of Physical Anthropology* 149(4):525-536.

Auerbach BM, DeLeon VB. 2013. Going out on a limb: functional and developmental integration in human limb long bones. *The FASEB Journal* 27:755.11

Auerbach B, Raxter M. 2008. Patterns of clavicular bilateral asymmetry in relation to the humerus: variation among humans. *Journal of Human Evolution* 54:663-674.

Auerbach BM, Ruff CB. 2004. Human body mass estimation: a comparison of "morphometric" and "mechanical" methods. *American Journal of Physical Anthropology* 125(4):331-342.

Auerbach BM, Ruff CB. 2006. Limb bone bilateral asymmetry: Variability and commonality among modern humans. *Journal of Human Evolution* 50:203-218.

Aufdemorte TB, Fox WC, Miller D, Buffum K, Holt GR, Carey KD. 1993. A non-human primate model for the study of osteoporosis and oral bone loss. *Bone* 14:581-586.

Bailey-Wilson JE, Wilson AF. 2011. Linkage analysis in the next-generation sequencing era. *Human Heredity* 72:228-236.

Bareggi R, Grill V, Zweyer M, Sandrucci MA, Martelli AM, Narducci P, Forabosco A. 1996. On the assessment of the growth patterns in human fetal limbs: longitudinal measurements and allometric analysis. *Early Human Development* 45:11–25.

Benazet JD, Zeller R. 2009. Vertebrate Limb Development: Moving from Classical Morphogen Gradients to an Integrated 4-Dimensional Patterning System. *Cold Spring Harbor Perspectives in Biology* 1(4):a001339–a001339.

Bender W, Spierer P, Hogness DS. 1983.Chromosomal walking and jumping to isolate DNA from the *Ace* and *rosy* loci and the bithorax complex in *Drosophila melanogaster*. *Journal of Molecular Biology* 168:17-83.

Berge C. 1994. How did the australopithecines walk? A biomechanical study of the hip and thigh of *Australopithecus afarensis*. *Journal of Human Evolution* 26:259-273.

Berger L. 2006. Comments on Dobson (2005), body proportions in early hominins, and the joint and limb proportion differences between Stw 431 (*A. africanus*) and A.L. 299-1 (*A. afarensis*). *Journal of Human Evolution* 51:109-110.

Bergmann, C. 1847. Ueber die Verhältnisse der wärmeökonomie der Thiere zu ihrer Grösse. *Göttinger Studien* 3:595-708.

Betti L, Carom-Taubadel NV, Lycett SJ. 2012. Human pelvis and long bones reveal differential preservation of ancient population history and migration out of Africa. *Human Biology* 84(2):139-152.

Biewener AA, Bertram EA. 1994. Structural response of growing bone to exercise and disuse. *Journal of Applied Physiology* 76:946-955.

Blangero J, Williams JT, Almasy L. 2000. Quantitative trait locus mapping using human pedigrees. *Human Biology* 72:35-62.

Blangero J, Williams JT, Almasy L, Williams-Blangero S. 2007. Mapping genes influencing human quantitative trait variation. In: Crawford M, editor. *Anthropological Genetics*. New York: Cambridge University Press. pp. 306-333.

Bogin B. 1997. Evolutionary hypotheses for human childhood. *Yearbook of Physical Anthropology* 40:63–89.

Boocock GRB, Morrison JA, Popovic M, Richards N, Ellis L, Durie PR, Rommens JM.. 2003. Mutations in SBDS are associated with Shwachman-Diamond syndrome. *Nature Genetics* 33:97.

Botstein D, White RL, Skolnick M, Davis RW. 1980. Construction of a genetic linkage map in man using restriction fragment length polymorphisms. *American Journal of Human Genetics* 32:314-331.

Bridges P. 1989. Bone Cortical Area in the Evaluation of Nutrition and Activity Levels. *American Journal of Human Biology* 1:785-792.

Bridges P. 1995. Skeletal Biology and Behavior in Ancient Humans. *Evolutionary Anthropology* 4(4):112-120.

Brommage R. 2001. Perspectives on using nonhuman primates to understand the etiology and treatment of postmenopausal osteoporosis. *Journal of Musculoskeletal and Neuronal Interactions* 1:307-325.

Brommer J. 2011. Whither pst? The approximation of qst by pst in evolutionary and conservation biology. *Journal of Evolutionary Biology* 24(6):1160-1168.

Brookes, AJ. 1999. The essence of SNPs. *Gene* 234(2):177-186.

Bui TD, Lako M, Lejeune S, Curtis ARJ, Strachan T, Lindsay S, Harris AL. 1997. Isolation of a full-length human WNT7A gene implicated in limb development and cell transformation, and mapping to chromosome 3p25. *Gene* 189:25-29.

Buikstra JE, Ubelaker DH. 1994. *Standards for Data Collection from Human Skeletal Remains*. Arkansas Archaeological Survey Research Series No. 44. Fayetteville, AR: Arkansas Archaeological Survey.

Buschang PH. 1982. The relative growth of limb bones for *Homo sapiens* – As compared to anthropoid apes. *Primates* 23(3):465-468.

Byard PJ, Sharma K, Russell JM, Rao DC. 1984. A family study of anthropometric traits in a Punjabi community: II. An investigation of familial transmission. *American Journal of Physical Anthropology* 64:97-104.

Cameron N, Tanner JM, Whitehouse RH. 1982. A longitudinal analysis of the growth of limb segments in adolescence. *Annals of Human Biology* 9:211–220.

Carmichael CM, McGue M. 1996. A cross-sectional examination of height, weight, and body mass index in adult twins. *Journal of Gerontology Series A: Biological Sciences and Medical Sciences* 50:B237-B244.

Carrier DR, Chase K, Lark KG. 2005. Genetics of canid skeletal variation: Size and shape of the pelvis. *Genome Research* 15:1825–1830.

Carroll SB, Grenier JK, Weatherbee SD. 2001. *From DNA to Diversity: Molecular Genetics and the Evolution of Animal Design*. Blackwell Science: Malden.

Carson EA. 2006. Maximum likelihood estimation of human craniometric heritabilities. *American Journal of Physical Anthropology* 131:169-180.

Carter D, Beaupré G. 2001. *Skeletal Function and Form*. New York: Cambridge University Press.

Carter DR, Wong M. 1988. The role of mechanical loading histories in the development of diarthrodial joints. *Journal of Orthopaedic Research* 6(6):804–816.

Carter D, Van der Meulen M, Beaupré G. 1996. Mechanical factors in bone growth and development. *Bone* 18(1):5S-10S.

Caspi A, Sugden K, Moffitt TE, Taylor A, Craig IW, Harrington H, McClay J, Mill J, Martin J, Braithwaite A, Poulton R. 2003. Influence of life stress on depression: moderation by a polymorphism in the 5-HTT gene. *Science* 301:386-389.

Chase K, Carrier D, Adler F, Jarvik T, Ostrander E, Lorentzen T, and Lark K. 2002. Genetic Basis for Systems of Skeletal Quantitative Traits: Principal Component Analysis of the Canid Skeleton. *Proceedings of the National Academy of Sciences* 99(15):9930-9935.

Cheverud JM. 1982. Phenotypic, genetic, and environmental morphological integration in the cranium. *Evolution* 36:499–516.

Cheverud JM. 1984. Quantitative genetics and developmental constraints on evolution by selection. *Journal of Theoretical Biology* 110:155-171.

Cheverud JM. 1988. A comparison of genetic and phenotypic correlations. *Evolution* 42(5):958–968.

Cheverud JM. 1995. Morphological integration in the saddle-back tamarin (*Saguinus fuscicollis*) cranium. *The American Naturalist* 145:63-89.

Cheverud JM. 1996a. Developmental integration and the evolution of pleiotropy. *American Zoologist* 36:44–50.

Cheverud JM. 1996b. Quantitative genetic analysis of cranial morphology in the cotton-top (*Saguinus oedipus*) and saddle-back (*S. fuscicollis*) tamarins. *Journal of Evolutionary Biology* 9:5-42.

Cheverud JM. 2007. The relationship between development and evolution through heritable variation. *Tinkering: The Microevolution of Development: Novartis Foundation Symposium 285* 285:55-70.

Cheverud JM, Buikstra JE. 1981. Quantitative genetics of skeletal nonmetric traits in the Rhesus Macaques on Cayo Santiago: I. Single trait heritabilities. *American Journal of Physical Anthropology* 54:43-49.

Cheverud JM, Buikstra, JE. 1982. Quantitative genetics of skeletal non-metric traits in the rhesus macaques on Cayo Santiago. III. Relative heritability of skeletal non-metric and metric traits. *American Journal of Physical Anthropology* 59:151-155.

Cheverud J, Dittus W. 1992. Primate population studies at Polonnaruwa. II. Heritability of body measurements in a natural population of Toque Macaques (*Macaca sinica*). *American Journal of Primatology* 27:145-156.

Cheverud JM, Tardif S, Henke MA, Clapp NK. 1993. Genetic epidemiology of colon cancer in the cotton-top tamarin (Saguinus oedipus). Human Biology 65(6):1005-1012.

Cheverud M, Routman E, Jaquish C, Tardif S, Peterson G, Belfiore N, Forman L. 1994. Quantitative and molecular genetic variation in captive cotton-top tamarins (Saguinus oedipus). Conservation Biology 8(1):95-105.

Chinappen-Horsley U, Blake G, Fogelman I, Kato B, Ahmandi K, and Spector T. 2008. Quantitative Trait Loci for Bone Lengths on Chromosome 5 Using Dual Energy X-Ray Absorptiometry Imaging in the Twins UK Cohort. *PloS One* 3(3):e1752.

Christians J, Bingham V, Oliver F, Heath T, Keightley P. 2003. Characterization of a QTL affecting skeletal size in mice. *Mammalian Genome* 14:175–183.

Clapp NK, Tardiff SD. 1985. Marmoset husbandry and nutrition. *Digestive Diseases and Sciences* 30:17S-23S.

Clark PJ. 1956. The heritability of certain anthropometric characters as ascertained from measurements of twins. *American Journal of Human Genetics* 8:49-54.

Comuzzie AG, Hixson JE, Almasy L, Mitchell BD, Mahaney MC, Dyer TD, Stern MP, MacCluer JW, Blangero J. 1997. A major quantitative trait locus determining serum leptin levels and fat mass is located on human chromosome 2. *Nature Genetics* 15:273–275.

Cowgill L, Hager L. 2007. Variation in the Development of Postcranial Robusticity: An Example from Catalhoyuk, Turkey. *International Journal of Osteoarchaeology* 17:235-252.

Cowgill LW, Eleazer CD, Auerbach BM, Temple DH, Okazaki K. 2012. Developmental variation in ecogeographic body proportions. *American Journal of Physical Anthropology* 148:557–570.

Cox LA, Mahaney MC, VandeBerg JL, Rogers J. 2006. A second-generation genetic linkage map of the baboon (*Papio hamadryas*) genome. *Genomics* 88:274-281.

Crawford M. 2005. Genetics of biological aging in Mennonites of Midwestern United States. *Przeglad antropologiczny* 68:3-18.

Crawford MH, Rogers L. 1982. Population genetic models in the study of aging and longevity in a Mennonite community. *Social Science and Medicine* 16:149-153.

Crawford MH, Demarchi D, Ellerd M, Puppala S. 2000. Body morphology and aging among the Mennonites of Kansas and Nebraska. In: Crawford MH, editor. *Different Seasons: Biological Aging Among the Mennonites of the Midwestern United States*. Lawrence, Kansas: University of Kansas, Lawrence. pp. 55-67.

Dario C, Carnicella D, Dario M, Bufano G. 2006. Morphological evolution and heritability estimates for some biometric traits in the Murgese horse breed. *Genetics and Molecular Research* 5:309-314.

Darwin C. 2003. *Signet Classics: The Origin of Species*. Penguin Group: New York.

Davenport CB. 1930. The crural index. *American Journal of Physical Anthropology* 17(8):333-353.

DeLeon VB, Auerbach BM. 2007. Morphological integration in human long bones. *American Journal of Physical Anthropology* 132(S44):96.

Deng H-W, Shen H, Xu F-H, Deng H, Conway T, Liu Y-J, Liu Y-Z, Li J-L, Huang Q-Y, Davies KM, Recker RR. 2003. Several genomic regions potentially containing QTLs for bone size variation were identified in a whole-genome linkage scan. *American Journal of Medical Genetics* 119A:121-131.

Denhardt DT, Guo X. 1993. Osteopontin: a protein with diverse functions. *The FASEB Journal* 7(15):1475-82.

Dettwyler KA. 1992. Nutritional status of adults in rural Mali. *American Journal of Physical Anthropology* 88:309-321.

Devor EJ, McGue M, Crawford MH, Lin PM. 1986a. Transmissible and nontransmissible components of anthropometric variation in the Alexanderwohl Mennonites: I. Description and familial correlations. *American Journal of Physical Anthropology* 69:71-82.

Devor EJ, McGue M, Crawford MH, Lin PM. 1986b. Transmissible and nontransmissible components of anthropometric variation in the Alexanderwohl Mennonites: II. Resolution by path analysis. *American Journal of Physical Anthropology* 69:83–92.

Devoto M, Specchia C, Li H-H, Caminis J, Tenenhouse A, Rodriguez H, Spotila LD. 2001. Variance component linkage analysis indicates a QTL for femoral neck bone mineral density on chromosome 1p36. *Human Molecular Genetics* 10(21):2447-2452.

Doerge, RW. 2002. Mapping and analysis of quantitative trait loci in experimental populations. *Nature Reviews: Genetics* 3:43-52.

Drake T, Hannani K, Kabo J, Villa V, Krass K, Lusis A. 2001. Genetic loci influencing natural variations in femoral bone morphometry in mice. *Journal of Orthopedic Research* 19:511–517.

Duarte C, Maurício J, Pettitt PB, Souto P, Trinkaus E, van der Plicht H, Zilhão J. 1999. The early Upper Paleolithic human skeleton from the Abrigo do Lagar Velho (Portugal) and modern human emergence in Iberia. *Proceedings of the National Academy of Sciences USA* 96:7604-7609.

Duggirala R, Blangero J, Almasy L, Dyer TD, Williams KL, Leach RJ, O'Connell P, Stern MP. 1999. Linkage of type 2 diabetes mellitus and of age at onset to a genetic location on chromosome 10q in Mexican Americans. *American Journal of Human Genetics* 64(4):1127–1140.

Eleazer CD. 2013. *The interaction of mechanical loading and metabolic stress on human cortical bone: Testing anthropological assumptions using cross-sectional geometry and histomorphology*. Ph.D. dissertation. Knoxville, TN: University of Tennessee.

Eleazer CD, Cowgill LW, Auerbach BM. 2010. Variation in human body proportions during ontogeny. *American Journal of Physical Anthropology* 141(S50):100.

Eleazer CD, Jankauskas R. 2016. Mechanical and metabolic interactions in cortical bone development. *American Journal of Physical Anthropology* In press.

Eveleth PB, Tanner JM. 1990. *Worldwide Variation in Human Growth*. Cambridge: Cambridge University Press.

Falconer DS, Mackay TFC. 1996. *Introduction to Quantitative Genetics*, 4th Edition. Essex: Longman Group, Ltd.

Feingold E, Brown PO, Siegmund D. 1993. Gaussian models for genetic linkage analysis using complete high-resolution maps of identity by descent. *American Journal of Human Genetics* 53:234-251.

Fisher RA. 1918. The correlation between relatives on the supposition of Mendelian Inheritance. *Transactions of the Royal Society of Edinburgh* 52:399-433.

Fisher RA. 1930. *The Genetical Theory of Natural Selection*. Oxford: Clarendon Press.

Fleagle, JG. 1999. *Primate Adaptation and Evolution*. San Diego: Academic Press.

Fleagle JG, Samonds KW, Hegsted DM. 1975. Physical growth of cebus monkeys, *Cebus albifrons*, during protein or calorie deficiency. *American Journal of Clinical Nutrition* 28:246–253.

Floud R, Wachter K, Gregory A. 1990. *Height, health, and history: Nutritional status in the United Kingdom, 1750–1980*. Cambridge: Cambridge University Press.

Franz CH, O'Rahilly R. 1961. Congenital skeletal limb deficiencies. *The Journal of Bone and Joint Surgery* 43:1202.

Froehlich, JW. 1970. Migration and plasticity of physique in the Japanese–Americans of Hawaii. *American Journal of Physical Anthropology* 32:429–442.

Fulker DW, Cherny SS. 1996. An improved multipoint sibpair analysis of quantitative traits. *Behavior Genetics* 26:527–532.

Fulker DW, Cherny SS, Cardon LR. 1995. Multipoint interval mapping of quantitative trait loci, using sib pairs. *American Journal of Human Genetics* 56:1224-1233.

Gavan JA. 1953. Growth and development of the chimpanzee; a longitudinal and comparative study. *Human Biology* 25:93-143.

Gengozian N. 1969. Marmosets: their potential in experimental medicine. *Annals of the New York Academy of Sciences* 162:336-362.

Gilbert SF. 2013. Development of the tetrapod limb. In: *Developmental Biology*, Eighth Ed. Sunderland, MA: Sinauer Associates, Inc. pp 505-527.

Gordon CC, Churchill T, Clauser CE, Bradtmiller B, McConville JT, Tebbetts I, Walker RA. 1988. 1988 *Anthropometric Survey of U.S. Army Personnel: Methods and Summary Statistics*. Natick, Massachusetts: United States Army Natick Research, Development and Engineering Center.

Göring HHH, Terwilliger JD, Blangero J. 2001. Large upward bias in estimation of locus-specific effects from genomewide scans. *American Journal of Human Genetics* 69:1357-1369.

Graves GR. 1991. Bergmann's rule near the equator: latitudinal clines in body size of an Andean passerine bird. *Proceedings of the National Academy of Sciences USA* 88(6):2322-2325.

Green D, Gordon A, Richmond B. 2007. Limb-size proportions in *Australopithecus afarensis* and *Australopithecus africanus*. *Journal of Human Evolution* 52:187-200.

Greenberg CR, Evans JA, McKendry-Smith S, Redekopp S, Haworth JC, Mulivor R, Chodirker BN. 1990. Infantile hypophosphatasia: Localizatio within chromosome region 1p36.1-34 and prenatal diagnosis using linked DNA markers. *American Journal of Human Genetics* 46:286.

Greulich, WW. 1957. A comparison of the physical growth and development of American-born and native Japanese children. *American Journal of Physical Anthropology* 15:489–515.

Goldgar DE. 1990. Multipoint analysis of human quantitative genetic variation. *American Journal of Human Genetics* 47:957–967.

Gu C, Rao DC. 1997. A linkage strategy for detection of human quantitative-trait loci. I. Generalized relative risk ratios and power of sib pairs with extreme trait values. *American Journal of Human Genetics* 61:200-210.

Gu C, Todorov A, Rao DC. 1996. Combining extremely concordant sibpairs with extremely discordant sibpairs provides a cost effective way to linkage analysis of quantitative trait loci. *Genetic Epidemiology* 13513-533.

Gudbjartsson D, Walters G, Thorleifsson G, Stafansson H, Halldorsson B, Zusmanovich P, Sulem P, Throlacius S, Gylfason A, Steinberg S, Helgadottir A, Ingason A, Steinthorsdottir V, Olafsdottir EJ, Olafsdottir GH, Jonsson T, Borch-Johnsen K, Hansen T, Andersen G, Jorgensen T, Pedersen O, Aben KK, Witjes JA, Swinkels DW, den Heijer M, Franke B, Verbeek ALM, Becker DM, Yanek LR, Becker LC, Tryggvadottir L, Rafnar T, Gulcher J, Kiemeney LA, Kong A, Thorsteinsdottir U, Stefansson K. 2008. Many sequence variants affecting diversity of adult human height. *Nature Genetics* 40:609-615.

Haeusler M, McHenry H. 2004. Body proportions of *Homo habilis* reviewed. *Journal of Human Evolution* 46:433-465.

Haeusler M, McHenry H. 2007. Evolutionary reversals of limb proportions in early hominids? Evidence from KNM-ER 3735 (*Homo habilis*). *Journal of Human Evolution* 53:383-405.

Hadfield JD. 2010. MCMC methods for Multi-response Generalized Linear Mixed Models: The MCMCglmm R Package. *Journal of Statistical Software* 33(2):1-22.

Hadfield JD. 2012. MasterBayes: Maximum Likelihood and Markov chain Monte Carlo methods for pedigree reconstruction, analysis and simulation. www.R-project.org.

Hadfield J. 2014. MCMCglmm Course Notes. www.R-project.org.

Haldane JBS. 1919. The combination of linkage values, and the calculation of distances between linked factors. *Journal of Genetics* 8:299-309.

Haldane JBS. 1932. *The Causes of Evolution*. Longmans, Green and Co: New York.

Hallgrímsson B, Willmore K, Hall BK. 2002. Canalization, developmental stability, and morphological integration in primate limbs. *Yearbook of Physical Anthropology* 45:131-158.

Hallgrímsson B, Lieberman DE, Young NM, Parsons T, Wat S. 2007. Evolution of covariance in the mammalian skull. *Novartis Foundation Symposium* 284:164-190.

Hallgrímsson B, Jamniczky H, Young NM, Rolian C, Parsons TE, Boughner JC, Marcucio RS. 2009. Deciphering the palimpsest: Studying the relationship between morphological integration and phenotypic covariation. *Evolutionary Biology*, 36, 355–376.

Hansen HL, Bredbenner TL, Nicolella DP, Mahaney MC, Havill LM. 2009. Cross-sectional geometry of the femoral midshaft in baboons is heritable. *Bone* 45(5):892–897.

Hansen TF. 1997. Stabilizing selection and the comparative analysis of adaptation. *Evolution* 51(5):1341-1351.

Hansen TF, Houle D. 2008. Measuring and comparing evolvability and constraint in multivariate characters. *Journal of Evolutionary Biology* 21:1201-1219.

Hansen TF, Armbruster WS, Carlson ML, Pélabon C. 2003a. Evolvability and genetic constraint in *Dalechampia* blossoms: Genetic correlations and conditional evolvability. *Journal of Experimental Zoology (Molecular and Developmental Evolution)* 296B:23-39.

Hansen TF, Pélabon C, Armbruster WS, Carson ML. 2003b. Evolvability and genetic constraint in *Dalechampia* blossoms: Components of variance and measures of evolvability. *Journal of Evolutionary Biology* 16:754-765.

Hansen TF, Pélabon C, Houle D. 2011. Heritability is not evolvability. *Evolutionary Biology* 38:258-277.

Harcourt-Smith W, Aiello L. 2004. Fossils, feet and the evolution of human bipedal locomotion. *Journal of Anatomy* 204:403-416.

Harrison C. 2007. Xming version 6.9.0.31. http://sourceforge.net/projects/xming.

Hartwig-Scherer S, Martin RD. 1991. Was "Lucy" more human than her "child"? Observations on early hominid postcranial skeletons. *Journal of Human Evolution* 21:439–449.

Haseman JK, Elston RC. 1972. The investigation of linkage between a quantitative trait and a marker locus. *Behavior Genetics* 2:3–19.

Havill LM. 2007. Heritability of lumbar trabecular bone mechanical properties in baboons. *Journal of Musculoskeletal and Neuronal Interactions* 7(4):316-317.

Havill LM, Mahaney MC, Czerwinski SA, Carey KD, Rice K, Rogers J. 2003. Bone mineral density reference standards in adult baboons (*Papio hamadryas*) by sex and age. *Bone* 33:877-888.

Havill L, Mahaney M, Cox L, Morin P, Joslyn G, and Rogers J. 2005. A Quantitative Trait Locus for Normal Variation in Forearm Bone Mineral Density in Pedigreed Baboons Maps to the Ortholog of Human Chromosome 11q. *The Journal of Clinical Endocrinology* 90(6):3638-3645.

Higgins RW. 2014. The Effects of Terrain on Long Bone Robusticity and Cross-Sectional Shape in Lower Limb Bones of Bovids, Neandertals, and Upper Paleolithic Modern Humans. In: Carlson KJ, Marchi D, editors: *Reconstructing Mobility: Environmental, Behavioral, and Morphological Determinants*. New York: Springer. pp. 227-252.

Higgins RW, Ruff CB. 2011. The effects of distal limb segment shortening on locomotor efficiency in sloped terrain: Implications for Neandertal locomotor behavior. *American Journal of Physical Anthropology* 146(3):336-345.

Hintze, J. 2006. NCSS, PASS, and GESS. NCSS. Kaysville, Utah. www.NCSS.com

Hirschhorn JN, Daly MJ. 2005. Genome-wide association studies for common diseases and complex traits. *Nature Reviews Genetics* 6:95-108.

Hlusko LJ, Mahaney MC. 2009. The baboon model for dental development. In: VandeBerg JL, Williams-Blangero S, Tardif SD, editors. *The Baboon in Biomedical Research*. New York: Springer. pp. 207-224.

Hoaglin, DC, Iglewicz B. 1987. Fine tuning some resistant rules for outlier labeling. *Journal of the American Statistical Association*. 82:1147-1149.

Hoaglin, DC, Iglewicz B, Tukey JW. 1986. Performance of some resistant rules for outlier labeling. *Journal of the American Statistical Association* 81:991-999.

Holliday TW. 1995. *Body Size and Proportions in the Late Pleistocene Western Old World and the Origins of Modern Humans*. Ph.D. dissertation. Albuquerque, NM: The University of New Mexico.

Holliday T. 1997. Body proportions in Late Pleistocene Europe and modern human origins. *Journal of Human Evolution* 32:423-447.

Holliday T. 1999. Brachial and crural indices of European Late Upper Paleolithic and Mesolithic humans. *Journal of Human Evolution* 36:549-566.

Holliday T. 2002. Body size and postcranial robusticity of European Upper Paleolithic hominins. *Journal of Human Evolution* 43:513-528.

Holliday T, Falsetti A. 1995. Lower limb length of European early modern humans in relation to mobility and climate. *Journal of Human Evolution* 29:141-153.

Hood GM. 2011. PopTools version 3.2.5. www.poptools.org.

Houle D. 1992. Comparing evolvability and variability of quantitative traits. *Genetics* 130:195-204.

Hulsey BI, Cabana GS, Havill LM. 2010. The heritability of baboon limb bone morphometry. *American Journal of Physical Anthropology* 141(S50):131.

Hummert JR, Van Gerven DP. 1983. Skeletal growth in a Medieval population from Sudanese Nubia. *American Journal of Physical Anthropology* 60:471-478.

Hunt K. 1994. The evolution of human bipedality: ecology and functional morphology. *Journal of Human Evolution* 26:183-202.

Hutchison DW, Cheverud JM. 1995. Fluctuating asymmetry in tamarin (*Saguinas*) cranial morphology: Intra- and interspecific comparisons between taxa with varying levels of genetic heterozygosity. *Journal of Heredity* 86:280-288.

IBM Corp. 2012. IBM SPSS Statistics for Windows, Version 21.0. IBM Corp: Armonk, NY.

Ishimori N, Li R, Walsh K, Korstanje R, Rollins J, Petkov P, Pletcher M, Wiltshire T, Donahue L, Rosen C, Beamer W, Churchill G, Paigen B. 2006. Quantitative trait loci that determine

BMD in C57BL/6J and 129S1/SvImJ inbred mice. *Journal of Bone and Mineral Research* 21:105–112.

Jablonski N, Chaplin G. 1993. Origin and habitual terrestrial bipedalism in the ancestor of the Hominidae. *Journal of Human Evolution* 24:259-280.

Jacobs K. 1985. Climate and the hominid postcranial skeleton in Wurm and Early Holocene Europe. *Current Anthropology* 26:512-514.

James, FC. 1970. Geographic size variation in birds and its relationship to climate. *Ecology* 51:365-390.

Jansen RC. 1993. Interval mapping of multiple quantitative trait loci. *Genetics* 135(1):205-211.

Jantz RL. 2006. Anthropometry. In: Ubelaker D, editor. *Handbook of North American Indians, Volume 3: Environment, Origins and Populations*. Washington, DC: Smithsonian Institution. pp. 777-788.

Jantz RL, Owsley DW. 1984. Long bone growth variation among Arikara skeletal populations. *American Journal of Physical Anthropology* 63:13-20.

Jantz RL, Marr P, Jantz CA. 2010. Body proportions in recent Native Americans: Colonization history versus ecogeographical patterns. In: Auerbach BM, editor. *Human Variation in the Americas: The integration of archaeology and biological anthropology*. Carbondale: Southern Illinois University. pp. 172-214.

Jensen LJ, Kuhn M, Stark M, Chaffron S, Creevey C, Muller J, Doerks T, Julien P, Roth A, Simonovic M, Bork P, von Mering C. 2009. STRING 8 – a global view on proteins and their functional interactions in 630 organisms. *Nucleic Acids Research* 37:D412-6. www.string-db.org.

Johanson DC, Masao FT, Eck G, White TD, Walter RC, Kimbel WH, Asfaw B, Manega P, Ndessokia P, Suwa G. 1987. New partial skeleton of *Homo habilis* from Olduvai Gorge, Tanzania. *Nature* 327:205–209.

Jolly CJ. 2001. A proper study for mankind: Analogies from the Papionin monkeys and their implications for human evolution. *Yearbook of Physical Anthropology* 44:177-204.

Jones KL. 2006. *Smith's Recognizable Patterns of Human Malformation*. 6th Edition. Philadelphia: Elsevier Saunders

Jungers WL. 1982. Lucy's limbs: skeletal allometry and locomotion in *Australopithecus afarensis*. *Nature* 297:676–678.

Jungers WL. 1985. Body size and scaling of limb proportions in primates. In: Jungers WL, editor. *Size and scaling in primate biology*. New York: Plenum Press. pp. 345–351.

Kammerer CM, Rainwater DL, Cox LA, Schneider JL, Mahaney MC, Rogers J, VandeBerg JL. 2002. Locus controlling LDL cholesterol response to dietary cholesterol is on baboon homologue of human chromosome 6. *Arteriosclerosis, Thrombosis, and Vascular Biology* 22:1720.

Karolchik D, Barber GP, Casper J, Clawson H, Cline MS, Diekhans M, Dreszer TR, Fujita PA, Guruvadoo L, Haeussler M, Harte RA, Heitner S, Hinrichs AS, Learned K, Lee BT, Li CH, Raney BJ, Rhead B, Rosenbloom KR, Sloan CA, Speir ML, Zweig AS, Haussler D, Kuhn RM, Kent WJ. 2014. The UCSC Genome Browser database: 2014 update. *Nucleic Acids Research* 42(1):D764-D770.

Kaur DP, Singh R. 1981. Parent-adult offspring correlations and heritability of body measurements in a rural Indian population. *Annals of Human Biology* 8:333-339.

Kenney-Hunt J P, Vaughn TT, Pletscher LS, Peripato A, Routman E, Cothran K, Durand D, Norgard E, Perel C, Cheverud JM. 2006. Quantitative trait loci for body size components in mice. *Mammalian Genome* 17: 526–537.

Kenney-Hunt JP, Wang B, Norgard EA, Fawcett G, Falk D, Pletscher LS, Jarvis JP, Roseman C, Wolf J, Cheverud JM. 2008. Pleiotropic patterns of quantitative trait loci for 70 murine skeletal traits. *Genetics* 178:2275-2288.

Kent WJ, Sugnet CW, Furey TS, Roskin KM, Pringle TH, Zahler AM, Haussler D. 2002. The human genome browser at UCSC. *Genome Research* 12(6):996-1006.

Kesavan C, Mohan S, Srivastava A, Kapoor S, Wergedal J, Yu H, Baylink D. 2006. Identification of genetic loci that regulate bone adaptive response to mechanical loading in C57BL/6J and C3H/HeJ mice intercross. *Bone* 39:634–643.

Kimbel WH, Delezene LK. 2009. "Lucy" redux: A review of research on *Australopithecus afarensis*. *Yearbook of Physical Anthroplogy* 52:2-48.

Kimmel CB, Ullmann B, Walker C, Wilson C, Currey M, Phillips PC, Bell MA, Postlethwait JH, Cresko WA. 2005. Evolution and development of facial bone morphology in threespine sticklebacks. *Proceedings of the National Academy of Sciences* 102(16):5791-5796.

Klein R, Mitchell S, Phillips T, Belknap J, Orwoll E. 1998. Quantitative trait loci affecting peak bone mineral density in mice. *Journal of Bone and Mineral Research* 13:1648–1656.

Klingenberg CP. 2008. Morphological integration and developmental modularity. *Annual Review of Ecology, Evolution, and Systematics* 39:115–132.

Klingenberg C, Leamy L, Cheverud J. 2004. Integration and modularity of quantitative trait locus effects on geometric shape in the mouse mandible. *Genetics* 166:1909–1921.

Kohn LAP, Olson P, Cheveru JM. 1997. Age of epiphyseal closure in tamarins and marmosets. *American Journal of Primatology* 41:129-139.

Koller DL, Econs MJ, Morin PA, Christian HC, Hui SL, Parry P, Curran ME, Rodriguez LA, Conneally PM, Joslyn G, Peacock M, Johnston CC, Foroud T. 2000. Genome screen for QTLs contributing to normal variation in bone mineral density and osteoporosis. *The Journal of Clinical Endocrinology & Metabolism* 85(9):3116-3120.

Koller DL, Liu G, Econs MJ, Morin P, Christian JC, Hui SL, Rodriguez LA, Conneally PM, Joslyn G, Johnston CC, Foroud T, Peacock M. 2001. Genome screen for QTLs contributing to normal variation in femoral structure. *Journal of Bone and Mineral Research* 16:985–991.

Komlos J. 1990. Height and social status in eighteenth century Germany. *Journal of Interdisciplinary History* 20:607–621.

Komlos J. 1994. *Stature, living standards, and economic development: Essays in anthropometric history*. Chicago: University of Chicago Press.

Komori T. 2010. Regulation of osteoblast differentiation by Runx2. *Advances in Experimental Medicine and Biology* 658:43-9

Konigsberg LW. 2000. Quantitative variation and genetics. In: Stinson S, Bogin B, Huss-Ashmore R, O'Rourke D, editors. *Human Biology: An Evolutionary and Biocultural Perspective*. New York: Wiley-Liss. pp. 135-162.

Korey, KA. 1990. Deconstructing reconstruction: the OH 62 humerofemoral index. *American Journal of Physical Anthropology* 83:25–33.

Kramer A. 2005. Biospeciation versus morphospeciation in the later human fossil record: Lessons learned from non-human primate socioecology. *Anthropologie - International Journal of the Science of Man* 43:199-296.

Kramer P, and Eck G. 2000. Locomotor energetics and leg length in hominid bipedality. *Journal of Human Evolution* 38:651-666.

Kruglyak L, Lander ES. 1995. Complete multipoint sib-pair analysis of qualitative and quantitative traits. *American Journal of Human Genetics* 57:439–454.

Kurki H, Ginter J, Stock J, Pfeiffer S. 2008. Adult proportionality in small-bodied foragers: A test of ecogeographic expectations. *American Journal of Physical Anthropology* 136:28-38.

Lande R. 1979. Quantitative genetic analysis of multivariate evolution applied to brain:body size allometry. *Evolution* 33:402-416.

Lander ES, Botstein D. 1989. Mapping Mendelian factors underlying quantitative traits using RFLP linkage maps. *Genetics* 121:185-199.

Lander E, Kruglyak L. 1995. Genetic dissection of complex traits: guidelines for interpreting and reporting linkage results. *Nature Genetics* 11:241-247.

Lander ES, Schork NJ. 1994. Genetic dissection of complex traits. *Science* 265(5181):2037-2048.

Lanyon LE., 1980. The influence of function on the development of bone curvature. An experimental study on the rat tibia. *Journal of Zoology* 192:457-466.

Lapin BA, Fridman E. 1965. *Monkeys for science*. Novosti Press: Moscow.

Larsen C. 1997. Stress and development during the years of growth and development and adulthood. *Bioarchaeology: Interpreting behavior from the human skeleton*. New York: Cambridge University Press. p 6-63.

Latimer B, Ohman JC. 2001. Axial dysplasia in *Homo erectus*. *Journal of Human Evolution* 40:A12.

Leamy L. 1974. Heritability of osteometric traits in a randombred population on mice. *The Journal of Heredity* 65:109-120.

Leamy L, Pomp D, Eisen E, and Cheverud J. 2002. Pleiotropy of quantitative trait loci for organ weights and limb bone lengths in mice. *Physiological Genomics* 10:21-29.

Leamy LJ, Kelly SA, Hua K, Farber CR, Pompc D. 2013. Quantitative trait loci for bone mineral density and femoral morphology in an advanced intercross population of mice. *Bone* 55:222-229.

Lee MMC, Chu PC, Chan HC. 1969. Effects of cold on the skeletal growth of albino rats. *American Journal of Anatomy* 124:239–250.

Leigh S. 2009. Growth and Development of Baboons. In: VandeBerg JL, Williams-Blangero S, Tardif SW, editors. *The Baboon in Biomedical Research*. New York: Springer. pp. 57-88

Leonard W, and Robertson M. 1995. Energetic Efficiency of Human Bipedality. *American Journal of Physical Anthropology* 97:335-338.

Lettre G, Jackson AU, Gieger C, Schumacher FR Berndt SI, Sanna S, Eyher(amendy S, Voight BF, Butler JL, Guiducci C, Illig T, Hackett R, Heid IM, Jacobs KB, Lyssenko V, Uda M, The Diabetes Genetics Initiative, FUSION, KORA, The Prostate, Lung Colorectal and Ovarian - Cancer Screening Trial, The Nurses' Health Study, SardiNIA, Boehnke M, Chanock SJ, Groop LC, Hu FB, Isomaa B, Kraft P, Peltonen L, Salomaa V, Schlessinger D, Hunter DJ, Hayes RB, Abecasis GR, Wichmann HE, Mohlke KL, Hirschhorn JN. 2008. Identification of ten loci associated with height highlights new biological pathways in human growth. *Nature Genetics* 40:584-591.

Lewton KL. 2012. Evolvability of the primate pelvic girdle. *Evolutionary Biology* 39:126-139.

Livshits G, Roset A, Yakovenko K, Trofimov S, Kobyliansky E. 2002. Genetics of human body size and shape: body proportions and indices. *Annals of Human Biology* 29:271-289.

Lodish H, Berk A, Matsudaira P, Kaiser CA, Krieger M, Scott MP, Zipursky L, Darnell J. 2004. *Molecular Cell Biology*, Fifth Edition. San Francisco: WH Freeman.

Lordkipanidze D, Ponce de León MS, Margvelashvili A, Rak Y, Rightmire GP, Vekua A, Zollikofer CPE. 2013. A complete skull from Dmanisi, Georgia, and the evolutionary biology of early *Homo*. *Science* 342:326-331.

Lovejoy C. 2005. The natural history of human gait and posture: Part 2. Hip and thigh. *Gait and Posture* 21:113-124.

Lumer H. 1939. Relative growth of the limb bones in the anthropoid species. *Human Biology* 11:379-392.

Lush JL. 1940. Intra-sire correlations or regressions of offspring on dam as a method of estimating heritability of characteristics. *Proceedings of the American Society of Animal Production* 33:293-301.

Lynch M, Walsh B. 1998. *Genetics and Analysis of Quantitative Traits*. Sunderland, MA: Sinauer Associates.

Macgregor S, Cornes BK, Martin NG, Visscher PM. 2006. Bias, precision and heritability of self-reported and clinically measured height in Australian twins. *Human Genetics* 120:571-580.

Mackem S, Lewandoski M. 2011. Limb Cells Don't Tell Time. *Science* 332(6033):1038–1039.

Magwene PM. 2001. New tools for studying integration and modularity. Evolution 55(9):1734-1745.

Malina R, Peña Reyes M, Tan S, Buschang P, Little B, Koziel S. 2004. Secular change in height, sitting height and leg length in rural Oaxaca, southern Mexico: 1968-2000. *Annals of Human Biology* 31(6):615-633.

Malina RM, Peña Reyes ME, Little BB. 2008. Secular change in the growth status of urban and rural school children aged 6-13 years in Oaxaca, southern Mexico. *Annals of Human Biology* 35:475–489.

Mantel N. 1967. The detection of disease clustering and a generalized regression approach. *Cancer Research* 27:209-220.

Mao H, Guo Y, Yang G, Yang B, Ren J, Liu S, Ai H, Ma J, Brenig B, Huang L. 2008. A genome-wide scan for quantitative trait loci affecting limb bone lengths and areal bone mineral density of the distal femur in a White Duroc × Erhualian F2 population. *BMC Genetics* 9:63-70.

Mariani FV, Ahn CP, Martin GR. 2008. Genetic evidence that FGFs have an instructive role in limb proximal–distal patterning. *Nature* 453(7193):401–405.

Marroig G, Shirai LT, Porto A, de Oliveira FB, De Conto V. 2009. The evolution of modularity in the mammalian skull II: Evolutionary consequences. *Evolutionary Biology* 36:136-148.

Martin LJ, Carey KD, Comuzzie AG. 2003. Variation in menstrual cycle length and cessation of menstruation in captive raised baboons. *Mechanisms of Ageing and Development* 124:865-871.

Martin, R. 1928. *Lehrbuch der Anthropologie in systematischer Darstellung*. Jena.

Martin RB, Burr DB, Sharkey NA, Fyhrie DP. 2015. *Skeletal Tissue Mechanics*. New York: Springer.

Martínez-Abadías N, Esparza M, Sjøvold T, González-José R, Santos M, Hernández M. 2009. Heritability of human cranial dimensions: comparing the evolvability of different cranial regions. *Journal of Anatomy* 214:19-35.

Martorell R, Malina RM, Castillo FS, Pawson IG. 1988. Body proportions in three ethnic groups: children and youths 2–17 years in NHANES II and NHANES. *Human Biology* 60:205–222.

Masinde G, Wergedal J, Davidson H, Mohan S, Li R, Li X, Baylink D. 2003. Quantitative trait loci for periosteal circumference (PC): Identification of single loci and epistatic effects in F2 MRL/SJL mice. *Bone* 32:554–560.

Maynard Smith J, Burian R, Kaufman S, Alberch P, Campbell J, Goodwin B, Lande R, Raup D, Wolpert L. 1985. Developmental constraints and evolution. *The Quarterly Review of Biology* 60: 265–287.

Mayr E. 1956. Geographical Character Gradients and Climatic Adaptation. *Evolution* 10(1):105-108.

McHenry H. 1986. The first bipeds: A comparison of the *A. afarensis* and *A. africanus* postcranium and implications for the evolution of bipedalism. *Journal of Human Evolution* 15:177-191.

McHenry H, Berger L. 1998. Body proportions in *Australopithecus afarensis* and *A. africanus* and the origin of the genus *Homo*. *Journal of Human Evolution* 35:1-22.

Meadows Jantz L, Jantz RL. 1999. Secular Change in Long Bone Length and Proportion in the United States, 1800-1970. *American Journal of Physical Anthropology* 110:57-67.

Mitteroecker P, Bookstein F. 2008. The evolutionary role of modularity and integration in the hominoid cranium. *Evolution* 62(4):943–958.

Montagu, MFA. 1960. *A Handbook of Anthropometry*. Springfield, Illinois: Charles C Thomas Publisher.

Morton NE. 1955. Sequential tests for the detection of linkage. *American Journal of Human Genetics* 7(3):277–318.

Mosimann JE. 1970. Size allometry: size and shape variables with characterizations of the lognormal and generalized gamma distributions. *Journal of the American Statistics Association* 65:930–945.

Mousseau TA, Roff DA. 1987. Natural selection and the heritability of fitness components. *Heredity* 59:181-197.

Mullis K, Faloona F. 1987. Specific synthesis of DNA in vitro via a polymerase-catalyzed chain reaction. *Methods in Enzymology* 155:335-350.

Mullis K, Faloona F, Scharf S, Saiki R, Horn G, Erlich H. 1986. Specific enzymatic amplification of DNA in vitro: the polymerase chain reaction. *Cold Spring Harbor Symposium in Quantitative Biology* 51:263-273.

Nakata M, Yu P-L, Davis B, Nance WE. 1974. Genetic determinants of cranio-facial morphology: a twin study. *Annals of Human Genetics* 37:431-443.

Norgard E, Roseman C, Fawcett G, Pavlicev M, Morgan C, Pletscher L, Wang B, and Cheverud J. 2008. Identification of Quantitative Trait Loci Affecting Murine Long Bone Length in a Two-Generation Intercross of LG/J and SM/J Mice. *Journal of Bone and Mineral Research* 23(6):887-895.

Norgard EA, Jarvis JP, Roseman CC, Maxwell TJ, Kenney-Hunt JP, Samocha KE, Pletscher LS, Wang B, Fawcett GL, Leatherwood CJ, Wolf JB, Cheverud JM. 2009. Replication of long-bone length QTL in the F9-F10 LG,SM advanced intercross. *Mammalian Genome* 20:224–235.

Nowlan NC, Murphy P, Prendergast PJ. 2007. Mechanobiology of embryonic limb development. *Annals of the New York Academy of Sciences* 1101:389–411.

Nowlan NC, Sharpe J, Roddy KA, Prendergast PJ, Murphy P. 2010. Mechanobiology of embryonic skeletal development: Insights from animal models. *Birth Defects Research Part C: Embryo Today: Reviews* 90(3):203–213.

Nudds RL, Oswald SA. 2007. An interspecific test of Allen's rule: Evolutionary implications for endothermic species. *Evolution* 61(12):2839-2848.

Ogle C, Mills CA. 1933. Animal adaptation to environmental temperature conditions. *American Journal of Physiology* 103:606-628.

Ohuchi H, Takeuchi J, Yoshioka H, Ishimaru Y, Ogura K, Takahashi N, Ogura T, Noji S. 1998. Correlation of wing-leg identity in ectopic FGF-induced chimeric limbs with the differential expression of chick Tbx5 and Tbx4. *Development* 125: 51-60.

Olson EC, Miller RC. 1958. *Morphological Integration*. Chicago: University of Chicago Press.

Open Helix website. 2014. www.openhelix.com/ucsc.

O'Rourke DH. 1980. *Inbreeding Effects on Morphometric Characters in the Papio hamadryas Colony at Sukhumi*. Ph.D. dissertation. Lawrence, Kansas: University of Kansas, Lawrence.

Osborne R, DeGeorge F. 1959. *Genetic Basis of Morphological Variation*. Cambridge: Harvard University Press.

Ott J. 1999. *Analysis of Human Genetic Linkage*. Third Edition. Baltimore, MD: Johns Hopkins University Press.

Ott J, Wang J, Leal SM. 2015. Genetic linkage analysis in the age of whole-genome sequencing. *Nature Reviews: Genetics* 16:275-284.

Paganini-Hill A, Martin AO, Spence MA. 1981. The S-leut anthropometric traits: Genetic analysis. *American Journal of Physical Anthropology* 55:55-67.

Pavličev M, Kenney-Hunt JP, Norgard AE, Roseman CC, Wolf J, and Cheverud JM. 2007. Genetic variation in pleiotropy: Differential epistasis as a source of variation in the allometric relationships between bone lengths and body weight. *Evolution* 62(1): 199-213.

Pavličev M, Cheverud JM, Wagner GP. 2009. Measuring morphological integration using eigenvalue variance. *Evolutionary Biology* 36:157-170.

Pearson O. 2000. Activity, climate, and postcranial robusticity. *Current Anthropology* 41(4):569-607.

Pearson OM, Lieberman DE. 2004. The aging of Wolff's ''law:'' Ontogeny and responses to mechanical loading in cortical bone. *Yearbook of Physical Anthropology* 47:63-99.

Perola M, Sammalisto S, Hiekkalinna T, Martin NG, Visscher PM, Montgomery GW, Benyamin B, Harris JR, Boomsma D, Willemsen G, Hottenga J-J, Christensen K, Kyvik KO, Sørensen TIA, Pedersen NL, Magnusson PKE, Spector TD, Widen E, Silventoinen K, Kaprio J, Palotie A, Peltonen L, GenomEUtwin Project . 2007. Combined genome scans for body stature in 6,602 European twins: evidence for common Caucasian loci. *PLoS Genetics* 3:e97.

Petes TD, Botstein D. 1977. Simple Mendelian inheritance of the reiterated ribosomal DNA of yeast. *Proceedings of the National Academy of Sciences* 74(11):5091-5095.

Pontzer H, Raichlen D, Sockol M. 2009. The metabolic cost of walking in humans, chimpanzees, and early hominins. *Journal of Human Evolution* 56:43-54.

Pontzer H, Rolian C, Rightmire GP, Jashashvili T, Ponce de León MS, Lordkipanidze D, Zollikofer CP. 2010. Locomotor anatomy and biomechanics of the Dmanisi hominins. *Journal of Human Evolution* 58(6):492-504.

Porter A. 1999. Modern human, Early Modern Human and Neanderthal limb proportions. *International Journal of Osteoarchaeology* 9:54-67.

Potti J, Merino S. 1994. Heritability estimates and maternal effects on tarsus length in pied flycatchers, *Ficedula hypoleuca*. *Oecologia* 100(3):331-338.

Potts R. 1998. Environmental hypotheses of hominin evolution. *Yearbook of Physical Anthropology* 41(S27):93-136.

Pratt SC, Daly MJ, Kruglyak L. 2000. Exact multipoint quantitative-trait linkage analysis in pedigrees by variance components. *American Journal of Human Genetics* 66:1153-1157.

Preece MA. 1996. The genetic contribution to stature. *Hormonal Research* 45:56-58.

Preisinger R, Flock DK. 2000. Genetic changes in layer breeding: Historical trends and future prospects. In: Hill WG, Bishop SC, McGuirk B, McKay JC, Simm G, Webb AJ, editors. *The Challenge of Genetic Change in Animal Production*. Occasional Publication No. 27. Edinburgh: British Society of Animal Science.

Prost J. 1980. Orign of bipedalism. *American Journal of Physical Anthropology* 52:175-189.

Pulst SM. 1999. Genetic linkage analysis. *Archives of Neurology* 56:667-672.

Quinn AR, Blanco CL, Perego C, Finzi G, La Rosa S, Capella C, Guardado-Mendoza R, Casiraghi F, Gastaldelli A, Johnson M, Dick Jr EJ, Folli F. 2012. The ontogeny of the endocrine pancreas in the fetal/newborn baboon. *Journal of Endocrinology* 214:289-299

R Core Team. 2014. R project. www.r-project.org.

Raff RA. 1996. *The shape of life: genes, development, and the evolution of animal form*. University of Chicago Press: Chicago.

Ralston SH, Galwey N, MacKay I, Albagha OME, Cardon L, Compston JE, Cooper C, Duncan E, Keen R, Langdahl B, McLellan A, O'Riordan J, Pols HA, Reid DM, Uitterlinden AG, Wass J, Bennett ST. 2005. Loci for regulation of bone mineral density in men and women identified by genome wide linkage scan: the FAMOS study. *Human Molecular Genetics* 14(7):943-951.

Rankinen T, Zuberi A, Chagnon YC, Weisnagel SJ, Argyropoulos G, Walts B, Pérusse L, Bouchard. 2006. The human obesity gene map: The 2005 update. *Obesity* 14(4):529-644.

Reeves NM, Auerbach BM, Sylvester AD. 2016. Fluctuating and directional asymmetry in the long bones of captive cotton-top tamarins (*Saguinus oedipus*). *American Journal of Physical Anthropology* In Press.

Reno P, DeGusta D, Serrat M, Meindl R, White T, Eckhardt R, Kuperavage A, Galik K, Lovejoy C. 2005. Plio-Pleistocene Hominid Limb Proportions. *Current Anthropology* 46(4):575-588.

Richmond B, Aiello L, Wood B. 2002. Early hominin limb proportions. *Journal of Human Evolution* 43:529-548.

Riddle RD, Johnson RL, Laufer E, Tabin C. 1993. *Sonic hedgehog* mediates the polarizing activity of the ZPA. *Cell* 75:1401-1416.

Riesenfield A. 1973. The effect of extreme temperatures and starvation on the body proportions of the rat. *American Journal of Physical Anthropology* 39:427–460.

Risch N, Zhang H. 1995. Extreme discordant sib pairs for mapping quantitative trait loci in humans. *Science* 268:1584-1589.

Robb JE. 1998. The interpretation of skeletal muscle sites: A statistical approach. *International Journal of Osteoarchaeology* 8:363–377.

Roberts DF. 1978. *Climate and Human Variability*. Menlo Park, CA: Cummings.

Robling A, Li J, Shultz K, Beamer W, Turner C. 2003. Evidence for a skeletal mechanosensitivity gene on mouse chromosome 4. *FASEB Journal* 17:324–326.

Robling AG, Castillo AB, Turner CH. 2006. Biomechanical and molecular regulation of bone remodeling. *Annual Review of Biomedical Engineering* 8:455-498.

Robling AG, Fuchs RK, Burr DB. 2014. Mechanical Adaptation. In: Burr DB, Allen MR, editors: *Basic and Applied Bone Biology*. New York: Elsevier. pp. 175-204.

Rodman P, McHenry H. 1980. Bioenergetics and the Origin of Homind Bipedalism. *American Journal of Physical Anthropology* 52:103-106.

Rogers J, Mahaney MC, Witte SM, Nair S, Newman D, Wedel S, Rodriguez LA, Rice KS, Slifer SH, Perelygin A, Slifer M, Palladino-Negro P, Newman T, Chambers K, Joslyn G, Parry P, Morin PA. 2000. A genetic linkage map of the baboon (*Papio hamadryas*) genome based on human microsatellite polymorphisms. *Genomics* 67:237-247.

Rogers J, Kochunov P, Lancaster J, Shelledy W, Glahn D, Blangero J, Fox P. 2007. Heritability of brain volume, surface area and shape: An MRI study in an extended pedigree of baboons. *Human Brain Mapping Special Issue: Genomic Imaging Volume* 28(6):576–583.

Rolian C. 2009. Integration and evolvability in primate hands and feet. *Evolutionary Biology* 36:100-117.

Rolian C, Willmore KE. 2009. Morphological integration at 50: Patterns and processes of integration in biological anthropology. *Evolutionary Biology* 36:1-4.

Roseman CC, Auerbach BM. 2015. Ecogeography, genetics, and the evolution of human body form. *Journal of Human Evolution* 78:80-90.

Roseman CC, Willmore KE, Rogers J, Hildebolt C, Sadler BE, Richtsmeier JT, Cheverud JM. 2010. Genetic and environmental contributions to variation in baboon cranial morphology. *American Journal of Physical Anthropology* 143:1-12.

Rubicz RC, Melton PE, Crawford MH. 2007. Molecular markers in anthropological genetic studies. In: Crawford M, editor. *Anthropological Genetics*. New York: Cambridge University Press. pp. 141-186.

Rubin C, Brandstrom H, Wright D, Kerje S, Gunnarsson U, Schutz K, Fredriksson R, Jensen P, Andersson L, Ohlsson C, Mallmin H, Larsson S, Kindmark A. 2007. Quantitative trait loci for BMD and bone strength in an intercross between domestic and wildtype chickens. *Journal of Bone and Mineral Research* 22:375–384.

Ruff CB. 1990. Body mass and hindlimb bone cross-sectional and articular dimensions in anthropoid primates. In: Damuth J, McFadden BJ, editors. *Body Size in mammalian paleobiology: Estimation and biological implications.* Cambridge: Cambridge University Press. pp. 119-149.

Ruff CB. 1991. Climate and body shape in hominid evolution. *Journal of Human Evolution* 21:81-105.

Ruff CB. 1993. Climatic adaptation and hominid evolution: The thermoregulatory imperative. *Evolutionary Anthropology* 2:53-60.

Ruff CB. 1994. Morphological adaptation to climate in modern and fossil hominids. *Yearbook of Physical Anthropology* 37:65-107.

Ruff CB. 2002a. Variation in human body size and shape. *Annual Review of Anthropology* 31:211-232.

Ruff CB. 2002b. Long bone articular and diaphyseal structure in Old World monkeys and apes. I: Locomotor effects. *American Journal of Physical Anthropology* 119:305-342.

Ruff CB. 2003. Ontogenetic adaptation to bipedalism: age changes in femoral to hemoral length and strength proportions in humans, with a comparison to baboons. *Journal of Human Evolution* 45:317-349.

Ruff CB. 2006. Environmental influences on skeletal morphology. In: Ubelaker D, editor. *Handbook of North American Indians, Vol 3: Environment, Origins and Populations*. Washington, D.C.: Smithsonian Institution. pp. 685-694.

Ruff CB. 2007. Body size prediction from juvenile skeletal remains. *American Journal of Physical Anthropology* 133:698-716.

Ruff CB. 2008a. Biomechanical analyses of archaeological human skeletal samples. In: Saunders S, Katzenberg M, editors. *The Skeletal Biology of Past Peoples: Research Methods*. New York: Alan R. Liss. pp. 41-62.

Ruff C. 2008b. Femoral/humeral strength in early African *Homo erectus*. *Journal of Human Evolution* 54:383-390.

Ruff C. 2009. Relative Limb Strength and Locomotion in *Homo habilis*. *American Journal of Physical Anthropology* 138(1):90-100.

Ruff CB. 2010. Body size and shape in the early hominins – implications of the Gona Pelvis. *Journal of Human Evolution* 58(2):166-178.

Ruff CB, Walker A. 1993. Body size and body shape. In: Walker A, Leakey RE, editors: *The Nariokotome* Homo erectus *Skeleton*. Cambridge, MA: Harvard University Press. pp. 234-265.

Ruff CB, Scott WW, Liu AY-C. 1991. Articular and diaphyseal remodeling of the proximal femur with changes in body mass in adults. *American Journal of Physical Anthropology* 86:397-413.

Ruff C, Trinkaus E, Walker A, Larsen C. 1993. Postcranial Robusticity in *Homo*. I: Temporal Trends and Mechanical Interpretation. *American Journal of Physical Anthropology* 91:21-53.

Ruff CB, Walker A, Trinkaus E. 1994b. Postcranial robusticity in Homo, III: Ontogeny. *American Journal of Physical Anthropology* 93:35-54.

Saiki R, Scharf S, Faloona F, Mullis K, Horn G, Erlich H. 1985. Enzymatic amplification of beta-globin genomic sequences and restriction site analysis for diagnosis of sickle cell anemia. *Science* 230:1350-1354.

Sanna S, Jackson AU, Nagaraja R, Willer CJ, Chen WM, Bonnycastle LL, Shen H, Timpson N, Lettre G, Usala G, Chines PS, Stringham HM, Scott LJ, Dei M, Lai S, Albai G, Crisponi L, Naitza S, Doheny KF, Pugh EW, Ben-Shlomo Y, Ebrahim S, Lawlor DA, Bergman RN, Watanabe RM, Uda M, Tuomilehto J, Coresh J, Hirschhorn JN, Shuldiner AR, Schlessinger D, Collins FS, Smith GD, Boerwinkle E, Cao A, Boehnke M, Abecasis GR, Mohlke KL. 2008. Common variants in the GDF5-UQCC region are associated with variation in human height. *Nature Genetics* 40(2):198-203.

Savell KRR, Auerbach BM, Roseman CC. In review. Constraint, natural selection, and the evolution of human body form. *Proceedings of the National Academy of Sciences USA*.

Schiess R, Haeusler M. 2013. No skeletal dysplasia in the Nariokotome Boy KNM-WT 15000 (*Homo erectus*) - A reassessment of congenital pathologies of the vertebral column. *American Journal of Physical Anthropology* 150:365–374.

Schlosser G, Wagner G. 2004. Introduction: The modularity concept in developmental and evolutionary biology. In: Schlosser G, Wager G, editors. *Modularity in Development and Evolution*. Chicago: University of Chicago Press. pp. 1-11.

Schoenwolf G, Bleyl S, Brauer P, Francis-West P. 2015. *Larsen's Human Embryology*. New York: Churchill Livingstone.

Scholander, PF. 1955. Evolution of climatic adaptation in homeotherms. *Evolution* 9:15-26.

Schork NJ. 1993. Extended multipoint identity-by-descent analysis of human quantitative traits: efficiency, power and modeling considerations. *American Journal of Human Genetics* 53:1306-1319.

Schultz AH. 1923. Fetal growth in man. *American Journal of Physical Anthropology* 4:389–399.

Schultz AH. 1929. The technique of measuring the outer body of human fetuses and of primates in general. Carnegie Institution of Washintgon, no. 394. *Contributions to Embryology* 20(117):213-257.

Schultz AH. 1930. The skeleton of the trunk and limbs of higher primates. *Human Biology* 2(3):303-438.

Schultz AH. 1973. Age changes, variability and generic differences in body proportions of recent hominoids. *Folia Primatologica* 19(5):338-359.

Schwartz JH, Tattersall I, Chi Z. 2014. Comment on "A complete skull from Dmanisi, Georgia, and the evolutionary biology of early *Homo*." *Science* 344:360a.

Serrat MA, King D, Lovejoy CO. 2008. Temperature regulates limb length in homeotherms by directly modulating cartilage growth. *Proceedings of the National Academy of Sciences USA* 105(49):19348-19353.

Shang H, Tong H, Zhang S, Chen F, Trinkaus E. 2007. An early modern human from Tianyuan Cave, Zhoukoudian, China. *Proceedings of the National Academy of Sciences USA* 104:6573-6578.

Sherwood R, Duren D, Havill L, Rogers J, Cox L, Towne B, Mahaney M. 2008. A genomewide linkage scan for quantitative trait loci influencing the craniofacial complex in baboons (*Papio hamadryas spp*.). *Genetics* 180:619-628.

Showell C, Binder O, Conlon FL. 2004. T-box genes in early embryogenesis. *Developmental Dynamics* 229(1):201-18.

Silventoinen K, Kaprio J, Lahelma E, Koskenvuo M. 2000. Relative effect of genetic and environmental factors on body height: differences across birth cohorts among Finnish men and women. *American Journal of Public Health* 90:627-630.

Silventoinen K, Sammalisto S, Perola M, Boomsma DI, Cornes BK, Davis C, Dunkel L, De Lange M, Harris JR, Hjelmborg JV, Luciano M, Martin NG, Mortensen J, Nisticò L, Pedersen NL, Skytthe A, Spector TD, Stazi MA, Willemsen G, Kaprio J. 2003. Heritability of adult body height: a comparative study of twin cohorts in eight countries. *Twin Research* 6:399-408.

SNPRC Baboon to Humans Comparative Maps Website. 2014. http://baboon.txbiomedgenetics.org/Bab_Results/Comp MapsQuery.php and http://baboon.txbiomedgenetics.org/Bab_Results/CompMaps.php

SNPRC Website. 2014. http://txbiomed.org/primate-research-center.

SOLAR Documentation. 2013. Sequential Oligogenic Linkage Analysis Routines. http://solar.txbiomedgenetics.org.

Soller M, Brody T, Genizi A. 1979. On the power of experimental designs for the detection of linkage between marker loci and quantitative loci in crosses between inbred lines. *Theoretical and Applied Genetics* 47:35-39.

Soranzo N, Rivadeneira F, Chinappen-Horsley U, Malkina I, Richards JB, Hammond N, Stolk L, Nica A, Inouye M, Hofman A, Stephens J, Wheeler E, Arp P, Gwilliam R, Jhamai PM, Potter S, Chaney A, Ghori MJR, Ravindrarajah R, Ermakov S, Estrada K, Pols HAP, Williams FM, McArdle WL, van Meurs JB, Loos RJF, Dermitzakis ET, Ahmadi KR, Hart DJ, Ouwehand WH, Wareham NJ, Barroso I, Sandhu MS, Strachan DP, Livshits G, Spector TD, Uitterlinden AG, Deloukas P. 2009. Meta-analysis of genome-wide scans for human adult stature identifies novel loci and associations with measures of skeletal frame size. *PLoS Genetics* 5:e1000445.

SSH Communications Security Corp. 2003. SSH Secure Shell version 3.2.9. www.ssh.com.

Steckel RH. 1987. Growth depression and recovery: The remarkable case of American slaves. *Annals of Human Biology* 14(2):111-132.

Steckel RH. 1995. Stature and the standard of living. *Journal of Economic Literature* 32:1903-1940.

Steegmann AT. 1985. 18th century British military stature: growth cessation, selective recruiting, secular trends, nutrition at birth, cold and occupation. *Human Biology* 57:77–95.

Steegmann AT. 1986. Skeletal stature compared to archival stature in mid-eighteenth century America: Ft. William Henry. *American Journal of Physical Anthropology* 71:431–435.

Steegmann AT. 1991. Stature in a mid-19th century poorhouse population: Highland Park, Rochester, New York. *American Journal of Physical Anthropology* 85:261–268.

Steegmann AT, Jr. 2007. Human cold adaptation: an unfinished agenda. *American Journal of Human Biology* 19:218-227.

Steudel-Numbers K. 2006. Energetics in *Homo erectus* and other early hominins: The consequences of increased lower-limb length. *Journal of Human Evolution* 51:445-453.

Steudel-Numbers K, Tilkens M. 2004. The effect of lower limb length on the energetic cost of locomotion: implications for fossil hominins. *Journal of Human Evolution* 47:95-109.

Steudel-Numbers K, Weaver T, Wall-Scheffler C. 2007. The evolution of human running: Effects of changes in lower-limb length on locomotor economy. *Journal of Human Evolution* 53:191-196.

Stini WA. 1969. Nutritional stress and growth: sex difference in adaptive response. *American Journal of Physical Anthropology* 31:417–426.

Stinson S. 1985. Sex differences in environmental sensitivity during growth and development. *Yearbook of Physical Anthropology* 28:123–147.

Stock JT. 2006. Hunter-gatherer postcranial robusticity relative to patterns of mobility, climatic adaptation, and selection for tissue economy. *American Journal of Physical Anthropology* 131:194-204.

Stock JT, Pfeiffer SK. 2004. Long bone robusticity and subsistence behaviour among Later Stone Age foragers of the forest and fynbos biomes of South Africa. *Journal of Archaeological Science* 31:999-1013.

Stratford T, Horton C, Maden M. 1996. Retinoic acid is required for the initiation of outgrowth in the chick limb bud. *Current Biology* 6(9):1124–1133

Sturtevant AH. 1913. The linear arrangement of six sex-linked factors in *Drosophila*, as shown by their mode of association. *Journal of Experimental Zoology* 14:43-59.

Susanne C. 1975. Genetic and environmental influences on morphological characters. *Annals of Human Biology* 2:279-287.

Susanne C. 1977. Heritability of anthropological characters. *Human Biology* 49(4):573-580.

Susman RL, Stern JT Jr. 1982. Functional morphology of *Homo habilis*. *Science* 217, 931–934.Susman

Sylvester A. 2006. Locomotor decoupling and the origin of hominin bipedalism. *Journal of Theoretical Biology* 242:581-590.

Szklarczyk D, Franceschini A, Wyder S, Forslund K, Heller D, Huerta-Cepas J, Simonovic M, Roth A, Santos A, Tsafou K, Kuhn M, Bork P, Jensen L, von Mering C. 2015. STRING v10: protein-protein interaction networks, integrated over the tree of life. *Nucleic Acids Research* 43:D447-452.

Takamura K, Ohyama S, Yamada T, Ishinishi N. 1988. Changes in body proportions of Japanese medical students between 1961 and 1986. *American Journal of Physical Anthropology* 77:17-22.

Tanaka EM, Gann AAF. 1995. The budding role of FGF. *Current Biology* 5(6):594-597.

Tanner JM, Hayashi T, Preece MA, Cameron N. 1982. Increase in leg relative to trunk in Japanese children and adults from 1957 to 1977: comparison with British and with Japanese Americans. *Annals of Human Biology* 9:411–423.

Tarchini B, Duboule D. 2006. Control of *Hoxd* genes' collinearity during early limb development. *Developmental Cell* 10:93-103.

Tardieu C, Trinkaus E. 1994. Early ontogeny of the human femoral bicondylar angle. *American Journal of Physical Anthropology* 95:183-195.

Tardif SD, Carson RL, Gangaware BL. 1990. Infant-care behavior of mothers and fathers in a communal-care primate, the cotton-top tamarin (*Saguinus oedipus*). *American Journal of Primatology* 22(2):73-85.

Tatham, S. 2011. PuTTY. Release 0.62. www.putty.org.

Tattersall I, Schwartz JA. 1999. Hominids and hybrids: The place of Neanderthals in human evolution. *Proceedings of the National Academy of Sciences USA* 96(13):7117-7119.

Temple D, Auerbach B, Nakatsukasa M, Sciulli P, Larsen C. 2008. Variation in Limb Proportions Between Jomon Foragers and Yayoi Agriculturalists from Prehistoric Japan. *American Journal of Physical Anthropology* 137:164-174.

Todorov AA, Province MA, Borecki IB, Rao DC. 1997. Trade-off between sibship size and sampling scheme for detecting quantitative trait loci. *Human Heredity* 47:1-5.

Towers M, Tickle C. 2009. Growing models of vertebrate limb development. *Development* 136(2):179–190.

Towers M, Wolpert L, Tickle C. 2012. Gradients of signalling in the developing limb. *Current Opinion in Cell Biology* 24(2):181–187.

Towne B, Siervogel RM, Blangero J. 1997. Effects of genotype-by-sex interaction on quantitative trait linkage analysis. *Genetic Epidemiology* 14:1053–1058.

Trinkaus E. 1981. Neandertal limb proportions and cold adaptation. In: Stringer C, editor. *Aspects of Human Evolution*. London: Taylor and Francis. pp. 187-224.

Trinkaus E, Churchill S, Ruff C. 1994a. Postcranial Robusticity in *Homo*. II: Humeral Bilateral Asymmetry and Bone Plasticity. *American Journal of Physical Anthropology* 93:1-34.

Tukey JW. 1977. *Exploratory Data Analysis*. Reading, MA: Addison-Wesley.

Turner C. 1998. Three Rules for Bone Adaptation to Mechanical Stimuli. *Bone* 23(5):399-407.

UCSC Genome Browser Website. 2014. www.genome.ucsc.edu.

Vandenberg SG. 1962. How "stable" are heritability estimates? A comparison of heritability estimates from six anthropometric studies. *American Journal of Physical Anthropology* 20:331-338.

Van Valen L. 1965. The study of morphological integration. *Evolution* 19:347–349.

Villmoare B, Fish J, Jungers W. 2011. Selection, morphological integration, and strepsirrhine locomotor adaptations. *Evolutionary Biology* 38:88-99.

Vinson A, Mahaney MC, Cox LA, Rogers J, VandeBerg JL, Rainwater DL. 2008. A pleiotropic QTL on 2p influences serum Lp-PLA2 activity and LDL cholesterol concentration in a baboon model for the genetics of atherosclerosis risk factors. *Atherosclerosis* 196:667-673.

Visscher PM, Hill WG, Wray NR. 2008. Heritability in the genomics era – concepts and misconceptions. *Nature Review Genetics* 9:255-266.

Waddington CH. 1942. The canalization of development and the inheritance of acquired characters. *Nature* 150:563-565.

Wagner GP. 1996. Homologues, natural kinds and the evolution of modularity. *American Zoologist* 36(1):36–43.

Wagner GP, Altenberg L. 1996. Complex adaptation and the evolution of evolvability. *Evolution* 50:967-976.

Wagner GP, Pavlicev M, Cheverud JM. 2007. The road to modularity. *Nature Reviews Genetics* 8:921-931.

Walker A, Leakey RE, Editors. 1993. *The Nariokotome* Homo erectus *skeleton*. Cambridge: Harvard University Press.

Wallace IJ, Tommasini SM, Judex S, Garland Jr T, Demes S. 2012. Genetic variations and physical activity as determinants of limb bone morphology: An experimental approach using a mouse model. *American Journal of Physical Anthropology* 148:24-35.

Wang X, Paigen B. 2002. Quantitative trait loci and candidate genes regulating HDL cholesterol: A murine chromosome map. *Arteriosclerosis, Thrombosis, and Vascular Biology* 22:1390-1401.

Wang DG, Fan J-B, Siao C-J, Berno A, Young P, Sapolsky R, Ghandour G, Perkins N, Winchester E, Spencer J, Kruglyak L, Stein L, Hsie L, Topaloglou T, Hubbell E, Robinson E, Mittmann M, Morris MS, Shen N, Kilburn D, Rioux J, Nusbaum C, Rozen S, Hudson TJ, Lipshutz R, Chee M, Lander ES. 1998a. Large-scale identification, mapping, and genotyping of single-nucleotide polymorphisms in the human genome. *Science* 280:1077-1082.

Wang X, Mabrey JD, Agrawal CM. 1998b. An interspecies comparison of bone fracture properties. *Bio-Medical Materials and Engineering* 8:1-9.

Weaver TD. 2003. The shape of the Neandertal femur is primarily the consequence of a hyperpolar body form. *Proceedings of the National Academy of Sciences USA* 100(12):6926-6929.

Weaver ME, Ingram DL. 1969. Morphological changes in swine associated with environmental temperature. *Ecology* 50:710–713.

Weaver TD, Steudel-Numbers K. 2005. Does climate or mobility explain the differences in body proportions between Neandertals and their Upper Paleolithic successors? *Evolutionary Anthropology* 14:218-223.

Weber JL, May PE. 1989. Abundant class of human DNA polymorphisms which can be typed using the polymerase chain reaction. *American Journal of Human Genetics* 44:388-396.

Weedon MN, Letter G, Freathy RM, Lindgren CM, Voight BF, Perry JRB, Elliott KS, Hackett R, Guiducci C, Shields B, Zeggini E, Lango H, Lyssenko V, Timpson NJ, Burtt NP, Rayner

NW, Saxena R, Ardlie K, Tobias JH, Ness AR, Ring SM, Palmer CAN, Morris AD, Peltonen L, Salomaa V, The Diabetes Genetics Initiative, The Wellcome Trust Case Control Consortium, Smith GD, Groop LC, Hattersley AT, McCarty MI, Hirschhorn JN, Frayling TM. 2007. A common variant of *HMGA2* is associated with adult and childhood height in the general population. *Nature Genetics* 39:1245-1250.

Weedon MN, Lango H, Lindgren CM, Wallace C, Evans DM, Mangino M, Freathy RM, Perry JRB, Stevens S, Hall AS, Samani NJ, Shields B, Prokopenko I, Farrall M, Dominiczak A, Diabetes Genetics Initiative, The Wellcome Trust Case Control Consortium, Johnson T, Bergmann S, Beckmann JS, Vollenweider P, Waterworth DM, Mooser V, Palmer CNA, Morris AD, Ouwehand WH, Cambridge GEM Consortium, Caulfield M, Munroe PM, Hattersley AT, McCarthy MI, Frayling TM. 2008. Genome-wide association analysis identifies 20 loci that influence adult height. *Nature Genetics* 40:575-583.

Weiss, Elizabeth. 2003. The effects of rowing on humeral strength. *American Journal of Physical Anthropology* 121:293-302.

Wescott D. 2006. Ontogeny of femur subtrochanteric shape in Native Americans and American Blacks and Whites. *Journal of Forensic Science* 51(6):1240-1245.

West-Eberhard, Mary J. 2003. *Developmental Plasticity and Evolution*. Oxford: Oxford University Press.

Wheeler P. 1991. The thermoregulatory advantages of hominid bipedalism in open equatorial environments: the contribution of increased convective heat loss and cutaneous evaporative cooling. *Journal of Human Evolution* 21:107-115.

White TD. 2000. *Human Osteology*. Second Edition. New York: Academic Press.

Williams JT, Blangero J. 1999a. Power of variance component linkage analysis to detect quantitative trait loci. *Annals of Human Genetics* 63:545-563.

Williams JT, Blangero J. 1999b. Comparison of variance components and sibpair-based approaches to quantitative trait linkage analysis in unselected samples. *Genetic Epidemiology* 16:113-134.

Willis JH, Coyne JA, Kirkpatrick M. 1991. Can one predict the evolution of quantitative characters without genetics? *Evolution*, 45:441–444.

Wilson AJ, Réale D, Clements MN, Morrissey MM, Postma E, Walling CA, Kruuk LEB, Nussey DH. 2009a. An ecologist's guide to the animal model. *Journal of Animal Ecology* 79:13-26.

Wilson AJ, Réale D, Clements MN, Morrissey MM, Postma E, Walling CA, Kruuk LEB, Nussey DH. 2009b. Supplementary File 5: Tutorial for MCMCglmm version. *Journal of Animal Ecology* 79:1-8.

Wolański W, Kasprzak E. 1976. Stature as a measure of the effects of environmental change. *Current Anthropology* 17:548-552.

Wolpoff M. 1983. Lucy's lower limbs: long enough for Lucy to be fully bipedal? *Nature* 304:59-61.

Wright S. 1920. The relative importance of heredity and environment in determining the piebald pattern of guinea-pigs. *Proceedings of the National Academy of Sciences of the USA* 6:320-332.

Wright S. 1921. Systems of mating. *Genetics* 6:111-178.

Wright, S. 1968. *Evolution and the genetics of populations*. University of Chicago Press, Chicago.

Woolley TE, Baker RE, Tickle C, Maini PK, Towers M. 2013. Mathematical modelling of digit specification by a sonic hedgehog gradient. *Developmental Dynamics* 243(2):290–298.

Yang Y, Niswander L. 1995. Interaction between the signaling molecules WNT7a and SHH during vertebrate limb development: Dorsal signals regulate anteroposterior patterning. *Cell* 80:939-947.

Young NM, Wagner GP, Hallgrímsson B. 2010. Development and evolvability of human limbs. *Proceedings of the National Academy of Sciences of the USA* 107(8):3400-3405.

Young NM, Hallgrímsson B. 2005. Serial homology and the evolution of mammalian limb covariation structure. *Evolution* 59(12):2691-2704.

APPENDICES

Appendix I: Permissions to use data.

Mennonite Data:

From: Crawford, Michael H [crawford@ku.edu]
To: Hulsey, Brannon Irene [bjones32@utk.edu]
Sent: Sunday, November 21, 2010 11:36 AM
Subject: RE: letter of permission

Dear Brannon,
Here is the letter of information requested by your Office of Research and your Departmental Representative to the UT IRB.
The data were collected from 1979 to 1981 in the Mennonite communities of Goessel and Meridien, Kansas and Henderson, Nebraska. This research was conducted as a result of a three-year grant from the National Institute of Aging (NIH). A total of 25 researchers from the University of Kansas and Cornell University collected an assortment of data concerning biological aging. I was the PI for the project and supervised the collection of anthropometric measurements by three graduate student assistants. Written informed consent was obtained from every volunteer in the study.
You have my permission to further analyze the data that were collected in this field research for your Ph.D. dissertation. The participants maintain their anonymity because you were sent data sheets with identifying numbers but no names were listed.
Do not hesitate to contact me if any questions arise concerning the data and/or the analyses.
Michael H. Crawford, Ph.D.
Professor of Anthropology
University of Kansas
Lawrence, KS
crawford@ku.edu

Sukhumi Baboon Data:

From: Dennis H O'Rourke [dennis.orourke@anthro.utah.edu]
To: Hulsey, Brannon Irene [bjones32@utk.edu]
Sent: Tuesday, July 20, 2010 11:05 PM
Subject: RE:

Hi Brannon,

Of course you can use my old dissertation data. If it can be of help to you I'm happy for you to use it. Let me know if I can help in anyway. I no longer have a copy of the data, so glad to know Mike kept a version of it at Kansas.

Cheers, Dennis

Tamarin Data:

THE UNIVERSITY of TENNESSEE
College of Arts and Sciences
Department of Anthropology
250 South Stadium Hall
Knoxville, TN 37996-0720
Phone (865) 974-4408
Fax (865) 974-2686

15 January 2011

Dear Brannon,

This letter confirms permission for you to use the Oak Ridge Small Primate Skeletal Collection (tamarins) for nondestructive analysis as part of your dissertation research. The sample is available in the Osteometric Variation Analysis Lab in 321 South Stadium Hall, along with associated pedigree information. Please let me know if you have additional questions.

Best wishes,

Benjamin M. Auerbach
Interim Curator of Osteological Collections

TBRI Baboons:

TEXAS BIOMEDICAL RESEARCH INSTITUTE

Department of Genetics

Lorena M. Havill, Ph.D.

February 4, 2011

Brannon Hulsey
Dept. of Anthropology
University of Tennessee
Knoxville, TN

Dear Brannon:

I am writing in enthusiastic support of your dissertation research in which you will use the collection of baboon skeletal materials that I have built over the past 8 years. This collection includes femora, humeri, and other skeletal materials from in excess of 700 genotyped, pedigreed, adult baboons. I have used these materials to successfully test the hypothesis that genetic variation affects phenotypic variance in a number of skeletal traits. I look forward to seeing the results of your work with limb proportions in these baboons.

Sincerely,

Lorena M. Havill

Lorena M. Havill, Ph.D.
Assistant Scientist
Director, Genetics of Skeletal Aging Research Laboratory

Appendix II: TBRI Data Collection Sheets

Baboon Specimen Number: _____

Date: _____

HUMERUS

1. Maximum Length _____
2. 50% of Length _____
AP Diameter _____
ML Diameter _____
Deltoid Tuberosity Present? Y N
3. 40% of Length _____
AP Diameter _____
ML Diamter _____
4. Length of Head _____
5. Epicondylar Breadth _____
6. Distal Articular Breadth _____
Trochlear Breadth _____
Capitular Breadth _____
7. Olecranon Fossa Height _____
Breadth _____

NOTES:

Baboon Specimen Number: _____

Date: _____

FEMUR

1. Maximum Length _____
2. Bicondylar Length _____
3. Midshaft Length _____
AP Diameter _____
ML Diameter _____
4. 25% of Length _____
AP Diameter _____
ML Diameter _____
5. 75% of Length _____
AP Diameter _____
ML Diameter _____
6. Maximum Head Diameter _____
7. Bicondylar Breadth _____
8. Articular Breadth _____
9. Breadth of Medial Condyle _____
Lateral Condyle _____
10. Articular Depth - Medial Condyle _____
Lateral Condyle _____

NOTES:

Appendix III: Mennonite Lateral Malleolus Height Regression Equations

To calculate Lateral Malleolus Height for Males:

Lateral Malleolus Height (LMH)

Average = 67.07 mm

Std. Dev. = 0.547

Trochanteric Height (TH)

Average = 928.3 mm

Std. Dev. = 4.776

Covariance between LMH and TH = 0.339

$cov(xy) = 0.339 * 4.776 * 0.547 = 0.8856$

$var(x) = 4.776^2 = 22.810$

$b = cov(xy) / var(x) = 0.8856 / 22.810 = 0.03882$

$a = ybar – b * xbar = 67.07 – 0.3882 * 928.3 = 31.03$

Therefore, the regression equation for males is:

$LMH = 0.03882 * TH + 31.03$

To calculate Lateral Malleolus Height for Females:

Lateral Malleolus Height (LMH)

Average = 60.6 mm

Std. Dev. = 0.53

Trochanteric Height (TH)

Average = 861.6 mm

Std. Dev. = 4.52

Covariance between LMH and TH = 0.285

cov(xy) = 0.285 * 4.52 * 0.53 = 0.683

var(x) = 4.52^2 = 20.43

b = cov(xy) / var(x) = 0.683 / 20.43 = 0.03343

a = ybar – b * xbar = 60.6 – 0.3343 * 861.6 = 31.80

Therefore, the regression equation for females is:

LMH = 0.03343 * TH + 31.80

Appendix IV: Tables and Figures

Table 1 - TBRI Baboon skeletal measurements.

Measurement	Citation (alternative measurement name)
Humerus Measurements	
Maximum Length	Buikstra & Ubelaker, 1994:80, #40
Anterio-posterior Diameter: Midshaft and 40%	personal communication with B. Auerbach
Medio-lateral Diameter: Midshaft and 40%	personal communication with B. Auerbach
Length of Head	Buikstra & Ubelaker, 1994:80, #42 (vertical diameter of head)
Epicondylar Breadth	Buikstra & Ubelaker, 1994:80, #41
Distal Articular Breadth	Ruff, 2000:336 (HDML)
Trochlear Breadth	Ruff, 2002:336 (TRML)
Capitular Breadth	Ruff, 2002:336 (CPML)
Olecranon Fossa Height	personal communication with B. Auerbach
Olecranon Fossa Breadth	personal communication with B. Auerbach
Femur Measurements	
Maximum Length	Buikstra & Ubelaker, 1994:82, #60
Bicondylar Length	Buikstra & Ubelaker, 1994:82, #61
Anterio-posterior Diameter: 25%, Midshaft, and 75%	Buikstra & Ubelaker, 1994:82, #66
Medio-lateral Diameter: 75%, Midshaft, and 75%	Buikstra & Ubelaker, 1994:82, #67
Maximum Head Diameter	Buikstra & Ubelaker, 1994:82, #63
Bicondylar Breadth	Buikstra & Ubelaker, 1994:82, #62 (epicondylar breadth)
Articular Breadth	Ruff, 2002:334 (FCML)
Breadth of Medial Condyle	Ruff, 2002:334 (MCML)
Breadth of Lateral Condyle	Ruff, 2002:334 (LCML)
Articular Depth of Medial Condyle	Ruff, 2002:334 (MCSI)
Articular Depth of Lateral Condyle	Ruff, 2002:334 (LCSI)

Table 2 - Paired t-tests for right and left TBRI Baboon femoral measurements.

	Paired Differences							
				95% CI of the Difference				
Left side – Right side	Mean	Std. Dev.	Std. Error Mean	Lower	Upper	t	df	Sig. (2-tailed)
Maximum Length	-0.131	1.713	0.170	-0.467	0.206	-0.771	101	.442
Bicondylar Length	0.281	3.525	0.349	-0.411	0.974	0.806	101	.422
50% AP Diameter	0.272	0.435	0.043	0.187	0.357	6.333	102	**.000**
50% ML Diameter	-0.045	0.331	0.033	-0.110	0.020	-1.383	101	.170
25% AP Diameter	0.278	0.519	0.051	0.176	0.379	5.425	102	**.000**
25% ML Diameter	-0.057	0.583	0.057	-0.171	0.057	-0.988	102	.325
75% AP Diameter	0.128	0.336	0.033	0.062	0.194	3.859	102	**.000**
75% ML Diameter	-0.052	0.322	0.032	-0.115	0.011	-1.630	102	.106
Head Diameter	0.084	0.642	0.063	-0.041	0.210	1.330	102	.186
Bicondylar Breadth	0.020	0.684	0.069	-0.117	0.156	0.284	98	.777
Articular Breadth	-0.147	0.503	0.058	-0.263	-0.031	-2.525	74	**.014**
Medial Condyle Breadth	-0.124	0.573	0.067	-0.257	0.009	-1.858	73	.067
Lateral Condyle Breadth	0.088	0.405	0.040	0.008	0.168	2.191	100	**.031**
Medial Condyle Depth	0.014	0.797	0.081	-0.147	0.174	0.170	96	.865
Lateral Condyle Depth	-0.314	0.966	0.095	-0.502	-0.126	-3.313	103	**.001**

Table 3 - Tamarin summary statistics.

	Humerus Maximum Length	Radius Maximum Length	Femur Bicondylar Length	Tibia Maximum Length
Females - Sample Size	95	95	99	101
Mean	51.48	46.45	66.09	66.77
Standard Deviation	1.65	1.66	2.06	2.37
Range	47.47-54.90	42.83-49.87	61.29-70.87	61.97-71.68
Males - Sample Size	116	116	115	117
Mean	50.55	45.86	65.27	66.30
Standard Deviation	1.53	1.65	2.00	2.13
Range	47.13-54.11	42.64-49.77	61.03-69.91	60.30-70.82
Combined – Sample Size	211	211	214	218
Mean	50.97	46.13	65.65	66.52
Standard Deviation	1.65	1.68	2.06	2.26
Range	47.13-54.90	42.64-49.87	61.03-70.87	60.30-71.68

All measurements are in mm.

Table 4 - Sukhumi Baboon summary statistics.

	Arm Length	Forearm Length	Thigh Length	Leg Length
Females - Sample Size	124	124	109	112
Mean	173.27	201.46	212.77	171.07
Standard Deviation	8.74	8.70	10.33	6.70
Range	152-192	183-220	189-235	154-187
Males - Sample Size	65	65	60	66
Mean	202.49	236.42	250.38	201.08
Standard Deviation	10.92	9.54	13.00	8.11
Range	176-229	215-253	221-275	185-216
Combined – Sample Size	189	189	169	178
Mean	183.32	213.48	226.12	182.20
Standard Deviation	16.86	18.91	21.30	16.23
Range	152-229	183-253	189-275	154-216

All measurements are in mm.

Table 5 - Mennonite summary statistics.

	Arm Length	Forearm Length	Thigh Length	Leg Length
Females - Sample Size	180	180	186	186
Mean	308.24	240.92	463.63	383.96
Standard Deviation	14.84	14.08	28.27	18.22
Range	273-340	207-273	399.99-525.77	345-425
Males - Sample Size	184	181	183	183
Mean	334.07	268.02	484.22	421.17
Standard Deviation	16.15	14.20	28.53	15.63
Range	285-368	233-304	423.46-549.94	382-457
Combined – Sample Size	364	361	369	369
Mean	321.30	254.50	473.84	402.42
Standard Deviation	20.18	193.58	30.17	25.19
Range	285-368	207-304	399.99-549.94	345-457

All measurements are in mm.

Table 6 - TBRI Baboon summary statistics.

	Humerus Measurements					
	Maximum Length	50% AP Diameter*	50% ML Diameter*	Head Length	Distal Articular Breadth	Epicondylar Breadth
Females - Sample Size	308	318	318	324	323	333
Mean	190.99	15.33	14.64	22.71	26.52	36.13
St. Dev.	7.13	1.14	0.87	1.29	1.39	1.92
Range	169.50-220.50	12.01-18.61	12.66-17.43	18.57-26.93	22.79-31.15	31.00-42.00
Males - Sample Size	132	133	133	134	135	139
Mean	223.81	18.98	17.86	27.44	32	44.23
St. Dev.	8.68	1.37	1.04	1.94	1.63	2.25
Range	203.00-240.50	15.42-22.83	15.27-20.49	22.70-34.29	28.66-37.24	39.50-52.25
Combined – Sample Size	440	451	451	458	458	472
Mean	200.84	16.41	15.58	24.1	28.14	38.52
Standard Deviation	16.87	2.06	1.74	2.63	2.9	4.21
Range	169.50-240.50	12.01-22.83	12.66-20.49	18.57-34.29	22.79-37.24	31.00-52.52
	Left Femur Measurements					
	Bicondylar Length	50% AP Diameter*	50% ML Diameter*	Head Diameter	Articular Breadth	Bicondylar Breadth
Females - Sample Size	123	123	124	247	94	124
Mean	221.67	15.52	15.31	22.48	32.8	35.98
St. Dev.	8.68	0.90	0.89	0.91	1.49	1.81
Range	197.50-244.00	13.32-18.11	13.16-17.90	19.61-24.86	29.36-36.48	32.07-43.51
Males - Sample Size	76	76	76	124	65	73
Mean	261.08	19.18	18.36	26.83	39.55	43.47
St. Dev.	11.09	1.46	1.37	1.23	1.96	2.19
Range	234.75-290.00	16.42-22.81	16.07-23.67	23.46-29.74	35.59-44.79	38.78-49.11
Combined – Sample Size	199	199	200	371	159	197
Mean	236.72	16.92	16.47	23.94	35.56	38.76

Table 6 Continued.

	Left Femur Measurements					
	Bicondylar Length	50% AP Diameter*	50% ML Diameter*	Head Diameter	Articular Breadth	Bicondylar Breadth
Standard Deviation	21.48	2.11	1.84	2.3	3.74	4.12
Range	197.50-290.00	13.32-22.81	13.16-23.67	19.61-29.74	29.36-44.79	32.07-49.11
	Right Femur Measurements					
	Bicondylar Length	50% AP Diameter*	50% ML Diameter*	Head Diameter	Articular Breadth	Bicondylar Breadth
Females - Sample Size	222	222	221	235	194	236
Mean	224.14	15.58	15.43	22.59	33.49	36.59
St. Dev.	8.58	0.89	0.87	0.91	1.53	1.64
Range	198.25-250.00	12.90-18.14	13.28-18.18	20.09-25.22	29.42-38.14	32.37-41.03
Males - Sample Size	104	102	102	108	95	109
Mean	262.61	18.96	18.20	26.81	40.3	43.7
St. Dev.	10.68	1.21	1.06	1.38	1.94	1.98
Range	236.50-291.00	16.47-22.32	16.07-21.25	20.91-31.22	36.07-45.11	38.95-48.55
Combined – Sample Size	326	324	323	343	289	345
Mean	236.41	16.64	16.31	23.92	35.73	38.84
Standard Deviation	20.22	1.86	1.59	2.24	3.61	3.75
Range	198.25-291.00	12.90-22.32	13.28-21.25	20.09-31.22	29.42-45.11	32.37-48.55

All measurements are in mm.

* The 50% AP and ML diameter measurements were averaged for analyses, but their separate summary statistics are presented here.

Table 7 - Tamarin average intraobserver measurement error rates.

Measurement	Maximum Humerus Length	Maximum Radius Length	Bicondylar Femur Length	Maximum Tibia Length
Average Error	0.009	0.016	0.015	0.015

All error rates are from right side elements.

Table 8 - TBRI Baboon average intraobserver measurement error rates.

	Humerus Measurements					
	Maximum Length	50% AP Diameter*	50% ML Diameter*	Head Length	Distal Articular Breadth	Epicondylar Breadth
2009	0.145	0.584	1.301	1.013	0.820	1.111
2009-2011	0.091	0.481	0.607	1.155	0.881	1.054
2011	0.096	0.477	0.615	0.871	0.656	0.407
Overall	**0.100**	**0.490**	**0.692**	**0.915**	**0.696**	**0.548**
	Left Femur Measurements					
	Bicondylar Length	50% AP Diameter*	50% ML Diameter*	Head Diameter	Articular Breadth	Bicondylar Breadth
2009	0.204	0.547	0.294	0.315	0.154	0.261
2009-2011	0.074	0.371	0.234	0.872	0.398	0.462
2011	0.048	0.453	0.313	0.424	0.235	0.453
Overall	**0.114**	**0.454**	**0.275**	**0.466**	**0.284**	**0.394**
	Right Femur Measurements					
	Bicondylar Length	50% AP Diameter*	50% ML Diameter*	Head Diameter	Articular Breadth	Bicondylar Breadth
2009	0.748	0.487	0.465	0.683	0.261	0.775
2009-2011	0.074	0.579	0.372	0.415	0.566	0.469
2011	0.054	0.390	0.218	0.362	0.269	0.574
Overall	**0.071**	**0.414**	**0.242**	**0.374**	**0.305**	**0.567**

* The 50% AP and ML diameter measurements were averaged for analyses, but their separate intraobserver measurement errors are presented here.

Table 9 - Sample model for within-bone morphological integration analyses: Femur articulations and muscle attachment integrated.

	Bicondylar Length	50% Diameter Avg.	Head Diameter	Articular Breadth	Bicondylar Breadth
Bicondylar Length					
50% Diameter Avg.	0				
Head Diameter	0	0			
Articular Breadth	0	0	1		
Bicondylar Breadth	0	0	1	1	

Table 10 - Phenotypic variance/covariance matrix for the Tamarins.

	Humerus	Radius	Femur	Tibia
Humerus	**2.772** (0.284) 2.218-3.319			
Radius	**2.424** (0.280) 1.961-3.031	**3.126** (0.317) 2.426-3.618		
Femur	**2.749** (0.319) 2.197-3.452	**2.883** (0.335) 2.321-3.595	**4.530** (0.444) 3.614-5.333	
Tibia	**2.836** (0.347) 2.426-3.765	**3.640** (0.367) 2.595-3.995	**4.329** (0.447) 3.338-5.068	**5.167** (0.515) 4.269-6.272

Variance/covariance estimates are in bold, standard error of the estimate is in parentheses, and the 95% credibility interval for the estimate is below.
See Table 38 for statistically significant differences between limb segments.

Table 11 - Genetic variance/covariance matrix for the Tamarins.

	Humerus	Radius	Femur	Tibia
Humerus	**1.276** (0.359) 0.605-1.967			
Radius	**1.143** (0.360) 0.449-1.827	**1.282** (0.391) 0.620-2.143		
Femur	**1.164** (0.430) 0.483-2.129	**1.400** (0.445) 0.454-2.159	**2.284** (0.590) 0.951-3.213	
Tibia	**1.617** (0.473) 0.485-2.284	**1.467** (0.494) 0.593-2.473	**2.000** (0.617) 0.790-3.158	**2.431** (0.701) 1.184-3.876

Variance/covariance estimates are in bold, standard error of the estimate is in parentheses, and the 95% credibility interval for the estimate is below.
See Table 40 for statistically significant differences between limb segments.

Table 12 - Environmental variance/covariance matrix for the Tamarins.

	Humerus	Radius	Femur	Tibia
Humerus	**1.407** (0.302) 0.923-2.079			
Radius	**1.166** (0.302) 0.770-1.930	**1.609** (0.332) 1.096-2.378		
Femur	**1.537** (0.356) 0.839-2.192	**1.519** (0.371) 0.851-2.306	**2.181** (0.486) 1.406-3.291	
Tibia	**1.549** (0.391) 0.913-2.446	**1.730** (0.410) 0.995-2.589	**2.146** (0.508) 1.247-3.217	**2.548** (0.575) 1.552-3.773

Variance/covariance estimates are in bold, standard error of the estimate is in parentheses, and the 95% credibility interval for the estimate is below.

Table 13 - Phenotypic correlation matrix for the Tamarins.

	Humerus	Radius	Femur	Tibia
Humerus	**1**			
Radius	**0.861** (0.020) 0.816-0.891	**1**		
Femur	**0.788** (0.027) 0.743-0.847	**0.794** (0.027) 0.734-0.840	**1**	
Tibia	**0.812** (0.026) 0.753-0.853	**0.830** (0.023) 0.775-0.863	**0.874** (0.018) 0.824-0.894	**1**

Variance/covariance estimates are in bold, standard error of the estimate is in parentheses, and the 95% credibility interval for the estimate is below.
See Table 39 for statistically significant differences between correlation coefficients for pairs of limb segments.

Table 14 - Genetic correlation matrix for the Tamarins.

	Humerus	Radius	Femur	Tibia
Humerus	**0.459** (0.107) 0.248-0.663			
Radius	**0.855** (0.058) 0.721-0.928	**0.445** (0.106) 0.235-0.644		
Femur	**0.807** (0.083) 0.599-0.895	**0.797** (0.085) 0.593-0.889	**0.506** (0.109) 0.275-0.704	
Tibia	**0.812** (0.075) 0.638-0.907	**0.840** (0.071) 0.669-0.921	**0.874** (0.055) 0.733-0.923	**0.527** (0.110) 0.276-0.699

Variance/covariance estimates are in bold, standard error of the estimate is in parentheses, and the 95% credibility interval for the estimate is below.
See Table 41 for statistically significant differences between correlation coefficients for pairs of limb segments.

Table 15 - Environmental correlation matrix for the Tamarins.

	Humerus	Radius	Femur	Tibia
Humerus	**0.540** (0.107) 0.337-0.752			
Radius	**0.883** (0.034) 0.791-0.919	**0.555** (0.106) 0.357-0.765		
Femur	**0.798** (0.049) 0.701-0.885	**0.801** (0.050) 0.698-0.885	**0.494** (0.109) 0.296-0.725	
Tibia	**0.831** (0.047) 0.713-0.900	**0.845** (0.041) 0.750-0.906	**0.881** (0.033) 0.804-0.929	**0.473** (0.110) 0.301-0.724

Variance/covariance estimates are in bold, standard error of the estimate is in parentheses, and the 95% credibility interval for the estimate is below.

Table 16 - Heritability, evolvability, and conditional evolvability estimates for the Tamarins.

	Humerus	Radius	Femur	Tibia
Trait Mean	50.97	46.13	65.65	66.52
Phenotypic Variance	2.772	3.126	4.530	5.167
Additive Genetic variance	1.276	1.282	2.284	2.431
Heritability (h^2)	0.459	0.445	0.506	0.527
h^2 95% Credibility Interval	0.248-0.663	0.235-0.644	0.275-0.704	0.276-0.699
Evolvability (*e*)	0.000519	0.000605	0.000527	0.000616
e 95% Credibility Interval	0.000240- 0.000757	0.000299- 0.000101	0.000219- 0.000743	0.000260- 0.000871
Conditional Evolvability (*c*)	0.000101	0.000129	0.000108	0.000120
c 95% Credibility Interval	0.000071- 0.000150	0.000091- 0.000195	0.000076- 0.000157	0.000082- 0.000161
Integration (*i*)	0.794	0.773	0.785	0.832
i 95% Credibility Interval	0.594-0.888	0.612-0.889	0.591-0.883	0.644-0.898

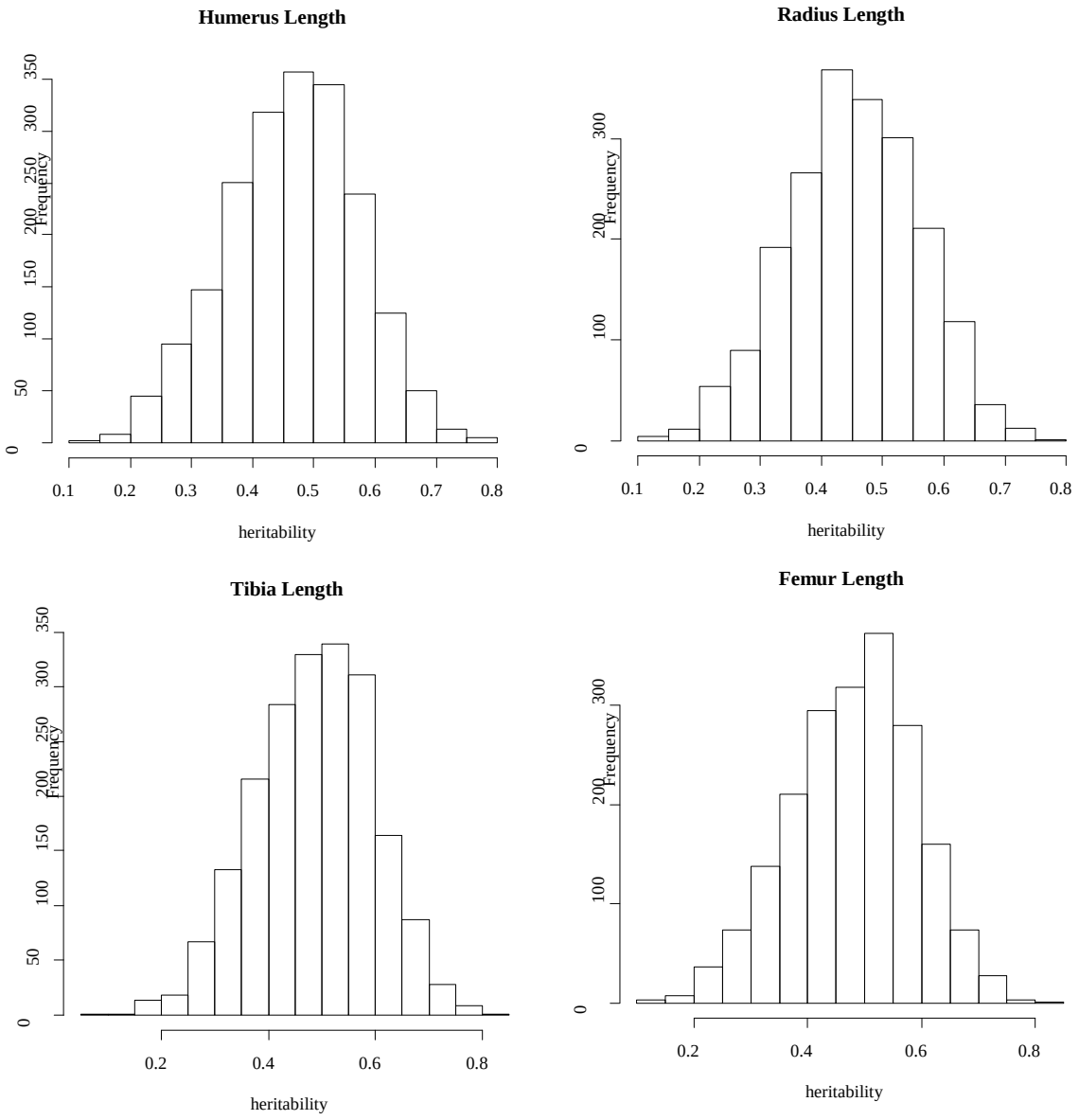

Figure 1 - Posterior distributions of heritability estimates for the Tamarin limb segments.

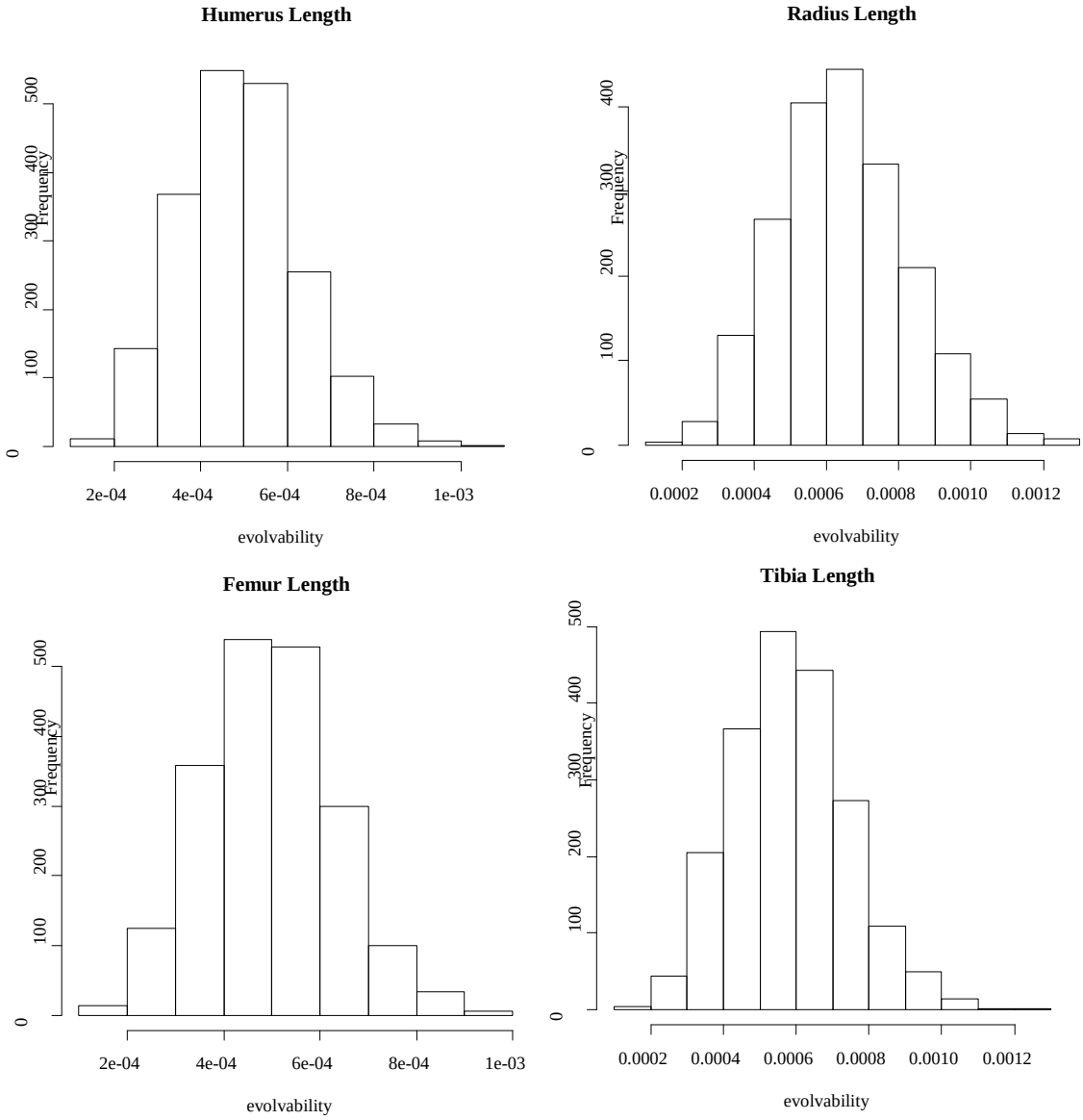

Figure 2 - Posterior distributions of evolvability estimates for the Tamarin limb segments.

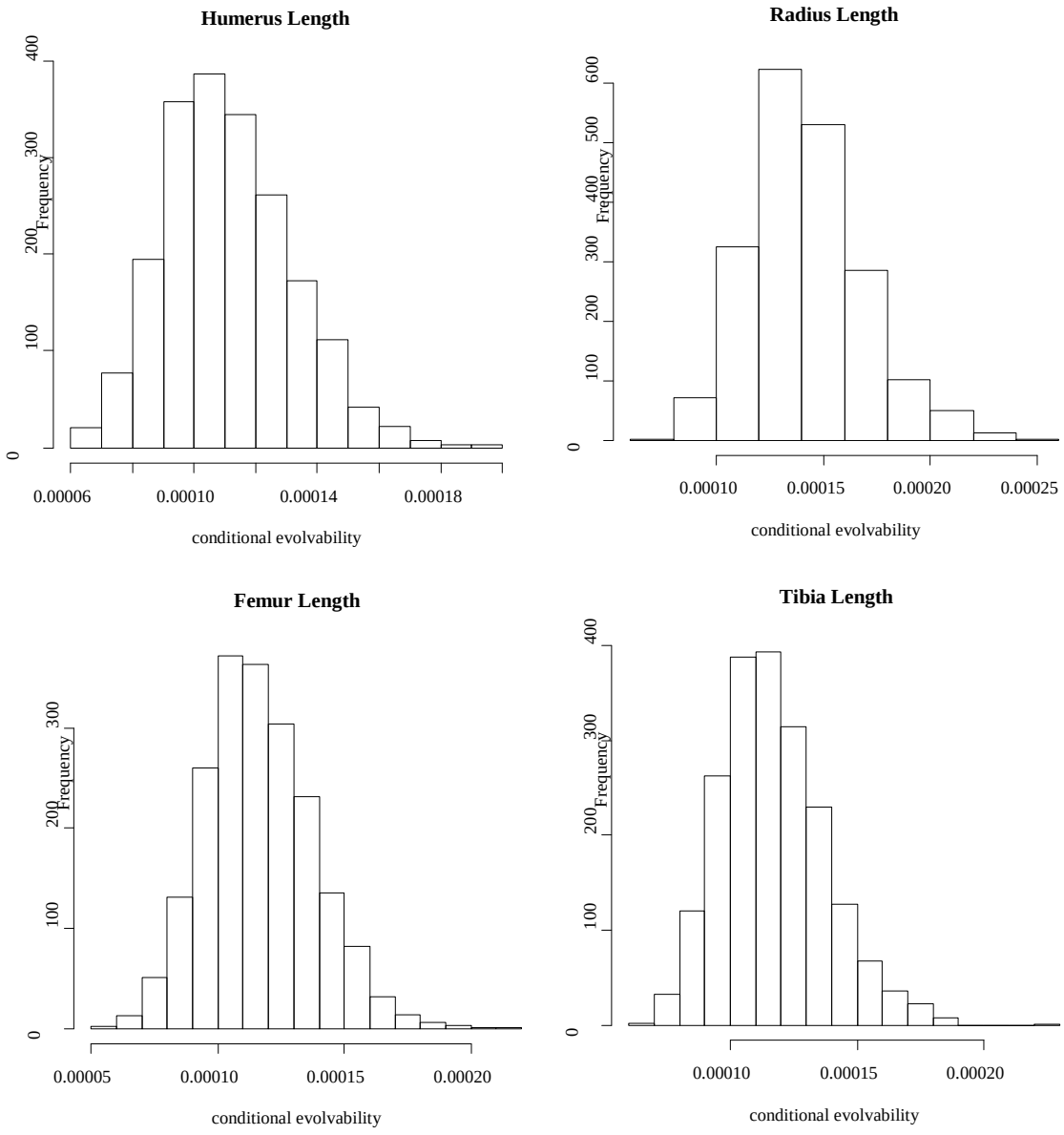

Figure 3 - Posterior distributions of conditional evolvability estimates for the Tamarin limb segments.

Table 17 - Phenotypic variance/covariance matrix for the Sukhumi Baboons.

	Arm	Forearm	Thigh	Leg
Arm	**113.738** (13.128) 92.704-141.587			
Forearm	**72.879** (10.422) 52.849-93.347	**101.940** (11.345) 85.144-127.935		
Thigh	**81.991** (13.736) 53.222-106.743	**82.828** (12.712) 57.652-106.501	**158.179** (20.358) 137.044-214.480	
Leg	**52.665** (8.630) 35.574-68.575	**56.854** (8.163) 40.916-72.276	**68.517** (10.986) 50.497-91.961	**66.366** (8.151) 54.567-85.464

Variance/covariance estimates are in bold, standard error of the estimate is in parentheses, and the 95% credibility interval for the estimate is below.
See Table 38 for statistically significant differences between limb segments.

Table 18 - Genetic variance/covariance matrix for the Sukhumi Baboons.

	Arm	Forearm	Thigh	Leg
Arm	**57.311** (17.034) 31.686-96.309			
Forearm	**38.216** (14.449) 14.307-69.412	**54.029** (14.726) 33.184-88.963		
Thigh	**46.666** (18.094) 11.538-83.656	**55.855** (17.219) 15.243-82.957	**102.449** (24.873) 46.212-140.287	
Leg	**30.397** (11.468) 8.271-52.682	**34.638** (10.966) 14.242-56.121	**41.515** (14.279) 14.587-68.763	**39.868** (9.728) 24.170-60.645

Variance/covariance estimates are in bold, standard error of the estimate is in parentheses, and the 95% credibility interval for the estimate is below.
See Table 40 for statistically significant differences between limb segments.

Table 19 - Environmental variance/covariance matrix for the Sukhumi Baboons.

	Arm	Forearm	Thigh	Leg
Arm	**54.608** (12.638) 32.034-81.826			
Forearm	**29.688** (10.330) 12.602-51.643	**39.875** (10.212) 25.667-65.423		
Thigh	**36.817** (13.476) 13.561-65.173	**31.205** (12.328) 8.980-56.216	**70.099** (18.377) 44.070-113.431	
Leg	**18.690** (8.205) 6.173-37.174	**22.278** (7.750) 8.000-37.426	**27.499** (10.242) 8.832-47.992	**28.191** (6.917) 16.085-42.600

Variance/covariance estimates are in bold, standard error of the estimate is in parentheses, and the 95% credibility interval for the estimate is below.

Table 20 - Phenotypic correlation matrix for the Sukhumi Baboons.

	Arm	Forearm	Thigh	Leg
Arm	**1**			
Forearm	**0.638** (0.045) 0.555-0.728	**1**		
Thigh	**0.580** (0.057) 0.457-0.677	**0.634** (0.050) 0.508-0.706	**1**	
Leg	**0.580** (0.054) 0.467-0.680	**0.650** (0.044) 0.576-0.744	**0.659** (0.048) 0.547-0.737	**1**

Variance/covariance estimates are in bold, standard error of the estimate is in parentheses, and the 95% credibility interval for the estimate is below.
See Table 39 for statistically significant differences between correlation coefficients for pairs of limb segments.

Table 21 - Genetic correlation matrix for the Sukhumi Baboons.

	Arm	Forearm	Thigh	Leg
Arm	**0.479** (0.112) 0.310-0.736			
Forearm	**0.710** (0.101) 0.442-0.811	**0.600** (0.104) 0.366-0.765		
Thigh	**0.634** (0.128) 0.324-0.787	**0.661** (0.104) 0.421-0.807	**0.552** (0.108) 0.322-0.734	
Leg	**0.627** (0.114) 0.353-0.784	**0.728** (0.085) 0.516-0.828	**0.725** (0.095) 0.455-0.812	**0.602** (0.100) 0.398-0.777

Variance/covariance estimates are in bold, standard error of the estimate is in parentheses, and the 95% credibility interval for the estimate is below.
See Table 41 for statistically significant differences between correlation coefficients for pairs of limb segments.

Table 22 - Environmental correlation matrix for the Sukhumi Baboons.

	Arm	Forearm	Thigh	Leg
Arm	**0.521** (0.112) 0.264-0.690			
Forearm	**0.643** (0.099) 0.420-0.782	**0.400** (0.104) 0.235-0.634		
Thigh	**0.608** (0.115) 0.347-0.774	**0.581** (0.111) 0.352-0.761	**0.448** (0.108) 0.266-0.678	
Leg	**0.543** (0.118) 0.287-0.723	**0.645** (0.102) 0.393-0.773	**0.669** (0.106) 0.378-0.778	**0.398** (0.100) 0.223-0.602

Variance/covariance estimates are in bold, standard error of the estimate is in parentheses, and the 95% credibility interval for the estimate is below.

Table 23 - Heritability, evolvability, and conditional evolvability for the Sukhumi Baboons.

	Arm	Forearm	Thigh	Leg
Trait Mean	183.32	213.48	226.12	182.20
Phenotypic Variance	113.738	101.940	158.179	66.366
Additive Genetic variance	57.311	54.029	102.449	39.868
heritability (h^2)	0.479	0.600	0.552	0.602
h^2 95% Credibility Interval	0.310-0.736	0.366-0.765	0.322-0.734	0.398-0.777
Evolvability (*e*)	0.001330	0.001000	0.001628	0.001000
e 95% Credibility Interval	0.000781-0.002395	0.000596-0.001612	0.000785-0.002327	0.000581-0.001505
Conditional Evolvability (*c*)	0.000715	0.000374	0.000639	0.000390
c 95% Credibility Interval	0.000466-0.001013	0.000288-0.000553	0.000462-0.000961	0.000295-0.000547
Integration (*i*)	0.515	0.646	0.571	0.625
i 95% Credibility Interval	0.252-0.714	0.394-0.779	0.301-0.749	0.376-0.766

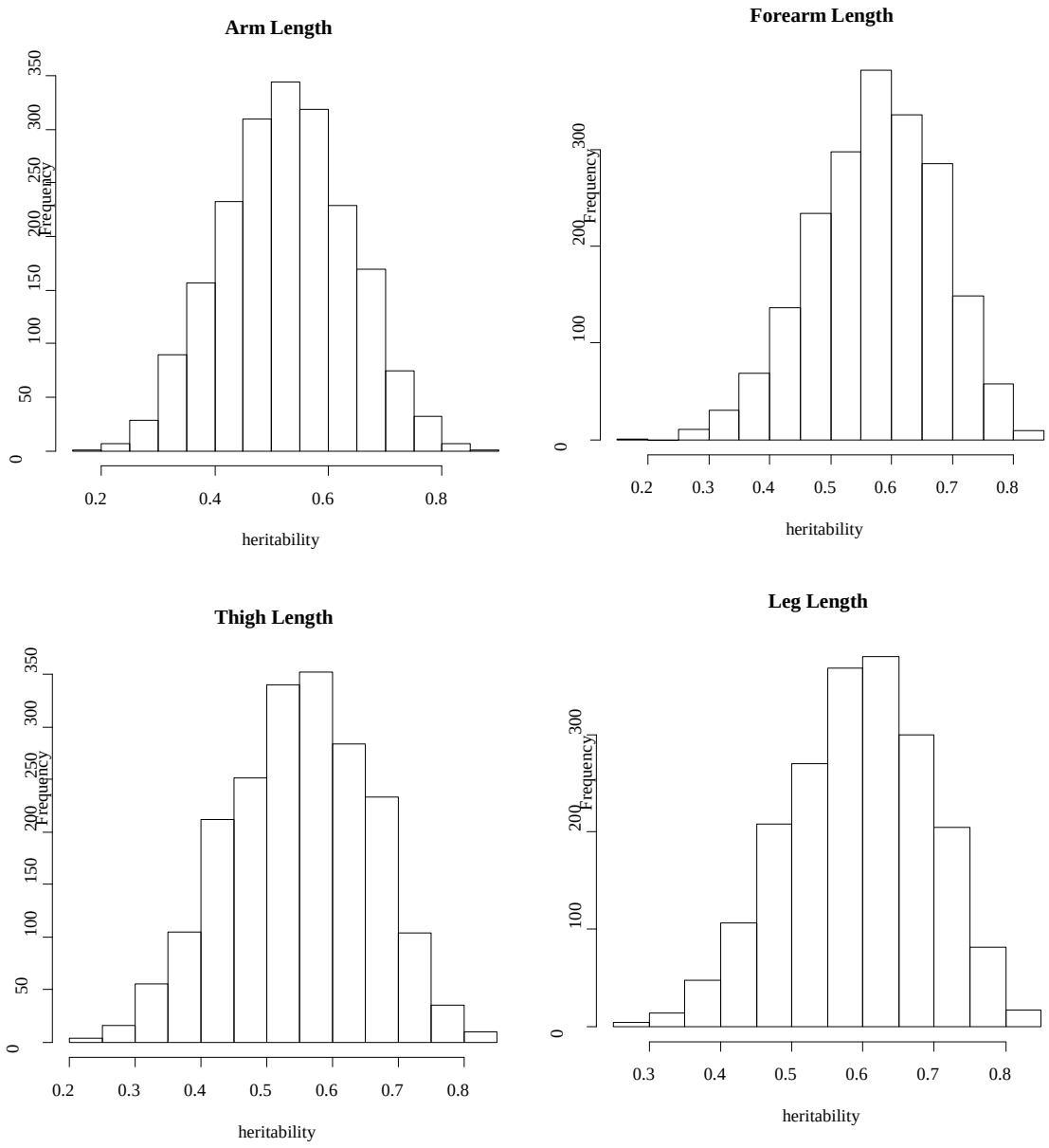

Figure 4 - Posterior distributions of heritability estimates for the Sukhumi Baboon limb segments.

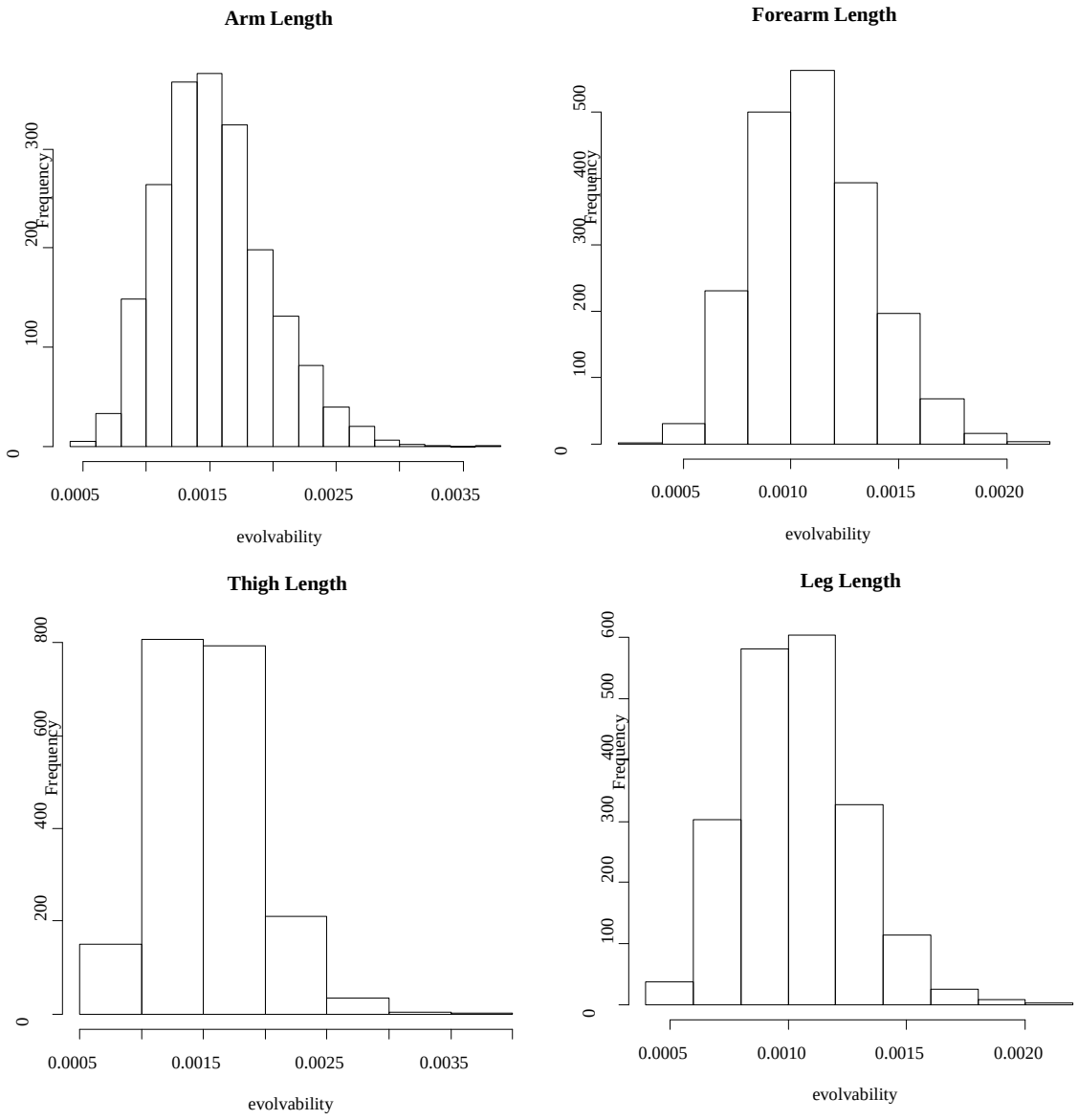

Figure 5 - Posterior distributions of evolvability estimates for the Sukhumi Baboon limb segments.

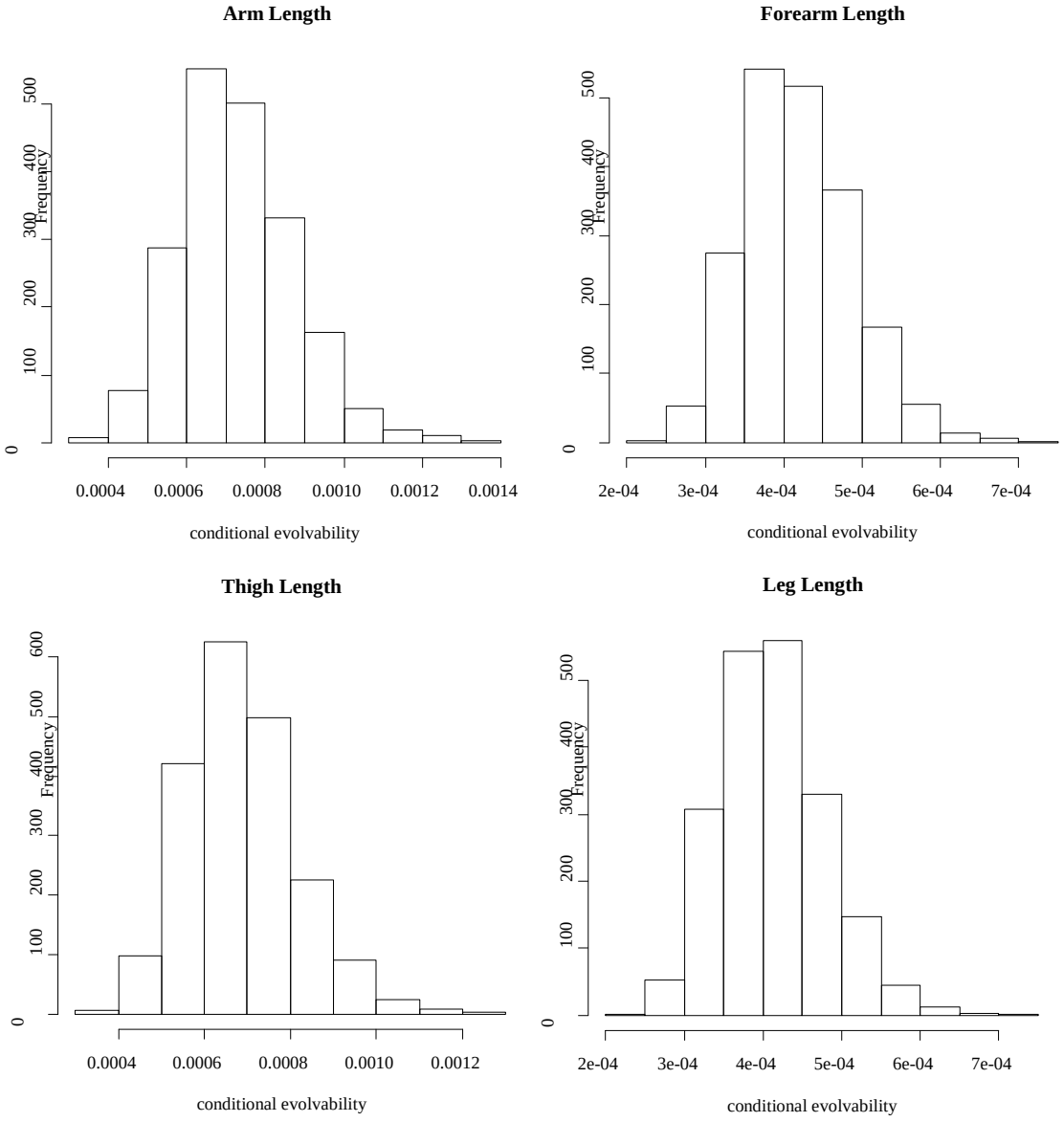

Figure 6 - Posterior distributions of conditional evolvability estimates for the Sukhumi Baboon limb segments.

Table 24 - Phenotypic variance/covariance matrix for the Mennonites.

	Arm	Forearm	Thigh	Leg
Arm	**244.357** (19.046) 207.050-281.479			
Forearm	61.188 (13.009) 33.347-83.602	**211.721** (16.175) 184.766-248.217		
Thigh	**210.123** (27.919) 149.515-257.525	**119.694** (24.140) 66.377-158.842	**821.957** (65.395) 706.015-953.125	
Leg	**135.630** (17.119) 101.954-170.187	**126.286** (15.367) 99.319-158.470	**177.759** (30.248) 125.219-245.368	**309.497** (24.465) 274.253-370.108

Variance/covariance estimates are in bold, standard error of the estimate is in parentheses, and the 95% credibility interval for the estimate is below.
See Table 38 for statistically significant differences between limb segments.

Table 25 - Genetic variance/covariance matrix for the Mennonites.

	Arm	Forearm	Thigh	Leg
Arm	**162.104** (24.749) 110.850-205.327			
Forearm	**35.414** (17.089) 7.927-74.002	**106.778** (22.432) 60.630-145.759		
Thigh	**184.706** (35.266) 133.443-270.165	**107.161** (33.072) 41.304-169.355	**541.050** (87.728) 421.342-753.439	
Leg	**77.855** (23.027) 46.139-136.917	**65.342** (21.672) 29.717-1113.290	**165.219** (41.841) 97.755-264.115	**154.188** (33.645) 100.195-229.781

Variance/covariance estimates are in bold, standard error of the estimate is in parentheses, and the 95% credibility interval for the estimate is below.
See Table 40 for statistically significant differences between limb segments.

Table 26 - Environmental variance/covariance matrix for the Mennonites.

	Arm	Forearm	Thigh	Leg
Arm	**81.671** (16.867) 52.481-118.318			
Forearm	**15.895** (13.019) -8.232-42.453	**102.271** (18.872) 77.780-150.753		
Thigh	**-5.805** (22.110) -39.926-45.743	**-5.349** (24.268) -40.280-54.336	**248.802** (55.422) 149.063-355.872	
Leg	**46.347** (17.102) 13.240-79.817	**47.403** (18.046) 22.522-93.373	**20.487** (28.609) -45.392-67.725	**152.834** (26.518) 106.001-209.952

Variance/covariance estimates are in bold, standard error of the estimate is in parentheses, and the 95% credibility interval for the estimate is below.

Table 27 - Phenotypic correlation matrix for the Mennonites.

	Arm	Forearm	Thigh	Leg
Arm	**1**			
Forearm	**0.249** (0.051) 0.157-0.352	**1**		
Thigh	**0.482** (0.045) 0.366-0.539	**0.261** (0.051) 0.166-0.360	**1**	
Leg	**0.490** (0.043) 0.390-0.559	**0.494** (0.041) 0.403-0.561	**0.344** (0.048) 0.261-0.447	**1**

Variance/covariance estimates are in bold, standard error of the estimate is in parentheses, and the 95% credibility interval for the estimate is below.
See Table 39 for statistically significant differences between correlation coefficients for pairs of limb segments.

Table 28 - Genetic correlation matrix for the Mennonites.

	Arm	Forearm	Thigh	Leg
Arm	**0.665** (0.072) 0.517-0.796			
Forearm	**0.376** (0.118) 0.100-0.553	**0.475** (0.088) 0.311-0.653		
Thigh	**0.694** (0.073) 0.513-0.788	**0.457** (0.109) 0.219-0.636	**0.716** (0.072) 0.560-0.828	
Leg	**0.592** (0.090) 0.360-0.707	**0.567** (0.105) 0.320-0.715	**0.560** (0.091) 0.364-0.740	**0.480** (0.085) 0.347-0.684

Variance/covariance estimates are in bold, standard error of the estimate is in parentheses, and the 95% credibility interval for the estimate is below.
See Table 41 for statistically significant differences between correlation coefficients for pairs of limb segments.

Table 29 - Environmental correlation matrix for the Mennonites.

	Arm	Forearm	Thigh	Leg
Arm	**0.335** (0.072) 0.204-0.483			
Forearm	**0.179** (0.128) -0.078-0.416	**0.525** (0.088) 0.347-0.689		
Thigh	**0.068** (0.156) -0.289-0.309	**-0.037** (0.147) -0.268-0.306	**0.284** (0.072) 0.172-0.440	
Leg	**0.453** (0.109) 0.177-0.600	**0.489** (0.098) 0.241-0.614	**0.084** (0.142) -0.239-0.313	**0.520** (0.085) 0.316-0.653

Variance/covariance estimates are in bold, standard error of the estimate is in parentheses, and the 95% credibility interval for the estimate is below.

Table 30 - Heritability, evolvability, and conditional evolvability for the Mennonites.

	Arm	Forearm	Thigh	Leg
Trait Mean	321.30	254.50	473.84	402.42
Phenotypic Variance	244.357	211.721	821.957	309.497
Additive Genetic variance	162.104	106.778	541.050	154.188
heritability (h^2)	0.665	0.475	0.716	0.480
h^2 95% Credibility Interval	0.517-0.796	0.311-0.653	0.560-0.828	0.347-0.684
Evolvability (*e*)	0.001463	0.001529	0.002263	0.000859
e 95% Credibility Interval	0.001018-0.001859	0.000850-0.002049	0.001787-0.003197	0.000544-0.001273
Conditional Evolvability (*c*)	0.000711	0.000903	0.001234	0.000443
c 95% Credibility Interval	0.000469-0.001016	0.000548-0.001334	0.000668-0.001656	0.000282-0.000659
Integration (*i*)	0.513	0.350	0.562	0.505
i 95% Credibility Interval	0.343-0.669	0.158-0.559	0.350-0.719	0.302-0.661

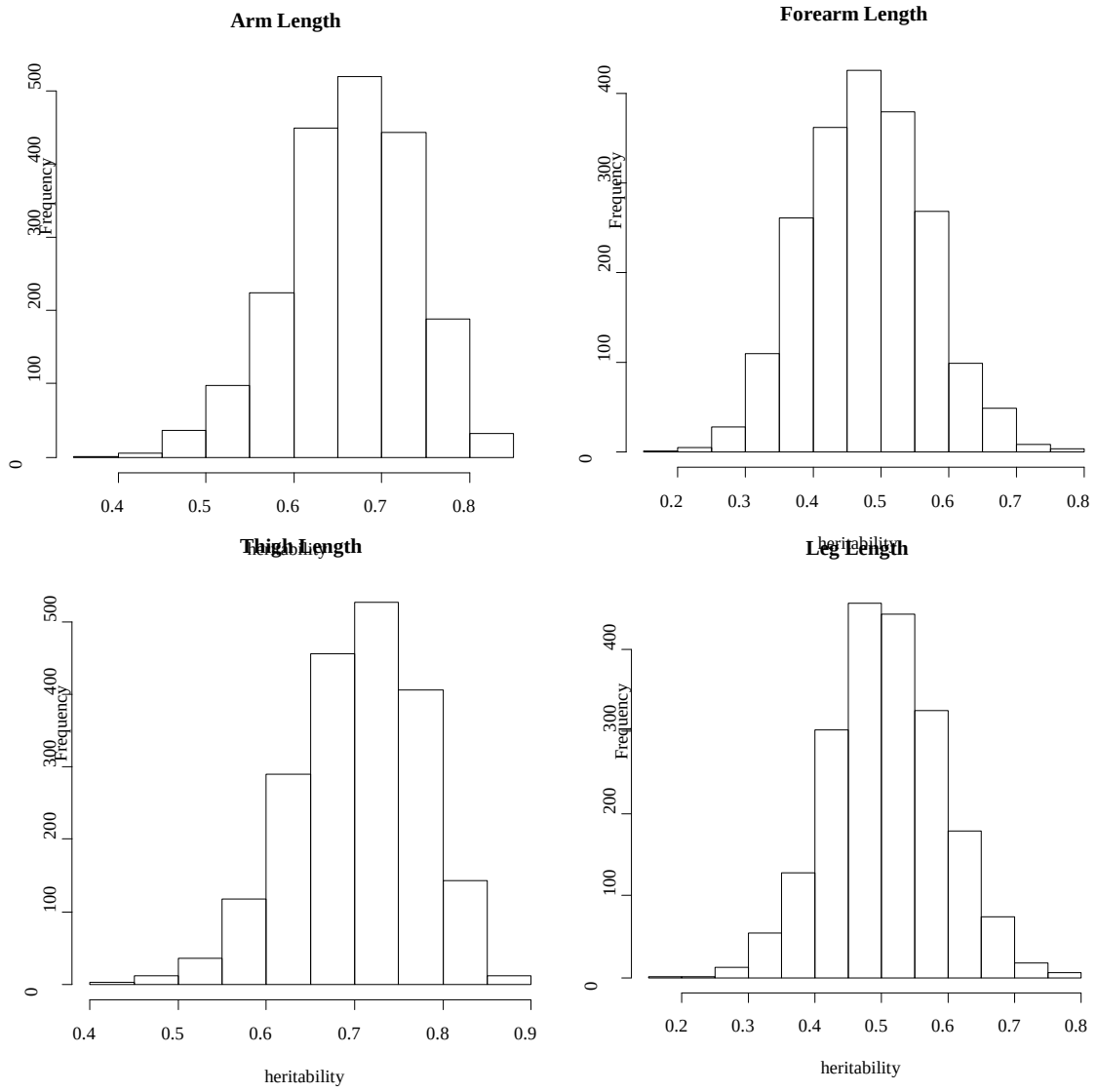

Figure 7 - Posterior distribution of heritability estimates for the Mennonite limb segments.

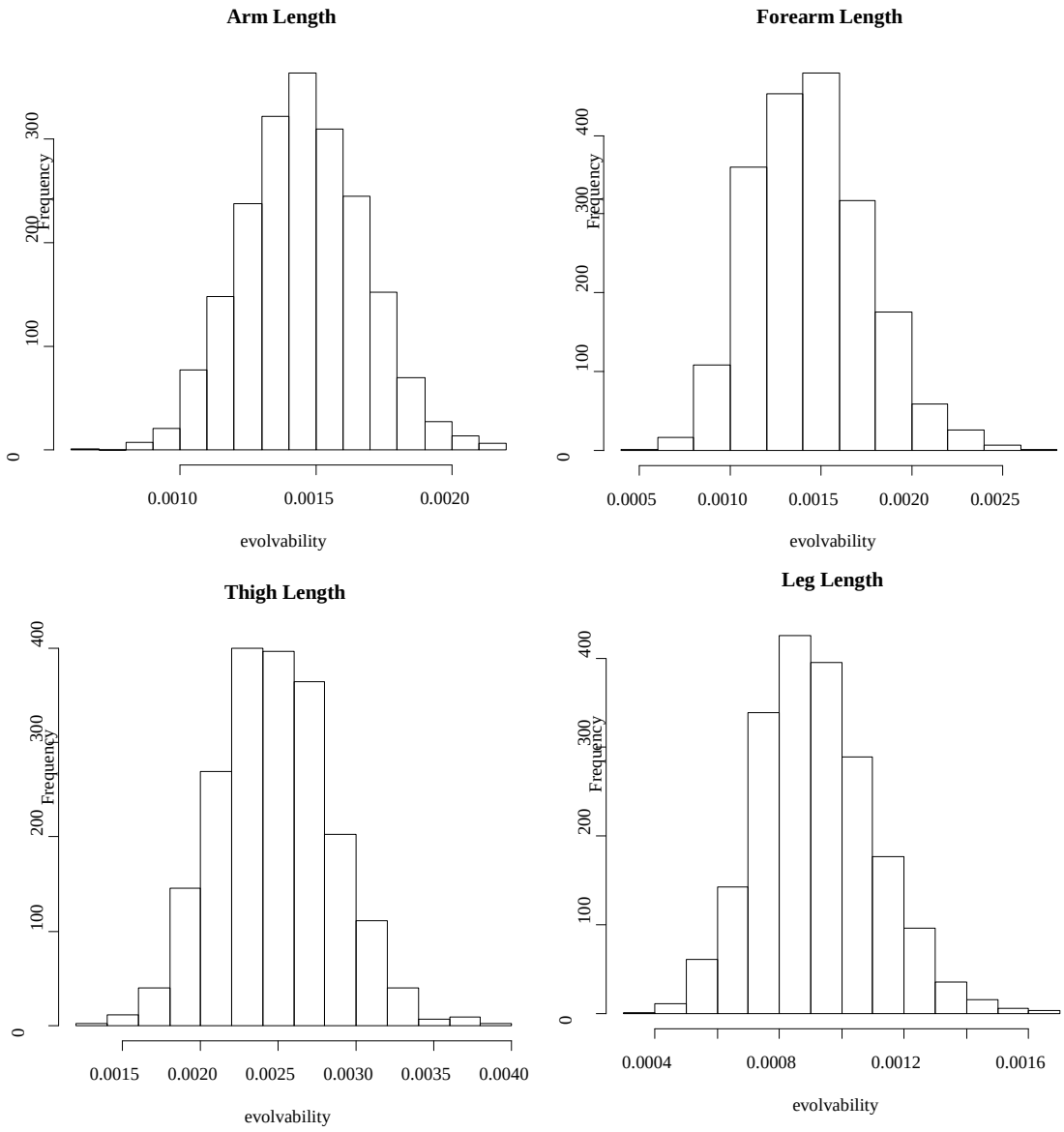

Figure 8 - Posterior distributions of evolvability estimates for the Mennonite limb segments.

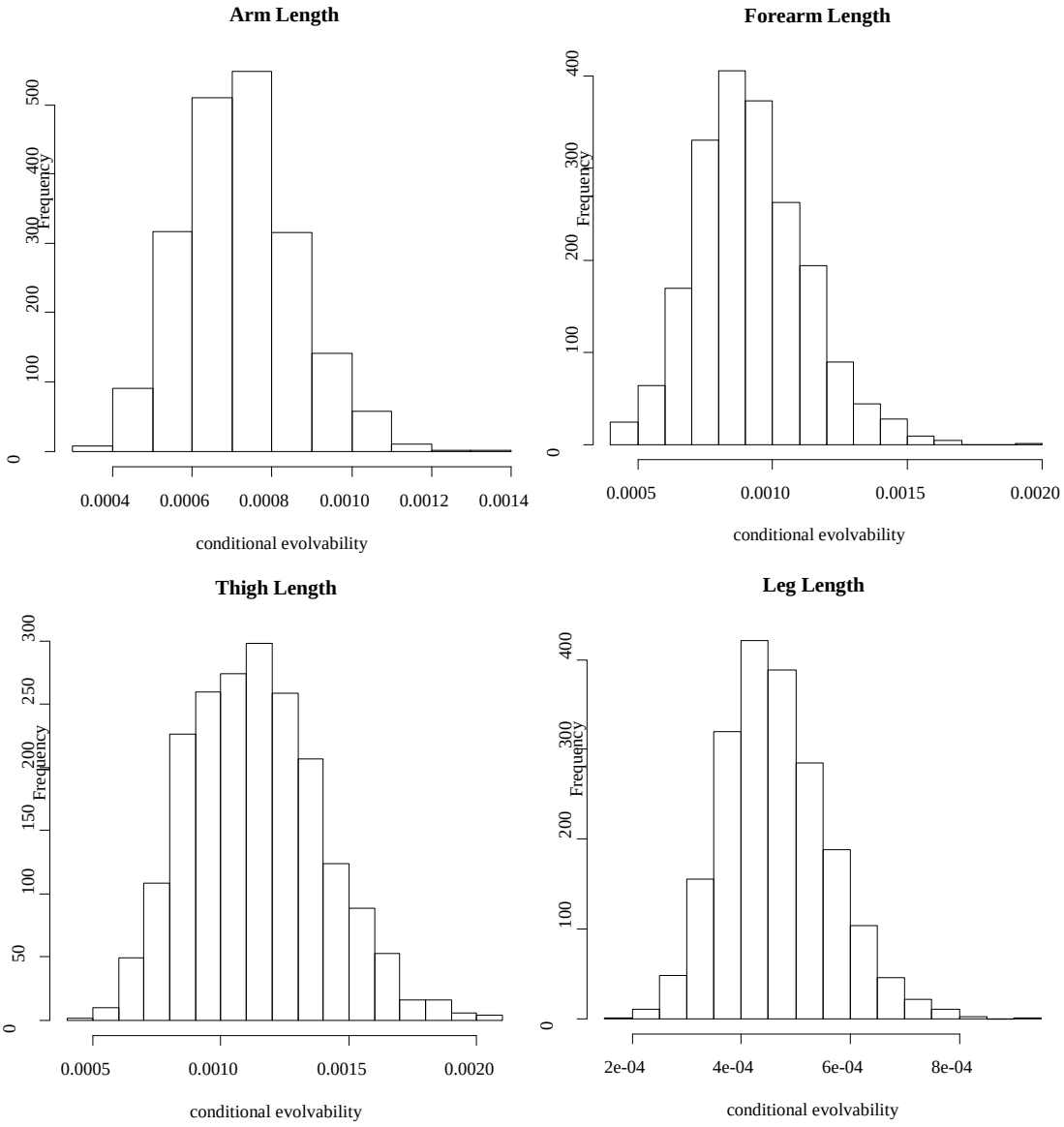

Figure 9 - Posterior distribution of conditional evolvability estimates for the Mennonite limb segments.

Table 31 - Phenotypic variance/covariance matrix for the TBRI Baboons.

	Humerus	Femur
Humerus	**66.546** (4.998) 58.893-77.984	
Femur	**64.592** (5.522) 55.208-76.722	**99.099** (5.522) 87.000-115.100

Variance/covariance estimates are in bold, standard error of the estimate is in parentheses, and the 95% credibility interval for the estimate is below.
See Table 38 for statistically significant differences between limb segments.

Table 32 - Genetic variance/covariance matrix for the TBRI Baboons.

	Humerus	Femur
Humerus	**39.818** (7.491) 25.311-55.056	
Femur	**34.761** (8.621) 23.608-57.693	**58.524** (10.892) 41.528-83.660

Variance/covariance estimates are in bold, standard error of the estimate is in parentheses, and the 95% credibility interval for the estimate is below.
See Table 40 for statistically significant differences between limb segments.

Table 33 - Environmental variance/covariance matrix for the TBRI Baboons.

	Humerus	Femur
Humerus	**26.709** (5.419) 17.786-38.327	
Femur	**24.940** (6.133) 12.670-35.863	**33.406** (7.799) 23.161-53.016

Variance/covariance estimates are in bold, standard error of the estimate is in parentheses, and the 95% credibility interval for the estimate is below.

Table 34 - Phenotypic correlation matrix for the TBRI Baboons.

	Humerus	Femur
Humerus	**1**	
Femur	**0.793** (0.020) 0.751-0.828	**1**

Variance/covariance estimates are in bold, standard error of the estimate is in parentheses, and the 95% credibility interval for the estimate is below.

Table 35 - Genetic correlation matrix for the TBRI Baboons.

	Humerus	Femur
Humerus	**0.595** (0.086) 0.423-0.758	
Femur	**0.827** (0.042) 0.725-0.886	**0.649** (0.083) 0.467-0.785

Variance/covariance estimates are in bold, standard error of the estimate is in parentheses, and the 95% credibility interval for the estimate is below.

Table 36 - Environmental correlation matrix for the TBRI Baboons.

	Humerus	Femur
Humerus	**0.405** (0.086) 0.242-0.577	
Femur	**0.770** (0.057) 0.640-0.851	**0.351** (0.083) 0.215-0.533

Variance/covariance estimates are in bold, standard error of the estimate is in parentheses, and the 95% credibility interval for the estimate is below.

Table 37 - Heritability, evolvability, and conditional evolvability for the TBRI Baboons.

	Humerus	Femur
Trait Mean	200.84	236.52
Phenotypic Variance	66.546	99.099
Additive Genetic variance	39.818	58.524
heritability (h^2)	0.595	0.649
h^2 95% Credibility Interval	0.423-0.758	0.467-0.785
Evolvability (*e*)	0.001064	0.001260
e 95% Credibility Interval	0.000693-0.001499	0.000822-0.001668
Conditional Evolvability (*c*)	0.000359	0.000410
c 95% Credibility Interval	0.000270-0.000461	0.000314-0.000525
Integration (*i*)	0.684	0.684
i 95% Credibility Interval	0.526-0.785	0.526-0.785

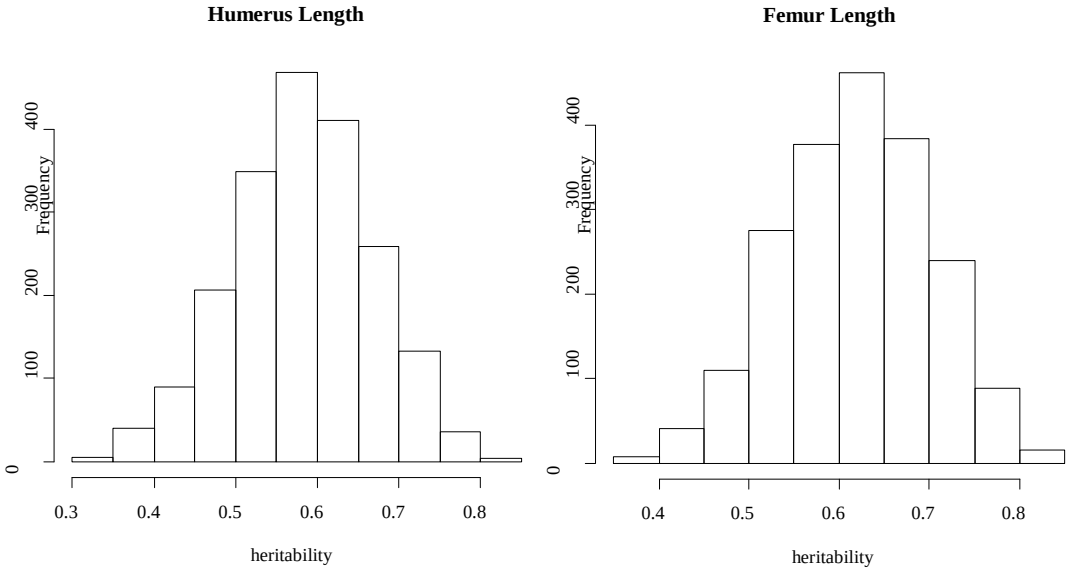

Figure 10 - Posterior distribution of heritability estimates for the TBRI Baboons.

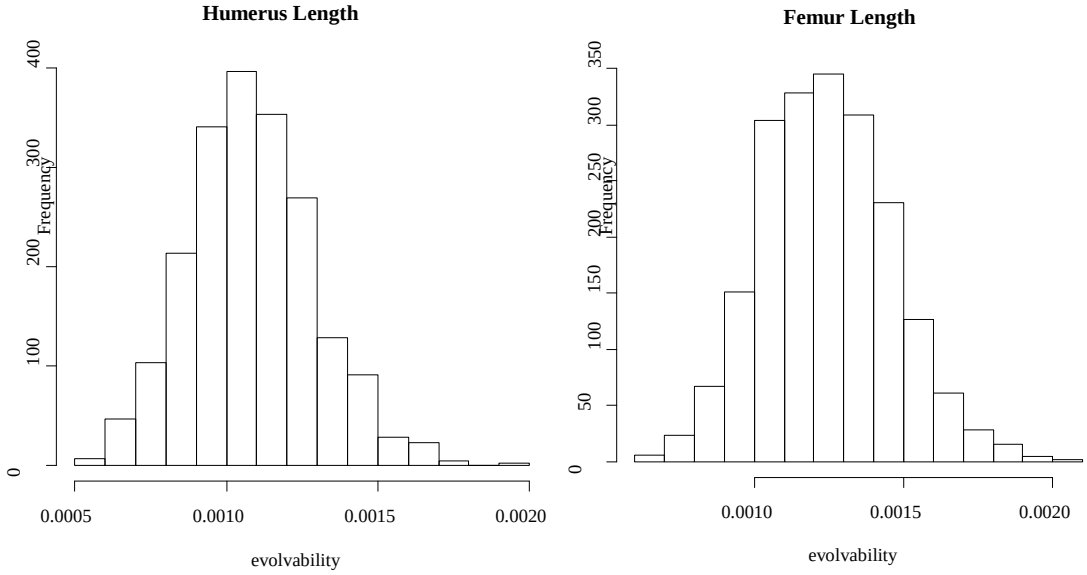

Figure 11 - Posterior distribution of evolvability estimates for the TBRI Baboons.

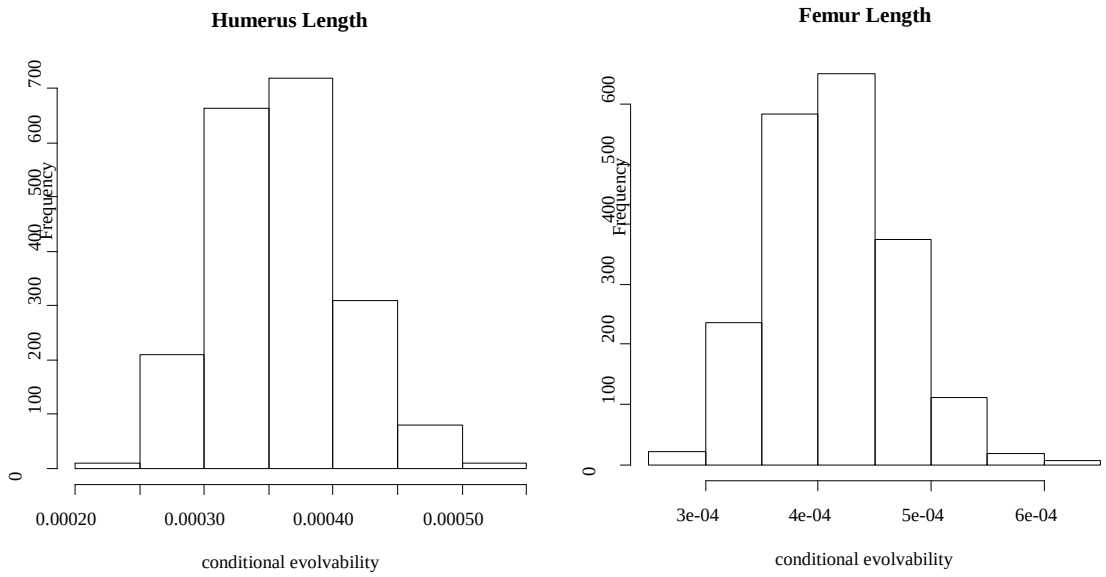

Figure 12 - Posterior distributions of conditional evolvability estimates for TBRI Baboons.

Table 38 - Intra-sample comparisons of phenotypic variance.

		Tamarins				Sukhumi Baboons				Mennonites				TBRI Baboons	
		H	R	F	T	H	R	F	T	H	R	F	T	H	F
Tamarin	H														
	R														
	F	X	X												
	T	X	X	X											
Sukhumi Baboons	H														
	R														
	F					X	X								
	T					X	X	X							
Mennonites	H														
	R														
	F									X	X				
	T									X	X	X			
TBRI	H														
	F													X	

An X indicates that the posterior distribution produced when comparing these two limb segments did not cross zero, meaning that the phenotypic variance estimates for these limb segments are statistically different. For ease of interpretation, all four samples use the abbreviations of H (humerus), R (radius), F (femur), and T (tibia) despite the fact that these limb segments are called the arm, forearm, thigh, and leg for the Sukhumi Baboons and Mennonites throughout the text. Gray cells indicate comparisons that are 1) redundant, 2) self-comparisons (e.g., H and H in Intra-Sample Comparisons), 3) not done (e.g., comparing the humerus of one sample to the tibia of another sample), or 4) not possible (because the TBRI Baboon sample is limited to two limb segments).

Table 39 - Intra- and inter-sample comparisons of phenotypic correlation.

		Tamarins						Sukhumi Baboons						Mennonites						TBRI
		HR	HF	HT	RF	RT	FT	HR	HF	HT	RF	RT	FT	HR	HF	HT	RF	RT	FT	HF
Tamarin	HR																			
	HF	X																		
	HT	X																		
	RF	X																		
	RT																			
	FT		X	X	X															
Sukhumi Baboons	HR	X																		
	HF		X																	
	HT			X																
	RF				X															
	RT					X														
	FT						X													
Mennonites	HR	X						X												
	HF		X											X						
	HT			X										X						
	RF				X						X				X	X				
	RT					X						X		X			X			
	FT						X						X		X	X		X		
TBRI	HF								X						X					

An X indicates that the posterior distribution produced when comparing these two correlations did not cross zero, meaning that the phenotypic correlation estimates are statistically different. For ease of interpretation, all four samples use the abbreviations of H (humerus), R (radius), F (femur), and T (tibia) despite the fact that these limb segments are called the arm, forearm, thigh, and leg for the Sukhumi Baboons and Mennonites throughout the text. Gray cells indicate comparisons that are 1) redundant, 2) self-comparisons (e.g., H and H in Intra-Sample Comparisons), 3) not done (e.g., comparing the humerus of one sample to the tibia of another sample), or 4) not possible (because the TBRI Baboon sample is limited to two limb segments).

Table 40 - Intra- and inter-sample comparisons of genetic variance.

		Tamarins				Sukhumi Baboons				Mennonites				TBRI Baboons	
		H	R	F	T	H	R	F	T	H	R	F	T	H	F
Tamarin	H														
	R														
	F	X	X												
	T	X	X												
Sukhumi Baboons	H														
	R														
	F														
	T							X							
Mennonites	H														
	R									X					
	F									X	X				
	T											X			
TBRI	H														
	F													X	

An X indicates that the posterior distribution produced when comparing these two limb segments did not cross zero, meaning that the genetic variance estimates for these limb segments are statistically different. Intra-sample comparisons use values from the VCV matrix, while inter-sample comparisons use values from the correlation matrix. For ease of interpretation, all four samples use the abbreviations of H (humerus), R (radius), F (femur), and T (tibia) despite the fact that these limb segments are called the arm, forearm, thigh, and leg for the Sukhumi Baboons and Mennonites throughout the text. Gray cells indicate comparisons that are 1) redundant, 2) self-comparisons (e.g., H and H in Intra-Sample Comparisons), 3) not done (e.g., comparing the humerus of one sample to the tibia of another sample), or 4) not possible (because the TBRI Baboon sample is limited to two limb segments).

Table 41 - Intra- and inter-sample comparisons of genetic correlation.

		Tamarins						Sukhumi Baboons						Mennonites						TBRI
		HR	HF	HT	RF	RT	FT	HR	HF	HT	RF	RT	FT	HR	HF	HT	RF	RT	FT	HF
Tamarin	HR																			
	HF																			
	HT																			
	RF																			
	RT																			
	FT																			
Sukhumi Baboons	HR																			
	HF																			
	HT																			
	RF																			
	RT																			
	FT																			
Mennonites	HR	X						X												
	HF													X						
	HT			X										X						
	RF				X															
	RT					X														
	FT						X													
TBRI	HF								X											

An X indicates that the posterior distribution produced when comparing these two correlations did not cross zero, meaning that the genetic correlation estimates are statistically different. For ease of interpretation, all four samples use the abbreviations of H (humerus), R (radius), F (femur), and T (tibia) despite the fact that these limb segments are called the arm, forearm, thigh, and leg for the Sukhumi Baboons and Mennonites throughout the text. Gray cells indicate comparisons that are 1) redundant, 2) self-comparisons (e.g., H and H in Intra-Sample Comparisons), 3) not done (e.g., comparing the humerus of one sample to the tibia of another sample), or 4) not possible (because the TBRI Baboon sample is limited to two limb segments).

Table 42 - Intra- and inter-sample comparisons of heritability.

		Tamarins				Sukhumi Baboons				Mennonites				TBRI Baboons	
		H	R	F	T	H	R	F	T	H	R	F	T	H	F
Tamarin	H														
	R														
	F														
	T														
Sukhumi Baboons	H														
	R														
	F														
	T														
Mennonites	H														
	R														
	F										X				
	T														
TBRI	H														
	F														

an X indicates that the posterior distribution produced when comparing these two limb segments did not cross zero, indicating that the heritability estimates for these limb segments are statistically different. For ease of interpretation, all four samples use the abbreviations of H (humerus), R (radius), F (femur), and T (tibia) despite the fact that these limb segments are called the arm, forearm, thigh, and leg for the Sukhumi Baboons and Mennonites throughout the text. Gray cells indicate comparisons that are 1) redundant, 2) self-comparisons (e.g., H and H in Intra-Sample Comparisons), 3) not done (e.g., comparing the humerus of one sample to the tibia of another sample), or 4) not possible (because the TBRI Baboon sample is limited to two limb segments).

Table 43 - Intra- and inter-sample comparisons of evolvability.

		Tamarins				Sukhumi Baboons				Mennonites				TBRI Baboons	
		H	R	F	T	H	R	F	T	H	R	F	T	H	F
Tamarin	H														
	R														
	F														
	T														
Sukhumi Baboons	H	X													
	R														
	F			X											
	T														
Mennonites	H	X													
	R		X												
	F			X						X	X				
	T											X			
TBRI	H	X													
	F			X								X			

An X indicates that the posterior distribution produced when comparing these two limb segments did not cross zero, indicating that the evolvability estimates for these limb segments are statistically different. For ease of interpretation, all four samples use the abbreviations of H (humerus), R (radius), F (femur), and T (tibia) despite the fact that these limb segments are called the arm, forearm, thigh, and leg for the Sukhumi Baboons and Mennonites throughout the text. Gray cells indicate comparisons that are 1) redundant, 2) self-comparisons (e.g., H and H in Intra-Sample Comparisons), 3) not done (e.g., comparing the humerus of one sample to the tibia of another sample), or 4) not possible (because the TBRI Baboon sample is limited to two limb segments).

Table 44 - Intra- and inter-sample comparisons of conditional evolvability.

		Tamarins				Sukhumi Baboons				Mennonites				TBRI Baboons	
		H	R	F	T	H	R	F	T	H	R	F	T	H	F
Tamarin	H														
	R														
	F														
	T														
Sukhumi Baboons	H	X													
	R		X			X									
	F			X											
	T				X	X		X							
Mennonites	H	X													
	R		X				X								
	F			X											
	T				X						X	X			
TBRI	H	X				X				X					
	F			X				X				X			

An X indicates that the posterior distribution produced when comparing these two limb segments did not cross zero, indicating that the conditional evolvability estimates for these limb segments are statistically different. For ease of interpretation, all four samples use the abbreviations of H (humerus), R (radius), F (femur), and T (tibia) despite the fact that these limb segments are called the arm, forearm, thigh, and leg for the Sukhumi Baboons and Mennonites throughout the text. Gray cells indicate comparisons that are 1) redundant, 2) self-comparisons (e.g., H and H in Intra-Sample Comparisons), 3) not done (e.g., comparing the humerus of one sample to the tibia of another sample), or 4) not possible (because the TBRI Baboon sample is limited to two limb segments).

Table 45 - Partial correlation coefficients for the TBRI Baboon humerus only.

	Maximum Length	50% Diameter Average	Head Length	Distal Articular Breadth	Epicondylar Breadth
Maximum Length					
50% Diameter Average	0.101				
Head Length	0.304	0.231			
Distal Articular Breadth	0.134	0.320	0.300		
Epicondylar Breadth	0.369	0.270	0.045	0.318	

Table 46 - Partial correlation coefficients for the TBRI Baboon femur only.

	Bicondylar Length	50% Diameter Average	Head Diameter	Articular Breadth	Bicodylar Breadth
Bicondylar Length					
50% Diameter Average	0.198				
Head Diameter	0.331	0.122			
Articular Breadth	0.197	-0.020	0.236		
Bicondylar Breadth	0.123	0.251	0.214	0.644	

Table 47 - Partial correlation coefficients for the TBRI baboon humerus and femur combined.

	Max. Length	H 50% Diameter Average	Head Length	Distal Articular Breadth	Epicond. Breadth	Bicond. Length	F 50% Diameter Average	Head Diameter	Articular Breadth	Bicond. Breadth
Max. Length										
H 50% Diameter Average	0.015									
Head Length	0.136	0.137								
Distal Articular Breadth	-0.123	0.177	0.135							
Epicond. Breadth	0.194	0.203	-0.063	0.254						
Bicond. Length	0.760	-0.020	-0.150	0.160	-0.022					
F 50% Diameter Average	-0.076	0.395	-0.085	-0.042	0.063	0.141				
Head Diameter	0.044	-0.051	0.220	0.293	-0.067	0.126	0.152			
Articular Breadth	-0.085	0.128	0.164	0.069	-0.124	0.232	-0.062	0.139		

Table 47 Continued.

	Max. Length	H 50% Diameter Average	Head Length	Distal Articular Breadth	Epicond. Breadth	Bicond. Length	F 50% Diameter Average	Head Diameter	Articular Breadth	Bicond. Breadth
Bicond. Breadth	0.144	-0.029	0.193	0.119	0.290	-0.091	0.179	0.049	0.548	

Table 48 - Edge exclusion deviance for the TBRI Baboon humerus only.

	Maximum Length	50% Diameter Average	Head Length	Distal Articular Breadth	Epicondylar Breadth
Maximum Length					
50% Diameter Average	4.276				
Head Length	40.436	22.867			
Distal Articular Breadth	7.556	45.049	39.328		
Epicondylar Breadth	61.036	31.564		44.456	

Table 49 - Edge exclusion deviance for the TBRI Baboon femur only.

	Bicondylar Length	50% Diameter Average	Head Diameter	Articular Breadth	Bicondylar Breadth
Bicondylar Length					
50% Diameter Average	13.758				
Head Diameter	39.918	5.159			
Articular Breadth	13.616		18.338		
Bicondylar Breadth	5.244	22.385	16.126	184.278	

Table 50 - Edge exclusion deviance for the TBRI Baboon humerus and femur combined.

	Max. Length	H 50% Diameter Average	Head Length	Distal Articular Breadth	Epicond. Breadth	Bicond. Length	F 50% Diameter Average	Head Diameter	Articular Breadth	Bicond. Breadth
Max. Length										
H 50% Diameter Average										
Head Length	5.974	6.063								
Distal Articular Breadth	4.878	10.186	5.886							
Epicond. Breadth	12.276	13.466		21.341						
Bicond. Length	275.777		7.282	8.299						
F 50% Diameter Average		54.282				6.426				
Head Diameter			15.875	28.723		5.121	7.480			
Articular Breadth		5.286	8.725		4.959	17.705		6.243		

Table 50 Continued.

	Max. Length	H 50% Diameter Average	Head Length	Distal Articular Breadth	Epicond. Breadth	Bicond. Length	F 50% Diameter Average	Head Diameter	Articular Breadth	Bicond. Breadth
Bicond. Breadth	4.186		12.147	4.564	28.111		10.421		114.275	

Table 51 - Edge strengths for the TBRI Baboon humerus only.

	Maximum Length	50% Diameter Average	Head Length	Distal Articular Breadth	Epicondylar Breadth
Maximum Length					
50% Diameter Average	0.005				
Head Length	0.048	0.027			
Distal Articular Breadth	0.009	0.054	0.047		
Epicondylar Breadth	0.073	0.038		0.053	

Table 52 - Edge strengths for the TBRI Baboon femur only.

	Bicondylar Length	50% Diameter Average	Head Diameter	Articular Breadth	Bicondylar Breadth
Bicondylar Length					
50% Diameter Average	0.020				
Head Diameter	0.058	0.007			
Articular Breadth	0.020		0.029		
Bicondylar Breadth	0.008	0.033	0.023	0.268	

Table 53 - Edge strengths for the TBRI Baboon humerus and femur combined.

	Max. Length	H 50% Diameter Average	Head Length	Distal Articular Breadth	Epicond. Breadth	Bicond. Length	F 50% Diameter Average	Head Diameter	Articular Breadth	Bicond. Breadth
Max. Length										
H 50% Diameter Average										
Head Length	0.009	0.009								
Distal Articular Breadth	0.008	0.016	0.009							
Epicond. Breadth	0.019	0.021		0.033						
Bicond. Length	0.431		0.011	0.013						
F 50% Diameter Average		0.085				0.010				
Head Diameter			0.025	0.045		0.008	0.012			
Articular Breadth		0.008	0.014		0.008	0.028		0.010		

Table 53 Continued.

	Max. Length	H 50% Diameter Average	Head Length	Distal Articular Breadth	Epicond. Breadth	Bicond. Length	F 50% Diameter Average	Head Diameter	Articular Breadth	Bicond. Breadth
Bicond. Breadth	0.007		0.019	0.007	0.044		0.016		0.179	

Table 54 - Correlation matrix for the TBRI Baboon humerus only.

	Maximum Length	50% Diameter Average	Head Length	Distal Articular Breadth	Epicondylar Breadth
Maximum Length	1				
50% Diameter Average	0.829	1			
Head Length	0.845	0.842	1		
Distal Articular Breadth	0.847	0.874	0.861	1	
Epicondylar Breadth	0.866	0.861	0.828	0.877	1

Table 55 - Correlation matrix for the TBRI Baboon femur only.

	Bicondylar Length	50% Diameter Average	Head Diameter	Articular Breadth	Bicondylar Breadth
Bicondylar Length	1				
50% Diameter Average	0.819	1			
Head Diameter	0.896	0.818	1		
Articular Breadth	0.896	0.819	0.912	1	
Bicondylar Breadth	0.895	0.843	0.913	0.954	1

Table 56 - Correlation matrix for the TBRI Baboon humerus and femur combined.

	Max. Length	H 50% Diameter Average	Head Length	Distal Articular Breadth	Epicond. Breadth	Bicond. Length	F 50% Diameter Average	Head Diameter	Articular Breadth	Bicond. Breadth
Max. Length	1									
H 50% Diameter Average	0.828	1								
Head Length	0.836	0.839	1							
Distal Articular Breadth	0.866	0.878	0.880	1						
Epicond. Breadth	0.864	0.861	0.820	0.886	1					
Bicond. Length	0.960	0.839	0.833	0.887	0.859	1				
F 50% Diameter Average	0.806	0.866	0.783	0.832	0.821	0.829	1			
Head Diameter	0.876	0.846	0.883	0.913	0.843	0.892	0.833	1		
Articular Breadth	0.883	0.872	0.989	0.913	0.861	0.903	0.835	0.913	1	

Table 56 Continued.

	Max. Length	H 50% Diameter Average	Head Length	Distal Articular Breadth	Epicond. Breadth	Bicond. Length	F 50% Diameter Average	Head Diameter	Articular Breadth	Bicond. Breadth
Bicond. Breadth	0.889	0.879	0.902	0.921	0.897	0.895	0.856	0.910	0.956	1

Table 57 - Ten models used to perform Mantel tests for integration.

Model Number	Integrated Traits
1*	Lengths
2	Articulations
3*	Diaphyses
4*	Muscle Attachments
5	Length & Articulations
6	Length & Diaphysis
7	Length & Muscle Attachment
8	Articulations & Diaphysis
9	Articulations & Muscle Attachment
10	Diaphysis & Muscle Attachment

*These models can only be tested on the humerus and femur combined analysis

Table 58 - Results of Mantel tests between correlation matrices and model matrices.

	Model 1	Model 2	Model 3	Model 4	Model 5	Model 6	Model 7	Model 8	Model 9	Model 10
Humerus										
Correlation		0.163			-0.078	-0.479	0.269	0.238	0.089	0.154
p-value		0.320			0.488	0.792	0.203	0.188	0.300	0.389
Femur										
Correlation		0.261			0.355	-0.419	0.136	-0.384	**0.716**	-0.245
p-value		0.221			0.306	0.696	0.513	0.697	**0**	0.640
Humerus & Femur										
Correlation	**0.367**	0.318	-0.017	0.112	0.367	-0.162	0.258	0.010	0.340	-0.069
p-value	**0**	0.072	0.540	0.215	0.094	0.791	0.130	0.463	0.097	0.608

Table 59 - Relative eigenvalue variance for the Tamarins, Sukhumi Baboons, and Mennonites with 95% credibility intervals.

	Tamarins	Sukhumi Baboons	Mennonites
Upper Limb	0.730 (0.666-0.793)	0.408 (0.307-0.531)	0.062 (0.023-0.121)
Lower Limb	0.764 (0.679-0.800)	0.435 (0.289-0.530)	0.118 (0.063-0.194)
Proximal Elements	0.621 (0.551-0.717)	0.337 (0.207-0.456)	0.196 (0.132-0.289)
Distal Elements	0.690 (0.601-0.745)	0.423 (0.327-0.548)	0.244 (0.160-0.311)
All Elements	0.679 (0.618-0.733)	0.381 (0.296-0.468)	0.154 (0.119-0.202)

Table 60 - Intra- and inter-sample comparisons of relative eigenvalue variance.

		Tamarins					Sukhumi Baboons					Mennonites				
		A	U	L	P	D	A	U	L	P	D	A	U	L	P	D
Tamarin	A															
	U	X														
	L	X														
	P	X	X	X												
	D	X														
Sukhumi Baboons	A	X														
	U		X													
	L			X												
	P				X											
	D					X										
Mennonites	A	X					X									
	U		X					X				X				
	L			X					X							
	P				X								X	X		
	D					X					X	X	X	X		

A = all four limb segments, U = upper limb segments, L = lower limb segments, P = proximal limb segments, D = distal limb segments.

Table 61 - Residual kurtosis and significant covariates used in linkage analyses.

Trait	Kurtosis	Covariates	Heritability (p-value)
Humerus Maximum Length	0.3133	sex	0.68 ($6.6*10^{-14}$)
Humerus 50% Diameter Average	0.3503	sex, age*sex, age^2	0.73 ($6.6*10^{-21}$)
Humerus Head Length	0.3478	age, sex	0.75 ($2.5*10^{-14}$)
Humerus Distal Articular Breadth	0.5640	age, sex	0.74 ($9.2*10^{-12}$)
Humerus Epicondylar Breadth	0.5429	sex, age*sex, age^2	0.61 ($7.1*10^{-10}$)
Femur Bicondylar Length	0.3074	sex, age^2	0.92 ($1.7*10^{-20}$)
Femur 50% Diameter Average	-0.1563	age, sex	0.78 ($4.7*10^{-11}$)
Femur Head Diameter	-0.1532	age, sex	0.90 ($2.2*10^{-15}$)
Femur Articular Breadth	0.1816	age, sex	0.76 ($7.3*10^{-12}$)
Femur Bicondylar Breadth	0.0978	age, sex	0.71 ($1.1*10^{-9}$)

Table 62 - Suggestive and significant LOD scores in linkage analyses.

Trait	Human Chr #	Baboon Chr #	Location (cM)	Peak (cM)	LOD score
Humerus Maximum Length	12	11	30-51	42	1.7153
	12	11	71-73	73	1.6231
	12	11	79-85	83	1.5617
Humerus 50% Diameter Average	6	4	51-67	56	2.6765
Humerus Head Length	2q	12	65-71	67	2.0879
	2q	12	143-146	146	1.8870
	11	14	19-75	46	3.7985
Humerus Distal Articular Breadth	2q	12	129-133	132	1.8174
	19	19	103	103	1.5293
Humerus Epicondylar Breadth	10	9	0-2	0	1.5743
Femur Bicondylar Length	7_21	3	134-147	142	2.2739
	7_21	3	154-159	157	1.5812
	14_15	7	94-118	103	2.1954
Femur 50% Diameter Average	6	4	61-69	64	1.7824
	6	4	135-138	137	1.5973
Femur Head Diameter	2p	13	30-50	41	2.5065
Femur Articular Breadth	12	11	17-53	26	2.4012
	12	11	65-73	67	1.8259
Femur Bicondylar Breadth	2q	12	67	67	1.5137
	20_22	10	79-81	79	1.5785

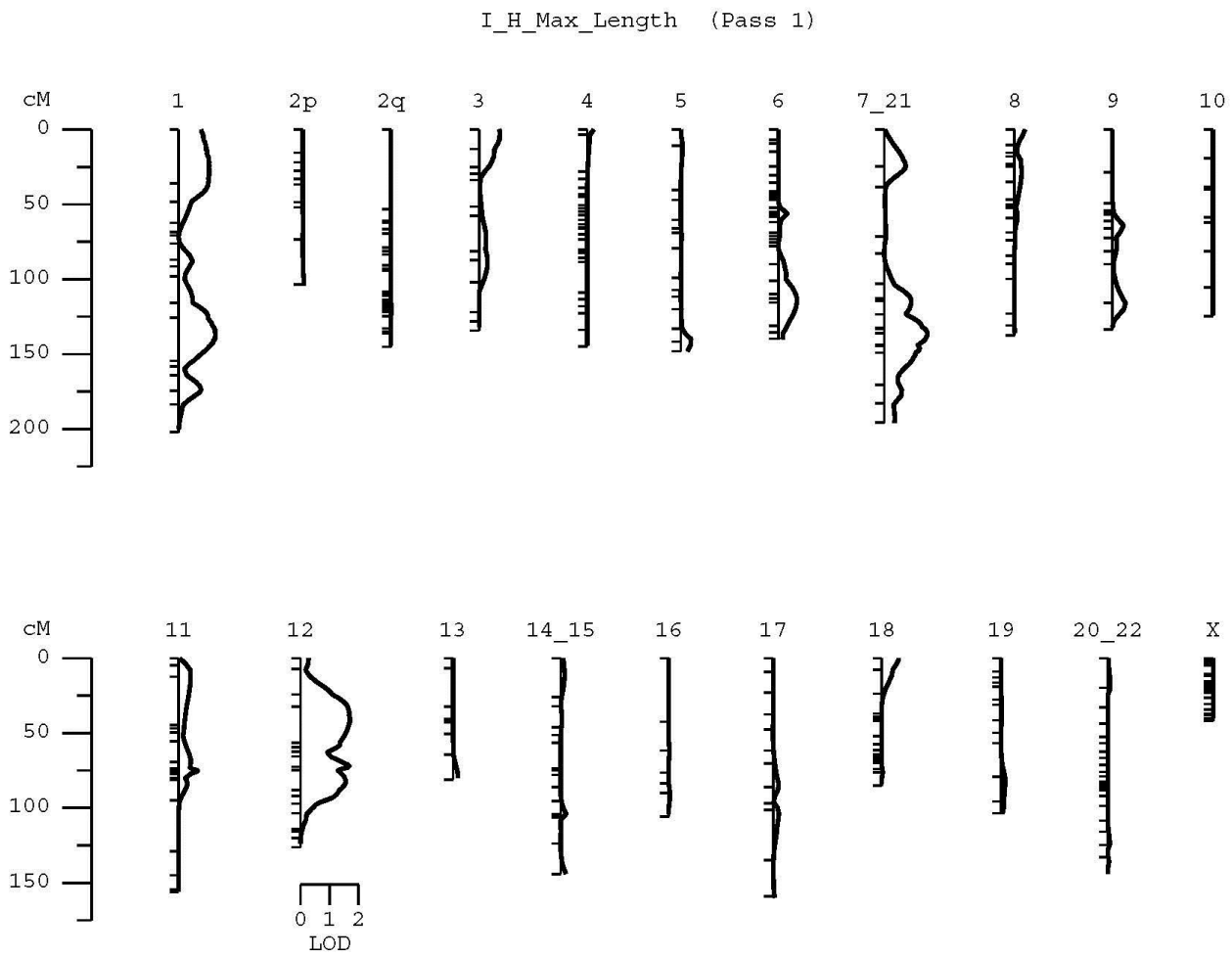

Figure 13 - String plot for Humerus Maximum Length.

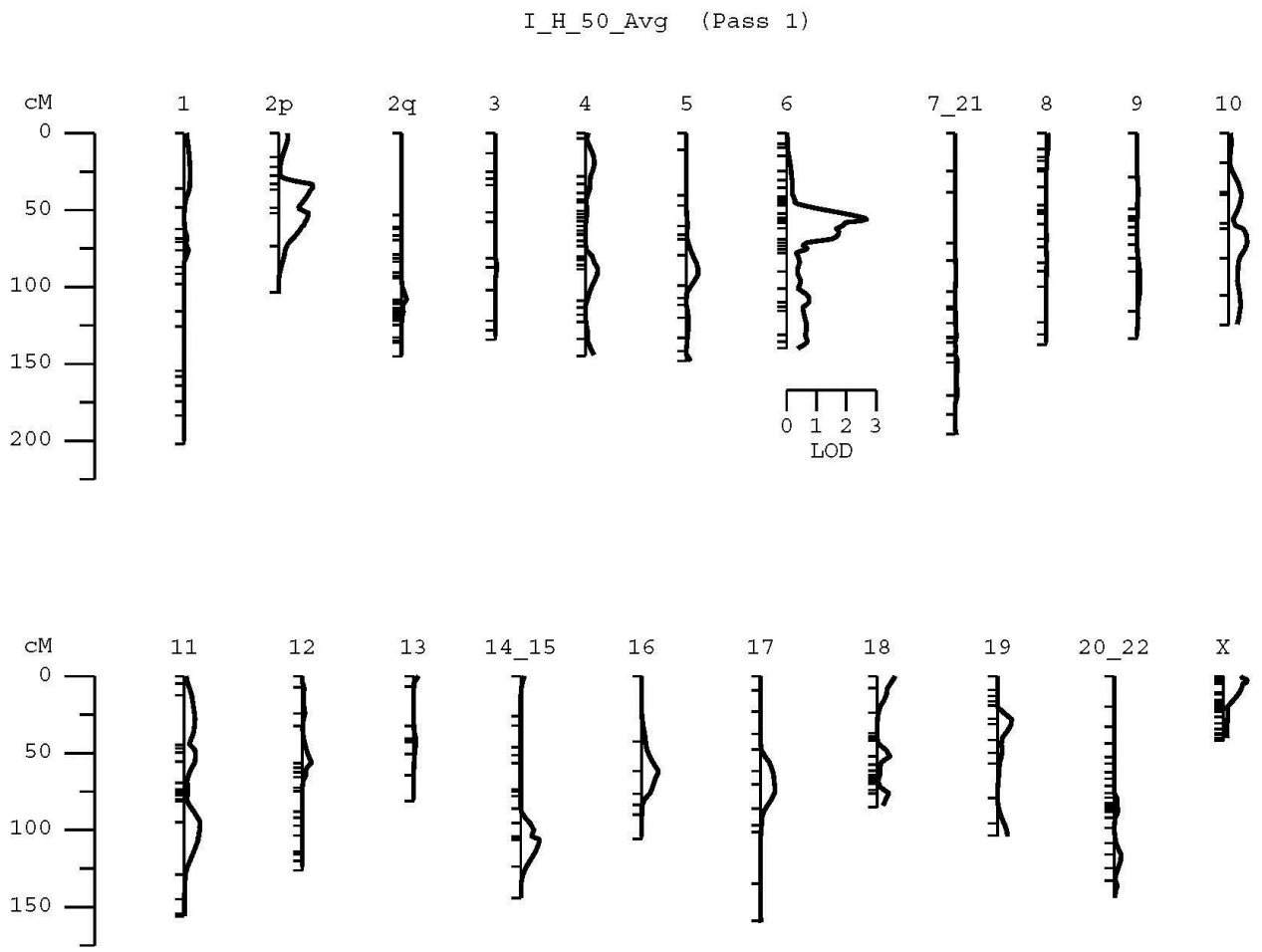

Figure 14 - String plot for Humerus 50% Diameter Average.

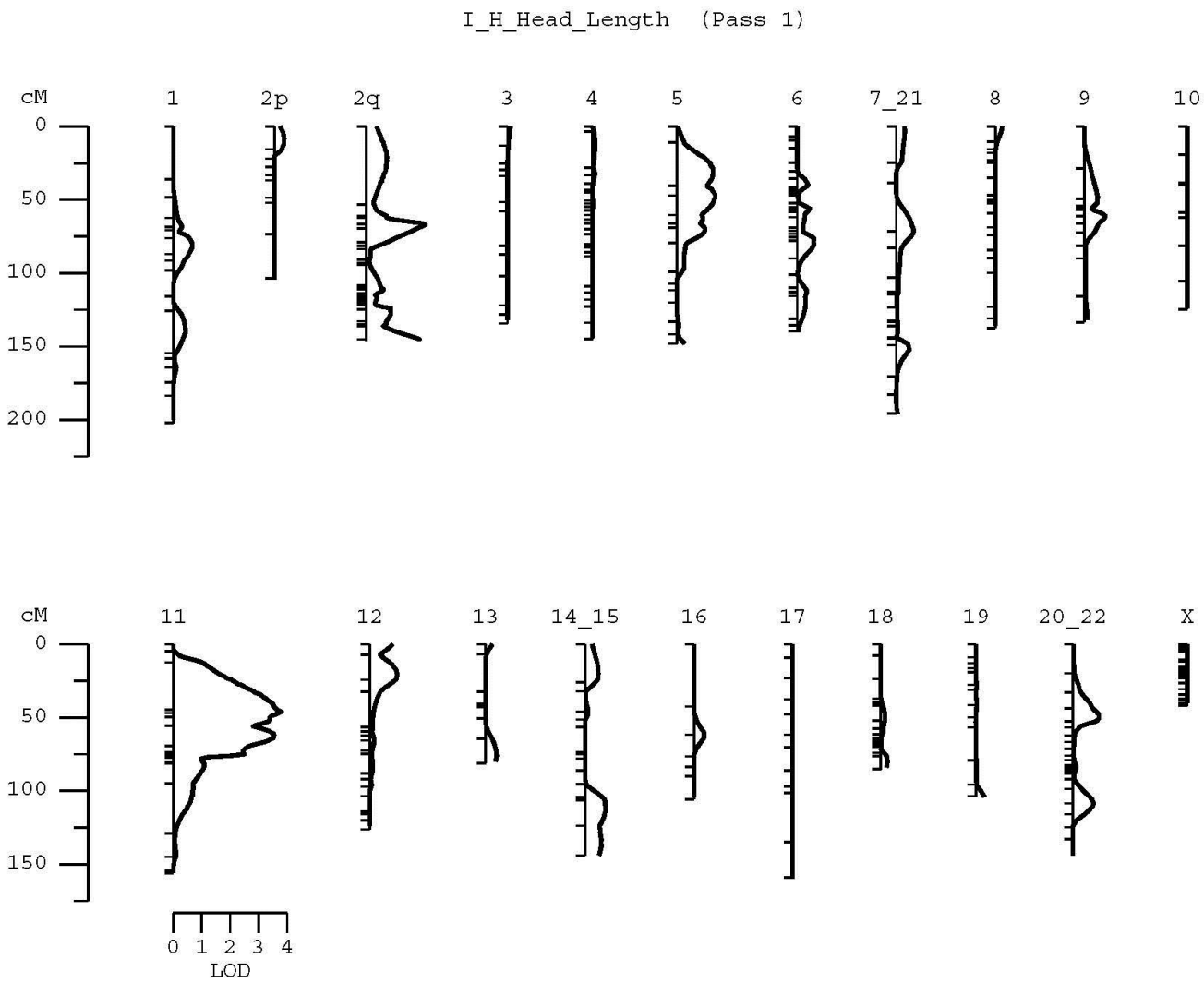

Figure 15 - String plot for Humerus Head Length.

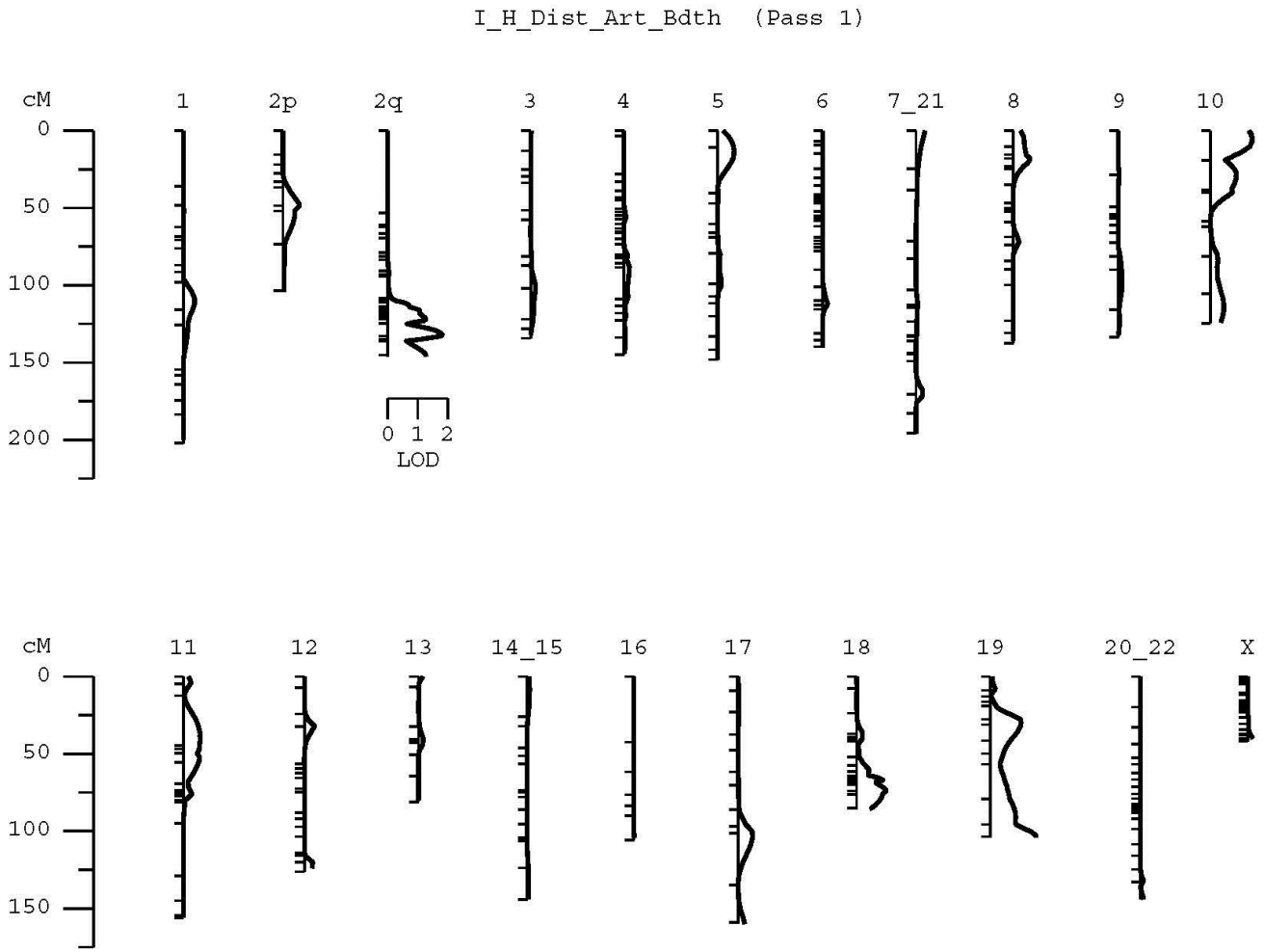

Figure 16 - String plot for Humerus Distal Articular Breadth.

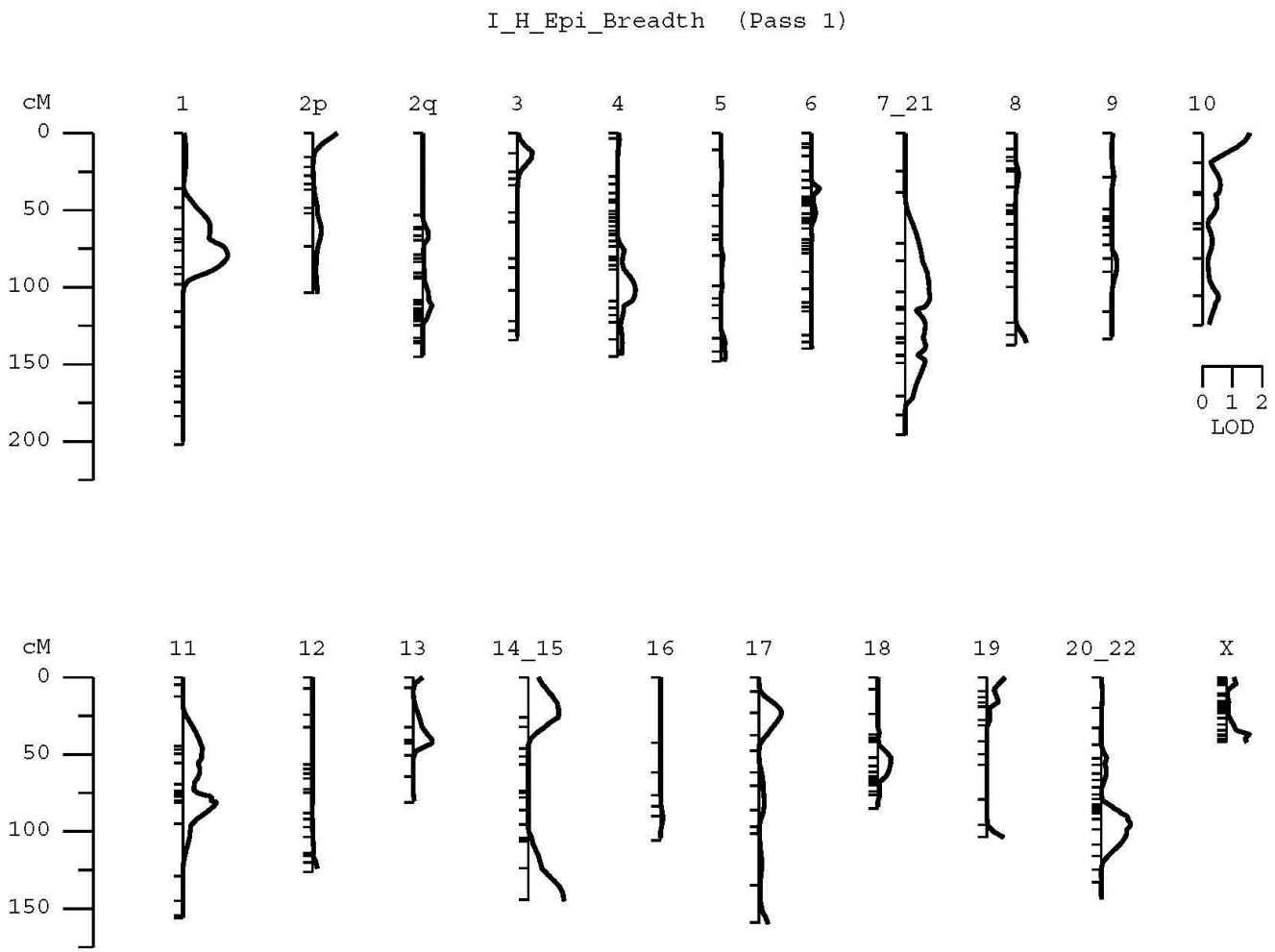

Figure 17 - String plot for Humerus Epicondylar Breadth.

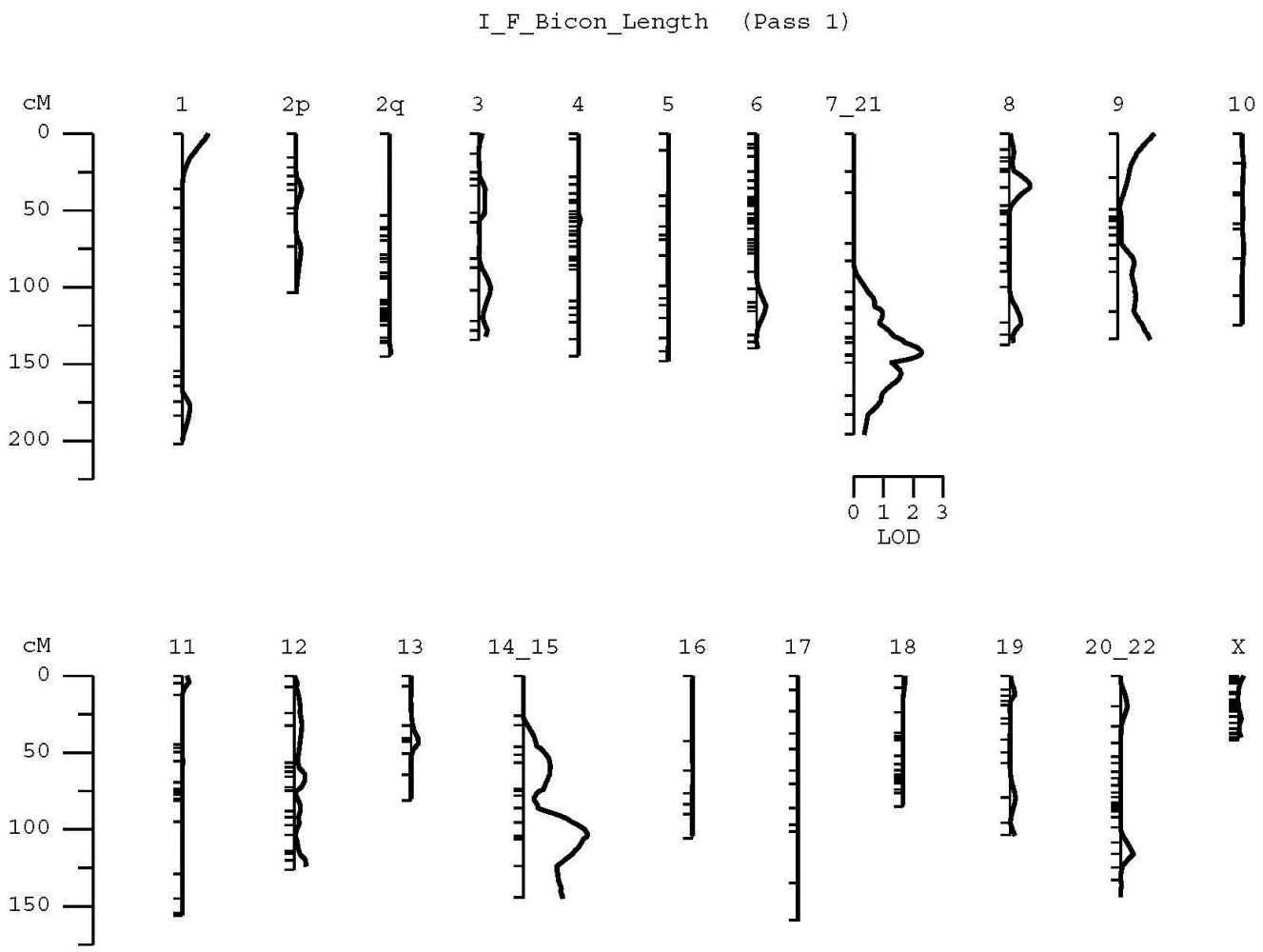

Figure 18 - String plot for Femur Bicondylar Length.

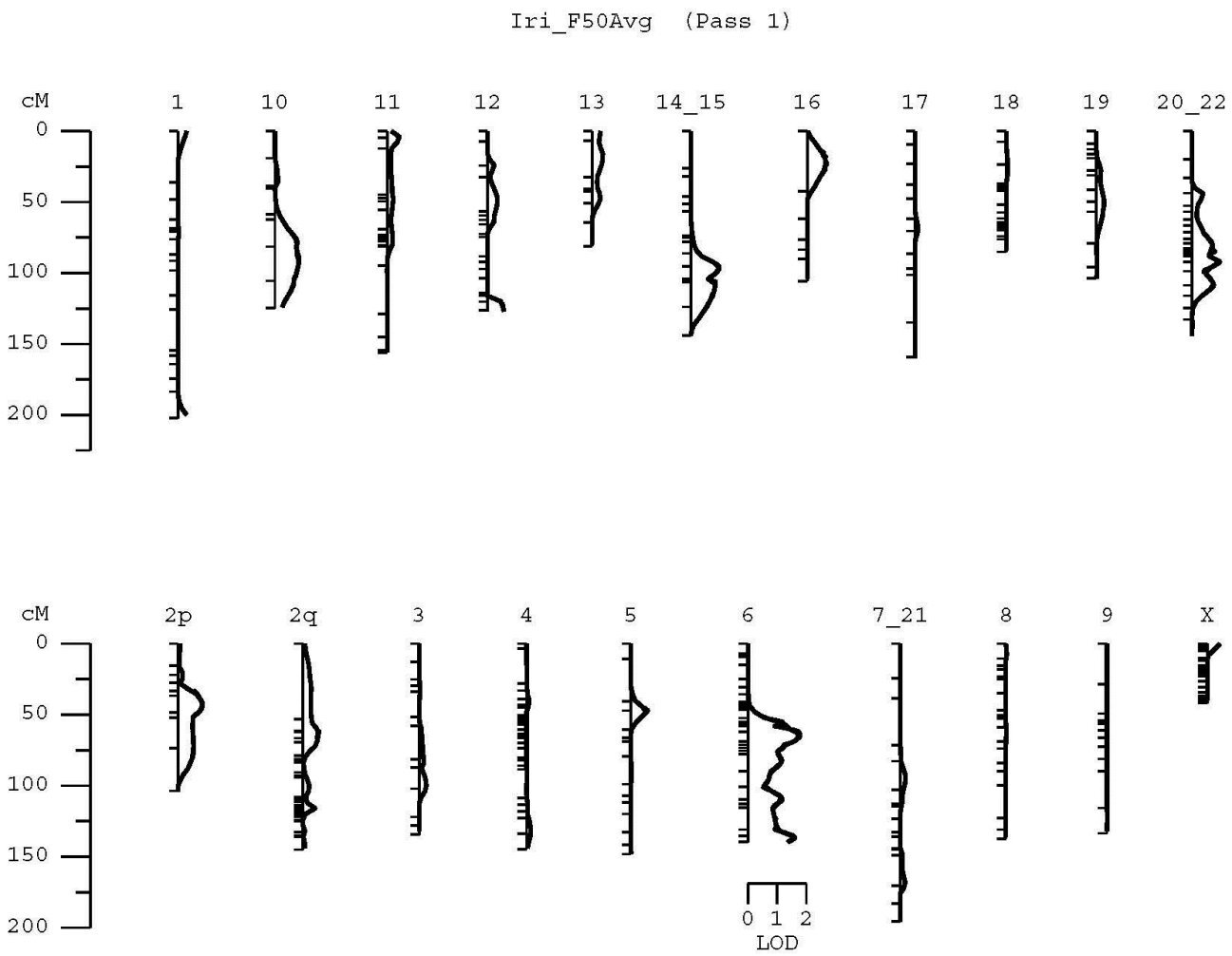

Figure 19 - String plot for Femur 50% Diameter Average.

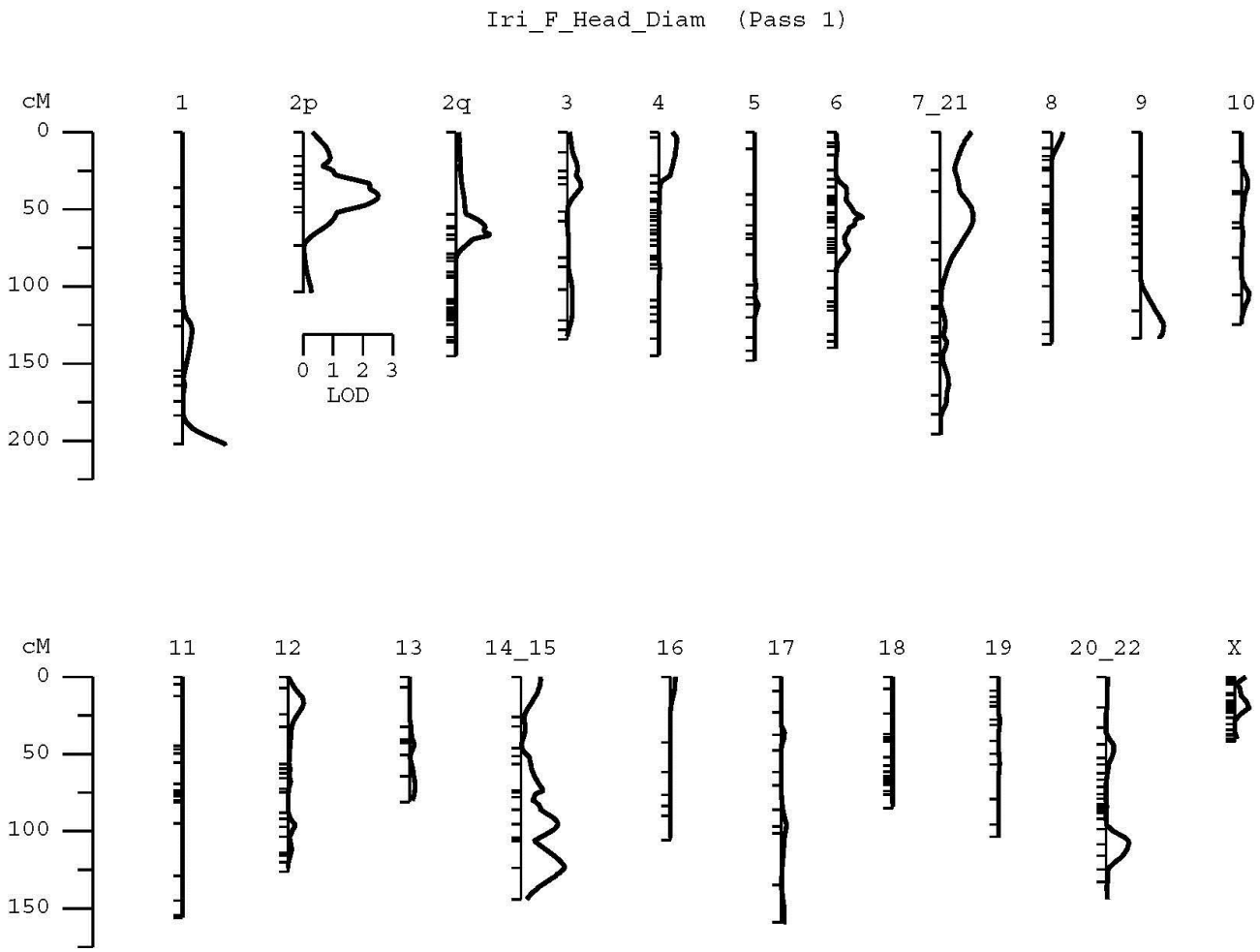

Figure 20 - String plot for Femur Head Diameter.

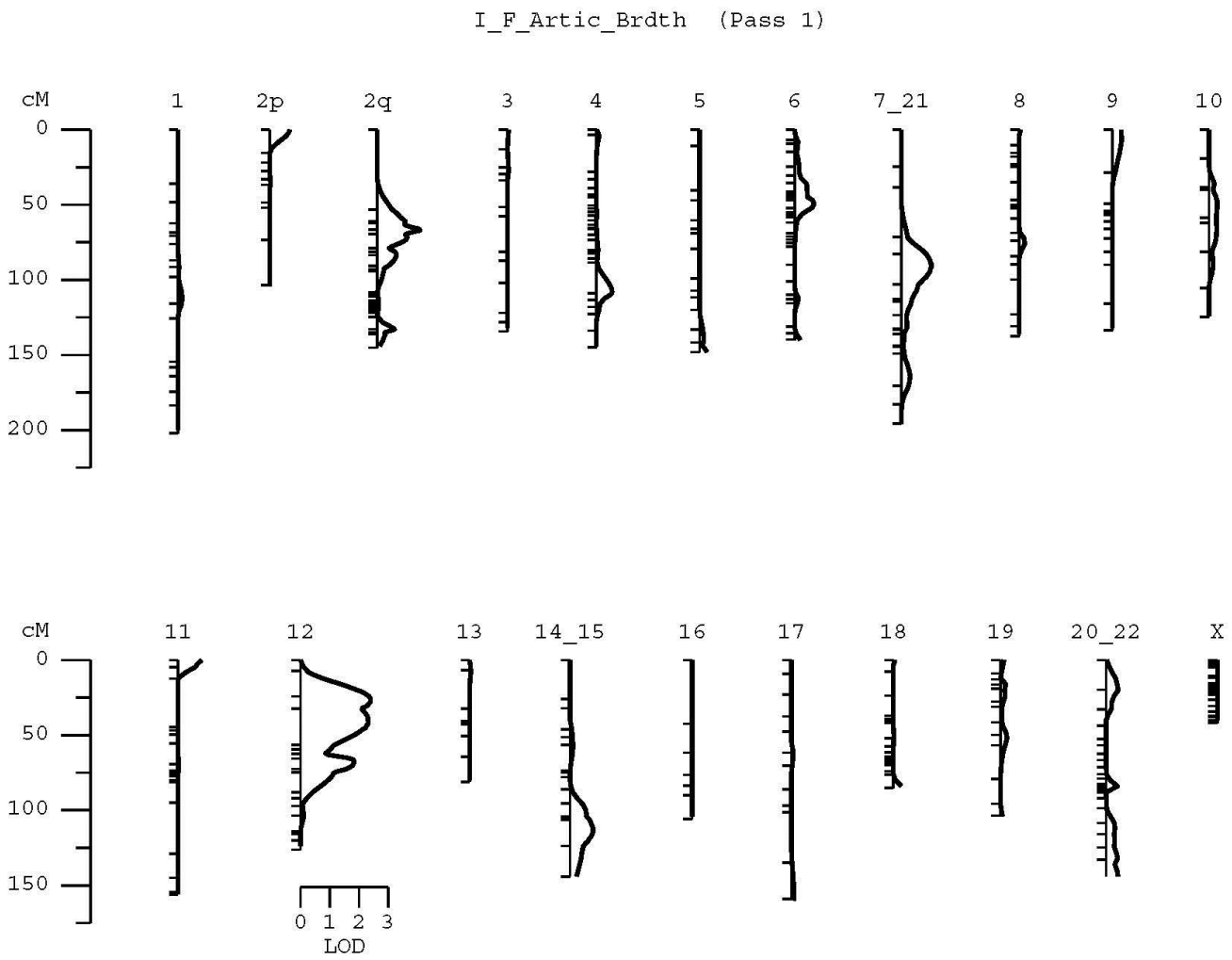

Figure 21 - String plot for Femur Articular Breadth.

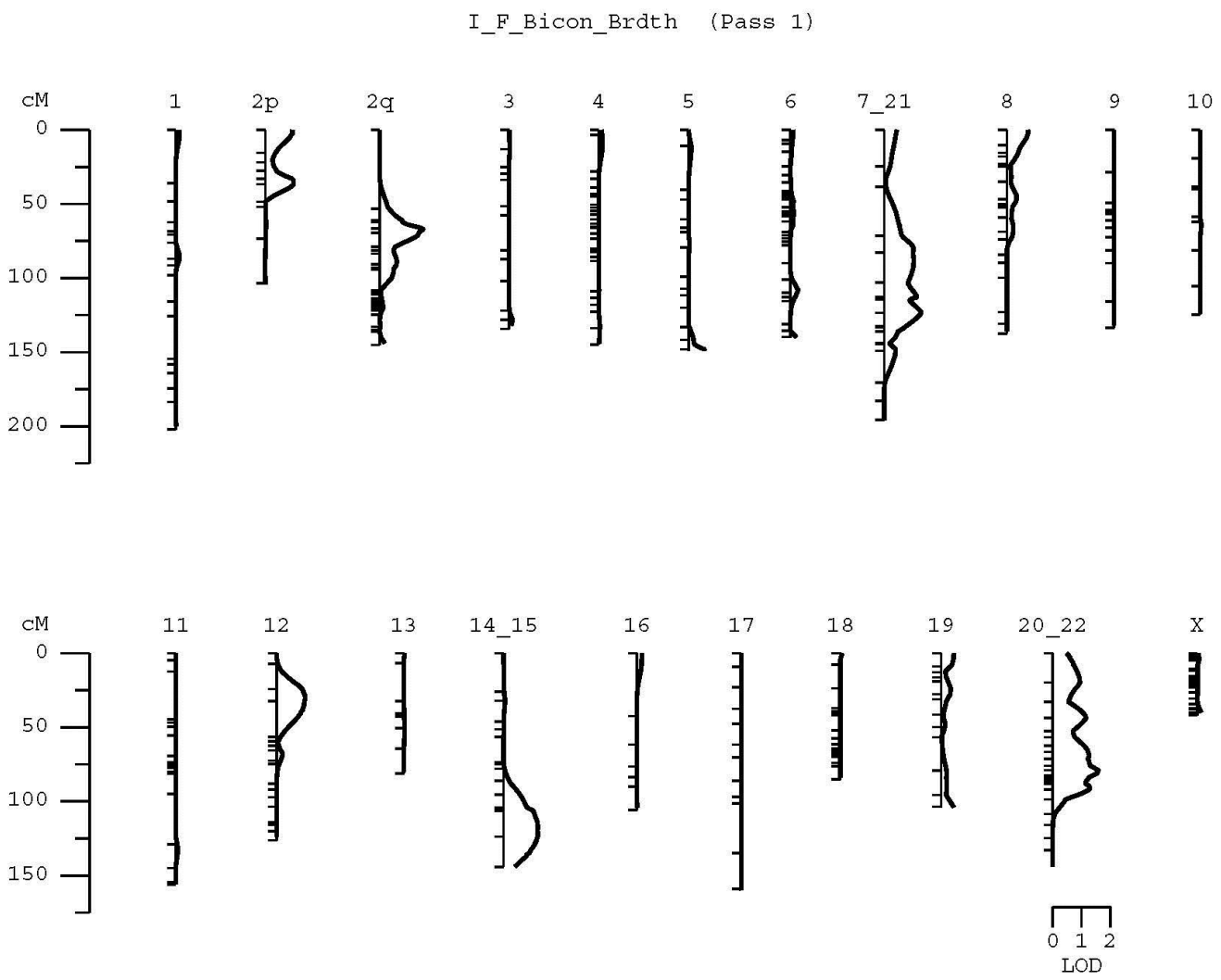

Figure 22 - String plot for Femur Bicondylar Breadth.

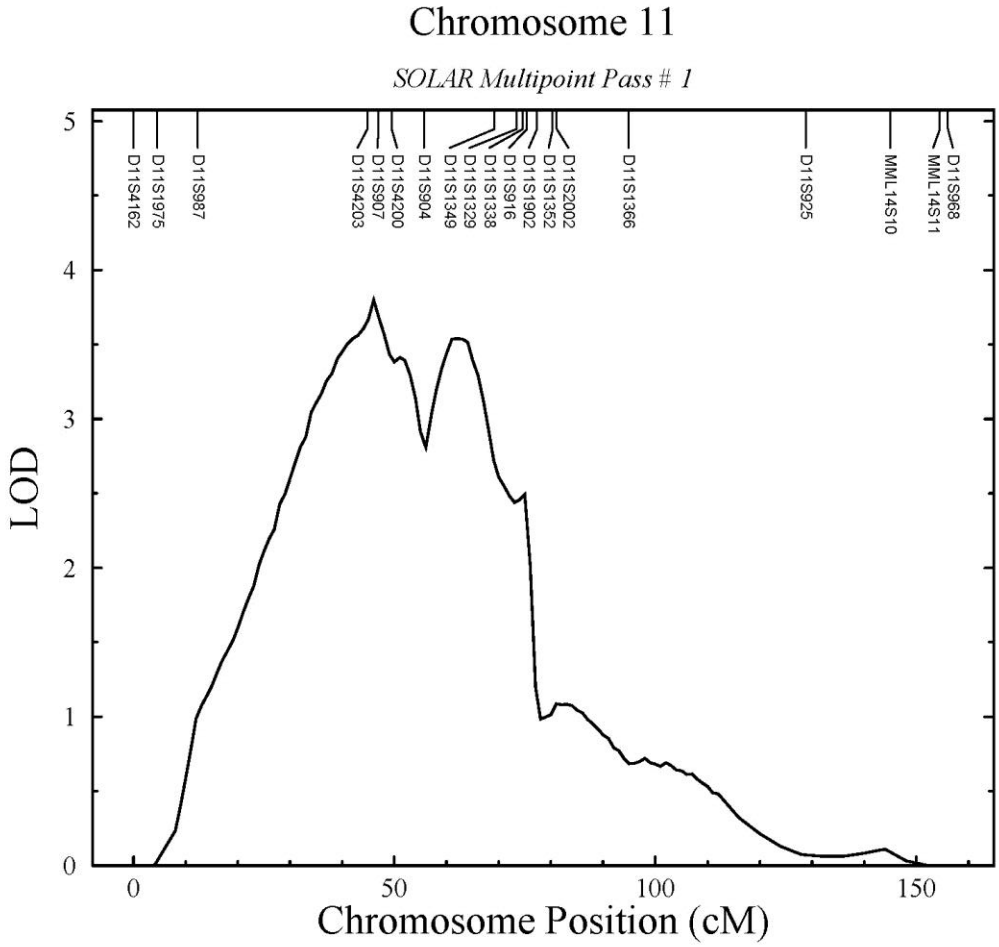

Figure 23 - Significant LOD score peak for Humerus Head Length on human chromosome 11 (baboon chromosome 14).

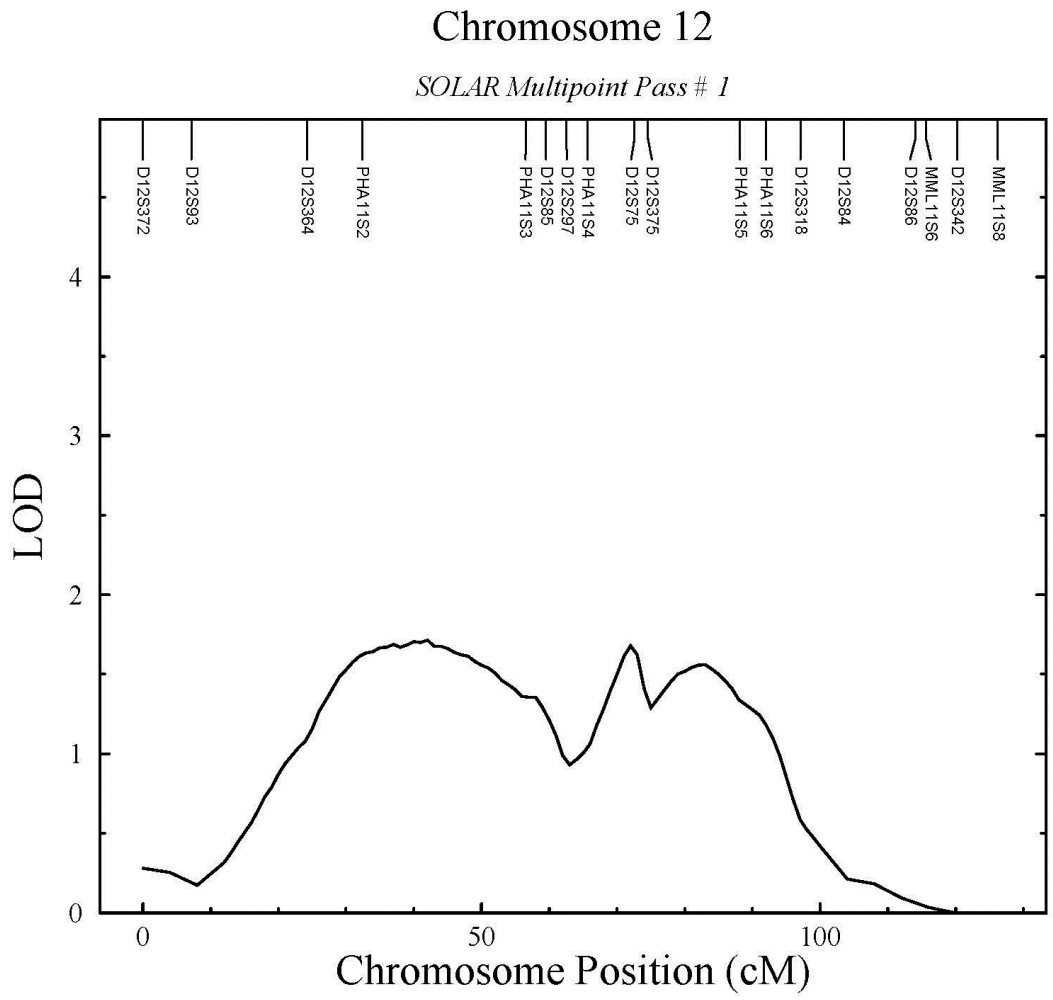

Figure 24 - Suggestive LOD score for Humerus Maximum Length on human chromosome 12 (baboon chromosome 11).

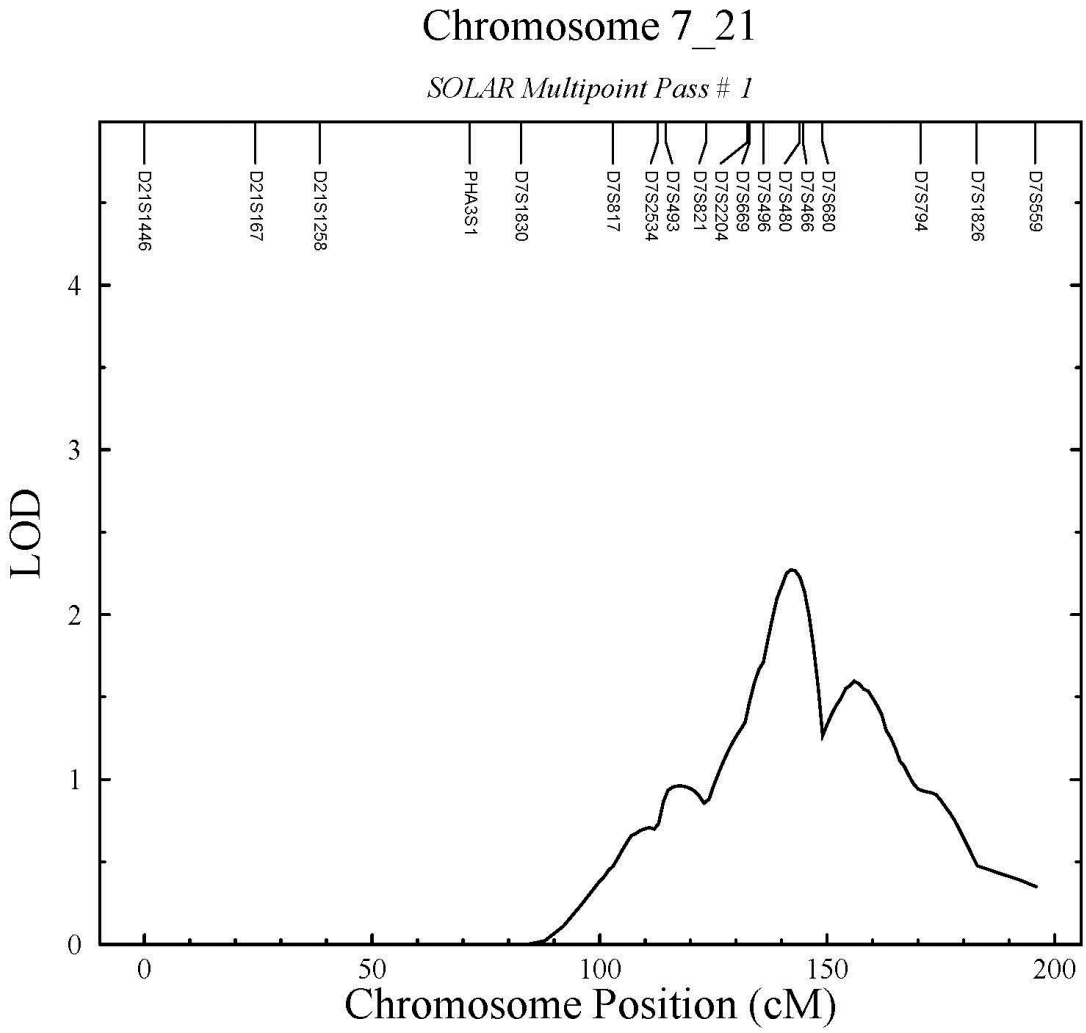

Figure 25 - Suggestive LOD score peak for Femur Bicondylar Length on human chromosome 7 (baboon chromosome 3).

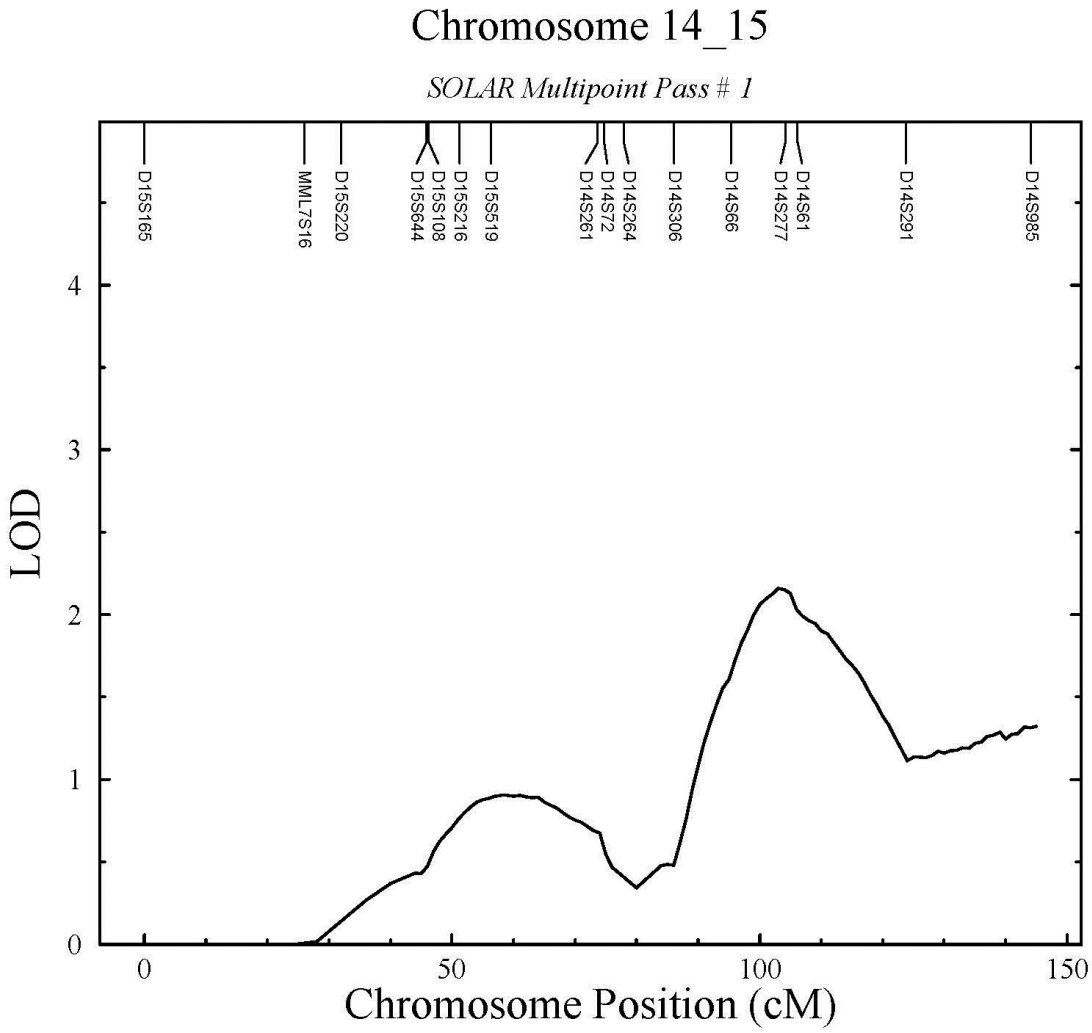

Figure 26 - Suggestive LOD score peak for Femur Bicondylar Length on human chromosome 14 (baboon chromosome 7).

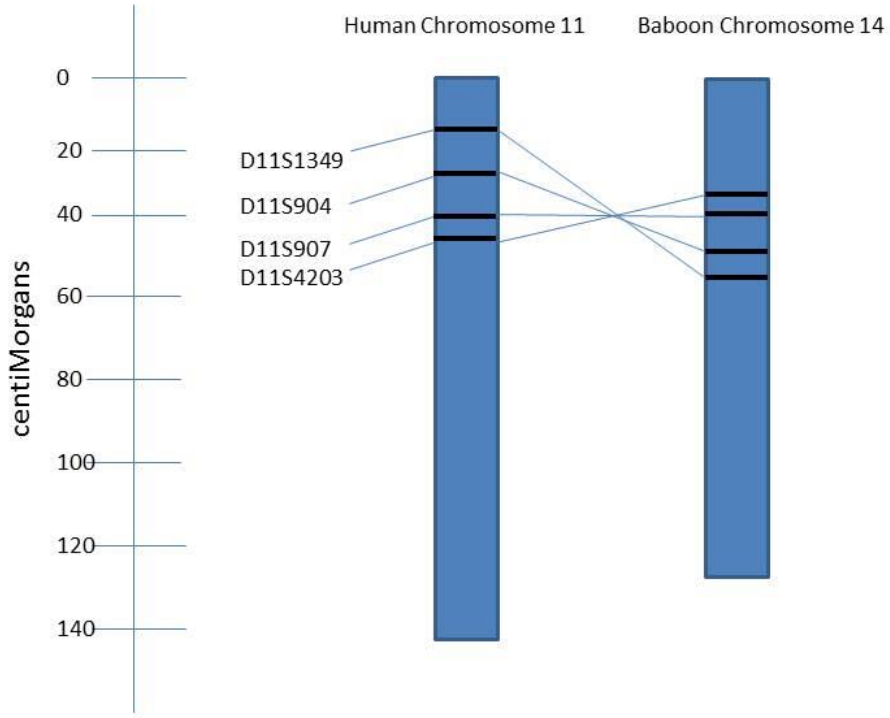

Figure 27 - Relative locations of STRs flanking the significant LOD score positions in human chromosome 11 and baboon chromosome 14.

Table 63 - Genes on chromosome 11 within are aof highest peak of significant LOD score for Humerus Head Length.

Gene Abbreviation	**UCSC name**	**Color**	**Coding/Non**	**Function** (unknown if left blank)
APIP	uc001mvs.2	dark blue	coding	negative regulator of ischemic/hypoxic injury
CD44	uc001mvu.3	black	coding	cell-cell interactions, Wnt signaling
EHF	uc009yke.2	dark blue	coding	transcription repressor involved in epithelial differentiation
FJX1	uc001mwh.3	dark blue	coding	ortholog of Drosophila gene for limb and wing development
MIR1343	uc021qfv.1	light blue	noncoding	microRNA
PAMR1	uc001mwf.3	dark blue	coding	muscle regeneration
PDHX	uc001mvt.3	black	coding	pyruvate dehydrogenase complex
SLC1A2	uc021qfx.1	dark blue	coding	transporter protein for clearing excitatory neurotransmitters
TRIM44	uc001mwi.2	dark blue	coding	differentiation and maturation of neuronal cells

Table 64 - Genes on chromosome 11 within area of secondary peak of significant LOD score for Humerus Head Length.

Gene Abbreviation	**UCSC name**	**Color**	**Coding/Non**	**Function** (unknown if left blank)
5S_rRNA	uc021qeb.1	light blue	noncoding	
7SK	uc021qea.1	light blue	noncoding	
ABCC8	uc001mnc.3	dark blue	coding	protein transport
AK026905	uc001mke.3	light blue	noncoding	
AK096475	uc001mmy.1	light blue	noncoding	
AL833346*	uc009ygt.3	light blue	coding	
ANO3	uc001mqt.4	dark blue	coding	transmembrane transport
ANO5	uc001mqi.2	dark blue	coding	transmembrane protein
ARNTL	uc001mkp.3	dark blue	coding	activates transcription
BC045791	uc001mqu.1	light blue	noncoding	
BTBD10	uc001mkz.3	dark blue	coding	
C11orf58	uc001mmk.2	dark blue	coding	small acidic protein
CALCA	uc001mlw.1	black	coding	calcitonin, regulates ossification and bone resorption
CALCB	uc001mlx.1	dark blue	coding	neurotransmitter
CCDC179	uc021qfb.1	dark blue	coding	
COPB1	uc001mli.2	dark blue	coding	intracellular protein transport
CSRP3	uc001mpk.3	black	coding	myogenesis
CYP2R1	uc001mls.1	black	coding	converts vitamin D
DBX1	uc021qey.1	dark blue	coding	central nervous system patterning
DD413619	uc021qdw.1	light blue	noncoding	
DKK3	uc001mjw.3	dark blue	coding	Wnt signaling, limb development
ERV9	uc010rdq.1	light blue	noncoding	endogenous retrovirus
FANCF	uc001mql.1	black	coding	DNA repair protein
FAR1	uc001mld.3	dark blue	coding	cellular lipid metabolism
GAS2	uc001mqm.3	dark blue	coding	cellular apoptosis
GTF2H1	uc001moi.2	black	coding	general transcription factor
HPS5	uc001mod.1	dark blue	coding	organelle biogenesis

Table 64 Continued.

Gene Abbreviation	**UCSC name**	**Color**	**Coding/Non**	**Function** (unknown if left blank)
HTATIP2	uc009yia.1	black	coding	tumor suppression
IGSF22	uc009yht.2	dark blue	coding	immunoglobulin superfamily
INSC	uc001mly.4	black	coding	influences bone density
JA429845	uc021qeq.1	light blue	noncoding	
KCNC1	uc001mnk.4	dark blue	coding	potassium ion transport
KCNJ11	uc001mnb.4	dark blue	coding	potassium channel
LDHA	uc001mok.3	black	coding	catalyzes final step of anaerobic glycolysis
LDHAL6A	uc001mop.1	dark blue	coding	carbohydrate metabolism
LDHC	uc001mon.4	dark blue	coding	sperm motility
LOC100126784*	uc010rdl.2	light blue	coding	
LOC100506305 (ENSG00000189332)	uc001mkl.2	light blue	noncoding	
LOC494141	uc009yhh.4	light blue	coding	mitochondrial carrier protein
LUZP2	uc001mqs.3	dark blue	coding	leucine zipper protein
Metazoa_SRP	uc021qeg.1	light blue	noncoding	
MICAL2	uc001mka.3	black	coding	
MICALCL	uc001mkg.1	dark blue	coding	spermatozoa production
Mir_340	uc021qes.1	light blue	noncoding	
MIR4486	uc021qeu.1	light blue	noncoding	microRNA involved in post-transcriptional gene regulation
MRGPRX1	uc001mpg.3	dark blue	coding	pain modulation
MRGPRX2	uc021qer.1	dark blue	coding	pain modulation
MRGPRX3	uc001mnu.3	dark blue	coding	pain modulation
MUC15	uc001mqw.3	dark blue	coding	
MYOD1	uc001mni.3	dark blue	coding	muscle cell differentiation and regeneration
NAV2	uc010rdm.2	black	coding	neuronal and sensory organ development
NAV2-AS4	uc021qet.1	light blue	noncoding	
NAV2-AS5	uc031pzi.1	light blue	noncoding	

Table 64 Continued.

Gene Abbreviation	**UCSC name**	**Color**	**Coding/Non**	**Function** (unknown if left blank)
NCR3LG1	uc001mmz.4	black	coding	natural killer cells, expressed on tumor cells
NELL1	uc001mqe.3	dark blue	coding	osteoblast cell differentiation and terminal mineralization
NUCB2	uc001mmw.3	dark blue	coding	calcium homeostasis
OR7E14P*	uc021qeh.1	light blue	coding	olfactory receptor
OTOG	uc031pzc.1	dark blue	coding	inner ear membranes
PARVA	uc001mki.4	dark blue	coding	cell adhesion
PDE3B	uc001mln.3	black	coding	fat metabolism
PIK3C2A	uc010rcw.2	black	coding	intracellular messenger
PLEKHA7	uc001mmo.3	dark blue	coding	zonula adherens biogenesis and maintenance
PRMT3	uc001mqb.3	black	coding	protein methylation
PSMA1	uc001mll.3	dark blue	coding	proteasome
PTH	uc001mlb.3	black	coding	parathyroid hormone, dissolves salts in bone, associated w adult height
PTPN5	uc001mpf.4	black	coding	neuronal cell survival
RASSF10*	uc021qdz.1	dark blue	coding	
RPS13	uc001mmp.3	dark blue	coding	ribosomal protein
RRAS2	uc021qec.1	black	coding	signal transducer
SAA1	uc021qem.1	dark blue	coding	cholesterol homeostasis, expressed in response to inflammation
SAA2	uc009yhj.3	dark blue	coding	
SAA2-SAA4*	uc021qel.1	dark blue	coding	fusion protein between two genes
SAA3P	uc001mnt.3	light blue	noncoding	
SAA4	uc001mny.3	dark blue	coding	
SAAL1	uc001mnq.3	dark blue	coding	
SCARNA16	uc021qdy.1	light blue	noncoding	
SERGEF	uc001mnm.3	dark blue	coding	influences body height
SLC17A6	uc001mqk.3	dark blue	coding	ion transport
SLC6A5	uc001mqd.3	dark blue	coding	neurotransmitter transporter

Table 64 Continued.

Gene Abbreviation	**UCSC name**	**Color**	**Coding/Non**	**Function** (unknown if left blank)
SnoMBII_202	uc021qef.1	light blue	noncoding	
SNORD14	uc021qei.1	light blue	noncoding	
SOX6	uc001mmg.3	dark blue	coding	sex determining region Y, required for normal chondrogenesis
SPON1*	uc001mle.3	black	coding	cell adhesion protein
SPTY2D1	uc001moy.3	dark blue	coding	
SPTY2D1-AS1	uc001mox.3	light blue	noncoding	
SVIP	uc001mqp.4	dark blue	coding	
TEAD1	uc021qdx.1	black	coding	organ size control and tumor suppression, Body height
TMEM86A	uc001moz.1	dark blue	coding	
TPH1	uc001mnp.2	black	coding	catalyzes the biosynthesis of serotonin
TRNA	uc021qfa.1	light blue	noncoding	
TSG101	uc001mor.3	black	coding	tumor susceptibility gene
TSH101*	uc009yhs.2	light blue	coding	tumor susceptibility gene
U7	uc021qee.1	light blue	noncoding	
UCH1C*	uc001mnf.3	black	coding	development of cochlear hair cells
UEVLD	uc010rde.3	black	coding	carbohydrate metabolism
USH1C	uc001mnd.3	black	coding	development of cochlear hair cells
USP47	uc001mjr.3	dark blue	coding	
ZDHHC13	uc001mpi.3	dark blue	coding	magnesium transport

Table 65 - Genes on chromosome 12 within area of suggestive LOD score for Humerus Maximum Length.

Gene Abbreviation	**UCSC name**	**Color**	**Coding/Non**	**Function** (unknown if left blank)
7SK	uc021qvo.1	light blue	noncoding	
ABCC9	uc001rfh.3	dark blue	coding	muscular multi-drug resistance
ABCD2	uc001rmb.2	dark blue	coding	protein transport
ADAMTS20	uc010skx.2	dark blue	coding	tissue remodeling
AEBP2	uc001ref.2	dark blue	coding	DNA-binding transcriptional repressor
AK000807	uc001rie.1	light blue	near coding	
AK094733	uc001rfu.1	light blue	noncoding	
AK096233	uc001rnk.1	light blue	near coding	
ALG10	uc001rlm.3	dark blue	coding	protein glycosylation
ALG10B	uc001rln.4	dark blue	coding	protein glycosylation
AMN1	uc001rkq.4	dark blue	coding	
ARHGDIB	uc001rcq.1	black	coding	cell signaling, proliferation, cytoskeletal organization, and secretion
ARNTL2	uc001rht.2	black	coding	partner of circadian and hypoxia factors
ART4	uc001rcl.1	dark blue	coding	Dombrock blood group system antigens
ASUN	uc001rhk.4	dark blue	coding	regulator of the mitotic cell cycle and development
ATF7IP	uc001rby.4	black	coding	multifunctional nuclear protein
AX746523	uc001riu.1	light blue	antisense	
BC039477	uc001rkg.3	light blue	noncoding	
BC040886	uc001rlq.3	light blue	noncoding	
BC041929	uc001rhc.3	light blue	noncoding	
BC043511	uc001rhx.3	light blue	antisense	
BC067269*	uc001rcb.3	light blue	coding	
BCAT1	uc001rgd.4	black	coding	catalyst
BHLHE41	uc001rhb.3	dark blue	coding	control of circadian rhythm and cell differentiation

Table 65 Continued.

Gene Abbreviation	**UCSC name**	**Color**	**Coding/Non**	**Function** (unknown if left blank)
BICD1	uc001rku.3	dark blue	coding	transport between Golgi apparatus and endoplasmic reticulum
C12orf39	uc001rfa.1	dark blue	coding	open reading frame
C12orf40	uc001rmc.3	dark blue	coding	open reading frame
C12orf60	uc001rcj.4	dark blue	coding	open reading frame
C12orf71	uc001rhq.3	dark blue	coding	open reading frame
C12orf77	uc001rgf.3	dark blue	coding	open reading frame
C2CD5	uc001rfq.3	dark blue	coding	protein transport
CAPRIN2	uc001rjh.1	dark blue	coding	erythroblast differentiation
CAPZA3	uc001rdy.3	dark blue	coding	morphogenesis of spermatids
CASC1	uc001rgj.3	dark blue	coding	cancer susceptibility candidate 1
CCDC91	uc001rip.1	black	coding	regulates membrane traffic
CMAS	uc001rfm.4	dark blue	coding	cell surface enzyme
CNTN1	uc001rmm.2	black	coding	mediates cell surface interactions during nervous system development
contactin1	uc001rmp.1	light blue	noncoding	
CPNE8	uc001rls.1	dark blue	coding	regulates molecular events at cell membrane/cytoplasm interface
DBX2	uc001rok.1	dark blue	coding	developing brain homeobox
DD157417	uc021qwd.1	light blue	anitsense	
DDX11	uc001rjt.1	dark blue	coding	DNA helicase involved in cellular proliferation
DDX11-AS1	uc001rjq.2	light blue	noncoding	
DENND5B	uc001rki.1	dark blue	coding	promotes exchange of GDP to GTP
DENND5B-AS1	uc031qgx.1	light blue	noncoding	
DERA	uc001rde.3	dark blue	coding	catalyst
DERA	uc010shx.1	light blue	coding	catalyst
DKFZp434C0631	uc001rjy.3	light blue	near coding	

Table 65 Continued.

Gene Abbreviation	**UCSC name**	**Color**	**Coding/Non**	**Function** (unknown if left blank)
DNM1L	uc001rld.2	dark blue	coding	mediates mitochondrial and peroxisomal division
EPS8	uc009zif.3	black	coding	regulates actin cytoskeleton dynamics and architecture
ERGIC2	uc001riv.3	dark blue	coding	transport between endoplasmic reticulum and Golgi apparatus
ERP27	uc001rco.3	black	coding	endoplasmic reticulum protein
ETNK1	uc001rft.3	dark blue	coding	phosphatidylethanolamine synthesis pathway
FAM60A	uc001rkd.3	dark blue	coding	repressor of genes in TGF-beta signaling pathway
FAR2	uc001ris.5	dark blue	coding	reduces fatty acids to fatty alcohols
FGD4	uc001rkz.3	dark blue	coding	regulation of actin cytoskeleton and cell shape
FGFR1OP2	uc001rhl.3	dark blue	coding	oncogene partner
FLJ13224*	uc001rkf.1	light blue	coding	
GOLT1B	uc009zit.2	light blue	near coding	Golgi transport
GUCY2C	uc001rcd.3	dark blue	coding	heat-stable enterotoxin receptor
GXYLT1	uc001rms.4	dark blue	coding	xylosyltransferase
GYS2	uc001rfb.3	dark blue	coding	liver protein involved in the synthesis of glycogen
H2AFJ	uc009zia.3	black	coding	core nucleosome component
H3F3C	uc001rkr.3	black	coding	core component of nuclesoome
HIST4H4	uc001rcf.4	black	coding	core nucleosome component
hsa-miR-3194-3p	uc021qwk.1	light blue	noncoding	
IAPP	uc001rev.3	black	coding	induces apoptotic cell death
IFLTD1	uc010sji.1	dark blue	coding	
O8	uc010sjt.2	dark blue	coding	nuclear protein import
IRAK4	uc001rnu.3	black	coding	innate immune response
ITPR2	uc001rhg.3	dark blue	coding	mediates the release of intracellular calcium
KCNJ8	uc001rff.4	dark blue	coding	potassium channel membrane protein
KIAA1551	uc001rks.3	dark blue	coding	

Table 65 Continued.

Gene Abbreviation	**UCSC name**	**Color**	**Coding/Non**	**Function** (unknown if left blank)
KIF21A	uc001rly.3	dark blue	coding	microtubule dependent transport
KLHL42	uc001rij.3	dark blue	coding	microtubule dynamics throughout mitosis
KNU6-78P	uc031qgy.1	light blue	noncoding	
KRAS	uc001rgp.1	black	coding	GTPase activity
LDHB	uc001rfd.3	black	coding	catalyzes conversion between lactate and pyruvate in glycolytic pathway
LINC00477	uc001rgb.1	light blue	noncoding	
LINC00941	uc001rjo.2	light blue	noncoding	
LMO3	uc001rdj.2	dark blue	coding	oncogene expressed in the brain
LOC100506393	uc021qvz.1	light blue	noncoding	
LRMP	uc001rgh.3	dark blue	coding	expressed in lymphoid cell lines and tissues
LRRK2	uc001rmg.4	black	coding	phosphorylation of proteins
LYRM5	uc001rgn.3	dark blue	coding	
MED21	uc001rhp.2	dark blue	coding	transcriptional regulation of RNA polymerase II transcribed genes
METTL20	uc009zjr.3	dark blue	coding	methyltransferase
MGP	uc021qvr.1	dark blue	coding	bone formation inhibitor, found in organic matrix of bone/cartilage
MGST1	uc001rdf.3	dark blue	coding	cellular defense against electrophilic compounds
Mir_720	uc021qwb.1	light blue	noncoding	
MIR3974	uc021qvv.1	light blue	noncoding	microRNA involved in post-transcriptional gene expression regulation
MIR4302	uc021qwe.1	light blue	noncoding	mircoRNA
MIR920	uc021qwc.1	light blue	noncoding	microRNA
MRPS35	uc001rih.3	dark blue	coding	encodes a mitochondrial ribosome protein
MUC19	uc021qwn.1	light blue	coding	
NELL2	uc001rof.3	dark blue	coding	neural cell growth and differentiation

Table 65 Continued.

Gene Abbreviation	**UCSC name**	**Color**	**Coding/Non**	**Function** (unknown if left blank)
OVCH1	uc001rix.1	light blue	coding	
OVCH1-AS1*	uc031qgv.1	light blue	coding	
OVOS2*	uc010sjy.1	light blue	coding	proteinase inhibitor
PDE3A	uc021qwa.1	black	coding	platelet aggregation and cardiovascular function
PDE6H	uc001rcr.3	dark blue	coding	transmission and amplification of vision signal
PDZRN4	uc010skn.2	dark blue	coding	
PIK3C2G	uc001rdt.3	black	coding	protein signaling pathway
PKP2	uc001rlj.4	black	coding	plays a role in junctional plaques
PLBD1	uc001rcc.1	dark blue	coding	phospholipase acting on phospholipids
PLCZ1	uc021qvx.2	dark blue	coding	sperm protein that initiates embryonic development
PLEKHA5	uc001reb.3	black	coding	mRNA associated with body height, weight, and BMI
PLEKHA8P1	uc001rom.2	light blue	coding	
PPFIBP1	uc001rib.2	dark blue	coding	mammary gland development
PPHLN1	uc010skq.2	dark blue	coding	epithelial differentiation and barrier formation
PRICKLE1	uc010skv.2	dark blue	coding	nuclear receptor
PTHLH	uc001rik.3	black	coding	parathyroid hormone family, regulates endochondral bone formation, mutations associated with brachydactyly type E2, inhibitor of osteoclastic bone resorption
PTPRO	uc001rcv.2	black	coding	regulation of osteoclast production, apical surface of polarized cells
PUS7L	uc009zkb.4	dark blue	coding	
PYROXD1	uc001rew.3	dark blue	coding	oxidation-reduction process
RACGAP1P	uc001rol.3	light blue	noncoding	
RASSF8	uc001rgx.3	black	coding	tumor suppressor protein
RASSF8-AS1	uc001rgu.1	light blue	noncoding	
RECQL	uc001rex.3	black	coding	helicase involved in DNA repair

Table 65 Continued.

Gene Abbreviation	**UCSC name**	**Color**	**Coding/Non**	**Function** (unknown if left blank)
REP15	uc001rig.1	dark blue	coding	facilitates transferrin receptor recycling
RERG	uc001rcs.3	black	coding	inhibits cell proliferation and tumor formation
RERGL	uc001rdq.3	dark blue	coding	binds GDP/GTP
RNY5	uc010slc.1	light blue	noncoding	
SKP1P2*	uc021qvt.1	light blue	coding	
SLC15A5	uc021qvs.1	light blue	coding	peptide transport
SLC2A13	uc010skm.2	dark blue	coding	glucose transport
SLCO1A2	uc010siq.2	light blue	coding	cellular uptake of organic ions in the liver
SLCO1B1	uc001req.4	dark blue	coding	liver-specific member of organic anion transporter family
SLCO1B3	uc001rel.4	dark blue	coding	bile acid and bilirubin transport
SLCO1B7	uc010sin.2	dark blue	coding	organic anion transporter family
SLCO1C1	uc001rei.3	dark blue	coding	mediates uptake of thyroid hormones in the brain
SMCO3 (C12orf69)	uc001rck.1	dark blue	coding	membrane component
SMOC2	uc010sjq.2	dark blue	coding	integral component of the membrane
SNORA75	uc021qwj.1	light blue	noncoding	
SOX5	uc001rfx.4	dark blue	coding	embryonic development and cell fate, perhaps chondrogenesis
SSPN	uc001rhd.3	dark blue	coding	structural component of muscle cells
ST8SIA1	uc001rfo.4	dark blue	coding	cell adhesion protein in Golgi apparatus
STK38L	uc001rhr.3	dark blue	coding	regulation of structural processes in neuronal cells
STRAP	uc001rdc.4	dark blue	coding	kinase receptor protein
SYT10	uc001rll.1	dark blue	coding	exocytosis of secretory vesicles
TM7SF3	uc010sjl.2	dark blue	coding	integral component of membrane
TMEM117	uc001rod.3	dark blue	coding	transmembrane protein
TMTC1	uc021qwi.1	dark blue	coding	membrane protein
TRNA_Lys	uc021qwh.1	light blue	noncoding	

Table 65 Continued.

Gene Abbreviation	**UCSC name**	**Color**	**Coding/Non**	**Function** (unknown if left blank)
TSPAN11	uc001rjp.3	dark blue	coding	integral component of the membrane
TWF1	uc001rob.3	dark blue	coding	actin monomer-binding protein
U5	uc021qwl.1	light blue	noncoding	
U6	uc021qvu.1	light blue	noncoding	
WBP11	uc001rci.3	dark blue	coding	WW domain binding protein
Y_RNA	uc021qvw.1	light blue	noncoding	
YAF2	uc001rmv.3	black	coding	negative regulation of muscle-restricted genes
YARS2	uc001rli.3	black	coding	mitochondrial protein that attaches tyrosine to tRNA
ZCRB1	uc001rmz.3	black	coding	component of the U12 spliceosome

Table 66 - Genes on chromosome 7 within area of suggestive LOD score for Femur Bicondylar Length.

Gene Abbreviation	**UCSC name**	**Color**	**Coding/Non**	**Function** (unknown if left blank)
5S_rRNA	uc003vil.3	light blue	noncoding	
AK097428	uc003vhr.4	light blue	noncoding	
ANKRD7	uc003vji.3	dark blue	coding	testis-specific protein
ASZ1	uc003vjb.2	dark blue	coding	spermatogenesis
BC022431	uc003vhh.1	light blue	noncoding	
BC039665	uc003vhi.4	light blue	noncoding	
BC040208	uc003vhn.1	light blue	antisense	
BC043243	uc003vfz.3	light blue	noncoding	
BCAP29	uc003vej.2	dark blue	coding	membrane protein transport from endoplasmic reticulum to Golgi
BD495725	uc003vhq.1	light blue	noncoding	
C7orf60	uc003vgo.1	dark blue	coding	open reading frame
C7orf66	uc003vfo.3	dark blue	coding	open reading frame
CAPZA2	uc003vil.3	dark blue	coding	actin capping protein
CAV2	uc003vid.3	dark blue	coding	scaffolding protein in caveolar membranes
CBLL1	uc003veq.3	dark blue	coding	plays a role in cell proliferation
CFTR	uc003vjd.3	black	coding	chloride channel associated with cystic fibrosis
CTTNPB2*	uc003vjf.3	dark blue	coding	regulates the actin cytoskeleton
DLD	uc003vet.3	black	coding	functions as either a dehydrogenase or a protease
DNAJB9	uc003vfn.3	black	coding	regulates ATPase activity and protects against apoptosis
DOCK4	uc003vfx.3	dark blue	coding	regulation of adherens junctions between cells
DQ656011	uc003vic.1	light blue	antisense	
DQ656015	uc003vhy.1	light blue	near coding	
DUS4L	uc003veh.4	dark blue	coding	catalyzes the synthesis of dihydrouridine
EF070117	uc003vhs.1	light blue	near coding	

Table 66 Continued.

Gene Abbreviation	**UCSC name**	**Color**	**Coding/Non**	**Function** (unknown if left blank)
EF070119	uc003vhu.1	light blue	near coding	
EF070122	uc003vht.1	light blue	near coding	
EIF3IP1*	uc003vfp.1	light blue	coding	translation initiation
FOXP2	uc003vgx.2	black	coding	development of speech and language regions of the brain
GPR22	uc003vef.3	dark blue	coding	multi-pass membrane protein
GPR85	uc010ljv.2	dark blue	coding	receptor that induces intracellular signaling cascade
IFRD1	uc003vgj.3	dark blue	coding	transcriptional coactivator/repressor during embryonic development
IMMP2L	uc003vfq.2	dark blue	coding	directs mitochondrial proteins to the mitochondria
ING3	uc003vjn.3	black	coding	tumor suppressor protein
KCND2	uc003vjj.1	dark blue	coding	potassium channel in the brain
LAMB1	uc003vew.2	dark blue	coding	noncollagenous component of basement membranes
LAMB4	uc010ljo.1	dark blue	coding	mediates organization of cells during embryonic development
LOC401397 (ENSG00000214194)	uc011kmt.2	light blue	coding	
LRRN3	uc003vft.4	dark blue	coding	membrane protein
LSMEM1	uc011kmq.2	dark blue	coding	membrane protein
MDFIC	uc003vhf.3	dark blue	coding	transcriptional regulation of viral genome expression
MET	uc011knf.2	black	coding	wound healing, organ regeneration, tissue remodeling
Mir_548	uc022ajy.1	light blue	noncoding	
Mir_875	uc022akb.1	light blue	noncoding	
MIR3666	uc022ake.1	light blue	noncoding	microRNA
NAA38	uc003vjg.3	dark blue	coding	component of the spliceosome
NRCAM	uc022aka.1	black	coding	neuronal cell adhesion molecule
PNPLA8	uc003vff.2	dark blue	coding	cleaves fatty acids from membrane phospholipids

Table 66 Continued.

Gene Abbreviation	**UCSC name**	**Color**	**Coding/Non**	**Function** (unknown if left blank)
PPP1R3A	uc010ljy.1	dark blue	coding	regulation of glycogen metabolism and muscle contractility
SLC26A3	uc003ver.2	dark blue	coding	intestinal chloride absorption
SLC26A4	uc003vep.3	dark blue	coding	associated with Pendred syndrome, a form of deafness
SLC26A4-AS1	uc003veo.3	light blue	antisense	
SNORA25	uc022akh.1	light blue	noncoding	
SnoU109	uc022ajx.1	light blue	noncoding	
ST7	uc003vin.3	dark blue	coding	tumor suppression
ST7-AS1*	uc003vim.4	light blue	coding	
ST7-AS2	uc003viu.3	light blue	noncoding	
ST7OT2	uc003vit.3	light blue	noncoding	
ST7-OT3	uc003viy.1	light blue	near coding	
ST7-OT4	uc003vip.1	light blue	coding	
TES	uc003vho.3	black	coding	tumor suppression
TFEC	uc003vhm.2	dark blue	coding	regulate expression of target genes, may co-regulate genes in osteoclasts
THAP5	uc003vfl.3	dark blue	coding	regulates cell cycle
TMEM168	uc003vgn.3	dark blue	coding	membrane protein
TSPAN12	uc003vjk.3	dark blue	coding	cell surface protein that mediates signal transduction events
U3	uc022ajz.1	light blue	noncoding	
U7	uc022akl.1	light blue	noncoding	
WNT2	uc003viz.3	dark blue	coding	signaling protein, regulation of cell fate and patterning during embryogenesis
Y_RNA	uc022akg.1	light blue	noncoding	
ZNF277	uc003vge.2	dark blue	coding	transcriptional regulation

Table 67 - Genes on chromosome 14 within area of suggestive LOD score for Femur Bicondylar Length.

Gene Abbreviation	**UCSC name**	**Color**	**Coding/Non**	**Function** (unknown if left blank)
5S_rRNA	uc021rva.1	light blue	noncoding	
ACTN1	uc001xkk.3	black	coding	anchors actin to a variety of intracellular structures
ACTN1-AS1	uc031qpf.1	light blue	noncoding	
ACTR10	uc001xdf.3	dark blue	coding	microtubule-based movement
ADAM20	uc001xme.3	dark blue	coding	sperm maturation and fertilization
ADAM20P1*	uc021rvr.1	light blue	coding	metallopeptidase activity
ADAM21	uc001xmd.3	dark blue	coding	sperm maturation and fertilization
ADAM21P1*	uc010ttg.2	light blue	coding	metallopeptidase activity
AK055910	uc021rum.1	light blue	near coding	
AK093892	uc001xmh.1	light blue	noncoding	
AKAP5	uc001xhd.4	black	coding	regulation of postsynaptic events in cerebral cortex
AP5M1	uc001xcv.3	dark blue	coding	protein complex involved in endosomal transport and cell death
ARG2	uc001xjs.3	black	coding	catalyzes the hydrolysis of arginine
ARID4A	uc010apg.1	black	coding	ubiquitous nuclear protein regulating cell proliferation and transcriptional repression
ATP6V1D	uc001xjf.3	dark blue	coding	mediates acidification of eukaryotic intracellular organelles
AX746582	uc001xji.1	light blue	noncoding	
BC035195	uc001xev.1	light blue	noncoding	
BC037850	uc001xci.3	light blue	noncoding	
BC047625	uc001xeo.3	light blue	noncoding	
BC050301	uc001xfm.3	light blue	noncoding	
BC052775	uc001xib.3	light blue	noncoding	
BC062762	uc021rvi.1	light blue	near coding	
BX161428	uc001xil.3	light blue	noncoding	
BX648502	uc031qov.1	light blue	noncoding	

Table 67 Continued.

Gene Abbreviation	**UCSC name**	**Color**	**Coding/Non**	**Function** (unknown if left blank)
C14orf105	uc001xcy.2	dark blue	coding	open reading frame
C14orf37	uc001xdc.3	dark blue	coding	open reading frame
C14orf39	uc001xez.4	dark blue	coding	eye development
CCDC175	uc021rtw.1	dark blue	coding	
CCDC177	uc031qpg.1	dark blue	coding	
CHURC1	uc001xhw.2	dark blue	coding	regulates FGF signaling during neural development
CHURC1-FNTB (ENSG00000125954)	uc010tso.2	black	coding	read-through transcription between neighboring genes
COX16	uc001xmb.3	dark blue	coding	mitochondrial protein
DAAM1	uc031qou.1	black	coding	scaffolding protein, regulates cell growth through stabilization of microtubules
DACT1	uc001xdx.3	dark blue	coding	regulates signaling pathways during development
DCAF5	uc001xkp.3	black	coding	substrate receptor
DHRS7	uc001xes.3	light blue	coding	oxidation/reduction of steroids and retinoids
DJ031130	uc010tsr.3	light blue	antisense	
EIF2S1	uc001xjg.3	black	coding	catalyzes first regulated step of protein synthesis
ERH	uc001xlc.2	black	coding	plays a role in the cell cycle
ESR2	uc001xha.1	black	coding	estrogen receptor and nuclear receptor transcription factor
EXD2	uc001xky.3	dark blue	coding	exonuclease activity
EXOC5	uc001xct.3	dark blue	coding	part of the exocyst complex
FAM71D	uc001xja.2	dark blue	coding	
FLJ22447	uc021rtz.1	light blue	noncoding	
FLJ31306	uc001xdl.3	light blue	near coding	
FUT8	uc001xip.3	black	coding	fucosyltransferases, contributes to malignancy of cancer cells
FUT8-AS1*	uc001xim.4	light blue	coding	

Table 67 Continued.

Gene Abbreviation	**UCSC name**	**Color**	**Coding/Non**	**Function** (unknown if left blank)
GALNT16 (WBSCR17)	uc001xlb.2	dark blue	coding	catalyzes oligosaccharide biosynthesis
GPHB5*	uc021rud.1	dark blue	coding	stimulates the thyroid
GPHN	uc001xiy.3	black	coding	involved in membrane protein-cytoskeleton interactions
GPR135	uc010apj.3	dark blue	coding	receptor
GPX2	uc021ruq.2	black	coding	protects against toxicity of ingested organic hydroperoxides
HIF1A	uc001xfq.2	black	coding	master regulator of hypoxia, involved in embryonic vascularization
HIF1A-AS2	uc021ruc.1	light blue	antisense	
HSPA2	uc001xhk.4	black	coding	stabilize preexisting proteins and mediate new polypeptide folding
JA429503	uc021rug.1	light blue	noncoding	
JB175233	uc021rtx.1	light blue	noncoding	
JKAMP	uc001xef.4	dark blue	coding	membrane protein
KCNH5	uc001xfy.3	dark blue	coding	voltage-gated potassium channel
KIAA0247	uc001xlk.3	dark blue	coding	membrane protein
KIAA0586	uc010trr.2	dark blue	coding	ciliogenesis and sonic hedgehog (SHH) signaling
KTN1	uc010trc.2	light blue	coding	membrane protein
L3HYPDH	uc001xee.1	dark blue	coding	metabolic activity
LINC00238	uc001xiu.3	light blue	noncoding	
LINC00520	uc010trd.2	light blue	noncoding	
LINC00643	uc010apt.2q	light blue	noncoding	
LOC100289511*	uc021rvk.1	light blue	coding	
LOC100506321	uc021ruv.1	light blue	antisense	
LOC145474	uc010ttl.2	light blue	noncoding	
LRRC9	uc001xep.1	light blue	noncoding	

Table 67 Continued.

Gene Abbreviation	**UCSC name**	**Color**	**Coding/Non**	**Function** (unknown if left blank)
MAP3K9	uc001xmm.3	black	coding	signal pathway to cellular responses evoked by environmental changes
MAX	uc001xif.2	black	coding	transcription regulator
MED6	uc001xmf.3	dark blue	coding	transcription mediator complex
Metazoa_SRP	uc021rvc.1	light blue	noncoding	
Mir_548	uc021rtl.1	light blue	noncoding	
Mir_548	uc021rtv.1	light blue	noncoding	
Mir_548	uc021run.1	light blue	noncoding	
Mir_625	uc021rux.1	light blue	noncoding	
Mir_633	uc021rtq.1	light blue	noncoding	
MIR4706	uc021ruu.1	light blue	noncoding	microRNA
MIR4708	uc021ruw.1	light blue	noncoding	microRNA
MNAT1	uc001xfd.3	black	coding	cell cycle control and RNA transcription
MPP5	uc001xjd.4	black	coding	participates in the polarization of differentiating cells
MTHFD1	uc001xhb.3	dark blue	coding	enzymatic activity
NAA30	uc001xcx.4	dark blue	coding	subunit of N-terminal acetyltransferase C complex
OTX2	uc031qor.1	dark blue	coding	transcription factor in brain, craniofacial, and sensory organ development
OTX2-AS1	uc021rtn.1	light blue	near coding	
PCNX	uc001xmo.2	dark blue	coding	membrane protein
PCNXL4	uc001xer.4	dark blue	coding	membrane protein
PELI2	uc001xch.3	black	coding	protein ubiquitination
PIGH	uc001xjr.1	dark blue	coding	produces a protein that anchors proteins to the cell surface
PLEK2	uc001xjh.1	black	coding	helps orchestrate cytoskeleton arrangement
PLEKHD1	uc010ttf.1	dark blue	coding	
PLEKHG3	uc001xhn.1	dark blue	coding	

Table 67 Continued.

Gene Abbreviation	**UCSC name**	**Color**	**Coding/Non**	**Function** (unknown if left blank)
PLEKHH1	uc001xjl.1	dark blue	coding	
PPM1A	uc010apn.3	black	coding	negative regulator of cell stress response pathway
PPP1R36	uc001xhl.1	dark blue	coding	inhibits phosphatse activity
PPP2R5E	uc001xgd.1	dark blue	coding	negative control of cell growth and division
PRKCH	uc010tsa.2	black	coding	regulates keratinocyte differentiation
PSMA3	uc001xdj.2	dark blue	coding	proteasome component
RAB15	uc001xhz.2	dark blue	coding	GTPase family
RAD51B	uc001xkd.3	dark blue	coding	DNA repair by homologous recombination
RDH11	uc001xjv.4	dark blue	coding	oxioreductive catalytic activity towards retinoids
RDH12	uc001xjz.4	dark blue	coding	oxioredcutive catalytic activity towards retinoids
RHOJ	uc001xgb.2	dark blue	coding	regulates angiogenesis
RNaseP_nuc	uc021ruo.1	light blue	noncoding	
RPL13AP3	uc010aos.3	light blue	noncoding	
RTN1	uc001xek.2	dark blue	coding	neuroendocrine secretion
SCARNA20	uc021rue.1	light blue	noncoding	
SGPP1	uc001xgj.3	dark blue	coding	regulates diverse biologic processes
SIPA1L1	uc001xmr.1	light blue	coding	
SIX6	uc001xfa.4	dark blue	coding	eye development
SLC10A1	uc001xlr.2	dark blue	coding	sodium/bile acid cotransporter
SLC35F4	uc021rtp.1	dark blue	coding	solute carrier family
SLC38A6	uc001xfg.2	dark blue	coding	solute carrier family
SLC39A9	uc021rvg.1	dark blue	coding	solute carrier
SLC8A3	uc001xly.3	dark blue	coding	sodium/calcium exchanger, maintains calcium homeostasis
SMOC1	uc001xlt.2	dark blue	coding	ocular and limb development
SNAPC1	uc001xft.3	dark blue	coding	required for transcription of RNA II and III snRNA genes

Table 67 Continued.

Gene Abbreviation	**UCSC name**	**Color**	**Coding/Non**	**Function** (unknown if left blank)
SNORD112	uc021rty.1	light blue	noncoding	
SNORD56B	uc001xmq.3	light blue	noncoding	
SPTB	uc001xht.3	black	coding	membrane organization and stability
SRSF5	uc001xlo.3	dark blue	coding	pre-mRNA splicing factor
SYNE2	uc001xgm.3	black	coding	tethers nucleus to cytoskeleton for structural integrity
SYNJ2BP	uc001xmc.4	black	coding	mitochondrial protein
SYNJ2BP-COX16*	uc021rvm.1	black	coding	read-through transcription between neighboring genes
SYT16	uc001xfu.1	dark blue	coding	trafficking and exocytosis of secretory vescicles
TEX21P	uc021ruj.2	light blue	noncoding	
TIMM9	uc010aph.3	dark blue	coding	mitochondrial intermembrane chaperone protein
TMEM229B	uc021rvb.1	dark blue	coding	transmembrane protein
TMEM260 (C14orf101)	uc001xcm.3	dark blue	coding	transmembrane protein
TMEM30B	uc001xfl.3	dark blue	coding	transmembrane protein
TOMM20L	uc001xdr.1	dark blue	coding	mitochondrial membrane
TRMT5	uc001xff.4	dark blue	coding	posttranscriptional modification of tRNAs
TRNA_Lys	uc021rts.1	light blue	noncoding	
TTC9	uc001xmi.2	dark blue	coding	cancer cell invasion and metastasis
U2	uc021rvp.1	light blue	noncoding	
VTI1B	uc001xjt.3	black	coding	mediates vesicle transport pathways
WDR89	uc001xgi.4	dark blue	coding	
ZBTB1	uc010aqg.3	dark blue	coding	transcriptional repressor
ZBTB25	uc001xhf.3	dark blue	coding	transcriptional regulation
ZFP36L1	uc001xki.2	black	coding	regulates response to growth factors
ZFYVE26	uc001xka.2	dark blue	coding	abcission step of cytokinesis, double-strand DNA break repair

Table 68 - Candidate genes.

Gene Abbreviation	Chromosome	Location (bps)	Function	Trait
DKK3	11	11,984,543 - 12,030,917	Wnt signaling, limb development	humerus head length
NELL1	11	20,691,117 - 21,597,229	osteoblast differentiation, bone mineralization	humerus head length
CD44	11	35,160,417 - 35,253,949	Wnt signaling, bone formation	humerus head length
FJX1	11	35,639,735 - 35,642,421	limb development	humerus head length
MGP	12	15,034,115 - 15,038,853	bone formation inhibitor	max humerus length
PTHLH	12	28,111,017 - 28,124,916	endochondral bone formation, skeletal homeostasis	max humerus length
PTPRO	12	15,475,191 - 15,751,265	osteoclast production	max humerus length
SOX5	12	23,685,231 - 24,102,637	embryonic development, chondrogenesis	max humerus length
TFEC	7	115,575,202 - 115,670,867	osteoclast regulation	femur bicond length
WNT2	7	116,916,686 - 116,963,343	patterning in embryogenesis	femur bicond length
KIAA0586	14	58,894,103 - 59,015,549	SHH signaling	femur bicond length
SMOC1	14	70,346,114 - 70,499,083	limb development	femur bicond length

Table 69 - Major proteins known to be involved in limb or bone formation.

Gene	Abbreviation (Alt. Name)	Location (chromosome:bps)	Function
Aldehyde Dehydrogenase1 Family, Member A2	ALDH1A2 (RALDH2)	chr15:58,245,622-58,358,121	catalyzes the synthesis of retinoic acid from retinaldehyde, which is necessary for limb bud formation
Bone morphogenetic protein 2	BMP2	chr20:6,748,745-6,760,910	induces cartilage and bone formation
Bone morphogenetic protein 3	BMP3	chr4:81,952,119-81,978,685	negatively regulates bone density
Bone morphogenetic protein 4	BMP4	chr14:54,416,455-54,421,270	induces cartilage and bone formation, involved in limb formation
Bone morphogenetic protein 5	BMP5	chr6:55,620,238-55,740,375	induces cartilage and bone formation
Bone morphogenetic protein 6	BMP6	chr6:7,727,011-7,881,961	induces cartilage and bone formation
Bone morphogenetic protein 7	BMP7	chr20:55,743,809-55,841,707	induces cartilage and bone formation, involved in calcium regulation and bone homeostasis
Fibroblast growth factor 4	FGF4	chr11:69,587,797-69,590,171	bone morphogenesis and limb development
Fibroblast growth factor 8	FGF8	chr10:103,529,887-103,535,759	required for limb development in embryogenesis
Fibroblast growth factor 9	FGF9	chr13:22,245,215-22,278,640	regulation of embryonic development
Fibroblast growth factor 17	FGF17	chr8:21900428-21906319	regulation of embryonic development
Fibroblast growth factor 18	FGF18	chr5:170,846,667-170,884,630	required for normal ossification and bone development
Frizzled-related Protein	FRZB	chr2:183,698,005-183,731,498	limb skeletogenesis, regulates chondrocyte maturation and long bone development
Growth differentiation factor 2	GDF2 (BMP9)	chr10:48,413,092-48,416,853	may be involved in bone formation

Table 69 Continued.

Gene	Abbreviation (Alt. Name)	Location (chromosome:bps)	Function
Growth differentiation factor 5	GDF5	chr20:34,021,149-34,026,027	involved in bone and cartilage formation
GLI family zinc finger 3	GLI3	chr7:42,000,548-42,276,618	plays a role in limb development, repressor of SHH pathway (see below), specifies limb digit number and identity, restricts zone of PTHLH expression (see below)
Gremlin 1	GREM1	chr15:33,010,205-33,026,870	plays a role in body patterning, relays SHH (see below) signal during limb bud outgrowth
Heart and neural crest derivatives expressed 2	HAND2	chr4:174,447,652-174,451,378	important in limb development by acting as a regulator of SHH (see below) induction in the limb bud
Homeobox D10	HOXD10	chr2:176,981,492-176,984,670	guides anterio-posterior positioning in the developing limb buds
Homeobox D11	HOXD11	chr2:176,972,084-176,974,316	plays a role in forelimb morphogenesis
Homeobox D12	HOXD12	chr2:176,964,530-176,965,488	involved in limb development
Homeobox D13	HOXD13	chr2:176,957,532-176,960,666	plays a role in development of the autopod
Indian Hedgehog	IHH	chr2:219,919,142-219,925,238	plays a role in bone growth and differentiation
LIM Homeobox Transcription Factor 1, Alpha	LMX1A	chr1:165,171,104-165,325,478	aids in dorsoventral patterning of the limb
Meis Homeobox 1	MEIS1	chr2:66,662,532-66,799,891	development of proximal limb structures
Meis Homeobox 2	MEIS2	chr15:37,183,222-37,392,341	development of proximal limb structures

Table 69 Continued.

Gene	Abbreviation (Alt. Name)	Location (chromosome:bps)	Function
Noggin	NOG	chr17:54,671,060-54,672,951	joint formation
Parathyroid Hormone-like Hormone	PTHLH	chr12:28,111,017-28,124,916	regulates endochondral bone development, required for skeletal homeostasis
Runt-related Transcription Factor 2	RUNX2	chr6:45,296,054-45,518,819	osteoblast differentiation and bone morphogenesis
Sonic Hedgehog	SHH	chr7:155,595,558-155,604,967	important in anterio-posterior limb axis patterning
SRY Box 9	Sox9	chr17:70,117,161-70,122,560	chondrocyte differentiation
Sp7 Transcription Factor	SP7 (osterix)	chr12:53,720,363-53,729,538	osteoblast differentiation and bone formation
T-box 4	TBX4	chr17:59,533,807-59,561,664	regulates limb development, specifies limb identity, expressed only in developing hindlimb
T-box 5	TBX5	chr12:114,791,735-114,843,968	plays a role in limb development, specifies limb identity, expressed in the developing forelimb
Wingless-type MMTV Integration Site Family, Member 7A	WNT7A	chr3:13,860,082-13,921,618	sets the dorsal-ventral axis for the developing limb bud

Gene locations are taken from the UCSC Genome Browser (Kent et al., 2002). Gene functions are taken from Kent et al., 2002 and Tickle et al., 2013.

Table 70 - Legend for line color in protein networks.

Type of Evidence	Color
Neighborhood	Dark Green
Gene Fusion	Red
Cooccurrence	Dark Blue
Coexpression	Black
Experiments	Pink
Databases	Light Blue
Textmining	Light Green

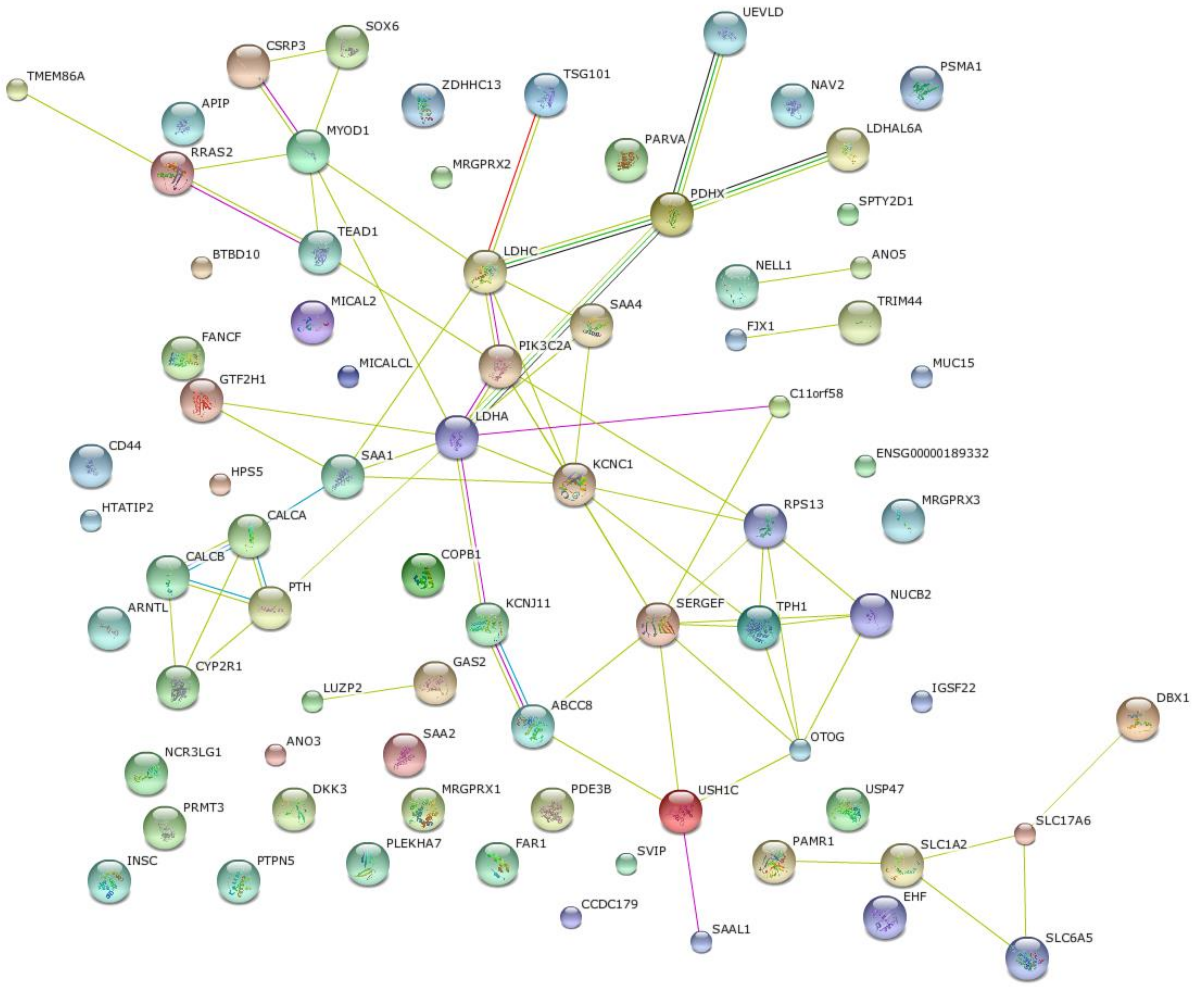

Figure 28 - Protein network for Humerus Head Length proteins.

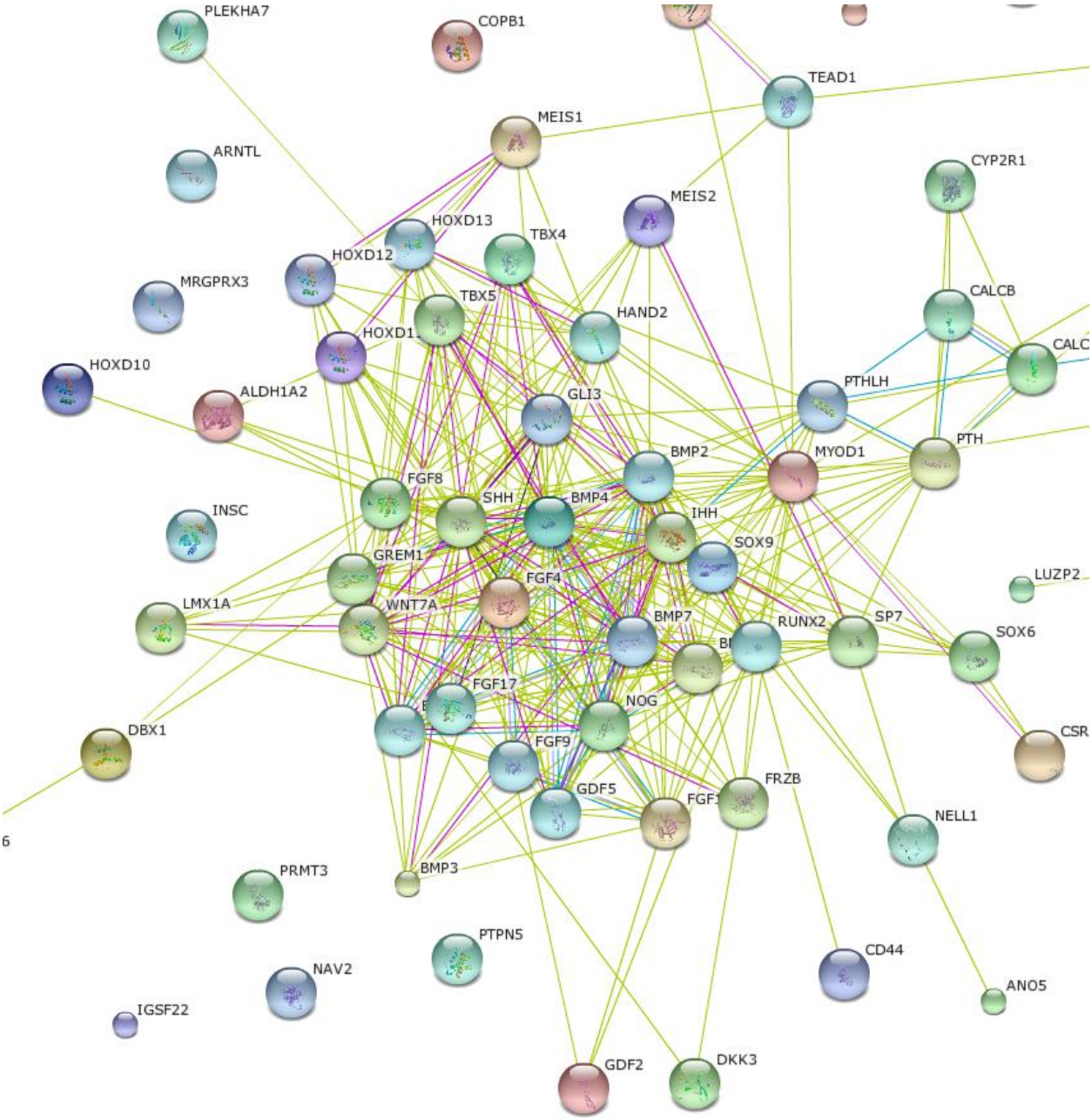

Figure 29 - Protein network for Humerus Head Length proteins and proteins known to be involved in bone or limb development. (Cropped from larger image.)

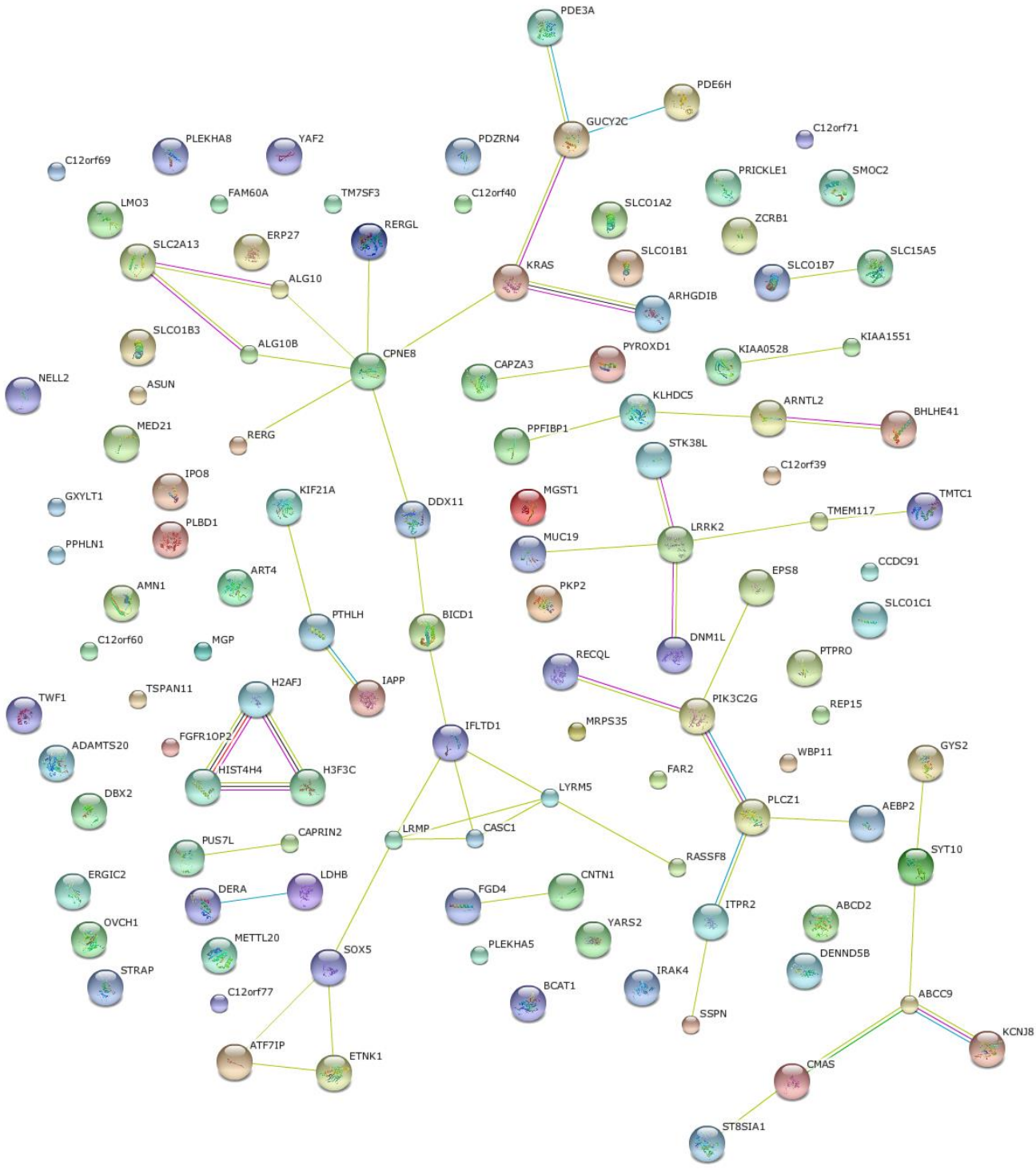

Figure 30 - Protein network for Humerus Maximum Length proteins.

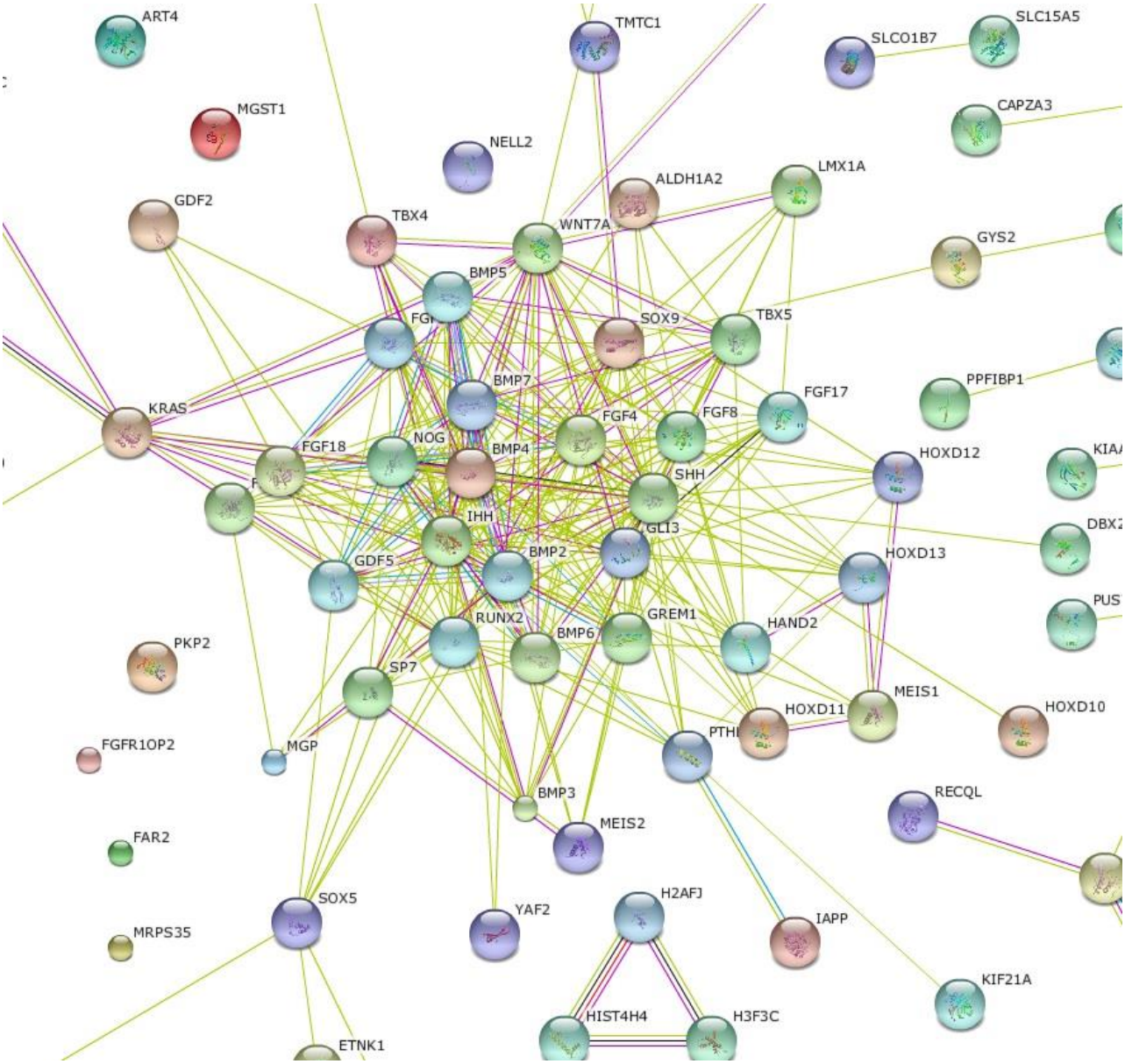

Figure 31 - Protein network for Humerus Maximum Length proteins and proteins known to be involved in bone or limb development. (Cropped from larger image.)

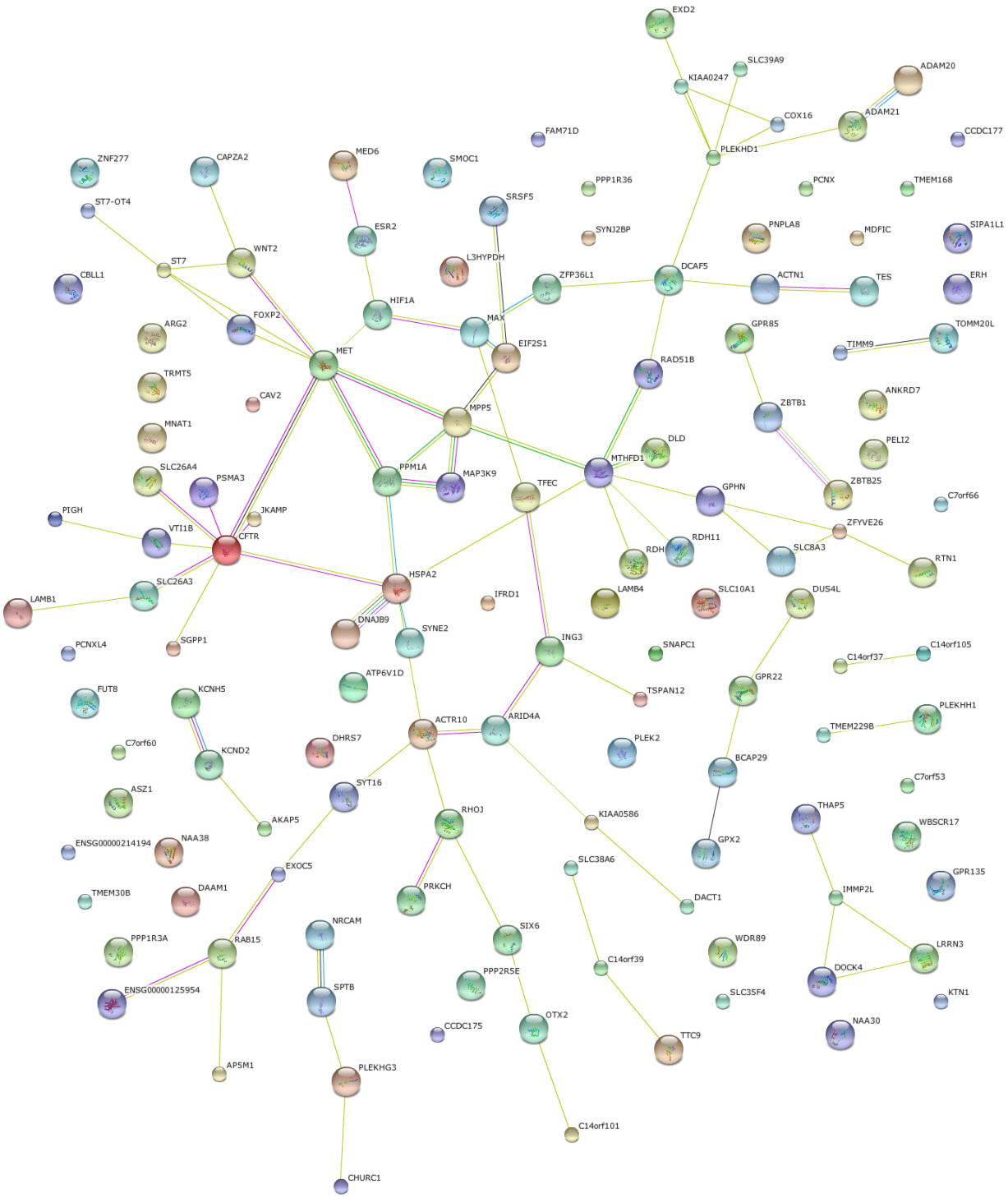

Figure 32 - Protein network for Femur Bicondylar Length proteins.

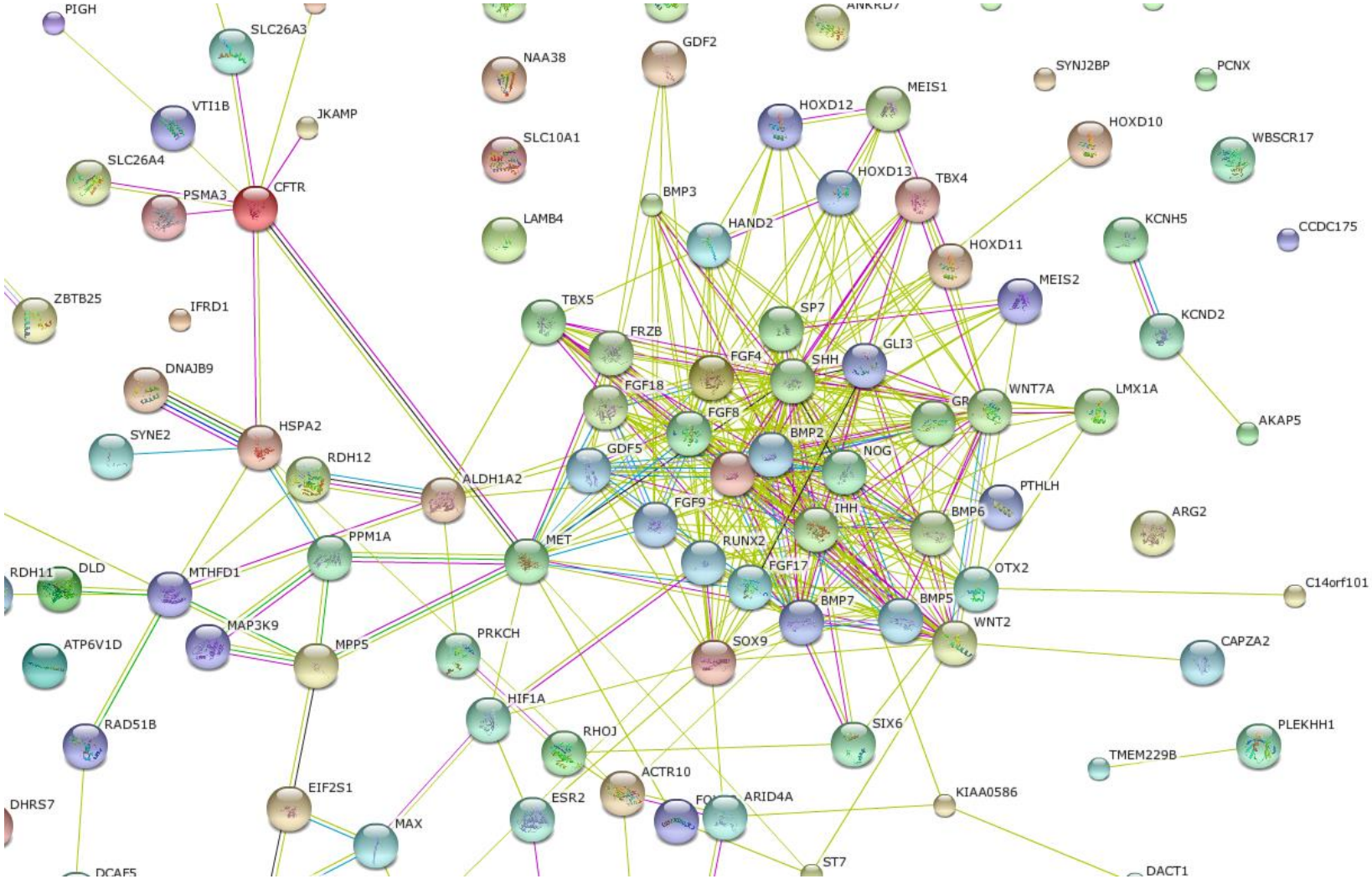

Figure 33 - Protein network for Femur Bicondylar Length proteins and proteins known to be involved in bone or limb development. (Cropped from larger image.)

VITA

Brannon (Jones) Hulsey was born in Fort Worth, Texas to parents Jeffrey and Susan Jones. She attended Richland High School in North Richland Hills, Texas and received her B.S. in Forensic Science with minors in Biology and Chemistry from Baylor University in Waco, Texas in 2004. She attended the University of Tennessee, Knoxville to pursue her interests in biological anthropology, obtaining an M.A. degree in 2006. She continued her doctoral work at the University of Tennessee and earned her Ph.D. in May 2016. During her tenure in graduate school, Brannon was the lab manager for the Molecular Anthropology Laboratories. She is currently a stay-at-home mom.